Autonomous Component Carrier Selection for 4G Femtocells

Garcia, Luis Guilherme Uzeda

Publication date:
2011

Document Version
Accepted author manuscript, peer reviewed version

Autonomous Component Carrier Selection for 4G Femtocells

Luis Guilherme Uzeda Garcia
Aalborg University
Denmark

A Dissertation submitted for the degree of
Doctor of Philosophy
December 2011.

Supervisors:
Preben E. Mogensen, PhD,
Professor, Aalborg University, Denmark.
Klaus I. Pedersen, PhD,
Senior Wireless Network Specialist, Nokia Siemens Networks, Aalborg, Denmark.

Opponents:
Petar Popovski, PhD
Associate Professor, Aalborg University, Denmark.
Rahim Tafazolli , PhD,
Professor and Head of the Centre for Communication Systems Research (CCSR), United Kingdom
Luis Lopes, PhD,
Director of Standards Strategy, Motorola, United Kingdom

To all those close to my heart.

"The wireless telegraph is not difficult to understand.
The ordinary telegraph is like a very long cat.
You pull the tail in New York, and it meows in Los Angeles.
The wireless is the same, only without the cat
Albert Einstein

"If you can't explain it simply,
you don't understand it well enough"
Albert Einstein

"Imagination will often carry us to worlds that never were.
But without it we go nowhere."
Carl Sagan

Abstract

It is envisioned that the ability to provide peak data rates of 1 Gbps in nomadic environments will be instrumental to the commercial success of 4^{th} generation mobile communication systems such as Long Term Evolution (LTE) Release 10, popularly known as LTE-Advanced. Increasing the *spectral efficiency per unit area*, taking the cellular concept to the extreme seems a promising path to achieve this ambitious target. As a result, low-power base stations such as indoor user-deployed femtocells have gained significant notoriety. The benefits are not without challenges though; femtocells introduce the concept of private and therefore potentially closed cells. Dense and uncoordinated deployment of femtocells, especially closed ones, will make severe inter-cell interference an inevitable reality if spectral resources are reused without any restriction. While inter-cell interference management has been extensively investigated in the context of conventional cellular networks; there are innumerous open problems related to networks comprising a diverse mix of base-stations types.

This Ph.D. thesis addresses some of these outstanding issues in the context of LTE-Advanced femtocells, paying special attention to the nuances of the interference footprint in the presence of closed cells. More specifically, this work entertains the idea of exploiting the Carrier Aggregation (CA) framework introduced in LTE-Advanced as a natural enabler of simple yet effective frequency domain interference management schemes. Carrier-based interference coordination is attractive because it is backward compatible and, above all, automatically offers intra-tier protection to both data and control channels even in the presence of closed cells. Something that is not currently possible. Control channel interference management is critical since improved data Signal to Interference plus Noise Ratio (SINR) is not useful if the User Equipment (UE) cannot decode control channels.

The research was chiefly carried out through Monte Carlo simulations. For this purpose, two semi-static system level simulators were developed in order to provide quantitative results. Simple analytical formulations provide additional insight and guide the qualitative evaluation. The investigations revolve around femtocell operating in a dedicated band. This assumption could also be interpreted as a global license-exempt band forming the basis of an envisioned "Femto Commons" spectrum, where spectrum sharing takes place among equals. The work covers both down- and uplinks; although the former admittedly receives more attention.

Femtocells venture into previously IEEE 802.11 (WiFi) exclusive territory. Hence the work begins with a characterization of the interference footprint of local area cellular deployments. In parallel, the performance of a hypothetical system employing Carrier Sense Multiple Access with Collision Avoidance (CSMA/CA) in an LTE-Advanced framework is evaluated. The findings motivate the solutions sought throughout the rest of this thesis.

The proposed Autonomous Component Carrier Selection (ACCS) framework constitutes the main contribution of this Ph.D. study. The core concept and some of its spinoffs included here flirt with cognitive radio networks and elements from game and especially graph theories. ACCS is a non-iterative heuristic, relying on unpretentious sensing (standard UE measurements) coupled with lightweight inter-node signaling, whereby autonomous decision makers (femtocells) tackle the complex combinatorial channel allocation optimization problem. The difficulties arise because the optimal sharing of radio resources amongst femtocells depends on many time-varying factors.The basic concept is extended as well as compared to both simpler and more complex alternatives. The goal is to assess how much complexity is required to provide efficient interference coordination on a component carrier level. This thesis also contains a comprehensive characterization of the performance of various practical carrier based strategies as a function of the network density and the traffic intensity.

Finally, the results provide strong empirical evidence that a concrete scheduler-independent and fully distributed carrier based solution is viable. ACCS and its generalizations are capable of curbing inter-cell interference, thereby boosting cell-edge user throughput by up to 500%, without compromising average and peak data-rates. As a result, ACCS grants the network the ability to self-adjust to variable traffic and deployment conditions.

Dansk Resumé[1]

Det er planlagt, at evnen til at levere maksimal datahastigheder på 1 Gbps i nomadiske miljøer vil være medvirkende til en kommerciel succes af fjerde generation af mobile kommunikationssystemer såsom Long Term Evolution (LTE), populært kendt som LTE-Avanceret. Øget spektral effektivitet per areal enhed for cellulære synes en lovende vej til at nå dette ambitiøse mål. Som følge heraf har energibesparende basisstationer som indendørs bruger-indsat femtocells opnået betydelig interesse. Fordelene er ikke uden udfordringer skønt; femtocells indføre begrebe som f.eks. privat adgangs kontrol. Tæt og ukoordineret anvendelse af femtocells, især med privat adgang, vil få alvorlige inter-celle indblanding blive en uundgåelig realitet, hvis spektrale ressourcerne genbruges uden nogen begrænsning. Inter-celle indblanding forvaltning har været grundigt undersøgt i forbindelse med konventionelle trådløse netværk, og der er utallige åbne problemer relateret til netværk bestående af et varieret mix af base-stationer typer.

Denne Ph.D. afhandling omhandler nogle af disse uafklarede spørgsmål i forbindelse med LTE-Avanceret femtocells, med særlig fokus på tilfælde med femtoceller med privat adgnag. Mere specifikt, dette arbejde underholder ideen om at udnytte Carrier Aggregation (CA) rammerne indført i LTE-avanceret som en naturlig katalysator af simple men effektive frekvensdomæne interferenskontrol løsniniger. Carrier-baserede interferens koordinering er attraktiv, fordi den er bagudkompatibel og frem for alt, automatisk tilbyder intra-tier beskyttelse til både data og kontrol kanaler. Noget, der er i øjeblikket ikke er muligt. Kontrol kanal interferens management er kritisk, da forbedrede data SINR er ikke nyttigt, hvis UE kan ikke afkode kontrol kanaler.

[1]Translated by Klaus I. Pedersen of Nokia Siemens Networks, Aalborg, Denmark.

Undersøgelsen blev hovedsageligt gennemført med brug af Monte Carlo simuleringer. Til dette formål blev to semi-statisk systemniveau simulatorer udviklet med henblik på at give kvantitative resultater. Simple analytiske formuleringer give yderligere indsigt og guide den kvalitative vurdering. Undersøgelserne drejer sig Femtocell opererer i et dedikeret band.

Femtocells anses ofte for at vove sig ind i IEEE 802.11 (WiFi) eksklusive område. Derfor begynder arbejdet med en karakterisering af interferens. Parallelt hermed, sammenligning af en hypotetisk system implementering af Carrier Sense Multiple Access with Collision Avoidance (CSMA/CA) for LTE-Advanced. Resultaterne motivere de løsninger der søges i resten af denne afhandling.

Den foreslåede Autonomous Component Carrier Selection (ACCS) løsning udgør det væsentligste bidrag til denne Ph.D. afhandling. Kernen koncept og nogle af dets spinoffs er kognitiv radionetværk og elementer fra "Game" teorier. ACCS er en ikke-iterativ heuristisk løsning med brug af standard UE målinger kombineret med letvægts inter-node signalering, hvorved autonome beslutningstagere (femtocells) håndtere det komplekse kombinatorisk kanalen tildeling optimering problem. Vanskelighederne opstår, fordi den optimale fordeling af radioressourcer blandt femtocells afhænger af mange tidsvarierende faktorer. Det grundlæggende koncept er udviklet, og sammenlignet med både enklere og mere komplekse alternativer. Målet er at vurdere, hvor meget kompleksitet er forpligtet til at yde effektiv indblanding koordinering på en komponent luftfartsselskab niveau. Denne afhandling indeholder også en omfattende karakterisering af system performance for tilfælde med tidsvariende bursty trafik.

De endelige resultater giver stærke empiriske beviser for, at en konkret scheduler-uafhængig og fuldt distribueret carrier-baserede løsning er attraktiv. ACCS og dens generaliseringer er i stand til at begrænse inter-celle interferens og dermed styrkelse af brugernes performance med op til 500%, uden at gå på kompromis med gennemsnitlige og peak data-rater. Som eksempel kan nævnes at ACCS giver netværket evne til selv at tilpasse sig til variabel trafik og implementering betingelser.

Preface and Acknowledgments

This thesis is the result of a three-year research project carried out at the Radio Access Technology (RATE) section, Institute of Electronic Systems, Aalborg University, Denmark. The work was carried out in parallel with the mandatory courses and teaching/working obligations required to obtain the Ph.D. degree.

The research project has been completed under the supervision and guidance of Professor Preben E. Mogensen (Aalborg University, Nokia Siemens Networks, Aalborg, Denmark) and Senior Wireless Network Specialist Dr. Klaus I. Pedersen (Nokia Siemens Networks, Aalborg, Denmark). It has been co-financed by the Faculty of Engineering, Science and Medicine, Aalborg University, Nokia Siemens Networks, Aalborg and the Danish Agency for Science, Technology and Innovation - Forskeruddannelsesudvalget (FUU).

The thesis investigates system level technologies to make uncoordinated deployments, i.e. without prior network planning, of LTE-Advanced femtocells viable and efficient. The work covers both down- and uplinks; although the former admittedly receives more attention. The reader is expected to have a basic knowledge of system level aspects of LTE.

I would like to express my sincere gratitude to my supervisors for their guidance, encouragement as well as sharing their knowledge with an enthusiastic mood. Not to mention their efforts reviewing this monograph. Their feedback and comments have greatly improved this text.

I am also deeply thankful to Lisbeth Schiønning Larsen, the secretary of our group, for the friendly assistance with all sorts of administrative issues. I am truly amazed by her efficiency, which is only outmatched by her kindness. I would also like to thank Jytte Larsen, the secretary at Nokia Siemens Networks, for proofreading my papers and thesis.

My deepest gratitude goes to all my current and former colleagues in the RATE group and Nokia Siemens Networks for the pleasant and stimulating environment. I will not cite all of their names here not risk committing the sin of leaving anyone out by accident. The exceptions being Dr. István Kovács, Dr. Yuanye Wang, Dr. Gilberto Berardinelli for their invaluable contributions and promptness, as well as my good old friend, Gustavo Wagner, with whom I had countless brainstorming sessions. The environment my colleagues have helped to create in Aalborg is truly unique in many positive ways. The technical discussions, the fantastic travel experiences, the relaxed atmosphere, the multinational community have been truly unforgettable.

I ought to mention my friends back home as well as the new ones I met in Denmark; I hope our friendship endures. Finally, special thanks to my family in Brazil, I could not have asked for a better one.

I now dedicate these last lines to my wife Sandra, who has accompanied me for nearly 5 years now. During this PhD study we have been blessed with a precious treasure, our beloved son, Vinícius. The sleepless nights certainly made things tougher, but so much more rewarding.

Luis Guilherme Uzeda Garcia, December 2011

Contents

Chapter 1

Introduction

In recent years, mobile broadband data traffic has witnessed astronomical annual growth rates [1, 2]. The driving force behind this prodigious expansion is the voracious need and desire to be "online" everywhere and at anytime. On the technology side, 3.5G High Speed Packet Access (HSPA) and 3.9G Long Term Evolution (LTE) systems [3–6] have made mobile broadband a reality. Consumers are now offered a synergistic combination of portable devices with high data transfer capabilities – smartphones, tablets, USB-dongles – and innumerous Internet-based applications such as social networks, video-sharing websites, just to mention a few.

Mobile traffic is still growing fast and there is a crying need for scalable wireless broadband communication solutions, especially in nomadic environments. A recent analysis indicates that up to 70% of the data usage is nomadic, i.e. generated at home, in schools or at work, whereas only 30% of the usage is truly mobile [7]. In 2010, according to [2], 31% percent of global smartphone traffic was offloaded onto the fixed network through Wireless Local Area Networks (WLANs) based either on the IEEE 802.11 standards [8] or low-power user-deployed cellular base-stations also known as femtocells [9]. That corresponds to 14.3 petabytes of data traffic being offloaded onto the fixed network each month. The same source projects that the average smartphone will generate 1.3 GB of traffic per month in 2015, a 16-fold increase over the 2010 average of 79 MB per month. By 2015, it is forecasted that over 800 million terabytes (800

exabytes) of mobile data traffic will be offloaded via local wireless solutions. The foregoing figures unquestionably attest the demand for complementary local area networks driven by an unrelenting desire for inexpensive yet efficient wireless broadband solutions allowing for improved indoor coverage, user experience and better cost/performance ratios as pointed in [10].

LTE Release 10, popularly known as LTE-Advanced [11], is an evolution of LTE which includes all the features of previous releases and adds several new ones – e.g. Carrier Aggregation (CA) [12] and improved support for heterogeneous deployments – in order to meet and surpass the targets set for future International Mobile Telecommunications-Advanced (IMT-A) [13, 14] 4G systems. Among such targets, is the ability to provide peak data rates of 1 Gbps for low-mobility scenarios such as nomadic/local wireless access.

While conventional cellular networks have been extensively investigated; there are numerous open problems related to femtocells and Heterogeneous Networks (HetNets) in general [9, 15–17]. This Ph.D. thesis addresses some of the outstanding issues, chiefly in the context of LTE-Advanced femtocells [9], paying special attention to the nuances of interference footprint in local area deployments. Owing to the *ad-hoc* nature of femtocell deployments, if resources are allowed be reused without any restriction, severe inter-cell interference will be an inevitable reality as future femtocell deployments become denser. A situation, in many ways, similar to existing WiFi networks [18]. Most notably, this project revolves around the development of self-adjusting autonomous schemes to mitigate inter-cell interference among femtocells operating in a dedicated band, i.e. macro cell and femtocell users are made orthogonal through bandwidth splitting.

The rest of this chapter is organized as follows. A short description of LTE-Advanced is given in Section 1.1. Section 1.2 discusses the need for femtocells in the context of current mobile communication networks, thus motivating the work reported in this thesis. Subsequently, Section 1.3 delineates the problem and defines the objectives of this Ph.D. project. The research methodology is described in Section 1.4; while Section 1.5 summarizes the publications derived from this Ph.D study. Finally, Section 1.6 provides an outline of the structure of the thesis highlighting the main contributions.

1.1 A Primer on LTE-Advanced

Long Term Evolution (LTE) is a wireless technology standardized by Third Generation Partnership Project (3GPP) and designed to support broadband Internet access via cell phones and handheld devices. The first version of LTE

was completed in March 2009 as part of 3GPP Release-8 (Rel-8) [3]. LTE offers flexible bandwidth options ranging from 1.4 MHz to 20 MHz and employs Orthogonal Frequency Division Multiple Access (OFDMA) and Single-carrier Frequency Division Multiple Access (SC-FDMA) as multiple access schemes in the down- and uplink respectively [3]. The 20 MHz bandwith can provide theoretic peak data rates exceeding 300 Mbit/s in the downlink if 4x4 Multiple Input Multiple Output (MIMO) [19,20] is used. The uplink data rates are limited to 75 Mbit/s because MIMO support is restricted to single layer transmissions [3, 5].

However, LTE Rel-8 does not meet the IMT-A requirements for 4G systems as defined by the International Telecommunications Union - Radio Communication Sector (ITU-R) such as peak data rates up to 1 Gbit/s [13, 14]. In March 2008, 3GPP started a new study item in order to further develop LTE towards LTE-Advanced targeting the IMT-A requirements [21, 22]. The LTE-Advanced study item was closed in March 2010. The outcome was a set of new radio features, which are now part of 3GPP Rel-10. The main technology components include: Carrier Aggregation (CA), MIMO evolution up to 8×8 and 4×4 in the Downlink (DL) and Uplink (UL) respectively, relay nodes and heterogeneous networks [23].

The remainder of this section gives an overview of LTE-Advanced. The discussion is primarily concerned with the technology components that impact this work. The interested reader can find detailed descriptions in [3, 11, 23, 24].

1.1.1 Heterogeneous Networks

A Heterogeneous Network (HetNet) is the outcome of a deployment strategy consisting of two or more cellular layers [25]. Therefore the resulting network comprises a diverse mix of base-stations types such as macro-, micro-, pico- and more recently femtocells. Although HetNets are not a radically new concept, there is much untapped potential stemming from new network topologies. Intuitively, since the demand for capacity is expected to vary drastically from rural areas to dense urban regions, cell areas should be inversely proportional to the traffic demand.

LTE-Advanced includes features that improve the support for heterogeneous deployments such as Enhanced Inter-Cell Interference Coordination (eICIC). A summary of possible solutions considered in 3GPP can be found in [26, 27]. As discussed in Section 1.2, this work is particularly interested in the latest addition to the base-station family, namely femtocells.

1.1.2 Carrier Aggregation

Carrier Aggregation (CA) is one of the distinguishing features of upcoming 4G systems. In fact, CA is the agreed method within 3GPP to achieve bandwidths up to 100 MHz in LTE-Advanced. CA is designed to be *backward compatible*, meaning that legacy Rel-8 and Rel-9 users should still be able to co-exist with LTE-Advanced on at least part of the total bandwidth. Thus, each individual spectrum chunk, denoted Component Carrier (CC), inherits the core physical layer design and numerology from LTE Rel-8.

The maximum supported bandwidth for LTE-Advanced of 100 MHz can be achieved via CA of 5 CCs of 20 MHz. However, only those User Equipments (UEs) supporting CA will be able to access all CCs simultaneously. Legacy UEs remain restricted to a single CC. The bandwidth of each CC follows those already supported by Rel-8, namely 1.4, 3, 5, 10, 15, and 20 MHz. The aggregated CCs may be either contiguous or non-contiguous, although the latter is more challenging from an Radio Frequency (RF) perspective. Moreover, nothing prevents the the aggregated CCs from having different bandwidths.

In practice, a phased approach is being used. New bandwidth combinations for interband CA are being agreed in standardization to cover the most interesting cases for operators around the world. To speed up the standardization work, different timescales are set for DL and UL. Therefore Rel-10 will only support interband CA in DL and for a limited number of bandwidth combinations, while full support for non-contiguous CA will come with Rel-11. However, all the related signaling procedures for CA in Rel-10 are standardized such that CA over other bands for both DL and UL can be added in future releases by specifying the RF requirements for the corresponding bandwidth combinations.

In order to avoid confusion, it is important to stress the distinction between CA on network and UE levels. The former is defined by the number of DL and UL CCs offered by the network in a cell. The latter is defined by the number of DL and UL CCs configured for a UE. As explained in [12], each served UE must be assigned a single primary serving CC – denoted *Pcell* – and possibly one or more additional serving CCs, called secondary serving cells (*SCells*) depending on its quality of service (QoS) requirements.

More importantly, with CA, it is possible to schedule UEs on multiple CCs independently. Each of which may exhibit different loads and radio channel characteristics such as interference levels. It then follows naturally, that CA could be employed as a new and promising instrument of Inter-Cell Interference Coordination (ICIC) on a CC level. Hence, due to the potential synergy, HetNets and CA are often discussed together in the literature.

1.1.3 The Access Network

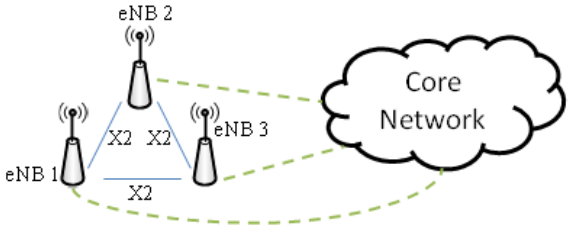

Fig. 1.1: Simplified representation of the access network of LTE.

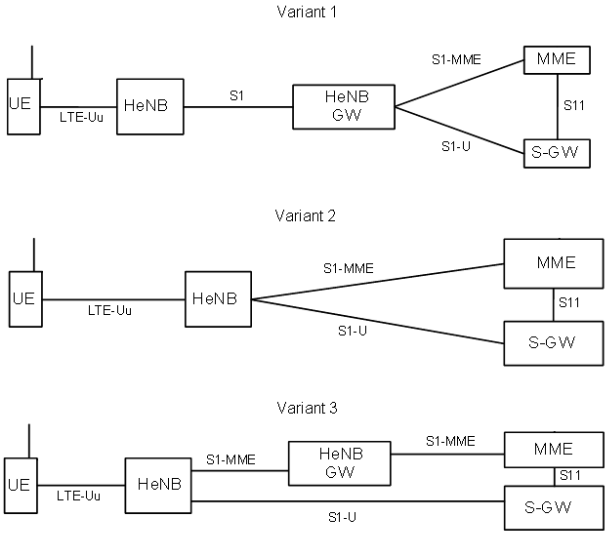

Fig. 1.2: The three agreed architectures in 3GPP for LTE femtocells. With a HeNB-GW (top), without a HeNB-GW (center) and with a HeNB-GW for the control plane (bottom). Adapted from [28].

LTE replaces the circuit-switched architecture by the so called Evolved Packet Core (EPC), an all-IP packet-switched architecture with a separation between control and user planes [3]. Additionally, as opposed to Wideband Code Division Multiple Access (WCDMA) [29], LTE is based on flat radio access network architecture without a centralized network controller [3]. As a result, the access network of LTE consists of collection of base stations, enhanced NodeBs (eNBs) in 3GPP parlance. Typically, eNBs are inter-connected by means of a standardized interface known as X2 as depicted in Fig. 1.1. Additionally, there is a set of S1 interfaces used to connect the eNBs to the EPC.

In the specific case of femtocells (See Section 1.2.1), three different architectures have been agreed within 3GPP. These variants shown in Fig. 1.2 differ with respect to the absence and functionalities of an optional node known as a Home eNB Gateway (HeNB-GW). When deployed, the HeNB-GW acts as an S1 concentrator for the control plane (optionally for the user plane as well), thus offering support for a large number of femtocells in a scalable manner. Readers can find a detailed description of architecture aspects related to femtocells in [28]. Even though LTE-Advanced introduces no new elements to the access network, the architecture inherited from LTE makes fully distributed algorithms, potentially relying on limited eNB to eNB communication, specially appealing. For those interested, [26] is suggested for further reading.

1.2 Why Go Local: Motivation

Despite the tremendous advances achieved by the mobile communications industry, the evolution needs to continue due to commercial as well as technical reasons. A prosaic yet compelling driver of incessant evolution is the end-user's expectation to have the same online experience irrespective of the access technology. In simple terms, from a utopian consumer's perspective, wireless and "wired" technologies should be indistinguishable in terms of delays and data rates, especially in nomadic environments.

This is a daunting challenge facing the wireless community. First and foremost, because, in contrast to the "wired" communication world, the designers of wireless systems cannot simply create more bandwidth by endlessly adding new physical resources. In mobile communication's jargon, resources often mean radio spectrum, which is a finite, scarce, extremely expensive and tightly regulated commodity. Complicating matters further is the fact that current cellular systems come very close to the fundamental limits imposed by the laws of physics in terms of *spectral efficiency per link* (bit/s/Hz). Another practical challenge is the fact that the current network deployment strategy based on macro cells becomes less economically viable for increasing data rates as pointed out in [30,31].

Despite the aforementioned major technical and financial hurdles, it is envisioned that the ability to provide peak data rates of 1 Gbps in Local Area Networks (LANs) will be instrumental to the commercial success of future IMT-A [13, 14] systems. Therefore solutions must be engineered. Increasing the *spectral efficiency per unit area*, taking the cellular concept to the extreme seems a promising direction. In this light, low-power base stations have recently reemerged as a promising technology component and many believe that increasingly smaller cells will definitely be one of the next steps in the evolutionary

path of cellular systems. The rationale is simple, smaller cells bring transmitters and receivers closer to each other thus yielding more spectrally efficient links. They also imply denser networks in order to cover the same area, bringing about exhaustive spatial reuse and therefore leading to the promise of higher spectral efficiency per unit area.

1.2.1 Femtocells

Femtocells are a major step towards network densification. They are miniature user-deployed and controlled base stations, compact enough to find a place in our homes and offices. Also known as Femto Access Point (FAP) or Home enhanced NodeBs (HeNBs), they rely on existing third party IP-based backhaul and offer significantly higher capacity per area when compared to traditional macro cells. As a consequence, femtocells are one of the candidates for high data rate provisioning in local areas, such as residences, apartment complexes, business offices and outdoor hotspot scenarios. Femtocells also represent an interesting alternative to provide last mile coverage in rural areas where the deployment of larger cells might be cost-inefficient.

In principle, LTE femtocells can use all bands defined by 3GPP and do not require dedicated frequency spectrum. However, it is up to each network operator to choose the deployment model that best suits its needs. Another advantage, especially when compared to WiFi is the seamless integration with the cellular network; the user never leaves the cellular domain. Femtocells can be configured to operate under open or closed access. The term Closed Subscriber Group (CSG) is commonly used to refer to cases when access to the FAP is limited to a small set of terminals explicitly approved by the femtocell owner. Conversely, open access, hereafter denoted as Open Subscriber Group (OSG) mode allows an arbitrary nearby cellular user to use the femtocell like any other ordinary cell. Unfortunately, the benefits are not without new challenges as discussed next.

1.2.2 Associated Challenges

The installation of many low-power base stations also poses new challenges in terms of interference management and efficient system operation [9, 15]. The latter is especially true for local area deployments, where end users start installing home base stations without any prior network planning, and without carefully considering where other people in the immediate surroundings have installed other home base stations.

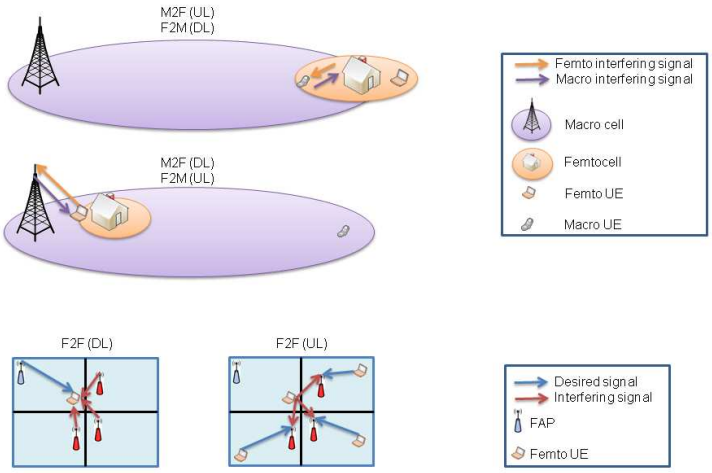

Fig. 1.3: Examples of severe inter-cell interference situations in a co-channel heterogeneous network assuming close access. Cross-tier (top and middle) and intra-tier (bottom).

The level of inter-cell interference in the six possible paths depicted in Fig. 1.3 – femto to macro (F2M), macro to femto (M2F), and femto to femto (F2F) (UL and DL)– depends largely on whether cells share spectrum, causing co-channel interference, and whether access is open or closed.

OSG femtocells clearly ameliorates the radio interference problem arising from the pseudo-chaotic placement of femtocells, but it also raises additional privacy, security, financial and even legal[1] issues [9, 30, 31]. Suddenly users might find themselves sharing their femtocell resources with uninvited passerby, possibly overstraining the backhaul. In OSG mode the main beneficiary is the network operator.

A femtocell owner would naturally prefer a CSG femtocell. Nonetheless, this access mode has the potential to wreak havoc on the nicely planned wide are (macro) cellular deployment, because all six interference paths come into play in co-channel setups. Strong radio interference and ultimately coverage holes may arise if the network topology is unfavorable e.g. a non-registered UE comes arbitrarily close to a femto base-station located near the edge of a macro cell.

[1] The licence conditions of most fixed private subscriber lines (e.g. ADSL) only permit its usage for the household.

This is particularly disturbing because the topology of the network is completely out of the operator's control [32].

The foregoing discussion leads to another key aspect challenging the success of femtocells: spectrum availability. The safest approach relies on separate spectrum for femtocells and large area macro cells. Dedicated bands are an effective way to prevent interference, narrowing the interference paths down to just the femto-to-femto interference paths. The disadvantage, however, is that it may lead to inefficient spectrum utilization. Moreover, many operators simply do not have a separate spectrum available for femtocells in urban areas.

As a result, most ongoing efforts focus on solutions to control the cross-tier (macro-femto) interference in case of co-channel deployments [15–17,33,34] and the references therein. An interesting hybrid approach stemming from the industry front based on the notion of a escape carrier, i.e. a femto-free carrier, is introduced in [35]. A summary of possible solutions considered in 3GPP can be found in [36]. Yet severe interference among femtocells will be an inevitable reality as future femtocell deployments become denser, similarly to existing WiFi networks [18]. Therefore new, practical, scalable and future-proof alternatives must be sought.

1.3 Scope and Objectives

As stated earlier, most of the really bit-rate-hungry traffic is expected to be generated indoors [2]. Currently, there are two competing technologies offering high data rates and offloading capabilities in local area scenarios, namely femtocells and the IEEE 802.11 (WiFi) family of standards [8,37]. The former is fully transparent to the mobile data user, i.e UEs never leave the cellular network. The latter is the current *de facto* standard for wireless local area communication and operates on unlicensed spectrum. Although this work concentrates on femtocells, there are lessons to be learned from WiFi, because both technologies face similar issues relating to access methods, backhaul,and deployment scenarios.

The random placement of femtocells alongside the foreseen CSG access mode is bound to result in chaotic inter-cell interference. While WiFi uses the Medium Access Control (MAC) protocol to ensure that its short-range links do not suffer from interference, cellular systems, especially those supporting universal frequency reuse, e.g. LTE, are inherently interference-limited. Because the complementary co-channel cross-tier (macro-femto) interference is already receiving significant attention [15–17, 33, 34], this project concentrates on the inter-cell interference among femtocells operating in a dedicated band, i.e. macro cell

and femtocell users are made orthogonal through bandwidth splitting.

An alternative and potentially more interesting interpretation is that femtocells operate in a license-exempt band [38] forming the basis of an an envisioned "Femto Commons" spectrum. In this case, femtocells would cater for additional capacity and complementary coverage in indoor/nomadic environments, thus seamlessly offloading the macro cells. The (ideally) globally license-exempt[2] (shared by multiple operators and private users deploying femtocells) would overcome the operators' potential spectrum shortage challenge.

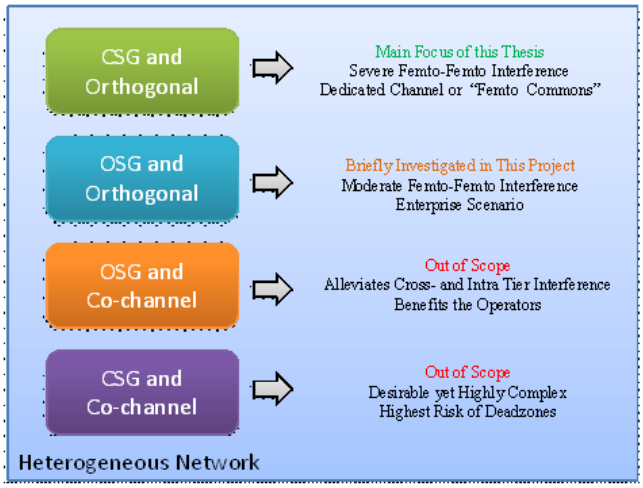

Fig. 1.4: Scope of this Thesis.

Such multi-operator approach would definitely call for new and scalable self-adjusting interference management techniques. Yet, finding the truly optimal division of frequency resources between low power base stations in a highly dynamic and partly chaotic environment is, in general, an iterative, non-linear, non-convex NP-hard optimization problem [40]. The difficulties arise because the optimal sharing of radio resources amongst femtocells depends on many time-varying factors such as the network topology, load, mobility and traffic conditions, etc.

Instead of striving for strict optimality, the fundamental problem addressed in this dissertation, whose scope is depicted in Fig. 1.4, is the design of practical, non-iterative and self-adjusting Component Carrier (CC) selection mechanisms to deal with interference in future LTE-Advanced femtocell deployments. This

[2] This spectrum arrangement differs from the unlicensed spectrum where WiFi operates in that the latter is based on coexistence and in the former is a form of spectrum sharing among equals [38, 39].

choice for simplicity is justified by several factors.

First, Carrier Aggregation (CA) is a crucial constituent of LTE-Advanced. However, because traffic requirements vary (on several time-scales), it is unlikely that all cells will continuously require all available CCs; particularly when one considers the much lower number of user attached to each femtocell. As a result CA can be exploited as a natural enabler of simple yet effective frequency domain interference management schemes, automatically offering protection to both data and control channels even under CSG mode.

Second, depending on the application it might be preferable to exchange optimality for inertia, i.e. resistance to reconfigurations. This can be easily understood when one considers that user-controlled femtocells can (re-)appear at anytime and anywhere. As a result, extremely dynamic and fine-grained iterative algorithms seeking optimality could lead to uncontrolled/unpredictable reconfigurations posing several practical problems that cannot be dismissed.

Cost also plays an important role. If a solution implies outrageous costs, nobody will use it. This clearly constrains the complexity of the algorithms that can be implemented on the limited hardware. In this respect, initial considerations in [9, 41] had already suggested that simple interference avoidance rather than suppression techniques are likely to form the basis of a sensible strategy to ensure high performing uncoordinated local area deployments. Granting cells the ability to autonomously "learn" what sensible means in the context of emerging local area deployments is the key aspect here. These self- scaling and -adjusting traits lead to a new autonomic paradigm with fully "robotic" base stations with the potential to reduce operational expenditures as highlighted in [42, 43].

To sum up, in view of the previous discussion, the four objectives of this thesis can be stated as:

- Characterize the interference footprint of local area cellular deployments.
- Investigate the suitability of well-established WLAN solutions in the context of cellular systems.
- Devise scheduler-independent, practical and fully distributed schemes that mitigate inter-cell interference without compromising average and peak data-rates.
- Identify the trade-offs and assess how much complexity is effectively required to provide efficient interference coordination on a CC level for future LTE-Advanced femtocell deployments.

Finally, the preceding goals will be pursued in light of the following design guidelines:

- Keep it simple
- Look for a good design; it need not be perfect
- Think about scalability
- Expect heterogeneity
- Exploit modularity
- Avoid static options and parameters

One might ask why. Simply, put these principles have proven to be fruitful in designing the grandest distributed system of all, the Internet. The interested reader can find a truly insightful discussion in the document that describes the architectural principles of the Internet [44]. In Chapter 6, a few final remarks examine how these guidelines came into being in the proposed solution in an attempt to put matters into perspetive.

1.4 Scientific Methodology

This section begins with a delineation of the process guiding the investigations during this Ph.D. project. The discussion proceeds with a critical analysis of the pros and cons of the selected assessment methodology, namely numerical simulations. The section then continues with a brief description of the simulation scenario followed by short summary of the tools employed to present the results.

The following steps provide a high-level overview of the scientific methodology. The nested structure reflects to some extent the iterative nature of the project; meaning that literature review and the final dissemination marked the beginning and the end of a full cycle, thus encapsulating the other activities.

- Literature review, brainstorming and problem delineation.
  - Research and development of practical solutions aiming at exploiting the nature of the problem being tackled as well as addressing issues not solved by prior art.

  - Intellectual Property Rights (IPR) considerations whenever applicable.
  - Analytical modeling whenever possible followed by qualitative analysis of the expected results.
  - Modeling, software implementation, testing and quantitative evaluation of the solutions/algorithms via system level simulations.
- Dissemination of knowledge through conference, journal papers or internal deliverables.

1.4.1 Why Simulations?

A cellular network is a complex system involving a phenomenal number of dynamic interactions. Consequently, a complete analytical treatment of the subject quickly becomes intractable as more elements and parameters are incorporated into the analysis.

Compounding the difficulties is the long-standing lack of a general capacity theory for wireless networks. In other words, with a handful of exceptions there are no general information-theoretic results on the Shannon capacity [45] of cellular systems. See [46] for an insightful discussion on the main obstacles hindering theoretic advancements. Recent progress in the field of stochastic geometry and theory of random geometric graphs [47] were able to shed some light on this cellular conundrum and are expected to become increasingly relevant over the next decades. However, it is undisputed that much more work is required. The most tractable results from stochastic geometry tend to rely on a few assumptions that may not accurately hold in practice as pointed out in [48].

Therefore, owing to the aforementioned analytical impediments, a choice for system level simulations has been made in order to characterize the performance of cellular networks in environments similar to those faced nowadays by IEEE 802.11 networks.

1.4.2 Precision and Accuracy

A substantial amount of time and energy was put into writing reliable simulators. Reliability is employed here in the sense that preliminary results were reproduced, calibrated and validated using public results in the literature as well as similar tools written by colleagues and former Ph.D. students. Additionally, each individual module was meticulously tested during the development phase.

The code also contains error treatment and several runtime checks to ensure that the integrated system would remain logically consistent. Particularly, the so-called 3GPP dense urban dual stripe model outlined in Section 1.4.3 was later implemented in a proprietary system level simulator fully aligned with LTE specifications, yielding very similar G-factor[3] distributions. While that attests the precision of the simulator, it says little about its accuracy.

The downside of simulators is that they are only as good as the models and assumptions that underpin them. In that respect, the simulation methodology and assumptions follow those defined in [22] for the evaluation of femtocells. The interested reader can find detailed descriptions of the underlying models in Appendix D.

The foregoing discussion on accuracy and precision of the results is concluded by claiming that performance figures included in this thesis should be interpreted as precise and accurate representatives of the relative trends; nevertheless the absolute values under conditions of actual operation could be widely divergent from those presented herein. For example, the impact of higher layers, e.g. Transmission Control Protocol (TCP) mechanisms such as flow and congestion control [49], are not modeled. Ultimately, an accurate performance evaluation of a complex cellular network cannot be carried out by means of either purely analytical or simulative work; it usually requires complementary field-tests.

1.4.3 Deployment Scenarios

During the early stages of this Ph.D., several scenarios were considered as representatives of the most common deployment environments for LANs, namely the indoor office and home scenarios. Both stemming from WINNER II channel and path loss models [50]. However, for the sake of consistency and in order to keep the computational effort at reasonable level, all results included in this thesis assume the simulation scenario and indoor path loss modeling defined by 3GPP in [22] for the evaluation of femtocells[4]. The scenario consists of two buildings, each with two stripes of apartments, each stripe having 10 apartments per floor. There is a 10m wide street between the two buildings. The scenario is illustrated in Fig. 1.5. Both femtocells and UEs are dropped uniformly at indoor random positions. To simulate the realistic case that an apartment may

[3] G-factor is the ratio of the total received wideband signal power and the interference plus noise power at the receiver side. It includes the effects of path loss and shadow fading, but is average over fast fading. It is equivalent to the average wideband Signal to Interference plus Noise Ratio (SINR) in a single antenna system.

[4] Results employing the WINNER model were published in the contributions 1-4 outlined in Section 1.5. The conclusions derived from both models are in agreement.

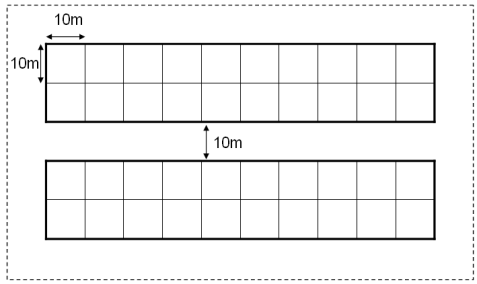

Fig. 1.5: Top view of the deployment scenario. Multiple floors are considered.

not have a femtocell, the "*deployment ratio*" parameter determines whether a femtocell is deployed or not. The deployment ratio can vary from 0 to 1.0. Detailed equations summarizing the model are reproduced in Appendix D for convenience.

1.4.4 Key Performance Indicators

Owing to the simulation based approach, a very large amount of data was generated during the course of this work. Summarizing and depicting this data in a concise manner is extremely relevant. In this thesis, results are summarized, displayed and compared using tools from descriptive statistics.

The upcoming chapters shall often resort to Empirical Cumulative Distribution Functions (ECDFs). The ECDF is an estimate of the underlying Cumulative Distribution Function (CDF) of the data samples. Given the data set $x_1, \ldots, x_n$, its ECDF $F(x)$ is given by

$$F(x) = \frac{1}{n} \sum_{i=1}^{n} 1\{x_i \leq x\},$$

where $1\{.\}$ denotes the indicator function. So that $F(x)$ is the proportion of data samples that do not exceed x. For the sake of brevity, the CDF term is used throughout this thesis; acknowledging that the true CDF is not known unless specifically stated otherwise. Additionally, instead of considering the entire CDF, this work make intensive use of the arithmetic mean as a measure of the central tendency as well as p percentiles. A p percentile of a distribution is the value P under which $p\%$ and above which $(100-p)\%$ of the observed samples lie. The following key performance indicators are extensively used throughout this thesis:

1. *Average user throughput:* This is the arithmetic mean of the user throughput averaged over all active radio frames for all simulated users.
2. *Outage user throughput:* This is the user throughput, corresponding to the 5%-tile taken from the user throughput CDF. Therefore the 5% worst users achieve equal or lower performance.
3. *Peak user throughput:* the achieved user throughput for the 95%-tile taken from the user throughput CDF. The 5% best users achieve higher – if Modulation and Coding Scheme (MCS) allows – or at least equal throughput values.

All user perceived throughput figures are calculated during active periods. A user is considered to be active from the moment the first packet of a session arrives until the reception of the last packet of the session. In full buffer simulations, all users are continuously active and the instantaneous throughput is considered instead. Other metrics are briefly introduced before their first appearance.

1.5 Publications

The following publications have been authored or co-authored during my Ph.D. studies. They are listed in chronological order of publication, which can differ from the actual order of submission.

- Luis G. U. Garcia, Yuanye Wang, Simone Frattasi, Nicola Marchetti, Preben Mogensen and Klaus Pedersen, "Comparison of Spectrum Sharing Techniques for IMT-A Systems in Local Area Networks," Vehicular Technology Conference. VTC-Spring 2009. IEEE 69th, Barcelona, 26-29 April 2009.
- Yuanye Wang, Sanjay Kumar, Luis G. U. Garcia, Klaus Pedersen, István. Kovács, Simone Frattasi, Nicola Marchetti and Preben Mogensen, "Fixed Frequency Reuse for LTE-Advanced Systems in Local Area Scenarios," Vehicular Technology Conference. VTC-Spring 2009. IEEE 69th, Barcelona, 26-29 April 2009.
- Luis G. U. Garcia, Klaus Pedersen and Preben Mogensen, "Autonomous Component Carrier Selection for Local Area Uncoordinated Deployment of LTE-Advanced," Vehicular Technology Conference. VTC-Fall 2009. IEEE 70th, Anchorage, 20-23 Sept. 2009.

- Luis G. U. Garcia, Klaus Pedersen and Preben Mogensen, "Autonomous component carrier selection: interference management in local area environments for LTE-advanced," Communications Magazine, IEEE , vol.47, no.9, pp.110-116, September 2009.

- Luis G. U. Garcia, Klaus Pedersen and Preben Mogensen,"" On Open versus Closed LTE-Advanced Femtocells and Dynamic Interference Coordination," Wireless Communications and Networking Conference (WCNC), 2010. IEEE, Sydney, 18-21 April 2010.

- Luis G. U. Garcia, Klaus Pedersen and Preben Mogensen,"Uplink Performance of Dynamic Interference Coordination under Fractional Power Control for LTE-Advanced Femtocells," Vehicular Technology Conference. VTC-Fall 2010. IEEE 72nd, Ottawa, 6-9 Sept. 2010

- Gustavo W. O. Costa, Luis G. U. Garcia, Andrea F. Cattoni, Klaus Pedersen and Preben Mogensen, "Self-Organizing Coalitions for Conflict Evaluation and Resolution in Femtocells," COST IC0902 Year 1 Annual Workshop - Joint workshop with COST2100, Italy, Bologna, November 2010

- Luis G. U. Garcia, Gustavo W. O. Costa, Andrea F. Cattoni, Klaus Pedersen and Preben Mogensen, "Self-Organizing Coalitions for Conflict Evaluation and Resolution in Femtocells," GLOBECOM 2010. IEEE Global Telecommunications Conference, Miami, 6-10 Dec. 2010

- Klaus Pedersen, Luis G. U. Garcia, Hung Nguyen, Yuanye Wang, Frank Frederiksen and Claudio Rosa, "Carrier aggregation for LTE-Advanced: functionality and performance aspects," Communications Magazine, IEEE, vol.49, no.6, pp.89-95, June 2011.

- Fernando Sanchez-Moya, Juan Villalba-Espinosa, Luis G. U. Garcia, Klaus Pedersen and Preben Mogensen, "On the Impact of Explicit Uplink Information on Autonomous Component Carrier Selection for LTE-A Femtocells," Vehicular Technology Conference. VTC-Spring 2011. IEEE 73rd, Budapest, 15-18 May 2011.

- Luis G. U. Garcia, Fernando Sanchez-Moya, Juan Villalba-Espinosa, Klaus Pedersen and Preben Mogensen, "Enhanced Uplink Carrier Aggregation for LTE-Advanced Femtocells," Vehicular Technology Conference. VTC-Fall 2011. IEEE 74rd, San Francisco, 5-8 Sept. 2011.

- Gustavo W. O. Costa, Luis G. U. Garcia, Andrea F. Cattoni, Klaus Pedersen and Preben Mogensen, "Dynamic Spectrum Sharing in Femtocells: a Comparison of Selfish versus Altruistic Strategies,"Vehicular Technology Conference. VTC-Fall 2011. IEEE 74rd, San Francisco, 5-8 Sept. 2011.

- Gustavo W. O. Costa, Luis G. U. Garcia, Andrea F. Cattoni, Klaus Pedersen and Preben Mogensen, "Comparison of Selfish versus Altruistic Strategies in Dynamic Spectrum Allocation for Cognitive Femtocells," Second International Workshop of the COST Action IC 0902 on Cognitive Radio and Networking for Cooperative Coexistence of Heterogeneous Wireless Networks, Barcelona, Oct. 2011.
- Luis G. U. Garcia, Gustavo W. O. Costa, Andrea F. Cattoni, Klaus Pedersen and Preben Mogensen, "Self-Organizing Coalition formation algorithm and policies," COST ACTION IC0902 Newsletter, Oct. 2011.
- Luis G. U. Garcia, Klaus Pedersen and Preben Mogensen, "Voice-Centric LTE Femtocells and Improper Graph Colorings," *to appear in IEEE VTC-Spring 2012*, May 2012.
- Luis G. U. Garcia, István. Kovács, Klaus Pedersen, Gustavo W. O. Costa and Preben Mogensen, "Autonomous Component Carrier Selection for 4G Femtocells – A fresh look at an old problem –," *to appear on the IEEE Journal On Selected Areas In Communications.*

1.6 Thesis Outline and Contributions

The thesis consists of 6 chapters and 5 appendices. This first chapter has set the framework of the study carried out in this project and explained the pursued goals. A general overview of the subsequent chapters is presented here; highlighting the main contributions in each chapter. Additionally, Fig. 1.6 presents a thesis map including some contextual information. The dashed circles depict closely related yet not specifically addressed topics.

- Chapter 2: Resource Sharing in Wireless Local Area Networks — This chapter is partially dedicated to a brief analysis of the fundamental concepts behind resource sharing and its inherent tradeoffs. The following conceptual question is also addressed: "Should contention based techniques be considered as a simple and inherently distributed spectrum sharing option for future femtocell deployments?". The performance of a hypothetical hybrid system employing Carrier Sense Multiple Access with Collision Avoidance (CSMA/CA) in an LTE-Advanced framework is compared with that of an ordinary LTE-Advanced system employing static frequent reuse schemes providing insightful benchmarking results.
- Chapter 3: Autonomous Component Carrier Selection — This chapter lays the foundation for the subsequent ones. The work proposes a fully

distributed and scalable solution based on minimal information exchange and negotiation between base stations where each individual FAP autonomously makes decisions without involving any centralized network control. The latter is considered to be the most attractive solution, especially for femtocells due to the expected large number of cells. The scheme mainly relies on measurements collected as a by-product of normal system operation, producing useful statistics for interference conditions in the network. In this way, each base station gathers knowledge about the surrounding environment and uses this information in the decision making process.

- Chapter 4: Applicability to The Uplink of LTE-Advanced — Addresses the UL particularities, such as the use of Fractional Power Control (FPC). This chapter provides qualitative and quantitative answers to questions such as what is the impact of FPC on femtocells and how to best configure it. In addition, it demonstrates that ACCS is equally attractive and applicable to the uplink even though most decisions are based on UE DL measurements. Furthermore, FPC information is incorporated and exploited by the carrier selection procedure. In its most general formulation, the method facilitates UE-specific component carrier configurations in femtocells.

- Chapter 5: Variable Traffic and Generalized ACCS — The main contribution of this chapter (G-ACCS) represents one step towards cognitive radio networks. The proposal extends the framework introduced earlier. A capacity-based algorithm is introduced to solve the CC selection problem. The proposed solution requires no explicit thresholds and employs power spectral density variations in a proactive fashion. This chapter also presents a systematic evaluation of the effects of inter-cell interference on the overall performance of femtocells through detailed system level simulations. Various CA based solutions – in increasing order of complexity – are evaluated under time-varying traffic conditions. The work focuses on the downlink and pays special attention to the often overlooked case of random session arrivals.

- Chapter 6: Conclusions and Future Work — Revisits the the overall study and formulates the recommendations for the deployment of future femtocells. Interesting topics for future investigations are also considered.

In order to support the work and provide further details, the following 5 appendices are included:

- Appendix A: Self-Organizing Coalitions for Conflict Evaluation and Resolution (SOCCER) paper reprints – despite being included here as an

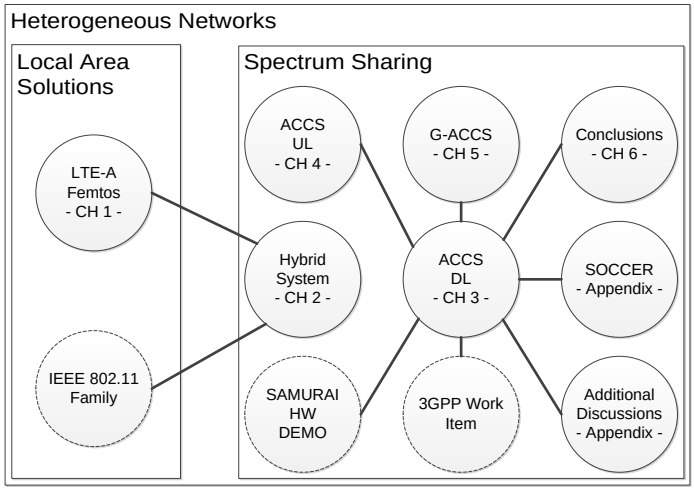

Fig. 1.6: Thesis map and contextualization.

appendix rather than being part of the main body of the thesis, (SOCCER) is one of the main contributions of this thesis due to its simplicity and efficacy. The algorithm builds on the framework introduced in Chapter 3 and can operate either as an add-on to Autonomous Component Carrier Selection (ACCS) or as an stand-alone method.

- Appendix B: A series of brief discussions examining complementary aspects related to the ACCS framework. The topics are examined separately, because they have not yet reached the same level of maturity as the other constituents of the ACCS framework. Among other subjects, the considerations pertain to timing aspects related to the implementation of ACCS and reactive recovery actions.

- Appendix C: On Open versus Closed LTE-Advanced Femtocells and Dynamic Interference Coordination – A paper reprint containing supplementary results and discussions about the differences between CSG and OSG deployments.

- Appendix D: Detailed simulation assumptions – The simulation assumptions as well as both simulators developed during this project are described carefully in this appendix.

- Appendix E: Mathematical functions – supporting material containing formal definitions of some of the functions employed in this dissertation.

1.6.1 Summary of Contributions

As a brief summary: during this Ph.D. project two IEEE Communications Magazine papers were published, while a third magazine paper on spectrum sharing and game theory has been written in collaboration with colleagues from Aalborg University. One article has been recently accepted and will soon appear on a special issue on femtocells of the IEEE Journal on Selected Areas in Communications (JSAC). Additionally, 11 conference papers have been submitted for publication, 9 of which have already been published at the time of writing; 12 patent applications have been submitted through Nokia Siemens Networks' patent office, while 2 more invention reports are being drafted. A proof-of-concept of some of the findings are being implemented in a hardware test bed by other Ph.D. colleagues within the European Union project Spectrum Aggregation and Multi-User MIMO: Real-World Impact (SAMURAI).

Other than the publications, one CSMA/CA based simulator was developed to carry out the preliminary WLAN investigations. A second tool for local area LTE-Advanced system was written. Both tools were developed in collaboration with a colleague from Aalborg University. The second tool has been used and further developed by several Ph.D. and master students, two of which were under my direct supervision. It also formed the basis of a third Nokia Siemens Networks proprietary simulator used in SAMURAI and for further investigation of carrier based ICIC concepts. Moreover several Nokia Siemens Networks internal deliverables and 3GPP contributions have been written. In that respect a Work Item (WI) has been recently created within 3GPP in response to an initial proposal by Nokia Siemens Networks. The goal of the "Carrier based HetNet ICIC for LTE" WI is to assess the feasibility of carrier based ICIC schemes for LTE-Advanced Rel-11 and beyond [51].

Chapter 2

Resource Sharing in Wireless Local Area Networks

2.1 Introduction

The IEEE 802.11 family of standards [8,37], popularly referred to as WiFi, was primarily designed for indoor use within a home or office environment. With the advent of femtocells, cellular technology – traditionally deployed over much larger areas – is now venturing into WiFi's territory. While the heart and soul of IEEE 802.11 is the contention based Distributed Coordination Function (DCF) [37]; cellular networks have historically relied on systematic (single-cell) scheduling schemes to control the access to the medium (channel). Despite its well known shortcomings, the WiFi standard has proven to be tremendously successful and is now the *de facto* standard for local wireless networking.

The explosive growth of mobile communications on one hand and the overly crowded and expensive spectrum on the other hand have fueled hot debates on spectrum sharing techniques, anticipating fundamental changes in spectrum regulation [38]. A key point of the discussions has been the need for empirical tests and validation of even the simplest spectrum sharing proposals already available. It is a sound idea to ask whether or not contention based techniques should be considered as a simple and inherently distributed spectrum sharing option for local area cellular deployments. Answering the previous ques-

tion is the central pillar of this chapter. Inspired by IEEE 802.11 Wireless Local Area Networks (WLANs), the performance of a hypothetical system is assessed. Such a system employs the Carrier Sense Multiple Access with Collision Avoidance (CSMA/CA) [49] based DCF in a Long Term Evolution (LTE)-Advanced framework. The performance is then compared with that of an ordinary LTE-Advanced system employing static frequent reuse schemes.

The analysis is carried out by means of system level simulations where femtocells are randomly placed without any prior considerations to minimize inter-cell interference. The results will make it clear that there is no fixed optimum configuration spanning all network topologies, and that a contention based approach, despite its beautiful simplicity, squanders resources due to random back-off timers and the well known exposed/hidden node issue. In all cases, a suitably chosen frequency reuse pattern proves to be a more interesting option.

The rest of this chapter is organized as follows: Section 2.2 starts with a discussion of the key conceptual difference between the two approaches, namely cellular and CSMA/CA. In Section 2.3 the examination proceeds to a brief analysis of the principles behind resource sharing and its inherent tradeoffs, outlining their implications regarding the considered sharing schemes. The simulation results and the discussions presented in Section 2.4 form the motivational basis for the alternative solutions sought throughout the rest of this thesis. Finally, conclusions are drawn in Section 2.5.

2.2 Understanding the Conceptual Differences

Even though femtocells and CSMA/CA based IEEE 802.11 networks have been designed to operate in similar propagation conditions, the techniques employed are radically different. The purpose of this section is to provide insights into the fundamental differences among these two contending approaches. The discussion begins with a very short description of some of the techniques commonly used by cellular networks to avoid completely erratic radio interference. The basic principles behind the DCF are also explained. Finally, the argumentation that follows, discusses the merits and problems of the DCF as a (i) Medium Access Control (MAC) protocol, (ii) a flexible duplexing scheme as well as a (iii) fully distributed spectrum sharing alternative.

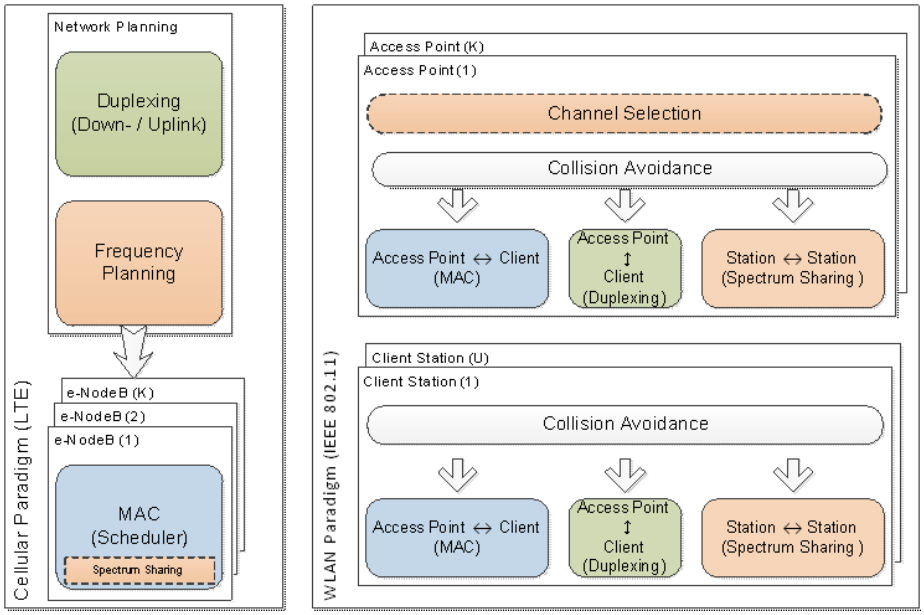

Fig. 2.1: Conceptual difference between cellular and CSMA/CA paradigms.

2.2.1 Cellular Systems

Cellular systems employ several strategies to make the best usage of resources within a network. Typically, the first step is the creation of two orthogonal transmission planes by means of duplexing. Therefore UL (reverse link) and DL (forward link) transmissions do not interfere with each other. Duplexing is commonly carried out in the frequency or time domain, denoted as Frequency Division Duplexing (FDD) or Time Division Duplexing (TDD), respectively [52].

Subsequently, sets of resources are assigned to the cells in the network. Such an assignment is commonly associated with frequency planning and may be static or dynamic, centralized or distributed. Irrespectively of how this assignment is performed, it serves one purpose: optimize overall system performance via mitigation of inter-cell interference.

Finally, within each cell multiple access techniques usually further subdivide the total signaling dimensions into S orthogonal, i.e. non-interfering, transmission planes which are then allotted to pairs of transmitters and receivers. As a result, users can be systematically scheduled by the base stations. This is represented on the left side of Fig. 2.1, where the green, orange and light blue colors denote

the duplexing, inter-cell interference mitigation and scheduling processes. Note that Inter-Cell Interference Coordination (ICIC) schemes can also be employed as part of the scheduling mechanism [4,53] in OFDMA systems as indicated by the dashed orange box.

As an example, in LTE-Advanced, the total system bandwidth is divided into Component Carriers (CCs) as described in Section 1.1.2. The frequency-domain resources within each CC are divided into S_{cc} blocks of 12 OFDM sub-carriers named Physical Resource Blocks (PRBs), which are the basic scheduling unit. The value of S_{cc} depends solely on the bandwidth of each CC.

2.2.2 IEEE 802.11 Networks

In contrast, the DCF plays all three roles simultaneously. As explained in the upcoming sections, this behavior is due to the coupling between the PHY and MAC layers in WiFi systems. Assuming full connectivity, i.e. all stations[1] are within radio range of each other, CSMA/CA works as:

i) A Medium Access Control (MAC) technique: Signals to/from different stations share a common channel in a traffic adaptive TDMA fashion.

ii) A flexible duplexing scheme: CSMA/CA leads to a device-centric traffic adaptive time division duplexing TDD of the resources.

iii) A simple *fully distributed* time-domain spectrum sharing scheme whereby a station seizes either the entire spectrum or no spectrum at all.

This is depicted on the right side of Fig. 2.1. Notice that the only difference between APs and client stations is the channel selection block. The former constitutes an underused interference mitigation possibility. Studies have found that up to 40% of WiFi APs are configured to use channel number 6 of the industrial, scientific and medical (ISM) radio band [54].

The description that follows is limited to key aspects required to understand the current work. The literature on IEEE 802.11 networks and its medium access mechanism is monumental, and a proper survey is beyond the scope of this thesis, however, the seminal paper in [55] is suggested for further reading. Additionally, the available literature on multi-cell WiFi networks is relatively modest when compared to the single-cell case. Nonetheless readers are referred

[1] In WLANs terminology all devices, be them either Access Points (APs) or user terminals (client stations) are generally referred to as stations.

to the work in [18, 56, 57]. In special, the work in [18] presents a perceptive characterization of inter-cell interference effects in unplanned IEEE 802.11 deployments and proposes a practical inter-cell interference mitigation technique based on adaptive contention windows. However, to the best of the author's knowledge there is no work considering CSMA/CA based schemes outside the scope of IEEE 802.11 WLANs. This lacuna is especially evident in the context of systems with resilient link level performance, where collisions, i.e. simultaneous transmissions from two stations, do not necessarily imply reception failures.

2.2.2.1 The DCF as a Medium Access Control Protocol

In many ways, WiFi resembles the early hub-based days of Ethernet where stations contended for the available bandwidth of a shared medium. As such, it carried over many of the advantages of Ethernet, particularly in terms of protocol simplicity and fully distributed operation. The DCF basic mechanism is carefully described and analytically modeled in [55] and later refined in [58] but can be summarized as follows:

Any station (s) willing to transmit must first sense the channel as either idle or busy. If the channel is idle, s is free to send a packet. Otherwise, it defers transmission. Time is assumed to be slotted, and s initializes a backoff timer. The timer's initial value τ_s is modeled as random integer value drawn from a uniform distribution on the [0 CW(s)] interval, where CW(s) is the current size of the contention window of station (s). When the backoff timer reaches zero, station s may transmit over the entire bandwidth of the channel. Whenever the channel is sensed busy, station s stops decrementing its backoff timer. It resumes its countdown once the channel is sensed idle again. After each successful transmission – indicated by a positive acknowledgment from the destination – s resets CW(s) to its minimal value $\mathrm{CW}_{\min}$. Moreover, each time a station experiences a collision – inferred by the lack of positive acknowledgement – its collision window CW(s) size increases exponentially subject to $\mathrm{CW}_{\min} \leq \mathrm{CW}(s) \leq \mathrm{CW}_{\max}$, where $\mathrm{CW}_{\max}$ is the maximum collision window size [49].

Among the inherent advantages of CSMA/CA as a *random access* protocol are its fully distributed nature, the reduced control channel overhead and the capability to quickly adapt to traffic arriving in bursts. The downside is that channel access is not guaranteed, i.e. unbounded delays and poor Quality of Service (QoS) guarantees; an effect particularly visible when all stations always have packets ready for transmission (saturated network). Another disadvantage is the difficulty in exploiting the channel knowledge [59]. Therefore, the AP must serve its clients in a round-robin fashion. Such issues are either minimized or even nonexistent in systems employing *scheduled access*.

2.2.2.2 Flexible Duplexing and the DCF

As stated earlier, duplexing is used to make Downlink (DL) and Uplink (UL) transmissions orthogonal. In case of Frequency Division Duplexing (FDD) two paired frequency bands are employed, one for each direction. Both channels can be treated independently and used simultaneously. However, FDD is not able to adapt to asymmetric traffic conditions, where one direction (typically the DL) might suddenly demand more capacity than the other.

Time Division Duplexing (TDD) allows both links to share a single channel by taking turns. Therefore, by dynamically adjusting their respective time-shares, any potential asymmetry between DL and UL can at least in principle be compensated for. In a single cell system, there are no further considerations, however, when multiple cells are considered, the promise of TDD is compromised. The rationale is that transmissions from neighboring cells are no longer fully orthogonal if the transitions to/from DL from/to UL in all cells are not fully aligned. This obviously restricts one cell's ability to adapt to asymmetric traffic conditions.

In a IEEE 802.11 system, the notion of DL and UL is not so crystal clear. In fact, all devices abide by the rules imposed by the DCF and are essentially treated as equals. Therefore if the AP has significantly more traffic than the client station which, in this case, limits itself to sending short acknowledgment packets, the AP will automatically attain a larger share of the medium.

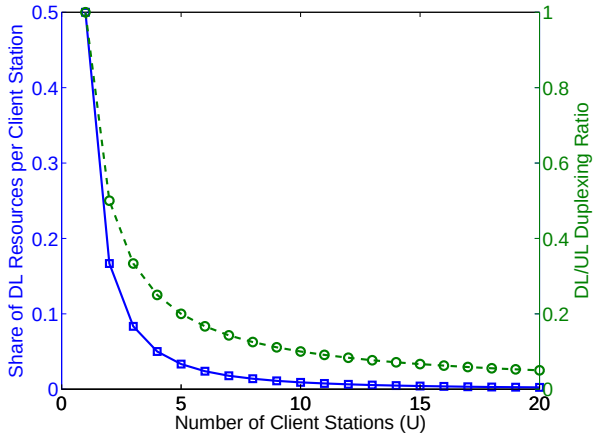

Fig. 2.2: An upper bound to the share of air time dedicated to the DL transmissions for each user (solid) and ideal DL/UL ratio (dashed) as a function of the number of clients in a single cell saturated IEEE 802.11 network.

However, this flexibility comes at a price. Because there are no fundamental distinctions among stations, a grave imbalance between DL and UL resources and subsequent DL starvation can easily arise. Assuming a single-cell saturated (full-buffer) network with U client stations, each client would be entitled to $1/U$ (round-robin) of the resources granted to the AP, which at best – although lower in practice due to the random backoff timers – would amount to $1/(U+1)$. Therefore the DL/UL capacity split will roughly equal $1/U$ while DL transmissions towards each client station is allotted at most $1/(U^2+U)$ of the air time[2]. Fig. 2.2 depicts the flexible duplexing effect, which ultimately leads to DL client starvation as U increases. This feature should be considered when comparing with LTE results. In this respect, we mainly look at the simpler single User Equipment (UE) per cell scenario as this roughly corresponds to a 50/50 DL/UL capacity split.

2.2.2.3 The DCF as a Spectrum Sharing Technique

Although 802.11 technology has been designed for single-cell WLANs, where basic coverage range was the primary objective; multi-cell deployments have become increasingly popular. As explained in Section 2.2.2.1, the basic DCF mechanism does not distinguish between transmissions performed by APs and client stations. Stations simply detect whether or not the channel is busy (based on received signal strength) and act accordingly. As a consequence, the contention mechanism automatically leads to inter-cell time-domain spectrum sharing whenever the coverage of two or more cells overlap. Ideally, only a single station transmits over the entire band at a time within a small area delimited by the sensing range. This range is defined to be the maximum distance from which a receiver can still detect a busy channel.

An interesting example based on the two simple scenarios depicted in Fig. 2.3 can be used to illustrate the inherent spectrum sharing capability of the DCF. For the sake of simplicity we assume that both Femto Access Points (FAPs)/AP transmit on the same band and always have data to transmit to their served users and that Closed Subscriber Group (CSG) is the access mode. To each user (receiver), the transmissions from other cells appear as interferers.

Notice that the network in the upper part of Fig. 2.3 would work without problems, irrespective of the selected solution, i.e. femtocells or WiFi. However, the lower network, where the location of the green transmitter and receiver has simply been swapped, poses a serious challenge to femtocells, practically mandating some form of coordination. In this case the interfering signal experiences a path loss much smaller than that of the desired signal. This is a possible

[2] A rigorous treatment of the saturation throughput of the DCF is found in [55]

outcome of CSG mode combined with randomly placed devices. A second and more subtle aspect is the existing asymmetry. The actions of the green base station have a much more profound impact on the cell served by the blue base station than the opposite. As a result both cells do not attain the same benefit from resource sharing. The next section reviews the technical foundations and the fundamental tradeoffs associated with resource sharing, while the potential asymmetry shall be revisited in upcoming chapters.

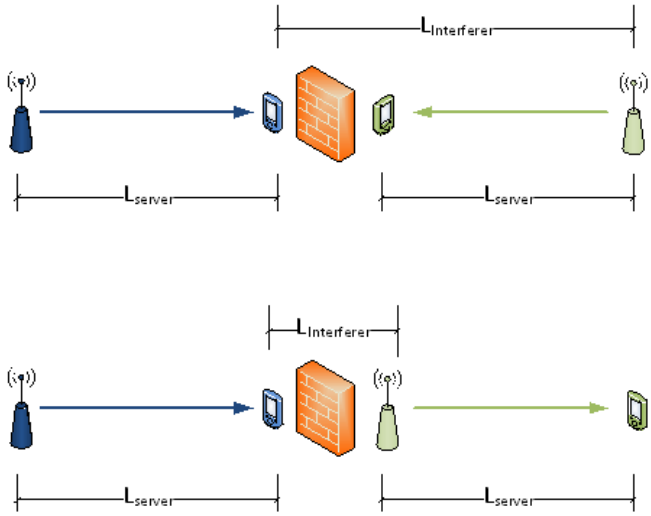

Fig. 2.3: A simple yet insightful example: For IEEE 802.11 networks, both topologies are essentially the same. However, if the base stations are FAPs, the upper and lower scenarios are very different and the lower one is likely to require some form of coordination.

2.3 Principles of Resource Sharing

Wireless systems employ several strategies to make the best usage of resources within a network. Without any coordination, all transmitters would have unrestricted access to the whole bandwidth at all times. Any sharing scheme will most likely impose some limits to the resources available. From a purely theoretical standpoint, it is irrelevant whether such division is carried out in the frequency, time or a combination of these domains[3]. It can easily be shown [60] that the capacity per user is identical in both cases. Nonetheless, it is important

[3] Albeit very common, channelization along space and/or code axes are not considered in this thesis.

to acknowledge that practical differences exist in terms of baseband processing, power amplifier requirements, Radio Frequency (RF) complexity, etc. Such distinctions should not be overlooked when designing a new system.

2.3.1 Frequency Domain Sharing

Frequency reuse is the most traditional way of sharing the spectrum. A basic hard frequency reuse scheme assigns to each cell a fraction $1/N$ of the whole spectrum, which usually differs from the assignment of neighboring cells. As a result, the experienced Signal to Interference plus Noise Ratio (SINR) is increased. However, this SINR improvement comes together with a reduction of the available spectrum per cell. Resorting to Shannon's famous capacity formula [45] for the Single Input Single Output (SISO) case and treating interference as noise, the maximum achievable data rate $R(N)$ can be expressed as a function[4] of the number of partitions $N \geq 2$:

$$R(N) = \frac{B}{N} \log_2[1 + \gamma(N)] \tag{2.1}$$

In (2.1) B (Hz) represents the total system bandwidth and $\gamma(N)$ corresponds to the attained SINR with N orthogonal partitions. Here the bandwidth-SINR tradeoff becomes evident. The logarithmically scaled increase in SINR must be able to overcome the linearly scaled loss in spectrum in order for frequency reuse to be beneficial. If we define $\gamma^*(N) \equiv \gamma(N) : R(N) = R(1)$, then by simple algebraic manipulation – starting from the equality $B/N \log_2[1 + \gamma^*(N)] = B \log_2[1 + \gamma(1)]$ – we can demonstrate that:

$$\frac{\gamma^*(N)}{\gamma(1)} = \sum_{i=0}^{N-1} \binom{N}{i} \gamma(1)^{N-1-i} \tag{2.2}$$

Equation (2.1) calculates the required gain in terms of SINR in order to ensure that the achievable data rate is not compromised by the bandwidth partition. The ratio is plotted in Fig. 2.4 as a function of $\gamma(1)$ (operation point) for several values of N. Additionally, the dashed line delimits the feasible region due to RF imperfections, which limit the effective SINR. Imperfections are unavoidable in real systems and must be considered, because they introduce an irreducible distortion term preventing the SINR from increasing as the inter-cell interference

[4] For the sake of simplicity we assume a broadcast (downlink) frequency-flat channel with a fixed power spectral density independent of N.

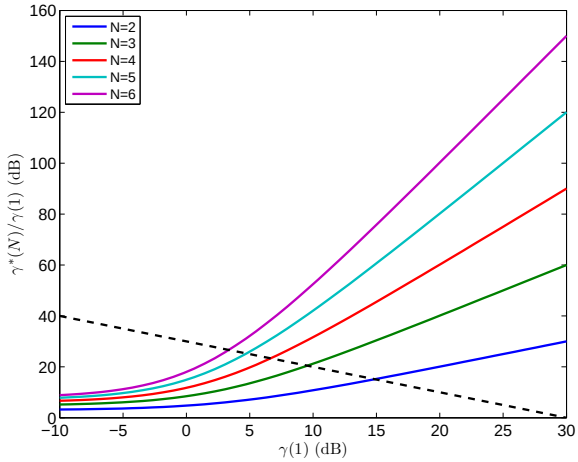

Fig. 2.4: Required SINR gain in dB to ensure the same data rate achievable with $N = 1$. SINR is asymptotically limited to 30 dB due to EVM.

falls off. Such limitations are commonly modeled by the concept of Error Vector Magnitude (EVM) (See Appendix D.1.4 for details).

Figure 2.4 clearly illustrates that the bandwidth could, at least in principle, be "arbitrarily" and beneficially sub-divided as long as $\gamma(1) \ll 0$dB. On the other hand, if the system is operating at SINR values higher than 10 dB, the bandwidth should be split judiciously. For example, $N \geq 3$ would only deliver a net profit in a region that cannot be achieved at all due to RF limitations. In spite of quantitative differences due to e.g. practical engineering assumptions, time-varying channel and traffic conditions, etc, the qualitative aspects of this fundamental tradeoff remain valid in a real system and are extremely useful in the interpretation of results.

2.3.2 Time Domain Sharing

Time-domain sharing is another option, where transmissions from different nodes take turns. Hence, the equivalent to hard frequency reuse would be strict time-domain coordination, whereby only one station within a small cluster transmits at a time. Thus in a saturated network, each station would ideally transmit

for $1/N$ of the time over the entire bandwidth.

$$R(N) = \left(\frac{1}{N}\right) B \log_2(1 + \gamma(N)) \tag{2.3}$$

That is what the basic DCF loosely tries to accomplish as discussed in Section 2.2.2. Although the situation is admittedly more complex – due to backoff timers, hidden and exposed nodes [61] as well as the positioning of stations – a simple analytical exercise can provide an intuitive understanding of the resource (time) partitioning deriving from the CSMA/CA mechanism.

Let us consider a simplified scenario where stations are randomly located in a large area according to a homogeneous planar Poissson Point Process (PPP) [47, 62] Φ, i.e. the location of each station is independent and given by a pair of independent (x, y) coordinates, whose station density per unit area is δ. Hence the intensity (the average number of stations in a circle of radius r) λ of Φ is then given by $\delta\pi r^2$.

By modeling the path loss at a particular location as a superposition of the mean distance-dependent value with a zero mean log-normally (normal in dB) distributed random variable ξ with standard deviation σ (dB), the received power $P_R(d)$ (in dBm) at any distance d from the transmitter with transmit power P_T (in dBm) is given by:

$$P_R(d) = P_T - [A + B \log_{10}(d) + \xi], \tag{2.4}$$

where A and B are parameters that depend on the antenna characteristics and the propagation environment. Because the path loss is a random variable with a normal distribution in dB about the distance dependent mean, the same can be stated about $P_R(d)$. The latter implies that the Q-function can be used to determine the probability that the received signal level will exceed a certain value $P_{\text{threshold}}$ [52] (See Appendix E for a formal definition of the Q-function).

In the context of CSMA/CA networks and assuming that there is one station transmitting at the origin, then all other stations are able to detect a busy channel with a given reliability (R_{level}), if the received signal level is above a certain threshold. For fixed $P_{\text{threshold}}$ and R_{level}, the sensing range r_s can be calculated as:

$$r_s = 10^{\left(\frac{P_T - P_{\text{threshold}} - A + \sigma z}{B}\right)}, \tag{2.5}$$

where z is a term accounting for the shadow fading, given by $z = Q^{-1}(R_{\text{level}})$ where $Q^{-1}(.)$ is the inverse of the Q-function. Resorting to the PPP assumption

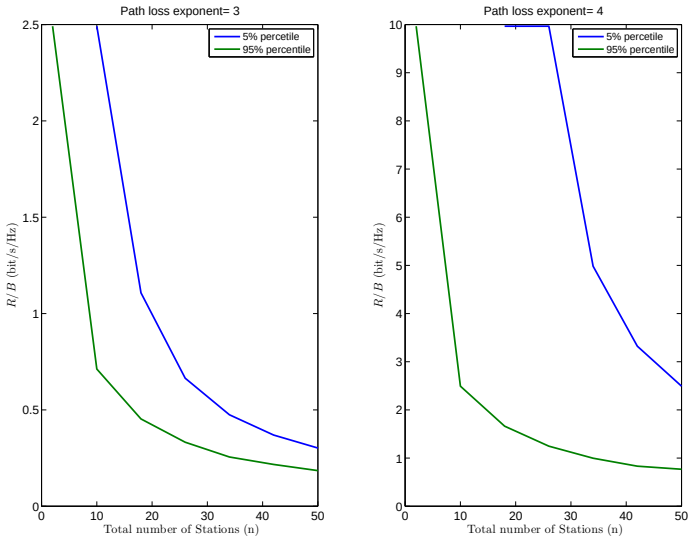

Fig. 2.5: Normalized spectral efficiency as a function of the total number of active stations for two different path loss exponents: 3 (left) and 4 (right). The estimated number of time-sharing stations is given by 5-th (blue) and 95-th (green) quantiles of the homogeneous PPP.

and using r_s to calculate the intensity of the process, one can estimate the number of stations (N) within sensing rage. These stations will be time-sharing the spectrum, thus yielding a maximum data rate $R(N)$ given by (2.3).

The results are plotted on the left-hand side of Fig. 2.5 for $R_{\text{level}} = 95\%$, $P_T = 20$ dBm and $P_{\text{threshold}} = -76$ dBm. The total number of uniformly distributed stations over an area of 2500 m^2 varied from $n = [2, \ldots, 50]$, thus $\delta = [8 \times 10^{-4}, \ldots, 0.02]$ stations/m^2. While the transmission power and sensing thresholds were selected to match typical WiFi values; the path loss model parameters, $A = 127, B = 30$ and $\sigma = 10$ as well as the simplified dense urban 5×5 -grid model – which led to the total area of 2500 m^2 – were taken from the 3GPP recommendations for femtocell studies [22]. The N-independent value of γ was set to 30 dB, which roughly corresponds to an EVM of 3%.

The blue (above) and green (below) curves represent maximum data rates normalized by the system bandwidth B according to the estimated number of time-sharing users given by 5-th and 95-th quantiles of the homogeneous PPP. Therefore, in 95% of the cases, N will be larger than the estimated values, and the

performance will be correspondingly lower than that predicted by the blue curve. Conversely, in 95% of the circumstances, the performance will be higher than that predicted by the green curve due to an effectively lower number of stations N sharing the channel. This characterization in terms of performance ranges is justified because the location of stations and thus the distances are subject to uncertainty. Despite the simplifications to make the analysis tractable, the results unquestionably attest that the resulting resource partitioning is severe even for a modest number of nearby stations.

The right-hand side of Fig. 2.5 uses the same set of parameters with the exception of $B = 40$, corresponding to a path loss exponent equal to 4. The goal was to try and capture the impact of the propagation environment. By comparing the values on the y-axis of both figures and the gaps between the curves, it becomes clear that the resulting number of stations N effectively sharing the medium and hence the data rates are significantly affected by the path loss exponent. That intuitively makes sense because a higher exponent leads to better insulation and consequently a reduced sensing range r_s.

In sum, contrary to the intuitive perception, dense CSMA/CA-based networks benefit from higher path losses associated with higher frequency bands. In spite of the improved coverage area, lower frequency bands are less attractive because the contention domain increases and fair share of each device becomes smaller.

2.4 Performance Evaluation

The high level goal of this section is to provide a comparative analysis of the two local area strategies outlined in Section 2.2. The effectiveness and efficiency of CSMA/CA as an implicit distributed time-domain spectrum sharing technique is compared to that of systematic scheduling approach, making use of hard frequency reuse patterns. The analysis is carried out via system level simulations. Finally, it is important to stress that the performance evaluation is not concerned with actual WiFi networks, but rather the viability of simple contention based solutions in the context of local area cellular networks.

2.4.1 Methodology and Assumptions

The performance was evaluated through semi-static system level simulations. In order to perform a meaningful comparative analysis, two simulators sharing the same structure were developed. The simulators are based on basic LTE specifi-

cations [63], but supporting bandwidths up to 100 MHz. The interested reader will find a detailed description of both simulators employed in Appendix D; nevertheless a basic description is provided next. Both tools rely on series of "snapshots", where each snapshot comprises thousands of radio frames. During each snapshot, path loss, shadowing and the location of nodes remain constant. Fast fading is not explicitly simulated. The statistical reliability of the simulations is ensured by (ensemble) averaging the results of thousands of snapshots. Both DL and UL are simulated. In summary, for each snapshot:

1. The cell layout is generated according to the deployment ratio.
2. Users are generated with uniformly distributed indoor locations.
3. SINR values are calculated and then averaged over a whole LTE frame (holding time in the CSMA/CA variant).
4. Frame SINR is mapped to achieved throughput, applying a modified Shannon fitting [64].
5. Several frames are simulated.

Some additional simplifications were made: There is no power control, hence all transmitting elements use their maximum power. Link layer is assumed to have the same capacity as in LTE systems; a modified Shannon's formula according to [64] is used to estimate the system performance. Implicitly this implies ideal Link Adaptation (LA). A 2×2 Multiple Input Multiple Output (MIMO) antenna configuration has been considered, thus allowing up to two code-words.

The considered simulation scenario is a single-floor version of the dense urban dual stripe introduced in Section 1.4.3. The deployment ratio (%) assumed the following six values [0.01 0.1 0.25 0.5 0.75 1]. The purpose is to mimic increasingly denser femtocell deployments; therefore the lowest deployment ratio corresponds to virtually isolated cells, while the highest implies one home base station in every apartment.

As discussed in Sections 2.3.1 and 2.3.2, the key difference between the cellular and the CSMA/CA paradigms is the way in which the channel is shared by all $U = \sum_{n=1}^{N} U_n$ users in the system, where N is the number of cells and U_n is the number of users served by each cell n. This distinction is reflected on both simulation tools as follows:

In the considered hypothetical system, a station s seizes all PRBs (See Section 2.2.1) over 40 MHz[5] whenever its back-off timer reaches zero. It then occupies the channel for a whole LTE radio frame (10 ms). The back-off timer mechanism works as described in Section 2.2.2.1 and the 0.5 ms LTE radio slot (half of a Transmission Time Interval (TTI) [3]) is employed as the time quantum[6] during the countdown.

In the LTE-Advanced compliant version, TDD is the selected duplexing scheme, and transmissions are continuously scheduled since full buffer traffic is assumed in both link directions. The same 40 MHz bandwidth is assumed, and femtocells have access to either 40, 20 or 10 MHz depending on whether the total spectrum is statically divided into 1, 2 or 4 chunks, respectively. The division effectively limits the number of available PRBs.

Keeping in mind that the focus is on the spectrum sharing aspect of CSMA/CA, the number of users served by each CSG home base station[7] is set at $U_n = 1 \, \forall \, n$. This serves three purposes: first the comparison becomes independent of the type of scheduler used by the cellular system, after all there is only one user to be served. Secondly, the DL starvation problem explained in Section 2.2.2.2 is avoided. Finally, because CSMA/CA brings about a DL/UL traffic ratio per cell close to $1/U_n$ as explained in Section 2.2.2.2, the single user per cell assumption leads to an approximate 50/50 capacity split, which is set accordingly in the pure LTE tool.

2.4.2 Numerical Results and Critical Analysis

The analysis focuses on DL performance; nonetheless similar figures were obtained for the UL. All throughput results presented here are normalized by the maximum capacity of the system. This emphasizes the relative trends rather than the absolute values. A normalized throughput of 100% implies uninterrupted transmission with the highest possible Physical Layer (PHY) data rate, i.e. over the entire system bandwidth at the maximum system spectral efficiency. Furthermore, throughput values are measured at the Medium Access Control (MAC) rather than the Physical Layer (PHY) layer [49]. This is particularly relevant in case of discontinuous transmissions induced by the contention mechanism.

[5] Akin to existing IEEE 802.11n systems [37].

[6] In WiFi systems the actual channel *holding time* varies as it depends on the physical layer throughput. Instead the maximum MAC Service Data Unit (MSDU) is fixed. Note that the selected 10 ms holding time comprises 20 LTE radio slots. This is roughly equivalent to the ratio (23.5) between the time needed to transmit the largest IEEE 802.11n MSDU of 7935 bytes at 300 Mbps and the WiFi slot time of $9\mu s$.

[7] Denoting both FAPs and APs.

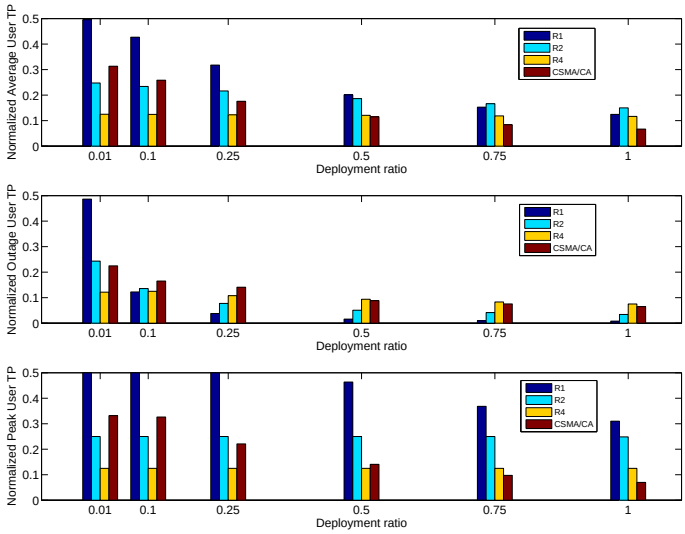

Fig. 2.6: Comparing the two paradigms under different network density levels. Results are normalized with respect to the theoretic maximum throughput.

Figure 2.6 summarizes the obtained results according to the performance indicators introduced in the first chapter (See Section 1.4.4). The upper part compares the two paradigms with respect to the attained average user throughput performance, while the middle and lower subfigures deal with the cell-edge and peak user throughput values respectively. Various characteristics of the interference footprint in WLANs and ultimately from the problem at hand can be inferred from the results. It can safely be stated that among the considered options, no single strategy consistently delivered the best performance over all possible deployment ratios and metrics of interest.

The leftmost group of bars in all three plots corresponds to the case where cells are virtually isolated. Consonant with the theoretic expectations discussed in Section 2.3 there is absolutely no reason to use any reuse pattern other than 1 (denoted R1 in Fig. 2.6), which grants the cell access to the whole spectrum and therefore maximizes all three metrics in the absence of significant inter-cell interference. Note that the saturation at 50% is due to duplexing. Moreover, the contention approach (CSMA/CA) squanders part of the resources. The duplexing is imperfect due to the random back-off timers leading to less than 50% airtime for the DL[8]. It is also plagued by possible collisions, even when

[8] Although not shown, for similar reasons, the UL traffic does not fill up the unused airtime,

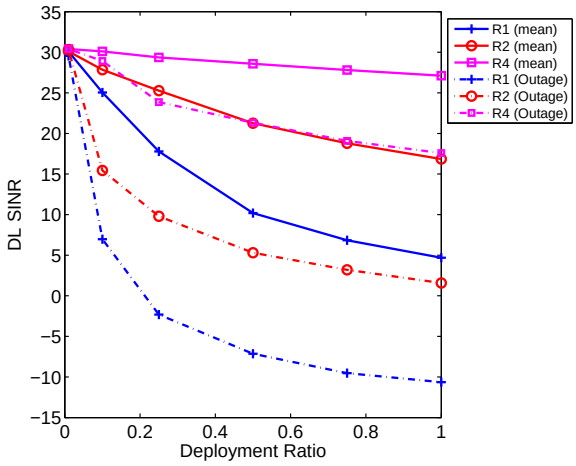

Fig. 2.7: Evolution of the average (solid) and outage (dashed) SINR for different static reuse patters as a function of the network density.

one assumes full connectivity. The client station and the AP start transmitting simultaneously whenever both randomly select the same back-off timers. In this case, both transmissions will be lost as stations cannot transmit and receive at the same time in the same frequency.

In multi-cell scenarios the balance gradually shifts towards resource partitioning; nevertheless the definition of an optimal configuration remains fuzzy and dependent on the considered performance indicator. For example, universal reuse is is a competitive solution in terms of simplicity, peak date rates and average user throughput. It consistently delivers the highest peak data rates. On the other hand, universal reuse is by far the worst option in terms of outage performance. As illustrated in Section 2.2.2.3, due to the randomized locations and the CSG mode, devices can receive critically high levels of interference in all but the sparsest deployments when all cells have unrestricted access to the full spectrum. Such interference is significantly attenuated by frequency reuse or CSMA/CA. This is particularly evident at higher deployment ratios where even basic sharing strategies yield improvement factors beyond 500% relative to the outage performance of reuse 1.

In terms of overall average performance, improvements only appear when the number of surrounding cells increases significantly. In this respect the moderate resource partitioning brought about by a 1/2 reuse pattern (R2) does deliver some gain in very dense networks. If there is no possibility to exploit the power

hence the imperfect duplexing.

domain or dynamically adjust the bandwidth, avoiding just the strongest interferer seems to be a sensible choice. The other schemes (CSMA/CA and R4) give rise to losses because the SINR improvement is not enough to offset the reduced transmission bandwidth. Such results are in good agreement with the discussion in Sections 2.2.2.3 and 2.3.1. Recall that effective time-slicing in CSMA/CA solely depends on the number of stations within sensing range, i.e the density of the network.

Figure 2.7 provides further insight as to why resource partitioning becomes more interesting as the deployment ratio is raised. The figure depicts the average as well as 5% outage DL user SINR values for different network densities. Three hard frequency reuse patterns are considered. CSMA/CA is not included therein, because unlike cellular networks, average SINR is a less meaningful indicator. Recap that by design, CSMA/CA always tries to ensure interference-free transmissions. It becomes clear that there is indeed room in the feasible SINR region for gains stemming from resource splitting in dense networks. The potential for cell-edge users is naturally even greater.

Additionally, in order to get further visual intuition, Fig. 2.8 shows SINR availability maps in a dense network assuming universal frequency reuse under CSG and OSG access modes. The small gray triangles represent the random location of the femtocell inside each apartment. Shadow fading is not included here for clarity, as a result each cell becomes a contiguous area, instead of comprising multiple "islands". Clearly, the introduction of OSG and hence the possibility to be served by the femtocell with the strongest signal makes the occurrence of extremely low SINR values (deep blue regions) much less frequent. Nonetheless, Open Subscriber Group (OSG) deployments can also benefit from resource sharing. Supplementary results and discussions about the differences between CSG and OSG can be found in Appendix C.

Finally, there is yet another subtle message in the results presented in Fig. 2.6; a message that underpins the lively discussions on cognitive radios [65] and the reform of spectrum sharing policies [38]. The traditional spectrum licensing policy managed by state regulators – through which access to radio spectrum is exclusively reserved to a few licensed operators – is analogous to the hard frequency reuse patterns. In this study case, a 1/4 static pattern has led to a performance, which is nearly insensitive to the network topology. It is unquestionably a safe approach, albeit very inefficient when cells are sparsely deployed. In short, predetermined and rigid spectral limits (the "status quo") are effective, but are not necessarily the most efficient solution even when the limited resources are cleverly assigned.

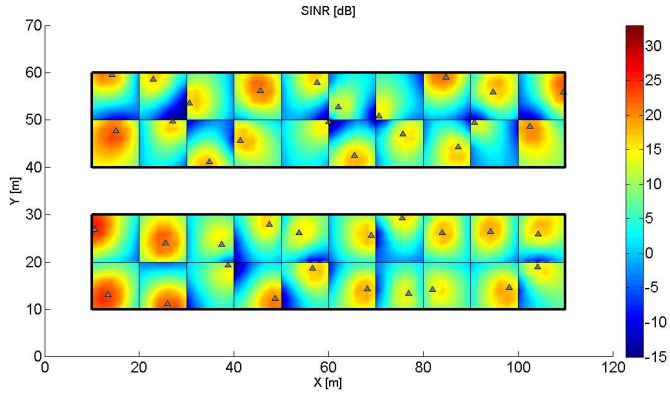

(a) CSG Cells

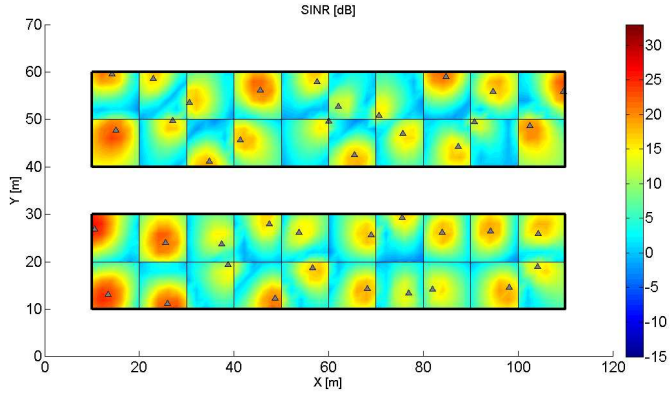

(b) OSG Cells

Fig. 2.8: CSG versus OSG Networks: One realization of the spatial distribution of downlink SINR with universal frequency reuse. Author's note: Depending on printer quality, differences might be less noticeable.

2.5 Conclusions

This chapter has addressed the first two objectives of this project. It has characterized the interference footprint of local area cellular deployments as well as investigated the suitability of well-established contention based solutions in the context of cellular systems.

The research was carried out by means of simple analytical models dealing with the fundamental aspects associated with resource sharing and through system level simulations based on the specifications of LTE-Advanced. The results revealed the multi-faceted nature of the problem and provided empirical evidence that even rudimentary spectrum sharing schemes can deliver substantial gains in local area networks, especially for the less privileged users.

The following conceptual question was also posed and answered: "Should contention based techniques be considered as a simple and inherently distributed spectrum sharing option for future femtocell deployments?". The rationale being the undisputed success of WiFi networks whose foundation stone is CSMA/CA. The performance of a hypothetical hybrid system employing CSMA/CA in an LTE-Advanced framework was compared with that of an ordinary LTE-Advanced system employing static frequent reuse schemes. The results presented herein indicated that CSMA/CA is in general not able to outperform simple frequency domain alternatives with a properly selected frequency reuse factor; thus making plain CSMA/CA less attractive.

Last but certainly not least, traditional frequency reuse requires network planning. This is not a scalable and viable solution in the context of local area networks. The foregoing observations coupled with problems that plague the contention based approach underlie the pursuit of new distributed algorithms capable of self-adjusting to the network conditions throughout the rest of this dissertation.

Chapter 3

Autonomous Component Carrier Selection

3.1 Introduction

The work in Chapter 2 demonstrated that the potential benefits offered by femtocells are not without new challenges in terms of interference management. Due to the expected large number of user-deployed cells, centralized network planning becomes unpractical and new scalable alternatives must be sought. In this chapter a decentralized and scalable carrier-based interference management solution is proposed. The concept relies on lightweight information exchange among cells and explores the possibilities offered by Carrier Aggregation (CA), an integral part of LTE-Advanced. Nonetheless, the concept remains useful even if terminals do not support CA. A series of system level simulation results demonstrate that a simple and robust interference management scheme, called Autonomous Component Carrier Selection (ACCS), allows each cell to dynamically select the most attractive frequency configuration. ACCS improves the experience of the least favored users without penalizing overall system capacity. Moreover, even though the developed scheme is applicable for both directions, in the current chapter, the discussion shall revolve around the Downlink (DL). The Uplink (UL) is dealt with in Chapter 4.

The rest of this chapter is organized as follows: Section 3.2 reviews the in-

terference and spectrum management literature and offers an overview of recent industrial advances. Section 3.3 introduces the design principles that have guided this work, highlighting the differences to prior contributions. Section 3.4 presents the system model as well as the basic assumptions behind the ACCS mechanism. Section 3.5 includes more detailed algorithm descriptions. Proof-of-concept system level simulation results are presented in Section 3.6. Finally, concluding remarks in Section 3.7 close this chapter.

3.2 Related Work and State of the Art

In general, one can categorize interference as either intra- or inter-cell interference. The former is typically not an issue in Orthogonal Frequency Division Multiple Access (OFDMA) networks because transmissions to/from mobiles within a cell are orthogonal. The latter, however, needs to be kept in check as it can bring about significant performance degradation.

Inter-cell interference management is a problem just as old as cellular systems. Not surprisingly, it has been extensively investigated, and a monumental amount of material is now available in the literature. A plethora of methods have been developed to mitigate inter-cell interference ranging from traditional static frequency planning to advanced signal processing at the receivers and transmitters [66].

This thesis investigates interference and spectrum management techniques in the ambit of Long Term Evolution (LTE) networks. More precisely, carrier-based Inter-Cell Interference Coordination (ICIC) among femtocells. Although inter-cell interference remains the crux of the matter, many of the original working assumptions have changed dramatically due to recent developments; thus making a fresh look at the old problem very opportune.

For example, LTE replaces the circuit-switched architecture by an all-IP packet-switched one. In the latter, due to fast statistical multiplexing, channels are shared, and hard blocking plays a much lesser role than in previous channel allocation studies. Furthermore packet bursts are much more ephemeral than voice calls. As a result multi-cell dynamic resource assignment on a packet or session basis is no easy feat. Last, but certainly not least, the advent of femtocells and the introduction of Closed Subscriber Group (CSG) cells have significantly changed the landscape as dominant interferers may take on a much more prominent and aggressive role. But before moving on hastily to the proposed solution, it is appropriate to review the existing literature available, both the academic and industrial line of works.

3.2.1 Academic Efforts

During the early days of cellular networks, channel assignment methods were of paramount importance due to the need for frequency planning. The latter was and still is the most traditional approach to guarantee a minimum carrier-to-interference ratio (C/I) at the expense of spectral resources available to cells (See Section 2.3.1).

At the heart of frequency planning lies the old channel allocation problem, whose essence is deciding how many, when and which channels should be used by each cell in the network. An excellent overview and systematic performance comparison of several channel allocation algorithms in the context of circuit-switched networks can be found in [67] and [68], respectively. An insightful theoretical analysis of the stability distributed dynamic channel allocation technique is presented in [69]. Readers will find a more up-to-date to overview in [66].

Mathematically, channel assignment is a combinatorial optimization problem which can be mapped into a conflict graph vertex (multi-) coloring[1] and is therefore NP-hard [40, 70]. Many contributions in the literature analyze the multi-cell spectrum allocation problem in light of graph (multi-) coloring [70–72]. Several centralized and distributed algorithms exist. While earlier studies were mostly based on the usage of unit disk graph to model ad-hoc networks [73], recent proposals deal with dense deployments of Wireless Local Area Network (WLAN) networks [74, 75].

With the emergence of decentralized packet switched cellular networks, dynamic spectrum approaches and cooperation gained momentum. These solutions typically consider a decentralized architecture with autonomous decision makers. Game Theory (GT) studies such interactions and has been applied to dynamic spectrum sharing in a number of recent proposals [76–78]. The work in [77] is an interesting example where GT is used to analyze the performance of a decentralized ICIC scheme. The working assumption is that each base station (player) will act independently towards the maximization of its cleverly tailored utility function, leading to overall interference reduction. In spite of its elegance and sound rationale, the method overlooks one critical trait of the spectrum sharing problem, as the amount of allocated channels is fixed. It is well known that interference levels alone do not fully characterize the cell capacity. The amount of spectrum employed by each cell is also extremely relevant. Whenever neighboring cells increase their shares of the total frequency resources, the spectral overlapping snowballs, which in turn compounds the inter-cell interference, ul-

[1] The cellular network is mapped into an interference graph $G = (V, E)$ where the node set V denotes Femto Access Points (FAPs) and the edge set E represents geographical adjacency of cells and therefore the possibility of co-channel interference [70].

timately degrading the performance of all cells. The noteworthy contribution in [78] does not require explicit information exchange and neither does it impose a hard limit to the resources. It retains the traditional GT player selfishness assumption (where players compete towards maximizing their utilities) but "artificially" yet cleverly frames the utility function in the context of diminishing returns. However the iterative scheme relies on previous interference levels and its convergence properties are not yet fully understood even under stationary topologies and well behaved interference patterns (full buffer).

Early efforts in [79] tackled the dynamic channel assignment problem based on the framework of real-time reinforcement learning, more precisely via a technique known as Q-learning [80]. Along similar lines, there is an emerging body of literature dealing with the application of distributed Q-learning and similar techniques to femtocells. Generally, these methods suggest that FAPs should gradually learn (by interacting with its local environment) through trials and errors, and adapt the channel selection strategy until convergence is reached [81]. The coexistence problem between macrocell and femtocell systems is also investigated in the light of reinforcement learning techniques in [82]. The former contribution also proposes a new docitive paradigm in order to speed up the slow and complex learning process. All of these contributions loosely fall under the umbrella of Cognitive Radio Networks (CRN) [65, 83]. The vision of CRNs has revamped the academic interest in the distributed version of the channel assignment problem due to its self-organizing nature and its potential to reduce operational expenditures. A survey of dynamic spectrum management in light of Cognitive Radio (CR) is presented in [84], while the authors of [85] propose CR-enabled femtocells that are able to access spectrum bands not only from macrocells, but also from other licensed systems.

Advanced distributed scheduling aiming for multi-cell capacity maximization [86] and ICIC [41, 53, 87, 88] have also sparked a lot of research within academia and standardization bodies. The noteworthy work in [89] introduces a semi-distributed hierarchical approach where two time scales are involved. A central controller operating on a time scale in the order of tens of milliseconds decides which resources should be used by each cell under its control, striving to maximize the overall multi-cell throughput. Then, in the short-term (a few milliseconds), each cell is free to decide how to schedule its users abiding by the restrictions imposed by the central controller. In [53], the authors do an excellent job reviewing the recent advances in ICIC research in the context of OFDMA networks; discussing the assumptions, advantages and limitations of some of the proposed mechanisms. They conclude that channel dependent (single cell) scheduling tends to limit the potential benefit of inter-cell coordination in macrocell networks.

Finally, stochastic geometry and related concepts have also been applied to in-

vestigate fully distributed networks consisting of randomly located devices, akin but not limited to femtocells [47]. The problem studied in [90] is particularly interesting. The authors derive simple analytical results for decentralized networks that clearly show the dependence of the optimal reuse factor on basic system parameters. Although they assume an off-line optimization and fixed rate transmissions, their results provide interesting insights. The key takeaway of their work is that an interference limited network should operate in a point that lies between the low-Signal to Interference plus Noise Ratio (SINR) and high-SINR regimes.

3.2.2 Industry Efforts

Despite being prolific sources of powerful insights and upper bounds, many of the studies in Section 3.2.1 lead to prohibitively complex implementations; thus often limiting their direct applicability. As a result, the ICIC mechanisms supported by LTE rely on notably less complex heuristics. The Rel-8 standardized solutions facilitate intra-carrier frequency domain ICIC methods on Physical Resource Block (PRB) resolution. Standardized signaling over the X2 interface [26] carries information on interference levels and scheduling decisions providing support for both reactive and proactive ICIC schemes. While the former is based on measurements of the past, the latter relies on sending out future scheduling decisions. For the DL the proactive Relative Narrowband Transmit Power (RNTP) indicator is available, whereas for the UL a reactive Overload Indicator (OI) and a proactive High Interference Indicator (HII) have been standardized. Generally, these indicators enable dynamic (re-)configuration of various frequency reuse patterns ranging from hard- to fractional- and soft-frequency reuse [41,87]. The interested reader can find more details about Rel-8 ICIC mechanisms in [3].

Three aspects deserve special attention. First, the aforementioned schemes are the outcome of studies conducted for macro cellular environments, hence not covering Heterogeneous Network (HetNet) scenarios. Second, the solutions are limited to data channels. Finally, there are no standardized handshake procedures between enhanced NodeBs (eNBs). This basically implies that it is up to vendors to decide when to transmit and how to react upon reception of such messages. In practice, this means that at best no actions or at worst conflicting actions might be taken in a multi-vendor network. In order to deal with the first limitation, Enhanced Inter-Cell Interference Coordination (eICIC) schemes are currently being finalized for LTE Rel-10. These are essentially intra-carrier time-domain interference management techniques designed to mitigate inter-cell interference problems in HetNets, i.e. between macro and Home enhanced NodeBs (HeNBs) (femtocells), as well as between macro and picocells. More details can be found at [26] and the references therein.

3.3 Design Choices and Rationale

Currently, LTE Rel-8 through Rel-10 does not include standardized interference management techniques, where the carrier domain is exploited, nor does it contain techniques for interference coordination for dense and uncoordinated deployment of small cells such as femto and picocells. Anticipating the need for such schemes, the ultimate goal of this work is to devise scheduler-independent, practical and fully autonomous carrier-based schemes that mitigate inter-cell interference without compromising average and peak data-rates. The preference for distributed as opposed to centralized schemes is justified by the the foreseen large scale deployment of user-deployed, which makes centralized schemes less attractive.

Conducting the interference coordination in the carrier domain is considered to be relevant as operators are likely to have multiple Component Carriers (CCs) available for LTE deployment in the future. Performing the interference coordination in the carrier domain also has the advantage of protecting both control and data channels. The protection offered to control channels is specially relevant in CSG scenarios. None of the existing mechanisms described in Section 3.2.2 were designed to shield these channels from intra-tier inter-cell interference, which can be disastrous[2] in case of unfavorable network topologies as exemplified in Section 2.2.2.3. Additionally, carrier-based mechanisms work with legacy User Equipments (UEs) and can easily be combined with CA techniques for Rel-10 UEs.

Carrier-based techniques also allow the resource assignment on a cell level to be decoupled from the sub-channel (PRB) scheduling. Therefore both problems are solved independently via a hierarchical resource management process carefully detailed in Section 3.4. Albeit suboptimal, such approach has two important practical advantages:

- Interoperability among vendors.
- Independence from scheduling decisions.

The benefit from interoperability is unequivocal because it is virtually impossible to get different vendors to agree upon cooperation rules built into their proprietary packet schedulers. In a decoupled framework, schedulers are free to request/distribute/relinquish the resources of the selected CCs among served UEs according to any internal metric.

[2] In time (frame) synchronized LTE networks, DL and UL control channels are always transmitted at the same time and frequency, hence unlike data channels collision is guaranteed.

The advantage of independence from (distributed) scheduling decisions might not be straightforward, but it is deep-rooted in the time-varying nature of the problem. Because traffic demand varies (on several time-scales), methods that rely purely on actual interference measurements, rather than potential potential interference coupling (detailed in Section 3.4.5), have to deal with two grave practical issues: (i) tracking a rapid moving target – interference varies due to scheduling, power, channel and traffic conditions – and (ii) adjusting the resources accordingly. However, by doing so, they modify the interference footprint, which mandates an iterative process and in a worst-case scenario can lead to a causality dilemma. For this reason, algorithms based on actual interference call for fast convergence properties, at least faster than the variations of signal and interference levels. Otherwise the system could be thrown into an inefficient oscillating (ping-pong) state.

Complicating matters further, user-controlled femtocells can (re-)appear anywhere and at anytime. This might put network stability on the line if algorithms strive for strict optimality. This quest could lead to virtually unpredictable reconfiguration storms. Consequently, depending on the application it might be preferable to exchange optimality for inertia, i.e. resistance to reconfigurations, for the sake of stability. In this view, it is a sensible to choice to have one anchor CC, enjoying certain privileges as described in Section 3.4.3.

Along the same line, this work has also purposefully targeted at mechanisms operating at time scales much longer than those of scheduling decisions, as it is not desirable to have cells switching on/off carriers on a very fast basis. This choice is aligned with the broad consensus regarding the time scale at which practical ICIC schemes should operate, as pointed out in [53].

3.4 Proposed Framework

3.4.1 System Model and Problem Formulation

Let a local area network be defined as a set of N femtocells, denoted by $\mathcal{N} = \{1, \ldots, N\}$ operating in a licensed band of $\mathcal{B}$ MHz. The spectrum is divided into a set $\mathcal{C}$ of CCs of cardinality $|\mathcal{C}| = C$. Without loss of generality, let us assume that $BW(c) = \mathcal{B}/C \ \forall \ c \in \mathcal{C}$ and that all CCs experience approximately the same propagation conditions. The problem at hand is then to find – given the topology and the current traffic conditions of the network – the subset $\Lambda(n) \subseteq \mathcal{C}$ of CCs that each cell n may deploy in order to maximize its overall capacity without endangering the less favored users in neighboring cells.

If each femtocell selects at least (but not limited to) one CC from the C available and is able to transmit with P power levels, then there are $(P^C - 1)^N$ different possible combinations. Clearly, some combinations may lead to severe inequities depending on many factors such as the mutual interference coupling among cells, traffic loads, etc. Making matters worse, the number and (un)suitability of combinations are time-varying due to mobility and the spatial- and temporally random bring-up/shutdown order of femtocells. As a result, finding the "best" combination entails a prohibitive computational complexity for all, but the simplest networks; thus methods based on heuristics are often employed.

3.4.2 Overview

The proposed Autonomous Component Carrier Selection (ACCS) concept is a fully distributed, non-iterative and scalable solution based on minimal information exchange between base stations (cells) where each individual low-power base station autonomously makes decisions without involving any centralized network control.

The cornerstone of ACCS is the division of CCs into two femtocell-specific categories as explained in Section 3.4.3. The other two central pillars of ACCS are the so-called Component Carrier Radio Allocation Table (CCRAT) and Background Interference Matrix (BIM). The former is detailed in Section 3.4.4, while the latter is explained in Section 3.4.5. Through these two pieces of information each FAP becomes aware of the existence of other FAPs and the interference conditions in the network. This knowledge is then used in the decision making process.

The proposed ACCS framework introduces a new Radio Resource Management (RRM) entity which deals solely with the CC acquisition rules whenever the need is raised by the independent packet schedulers. Therefore, each CC is eligible for use in any cell provided that certain (parameterized) requirements are satisfied. In other words, ACCS does not explicitly deal with traffic requirements and fairness governing neither the acquisition nor the waiver of CCs. Such requests are expected to come from lower RRM layers. ACCS merely grants or denies such solicitations. In summary, the framework revolves around three fundamental premises:

1. Each FAP always has the right to have at least one active Base Component Carrier (BCC) enabled from the set of possible candidate carriers.
2. For additional capacity, a FAP may choose to enable additional Supplementary Component Carriers (SCCs).

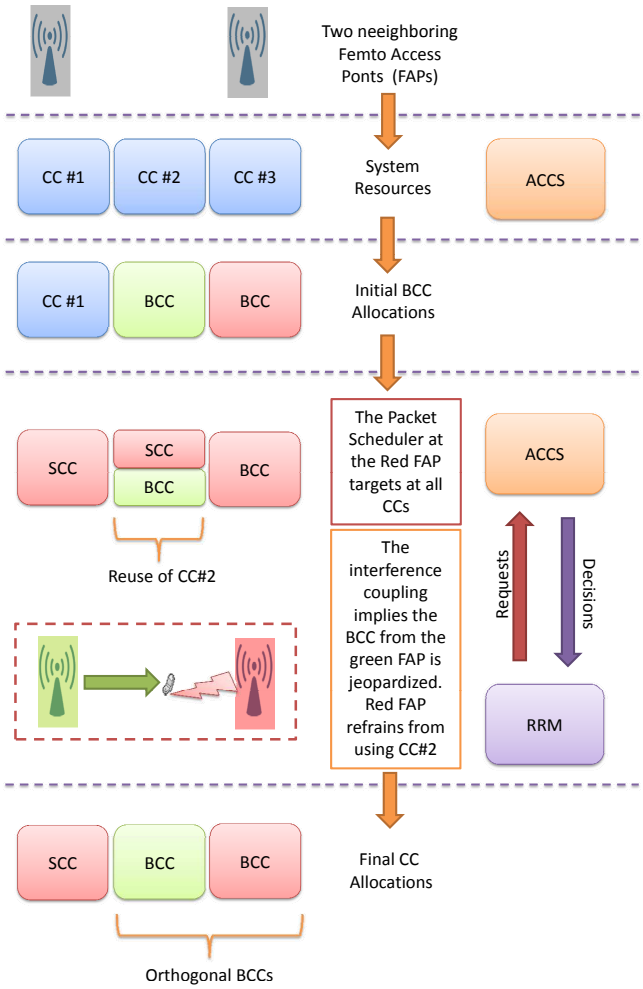

Fig. 3.1: An illustration of the ACCS framewrok in action. Two FAPs make their initial BCC selections. While the green FAP is satisfied with a single CC, the red FAPs needs more spectrum. However, it is able to infer autonomously that this new allocation will disrupt the neighboring cell.

3. A FAP is only allowed to enable additional carriers provided that this does not result in disruptive interference levels towards neighbors currently using the desired carrier.

In special, the last entry is a policy preventing so-called greedy cells from using all the available CCs for their own sake, even when this results in intolerable interference to the neighboring cells. It thus represents a shift from a selfish and opportunist paradigm to a cooperative competition, a.k.a. "coopetition". Cells need to heed their roles as sources of interference and not just mere victims. A notion that was subsequently followed by other contributions in the literature such as those in [91–95]. This idea is analyzed more carefully in Chapter 5.

Figure 3.1 provides a high level illustration of the framework and exemplifies the concept in action. The terminology and actions shall become clearer as the reader goes over the upcoming sections. The forthcoming description follows a conceptual rather than a functional sequence as originally employed in [96]. Although the latter arguably makes up for a smoother flow, it fails to decouple the general framework from the algorithms. For example, the material in the next two chapters, in Appendix A, as well as noteworthy independent work found in [95] build upon the same framework but use different algorithms. Consequently, the two CC categories, the so-called CCRAT as wells as BIMs are introduced first. The selection algorithms coming at a later stage.

3.4.3 Base and Supplementary Component Carriers

Due to the first aforementioned fundamental premise, each femtocell always has one active component carrier, denoted the Base Component Carrier (BCC). The BCC is selected by the femtocell when it is switched on and it is never relinquished. However, the quality of the BCC is constantly monitored and under special circumstances the selection might be reevaluated.

Depending on the offered traffic in the cell and the mutual interference coupling with the surrounding cells, transmission and/or reception on all component carriers may not always be the best solution. It is therefore proposed that each cell dynamically selects additional CCs upon demand (i.e. a second step after having selected the BCC). These extra CCs are referred to as Supplementary Component Carriers (SCCs)[3].

Additional discussions on quality monitoring, temporal aspects of ACCS, and

[3] All component carriers not selected are assumed to be completely muted (uplink/downlink) and not used by the cell.

many other implementation related issues have been included in Appendix B.2. For now, it suffices to clarify that BCCs have absolute priority of over SCCs in order to avoid BCC reselections as much as possible. BCC reselection is equivalent to resetting a cell, a process that inevitably leads to service interruptions. While BCC reselections shall occur over hours or even days, SCCs can be reselected on a much faster basis. Nonetheless, the (re-)selection of CCs occurs over a much longer time span (hundreds of milliseconds up to seconds) and is fairly slow when compared to fast packet scheduling (1 millisecond in LTE).

3.4.3.1 Relation to $\mathrm{P}_{\mathrm{cell}}$ and $\mathrm{S}_{\mathrm{cell}}$

In order to avoid confusion, it is important to stress that the proposed selection of CCs is femtocell-specific, which differs from the UE-specific CC assignment. As explained in [12], the latter implies that the set of CCs a base-station is allowed to use is pre-determined, but UEs can be configured independently. Each served UE must be supplied with a single primary serving CC – denoted *Pcell* – and possibly one or more additional serving CCs, called secondary serving cells (*SCells*) depending on its quality of service (QoS) requirements. Realize that, at least in theory, nothing prevents a SCC from being the *Pcell* for some UEs. Note that the set of CCs employed by UE u is then a subset of the CCs cell n has deployed such that $\Lambda(u) \subseteq \Lambda(n) \subseteq \mathcal{C}$.

3.4.4 Component Carrier Radio Allocation Table

One basic assumption in the ACCS framework is that the current allocation of CCs is signaled amongst cells periodically or whenever the allocation is changed, such that HeNBs know which CCs the neighboring cells are currently using. This information is of critical importance and is summarized in what we refer henceforth as the Component Carrier Radio Allocation Table (CCRAT). Essentially, such tables make femtocells aware of the existence of other femtocells.

The CCRAT consists of pieces of information aggregated by each femtocell via signaling expressing which CCs are currently in use and their respective allocations as either BCC or SCC. Without loss of generality and solely in order to preserve light notation, it is assumed that each femtocell has knowledge about the other $N-1$ cells in the network, understanding that for all distant and undetectable neighbors all CCs can be arbitrarily marked as unused. Notwithstanding, a practical implementation does not necessitate global knowledge.

The CCRAT can then be modeled as a $N \times C$ matrix $\boldsymbol{\Psi}^k = \begin{bmatrix} \boldsymbol{\psi}_k^1 & \boldsymbol{\psi}_k^2 & \dots & \boldsymbol{\psi}_k^C \end{bmatrix}$

where each $N \times 1$ vector $\boldsymbol{\psi}_k^c$ informs the usage – as seen by cell k – of component carrier c by the N cells in network and their respective (if any) PSD reduction. The n^{th} entry of $\boldsymbol{\psi}_k^1$ according to the CC usage is such that:

$$[\boldsymbol{\psi}_k^c]_n = \begin{cases} z_n^c & \text{c is used by cell n.} \\ \Re(z_n^c) = \infty & \text{c is unused by cell n.} \end{cases}$$

Where z_n^c is a complex number whose real part, $\Re(z_n^c)$, represents the Power Spectral Density (PSD) *reduction* (relative to a common maximum PSD) applied by cell n to CC c, while its imaginary part, $\Im(z_n^c)$, is set at 1 if CC c is used as an SCC by cell n or 0 otherwise. Notice that unused CCs are completely muted, hence the infinite PSD reduction in the real part of $[\boldsymbol{\psi}_k^c]_n$. Finally, the usage of complex notation does not imply that the algorithm entails complex operations. Rather, it is employed as mathematical artifice to distinguish the BCCs and SCCs in (3.3)-(3.6) during the SCC selection described in Section 3.5.2.

3.4.5 Background Interference Matrix

Background Interference Matrixs (BIMs) are built via a combination of local and exchanged pieces of information based exclusively on DL UE measurements and play a vital role in the SCC selection algorithm described in Section 3.5.2. The local information essentially predicts the *potential* DL (incoming) C/I experienced by the served UEs; realized when the given pair of cells (serving and interferer) use the same CC at the same time with equal transmit PSD. Similarly, the exchanged information makes cells aware of their individual contributions as *potential* sources of (outgoing) interference. Along the lines of the discussion in the previous section, it can be assumed that each femtocell has knowledge about the other $N-1$ cells in the network, understanding that the predicted C/I ratio can be set at an arbitrary high value for all distant and undetectable neighbors. The latter indicates the lack of interference coupling between these cells.

Each active UE connected to a cell performs measurements of Reference Signal Received Power (RSRP) [97] levels which are reported to its serving cell. These measurements conducted both towards the serving and surrounding cells do not represent an extra burden on the UE side, because such measurements are performed regularly for e.g. handover purposes. Each femtocell (k) then builds a local $M \times N$ matrix $\boldsymbol{\Gamma}^k$, where M is the number of served UEs, and N is the

number of cells in the network. Each γ^k_{mn} entry is given by the ratio:

$$\gamma^k_{mn} = \begin{cases} \dfrac{G_{\{m\}\leftarrow\{n\}}\rho_k}{\eta} & n = k \\ \dfrac{G_{\{m\}\leftarrow\{k\}}}{G_{\{m\}\leftarrow\{n\}}} & \text{otherwise.} \end{cases}$$

Above, $G_{\{x\}\leftarrow\{y\}}$ reflects the composite channel gain[4] between user x and femtocell y. The channel gains can readily be estimated by femtocell k in possession of the information fed back by UE m because the transmission power of reference symbols ρ_k is known a priori (the same in all cells or alternatively signaled between cells). Here, η is the thermal noise power assumed the same for all users.

In order to curb the control signaling overhead, the assumption in [96] is that this local information is first "fused" before being exchanged. Due to the very limited number of users served by femtocells, the proposed data fusion process is rather simple[5]. The $M \times N$ matrix is compressed into a $N \times 1$ (incoming) column vector $\mathbf{i}^k = \begin{bmatrix} i^k_1 & i^k_2 & \dots & i^k_N \end{bmatrix}^T$ such that $i^k_n \triangleq \min(\gamma^k_{*n})$, i.e. each element is taken as the minimum value of the corresponding column of $\mathbf{\Gamma}^k$. Conceptually, this implies that measurements from the UE that will experience the lowest C/I ratio in case of simultaneous usage of the same CC dictate the values that are effectively exchanged. Once mutual information exchange takes place between all pairs of cells – each cell sending and receiving a single quantized value to/from its peer – a second $N \times 1$ (outgoing) column vector $\mathbf{o}^k = \begin{bmatrix} o^k_1 & o^k_2 & \dots & o^k_N \end{bmatrix}^T$ such that $o^k_n \triangleq i^n_k$ becomes available. Finally the $N \times 2$ BIM of cell k is then:

$$\text{BIM}_k = \begin{bmatrix} \mathbf{i}^k & \mathbf{o}^k \end{bmatrix} \tag{3.1}$$

Essentially, a BIM entry is an estimate of Carrier to Interference Ratio (CIR) for a single interferer. For example, for a pair of cells, k and n, the incoming DL BIM of k is denoted $\text{DL}_{\{k\}\leftarrow\{n\}}$ and it is a representative value of the Signal to Interference Ratio (SIR) experienced by UEs at femtocell k if the FAP at n is the only interferer. Conversely, the outgoing DL BIM of k towards n is an appraisal of the CIR measured by UEs at femtocell n, when k is the only interferer. The outgoing BIM is denoted as $\text{DL}_{\{k\}\rightarrow\{n\}}$. Naturally, for a pair of cells the incoming BIM of a cell is the outgoing BIM of the other, thus by definition the following holds:

[4] Averaged over a period of time in order to yield a reasonably accurate estimate.

[5] The same framework can be extended to the context of pico and even macrocells. However, the data fusion process should be adapted.

$$\begin{aligned} DL_{\{k\}\leftarrow\{n\}} &\equiv \mathrm{BIM}_k(n,1) \\ &\equiv \mathrm{BIM}_n(k,2) \\ &\equiv DL_{\{n\}\rightarrow\{k\}} \end{aligned} \tag{3.2}$$

The entire process is illustrated in Fig. 3.2. The first stage – local information gathering – is common in cellular networks. The data fusion part is a research field on its own. It is linked to the filtering and post processing of the collected data in order to attain a meaningful yet compact characterization of the interference coupling among cells. In principle, nothing prevents the same BIM concept from being applied to e.g. picocells, but the data fusion process would most likely need to be changed. Picocells usually serve more users scattered around a larger area than femtocells, and as a result the simple data fusion process employed here is likely to be too restrictive. Finally, the information exchange among cells opens up many new possibilities, such as the novel algorithm developed as a spinoff of this project. It was proposed in [98] and is included in Appendix A.5 for convenience.

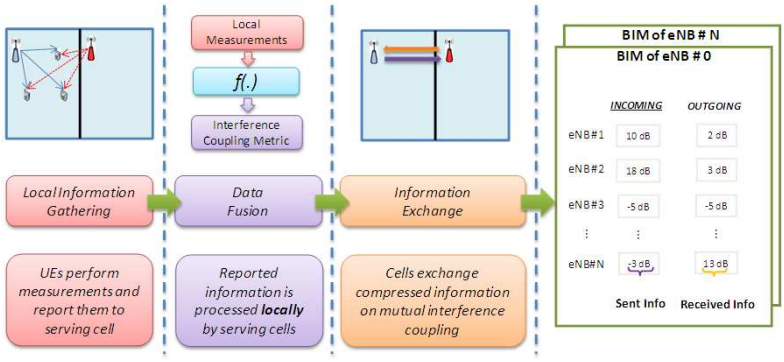

Fig. 3.2: Building Background Interference Matrices (BIMs).

3.5 Basic Selection Algorithms

3.5.1 Base Component Carrier Selection

When a FAP is powered on it needs to select at least a single CC in order to be able to serve UEs and carry traffic. As the HeNB is being initialized, it clearly cannot rely on UE assisted mechanisms. Therefore it shall autonomously select

the carrier based on information sensed, aggregated and processed locally. It is then proposed that each femtocell enters into a Network Listening Mode (NLM) mode immediately after being switched on[6]. In this state, the new entrant performs various DL air interface measurements, which are complemented by inter-cell signaling; thus gathering knowledge about surrounding cells. From this information the CCRAT (Section 3.4.4) is built, wideband UL received interference power, and the path loss to neighboring femtocells is estimated. As a result, after the NLM stage, the following information is assumed to be locally available:

- Neighboring cell indexes (cell IDs).
- Component carrier occupancy of each detectable neighbor as well as information on whether a CC is used as either base or supplementary
- Downlink Reference Signal Transmit (DL RS TX) power which represents the HeNB DL transmit power over reference symbols.
- Path loss estimates towards each neighboring FAP.
- Wideband UL Received Interference Power (RIP) for each CC.

The first three pieces of information make up the CCRAT, while the path losses are estimated based on the proposed inter-cell measurements based on the signaled DL RS TX. It is proposed that new entrants carry out the measurements on the BCCs. Notice that such inter-cell path loss measurements need not be frequent as they are only required by a new eNB when they are switched on.

The proposed scheme is illustrated in Fig. 3.3 with a simple example. There are four existing femtocells, and a fifth one is being switched on. The current selection of BCCs and SCCs is depicted for each FAP with "B" and "S", respectively. Component carriers not allocated are completely muted and therefore carry neither user nor control data.

Given the aforementioned information, a $C \times N'$ matrix similar to the one depicted in Fig. 3.3b is created. The number of columns $N' \leq N$ is not fixed and depends on the number of neighbors that can be detected while C corresponds to the number of CCs into which the total bandwidth is divided (Section 3.4.1). The N' columns (neighbors) are sorted according to the experienced path loss towards the FAP making the initial carrier selection. As depicted in Fig. 3.3b, only neighboring HeNBs within a certain path loss threshold are considered.

[6]In Frequency Division Duplexing (FDD) systems, this implies that HeNBs are able to listen to the DL band as well. Conversely, in Time Division Duplexing (TDD) systems, this is not an additional requirement, since UL and DL use the same band.

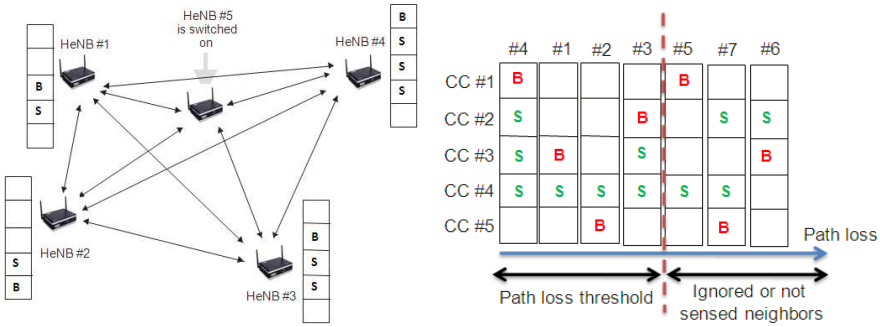

(a) Bootstrapping (b) Matrix

Fig. 3.3: Simple illustration of the Base Component Carrier Selection concept.

Neighboring femtocells with higher path loss are not taken into account as there is either marginal interference coupling, or these simply cannot be sensed. To account for possible errors, neighbors with similar estimated path losses (e.g 1 dB) can later be grouped as one entry. Moreover, whenever a grouping of two detected neighbors sharing the same carrier takes place, the lowest estimated path loss of these two neighbors is decreased, and the column ordering is reevaluated. Solely for simplicity, changes are made in steps of 3 dB. This is done to reflect the fact that two roughly equally strong sources of interference can be as detrimental as one single 3 dB stronger interferer. Based on this matrix, the following procedure for initial BCC selection is proposed:

1. If a fully idle component carrier is available, it will be selected. A fully idle component carrier means that a given row has neither "B" nor "S" entries. Otherwise go to 2.
2. If there are row entries without prior "B" entries, select one of those as base carrier. Select the row entry with the lowest number of "S" occurrences if there are multiple rows without "B" entries.
3. If all row entries include "B", select the component carrier with maximum path loss to the nearest[7] neighboring HeNB having the same component carrier as its BCC.
4. In cases, there are multiple BCC candidates according to the above rules, select the component carrier experiencing the lowest level of uplink interference. In other words, the decision is based on measurements of the uplink wideband received interference power.

[7]The proximity implied here is correlated yet not necessarily physical. Instead it is linked and inversely proportional to the inter-cell path loss as measured by the FAP.

3.5.1.1 A Critical View on the Proposed Algorithm

The problem at hand, i.e. the selection of a single component carrier is an embodiment of the classical frequency assignment problem, which can be mapped into a distributed graph coloring problem. Finding the proper carrier assignment is a combinatorial network optimization problem which has been extensively studied in the last decades. As opposed to the general problem outlined in Section 3.4.1, the search space in this case is smaller (C^N) and even naive methods such as exhaustive search algorithms might be feasible in a centralized case with few femtocells and limited CCs to choose from. Rapidly converging distributed algorithms exist as well. In this respect, the related work in [72] investigates the BCC selection and analyzes the characteristics of the different classes of graph coloring algorithms. The authors show that distributed selection of *conflict-free* BCCs converges with 5 or more CCs.

In principle, the BCC selection could be carried out using any of the algorithms/techniques in the literature. However, it was a deliberate design decision to put forward a simple set of rules aware of the interrelation between BCCs and the short-lived and hence less critical SCC allocations. Another pivotal element precluding the direct application of most distributed algorithms is the need to avoid "recoloring" as much as possible and ideally prevent them altogether as discussed in Section 3.3. The suggested rules assume absolute priority of base over supplementary component carriers and rely on recovery actions to vacate CCs crowded with SCCs, i.e. dig a spectrum hole, since each HeNB must always have at least one CC with full cell coverage. Such recovery actions can be understood as reactive defensive measures not allowing previous and/or potentially erroneous SCC allocations to catastrophically interfere with BCCs.

The inter-cell path loss measurements are used to ensure that only cells with the largest possible path loss separation select the same BCC. This means that FAPs will select a carrier $\hat{c}$ on which the closest node using $\hat{c}$ as a BCC is farthest (from a radio propagation perspective) away. It is worth mentioning that the proposed method was found sensitive to the bring up order of femtocells in case the number of CCs to choose from was 2. However, with more than 3 carriers, the sensitivity was rather small. Such results are documented in [99]. Additional considerations and complementary results are included in Appendix B in order to preserve the logical flow of this text. The analysis therein employs concepts from graph theory and assesses the values of receiver-side information. Additional discussions on the proposed, yet not thoroughly investigated, recovery actions are included there as well.

3.5.2 Supplementary Component Carrier Selection

As stated earlier, ACCS imposes certain constraints for selection of SCCs which basically implies that HeNBs have to take the interference created towards other cells into account. The goal is a flexible yet simple and efficient sharing of the spectral resources that will not prevent one cell from using the entire spectrum when this is a sensible choice. Granting femtocells the ability to "learn" what sensible means is the key aspect here. One of the design targets is to always ensure that the minimum estimated CIR on the BCC equals at least a parameterized ξ_{BCC}. A second goal is to select SCCs in order to maximize the cell throughput, subject to a configurable minimum CIR constraint ξ_{SCC} for users on SCCs. Typically, $\xi_{\mathrm{BCC}} \geq \xi_{\mathrm{SCC}}$ as BCCs are expected to provide full cell coverage, while SCCs could potentially have reduced coverage. It is fair to assume a priori and global knowledge of the aforementioned targets.

Once cell k detects that the capacity offered by its BCC alone is not sufficient to carry the offered traffic, it will use the information found in its CCRAT and BIM (Sections 3.4.4 and 3.4.5) to figure out whether or not the new allocation will jeopardize any existing allocation. The process is fairly straightforward and repeated for each desired CC in the set of candidate CCs $\Lambda^c(k) : \Lambda(k) \cup \Lambda^c(k) = \mathcal{C}$, where $\Lambda(k)$ is the set of component carriers already allocated to cell k.

In essence, for each $c \in \Lambda^c(n)$, femtocell k calculates a set four differences (in dB). These differences can be understood as neighbor and CC specific CIR margins with respect to the CIR thresholds ξ_{BCC} and/or ξ_{SCC}, depending on the CC usage of the interfered neighbor. If there is at least one neighbor using that particular CC for which any of the four margins – or just two in case of asymmetric DL/UL configurations – is found to be negative, that particular CC is not taken into use and another candidate CC is evaluated. Mathematically:

$$\boldsymbol{\Delta}_{\mathrm{dl}}^{\mathrm{inc}}(c) = \Re(\boldsymbol{\psi}_k^c) + \mathbf{i}^k - \boldsymbol{\xi}_{\mathbf{SCC}} \tag{3.3}$$

$$\boldsymbol{\Delta}_{\mathrm{dl}}^{\mathrm{out}}(c) = \Re(\boldsymbol{\psi}_k^c) + \Im(\boldsymbol{\psi}_k^c)\phi + \mathbf{o}^k - \boldsymbol{\xi}_{\mathbf{BCC}} \tag{3.4}$$

$$\boldsymbol{\Delta}_{\mathrm{ul}}^{\mathrm{inc}}(c) = \Re(\boldsymbol{\psi}_k^c) + \mathbf{o}^k - \boldsymbol{\xi}_{\mathbf{SCC}} \tag{3.5}$$

$$\boldsymbol{\Delta}_{\mathrm{ul}}^{\mathrm{out}}(c) = \Re(\boldsymbol{\psi}_k^c) + \Im(\boldsymbol{\psi}_k^c)\phi + \mathbf{i}^k - \boldsymbol{\xi}_{\mathbf{BCC}} \tag{3.6}$$

In (3.3)-(3.6) , ϕ is a scalar defined as $\phi \triangleq \xi_{\mathrm{BCC}} - \xi_{\mathrm{SCC}}$, i.e. the difference in dB between the BCC and SCC CIR thresholds. The vectors $\boldsymbol{\xi}_{\mathbf{BCC}}$ and $\boldsymbol{\xi}_{\mathbf{SCC}}$ correspond to the product of the respective threshold by the $(N \times 1)$ collum vector $\mathbf{1}$ whose entries are all equal to one; thus $\boldsymbol{\xi}_{\mathbf{xCC}} = \mathbf{1}\xi_{\mathrm{xCC}}$. The vectors $\mathbf{i}^k$ and $\mathbf{o}^k$ are the first and second columns of BIM_k respectively as defined in (3.1)

and (3.2). Intuitively, (3.3) means that femtocell k checks whether c is a suitable CC for DL usage as an SCC (*victim of interference*); whereas in (3.4) cell k estimates whether the new allocation entails excessive DL interference towards any of its neighbors (*source of interference*) currently employing the desired CC either as BCC or SCC. The CC usage distinction is based on the imaginary part of the information contained on cell's k CCRAT, which is multiplied by the scalar ϕ. The result of this product provides the required offset to the outgoing BIM CIR estimate, i.e. either 0 (BCC) or ϕ (SCC).

Similarly, (3.5) and (3.6) perform the same verifications for the UL. Notice, however, that the CIR estimates in these cases are rough approximations of the actual UL interference situation based on the measurements mobile terminals have made on the *interfered* side. The reasoning behind this is that incoming/outgoing DL interference propagates through the same path as the outgoing/incoming UL interference and therefore the DL CIR estimates contain correlated and useful information. This aspect is carefully considered in Section 4.4. Finally, the decision to allocate the desired CC is taken locally and can be formally expressed as:

$$\mathrm{DL}_{\mathrm{ok}}(c) = H\left\{\mathrm{sgn}\left\{\min\left[\boldsymbol{\Delta}_{\mathrm{dl}}^{\mathrm{inc}}(c)\right]\right\}\right\} \wedge H\left\{\mathrm{sgn}\left\{\min\left[\boldsymbol{\Delta}_{\mathrm{dl}}^{\mathrm{out}}(c)\right]\right\}\right\} \tag{3.7}$$

$$\mathrm{UL}_{\mathrm{ok}}(c) = H\left\{\mathrm{sgn}\left\{\min\left[\boldsymbol{\Delta}_{\mathrm{ul}}^{\mathrm{inc}}(c)\right]\right\}\right\} \wedge H\left\{\mathrm{sgn}\left\{\min\left[\boldsymbol{\Delta}_{\mathrm{ul}}^{\mathrm{out}}(c)\right]\right\}\right\} \tag{3.8}$$

In (3.7)-(3.8), the symbol $\wedge$ denotes the logical conjunction (AND), min(.) is a function that returns a scalar corresponding to the smallest element of its argument, sgn(.) is the signum function which extracts the sign of a real number. Finally, $H(.)$ represents the discrete form of the Heaviside step function whose value is one for non-negative arguments and zero otherwise. Formal definitions are included in Appendix E.

Using this approach, we ensure that a cell is only allowed to allocate more CCs to the extent where it does not violate the minimum CIR conditions in the surrounding cells. Moreover, if for whatever reason a cell requires just a subset of the set allowed component carriers ζ, the compatible CCs could be ranked and selected according to e.g. the incoming DL margins:

$$\hat{c} = \underset{c \in \zeta}{\arg\max}\ \min\left[\boldsymbol{\Delta}_{\mathrm{dl}}^{\mathrm{inc}}(c)\right]$$

3.6 Proof of Concept Results

This section deals with the potential benefits of the proposed ACCS framework and algorithms. The assessment is based on system-level simulations. It is never enough to remind that the analysis assumes that femtocells operate in a dedicated band, i.e. macro cell and femtocell users are made orthogonal through bandwidth splitting. The investigation encompasses the effects of variable CIR targets and those of spatial density (network topology). The goal is to grasp the behavior of ACCS as a function of controllable (CIR targets) and uncontrollable parameters (density).

The performance figures were generated using the same LTE tool outlined in Section 2.4.1, whose comprehensive description is found in in Appendix D. The simulation scenario is the one described in Section 1.4.3. A single femtocell and all its served user(s) are located inside the same apartment under CSG access mode. Private access is far more challenging than open access from an interference management perspective, yet OSG deployments may also benefit from it as evidenced in Appendix C. The number of UEs served by each FAP was set at 1. Results with variable number of UEs per cell were generated and did not alter the message in any fundamental way. The location of terminals within each apartment is random and uniformly distributed. In the absence of a FAP, a flat contains no active users. Three floors are considered.

The system operates with a 30 MHz bandwidth, the maximum transmission power of a FAP is 100 mW (20 dBm), and 3 dBi antenna gain is assumed. Synchronized TDD with fixed switching point is considered with a equal split between DL and UL, however only the former is considered here, thus assuming decoupled decisions. For simplicity, there is no DL power control, and the total transmission power is evenly divided among the 3 CCs into which the bandwidth is divided. Error Vector Magnitude (EVM) modeling is included (3%), thus SINR is asymptotically limited to 30.5 dB. A simple full-buffer traffic model and a simple round-robin packet scheduler are considered.

The numerical results were obtained as follows. In each snapshot, the deployed femtocells were activated; one at a time in a random sequence. Upon activation each femtocells selects a single BCC according to the rules defined in Section 3.3. The selected BCC is not changed afterwards. In a subsequent stage, after the activation of all cells, femtocells, picked one by one in a random order, attempt to activate additional CCs. Due to the the full load assumption, cells will target at as many SCCs as possible. Naturally, the resulting allocation will depend on the existing allocations of neighboring cells and the interference coupling. The information exchange is idealized, therefore FAPs are aware of previous decisions made by neighboring cells when attempting to activate additional CCs.

Simply put, decisions are never taken simultaneously. This assumption is lifted in Chapter 5. Signaling delays are briefly discussed in Appendix B. In all cases, the collection of results begins once all deployed femtocells have been switched on and had a chance to select SCCs.

Again, all throughput results presented next are normalized by the maximum throughput of the system. Hence, a normalized throughput of 100% implies a transmission over the whole bandwidth with the highest spectral efficiency allowed by Modulation and Coding Scheme (MCS) limitations. This emphasizes the relative trends rather than the absolute values.

Figures 3.4a and 3.4b look into the impact of different CIR targets. The performance of ACCS with 3 sets of CIR targets is compared; starting with aggressive (BCC=5 and SCC=2) and moving towards more conservative values (BCC=15 and SCC=8). These figures assumed a deployment ratio, $\delta = 25\%$, but trends remain the same in sparser and denser topologies. It is clear that more conservative (higher) values tend to shift the lower tail of the SINR distribution to the right. The flip side is seen on the CC utilization which becomes sparser. The SINR distributions for universal reuse and reuse 1/3 are depicted by dashed lines in order to facilitate comparisons and make the trade-offs more evident.

The curves in Fig 3.5 show how both effects displayed in Fig. 3.4 come together to yield the throughput distributions. The upshot is that ACCS retains the benefits of both sparse and tight frequency reuse patterns. In addition to that, by varying the CIR targets one can control the trade-off between average and outage performance in a controllable fashion.

The bar plots in Fig. 3.6 summarize the sensitivity of ACCS with respect to the number of CCs available. The sensitivity of the BCC selection algorithm as well as that of the complete algorithm (BCC and SCC selections) was evaluated in terms of average and outage performance. It is clear from Fig. 3.6a that a higher number of CCs leads to improved outage at the expense of average performance. This is perfectly aligned with the bandwidth/SINR trade-off discussed in Chapter 2 since more CCs to choose from imply narrower CCs[8]. On the other hand, the penalty in terms of average throughput is not observed in Fig. 3.6b at all. This is in perfect agreement with the findings of Fig. 3.5 and is due to the possibility to employ SCCs, thus lifting the hard restriction on bandwidth availability per cell. Moreover, it can be seen that the relative gains in outage performance tend to saturate. This is a good indication that the number of CCs does not need to be very large. In fact, 4 or perhaps even 3 carriers suffice to reap most of the benefits.

[8]The subdivision of 30 MHz into 4 and 5 CCs leads to a non-standard CC bandwidth, but that was neglected at this point since the goal was the assessment of the performance in terms of the degrees of freedom the algorithm enjoyed.

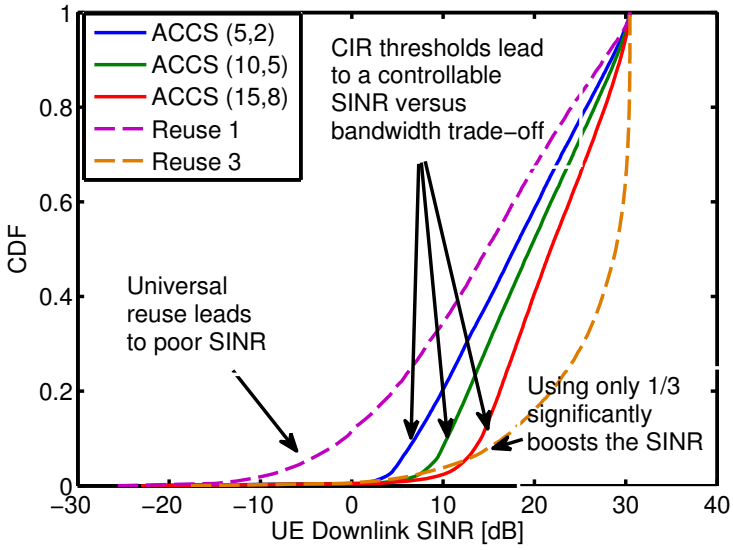

(a)

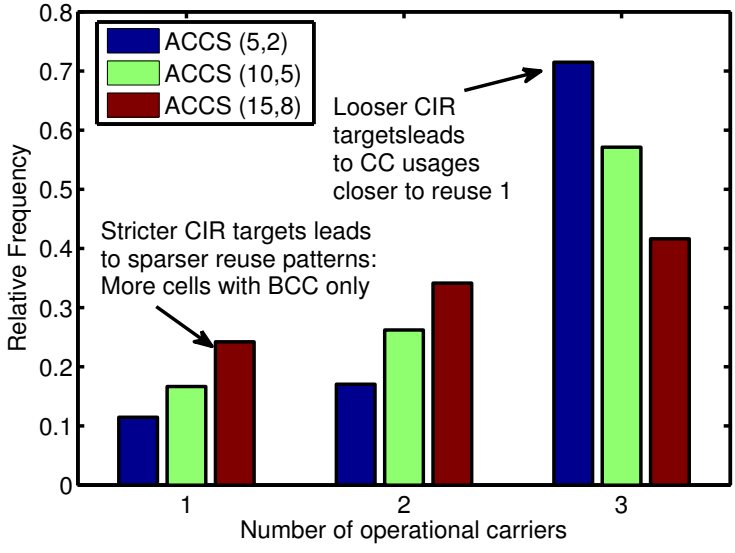

(b)

Fig. 3.4: Analyzing the effect of different CIR targets. The performance of ACCS with 3 sets of CIR targets (BCC,SCC) is compared. (a):SINR distributions for the three sets as well as 2 hard frequency reuse patterns are depicted. (b): CC utilization is shown for the three sets.

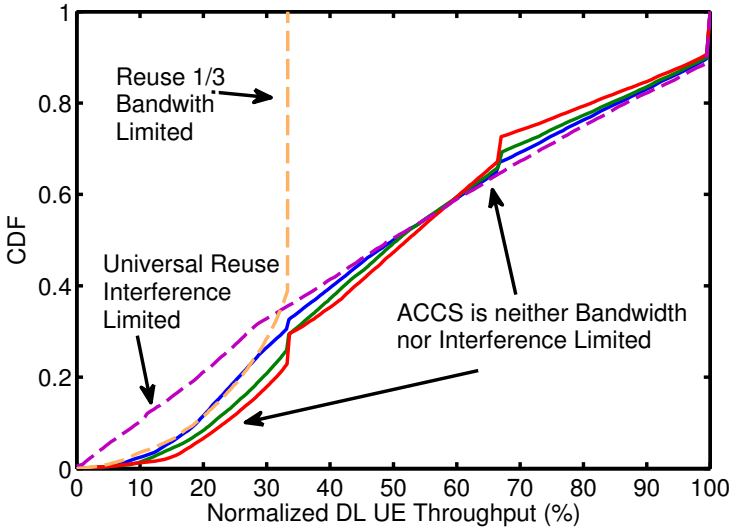

Fig. 3.5: ACCS retains the benefits of both sparse and tight frequency reuse patterns (dashed lines). The three solid lines depict the overall effect of varying the thresholds. By adjusting the CIR targets one can improve the outage performance by shifting the lower tail to the right at the expense of slightly lower average and peak performance.

Figure 3.7 is the key one as it summarizes the results. It depicts how ACCS adapts to the *spatial sparseness* (or alternatively the density) of the network. It should be read as follows: the size of each "bubble" is proportional to the relative improvement in terms of 5% outage performance where the corresponding reuse 1 outage throughput is the benchmark. The color indicates the percentage of the maximum throughput achieved by the best 5% users. While the x and y coordinates correspond to the normalized average and 5% outage throughput values. The lines connecting the dots simply highlight the trends.

Four values for the deployment ratio parameter, δ are considered; varying from 0.25 to 1 in steps of 0.25. The CIR targets assumed the intermediate set of values (BCC=10 and SCC=5). In order to provide a better understanding of ACCS behavior, a similar set of results was generated and included in the figure for two static hard frequency reuse patterns, namely universal reuse and reuse 1/3, labeled as R1 and R3 respectively in Fig. 3.7.

The results clearly show that there are modest gains to be had in the form of average throughput. The greatest potential lies in terms of outage performance, which can be boosted by a factor of 4 or more by sparser reuses at the expense of peak and average performances. This is again in perfect alignment with the

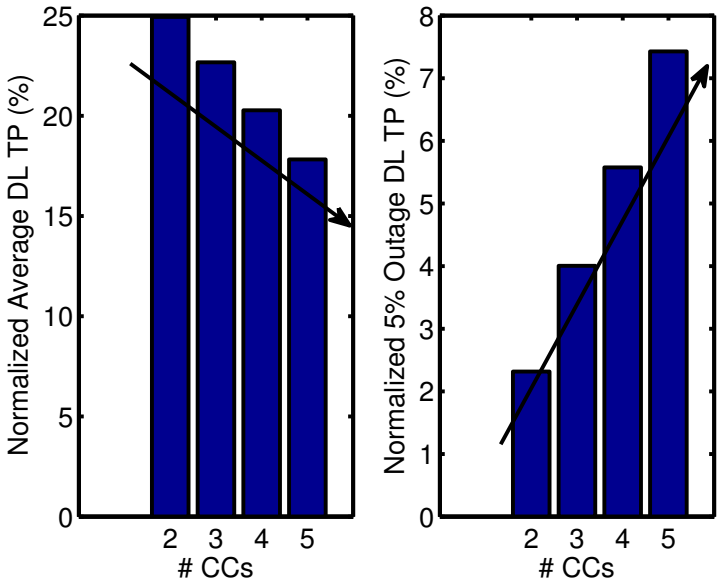

(a)

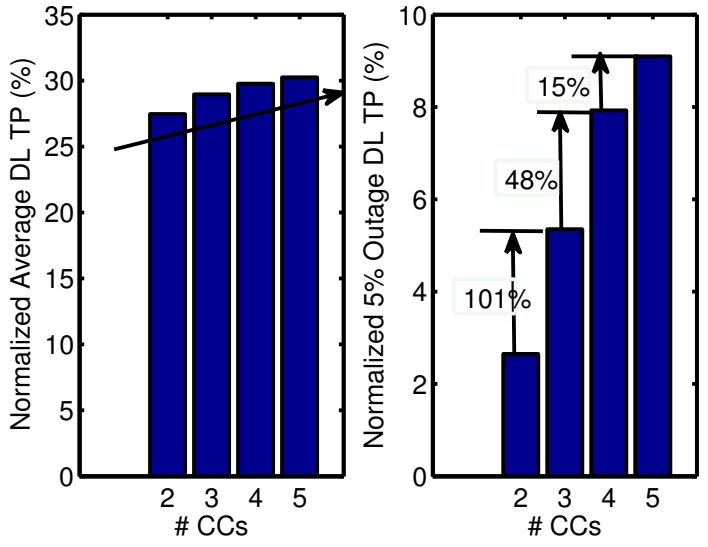

(b)

Fig. 3.6: Analyzing the sensitivity of the algorithm with respect to the number of CCs available for a fixed set of BCC=15 dB and SCC=8 dB CIR targets and 100% deployment ratio. (a): BCC selection only. (b): Complete ACCS.

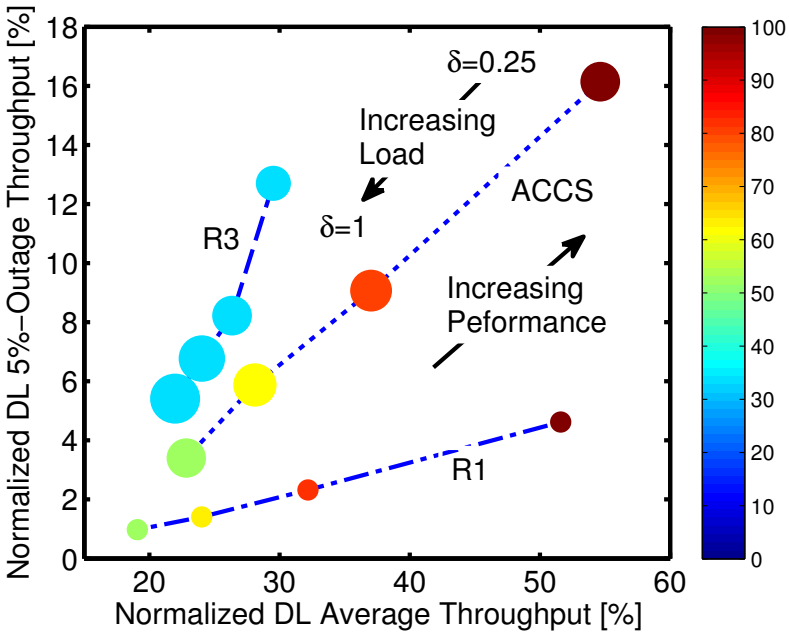

Fig. 3.7: The behavior of ACCS and two hard reuse patterns as a function of network density. The bigger, the darker and the closer to the uppermost right corner the better.

results from Fig. 2.6. In other words, universal reuse is not a bad option when it comes to average and even peak performance, especially in sparser deployments. Nonetheless, reuse one cannot be recommended since it is unfair, and above all, not fail proof due to the significant share of users with SINR values below 0 dB as seen in Fig. 3.4a even though the deployment ratio is 25%. The same goes for reuse 1/3, because a great deal of resources is wasted in sparser deployments.

Where ACCS excels is in its ability to retain the benefits from both sparse and tight frequency reuse patterns throughout the range of density levels. Average and peak throughput values are consistently on par or better than those of reuse 1 as the network gets denser, whereas the outage throughput retains most of the benefits from a sparse reuse pattern. Interested readers can find additional simulation results with different deployment scenarios in [96]. Observations therein lead to the same conclusions, as a result, it is valid to claim that ACCS endows the network with the capability to self-adjust dynamically towards an attractive frequency configuration.

3.7 Conclusions

In this chapter, a simple Autonomous Component Carrier Selection (ACCS) framework for femtocells has been introduced. Simulation results provide evidence that the presented concept successfully adapts to the spatial sparseness of the network, boosting outage user throughput when compared to universal frequency reuse without compromising average and peak user data rates. This renders the system much less sensitive to the density as well as the topology of the network. Hence, ACCS provides a fully distributed (scalable) and self-adjusting frequency reuse mechanism, which allows for uncoordinated deployment of femtocells without prior (expensive & manual) network planning. This result is of significant importance as the expected large scale deployment of HeNBs will call for interference management techniques. Each cell always selects one, and only one, base component carrier. Allocation of supplementary component carriers is possible if and only if the performance impact on neighboring cells is estimated to be acceptable. Apart from the need to standardize the allocation policy and the information exchange processes the concept entails minimal changes to the standard as it relies on existing UE measurement reports. Although merely hinted at in this chapter, the ACCS concept can be further extended to handle interference amongst picocells.

Chapter 4

Applicability to the Uplink of LTE-Advanced

4.1 Introduction

Unlike the preceding chapters, this one is devoted to the specificities of the Uplink (UL). In concrete terms, the previous chapters have claimed and attested that dynamic frequency domain interference coordination is indeed appealing in case of dense and uncoordinated deployments of femtocells. The foregoing Downlink (DL) performance results have supplied empirical evidence that the proposed Autonomous Component Carrier Selection (ACCS) concept is very effective. However, the encouraging DL performance does not automatically imply that ACCS is equally valid in the UL. ACCS considers UL conditions as well, but the decisions rely on DL based approximations. There could be a potential disconnect. For example, while the DL tackles channel and interference variations by means of scheduling and Link Adaptation (LA), the UL employs Fractional Power Control (FPC) to curtail inter-cell interference in Long Term Evolution (LTE) systems. Moreover, the DL is a broadcast channel whereas the UL is a multiple access medium. As a result, the interference range of DL transmissions does not depend on the location of the receiving terminal, this is clearly not the case in the UL. In view of the aforementioned reasons, a careful investigation of the applicability of ACCS to the UL of LTE-Advanced is deemed pertinent.

The description that follows summarizes the main discussions and findings of the aforementioned contributions. This chapter comprises four major blocks, the first one (Section 4.2) provides some background on FPC and discusses the potential mismatch between actual UL conditions and those inferred from DL measurements, in other words it exposes the problem with the Background Interference Matrix (BIM). Subsequently, Section 4.3 is devoted to an understanding of FPC in the context of femtocells. This perception is paramount to provide a decoupled interpretation of the impacts of ACCS and those from FPC. Section 4.4 builds upon the previous one and considers the coexistence of the pristine ACCS concept and FPCon the UL performance of ACCS associated with FPC. The final and novel step is introduced in Section 4.5. The basic ACCS scheme is enhanced to incorporate UL power control information into the carrier selection procedure in order to minimize the additional incurred signaling and to capitalize on Power Spectral Density (PSD) variations simultaneously. In its most general formulation, the suggested approach facilitates User Equipment (UE)-specific Component Carrier (CC) configurations in femtocells. Finally, Section 4.6 closes this chapter and points to future studies.

4.2 Preliminaries

4.2.1 Open-loop Fractional Power Control

Power Control (PC) is one staple element of modern cellular networks. It is used to keep the transmission power within a desired range according to certain criteria, normally linked to ensuring a required Signal to Interference plus Noise Ratio (SINR). Therefore, power control improves the overall system performance and yields power savings. LTE systems employ Fractional Power Control (FPC). In its simplified form, i.e. excluding closed loop and Modulation and Coding Scheme (MCS) power boosting correction factors, the total UE transmit power, expressed in dBm is given by [100]:

$$P_{TX} = \max\{P_{\min}, \min\{P_{\max}, P_0 + 10\log_{10} M + \alpha L_u^s\}\}, \tag{4.1}$$

where $P_{\min}$ and $P_{\max}$ are the minimum and maximum UE transmit powers respectively – typically -30 and 23 dBm – , P_0 is a UE-specific parameter, M is the number of Physical Resource Blocks (PRBs) assigned to a certain user, α is the cell-specific path loss compensation factor, and L_u^s is the DL path loss measured by UE u towards its serving cell based on the transmit power of the reference symbols [63]. This approach clearly decreases the transmit

power of cell-edge users much more intensely than cell-center ones. The main idea behind FPC is to make users with higher path loss operate at lower SINR requirements [101]. The rationale is that users with high path losses tend to be far away from their serving base stations and thus near neighboring base stations, therefore being probable sources of UL interference in macrocells. This point is revisited in Section 4.3, but in the context of femtocells.

Observe that the transmit PSD, i.e. the power per PRB, is independent of M and depends solely on the path loss to the serving cells[1]. As a consequence, for any UE pair (i, j) : $\text{PSD}_i \geq \text{PSD}_j \Leftrightarrow L_i^s \geq L_j^s \, \forall \, i, j$ provided that (i) P_0 and α are the same and (ii) the UEs are not power limited due to the combination of large values of M and L_u^s. The former is typically the case. The latter is also a valid assumption since UEs connected to femtocells, with all likelihood, will not become power-limited due to the very small cell radius. For simplicity, it is furthermore considered that any given femto-UE employs the same transmit PSD on all active CCs, according to (4.1). In other words, P_0 is UE- rather than CC-specific, and all CCs are on the same band and thus experience (roughly) equal path losses.

4.2.2 The Problem with BIMs

As explained in Section 3.4.5 BIMs are built based on DL measurements exclusively. In possession of this information, cells estimate their individual contributions as both victims (incoming) and sources of (outgoing) interference. The BIM information essentially predicts the Carrier to Interference Ratio (CIR) experienced whenever two cells use the same CC at the same time with equal transmit PSD values.

Unfortunately, it is not straightforward to build BIMs locally based on UL measurements directly. The difficulty lies in identifying the individual interference contributions[2] from each UE in neighboring cells. This occurs because the UL receiver at the Femto Access Point (FAP) only measures the total aggregate interference power. As a result, ACCS uses DL information to infer the UL conditions. A potential workaround is presented in [91]. Nonetheless, the pitfall therein is the substantially heavier inter-cell signaling. Moreover, the proposed solution also fails to consider the UEs transmit power settings in its estimation of the UL CIR, something whose importance will become particularly clear in the discussion that follows and especially in Section 4.5.

[1] Observe that the total mobile transmit power does vary as a function of M, the assigned number of PRB.

[2] This knowledge enables the outgoing interference estimation.

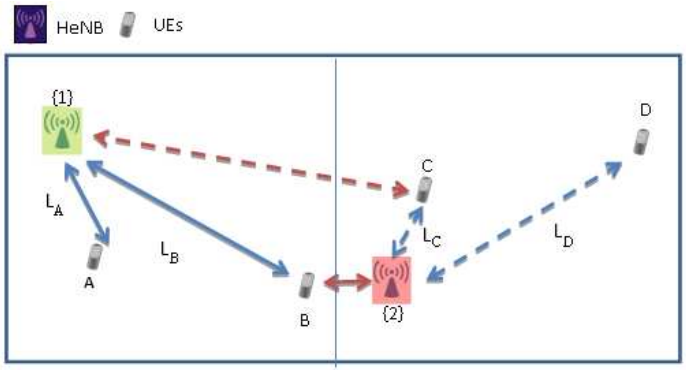

Fig. 4.1: Simplified scenario illustrating how worst case DL and UL C/I values are estimated.

Figure 4.1 helps us visualize the limitations of ordinary BIMs. For simplicity, just two Home enhanced NodeBs (HeNBs) {1}–{2} and four UEs (A–D) are considered; understanding that the example can be extended to incorporate additional terminals and/or cells. Taking HeNB {1} as the reference cell, the solid lines show the links (signal in blue and interference in red) used in the determination of the DL incoming BIM, hereafter denoted by $\mathrm{DL}_{\{1\}\leftarrow\{2\}}$. The dashed lines show the links involved in the determination of the DL outgoing BIM of cell {1} – gathered, fused and signaled back by HeNB {2} – denoted as $\mathrm{DL}_{\{1\}\rightarrow\{2\}}$. In this example, path loss measurements conducted by UEs [B] and [C] account for the exchanged incoming/outgoing information respectively as these are the users experiencing the lowest CIR values in Fig. 4.1 (Refer to Section 3.4.5 for details).

When it comes to UL carrier selection, the original ACCS makes the following two assumptions (See Section 3.5.2):

$$\mathrm{UL}_{\{1\}\leftarrow\{2\}} \approx \mathrm{DL}_{\{1\}\rightarrow\{2\}} \tag{4.2}$$

$$\mathrm{UL}_{\{1\}\rightarrow\{2\}} \approx \mathrm{DL}_{\{1\}\leftarrow\{2\}} \tag{4.3}$$

ACCS thus explicitly assumes that the worst-case UL incoming ($\mathrm{UL}_{\{1\}\leftarrow\{2\}}$) carrier to interference ratio is well approximated by the outgoing ($\mathrm{DL}_{\{1\}\rightarrow\{2\}}$) ratio. Similarly, the worst-case UL outgoing ($\mathrm{UL}_{\{1\}\rightarrow\{2\}}$) is approximated by the DL incoming ($\mathrm{DL}_{\{1\}\leftarrow\{2\}}$) ratio. This is due to the fact that the interference paths (red arrows) are the same, just in the opposite direction (channel reciprocity).

Clearly, not all UL desired signals (blue arrows) are being considered; hence the worst-case approximation in e.g. (4.3) is only valid if the path loss of the "farthest" UE is similar to L_C^2. As it can be seen, the latter is not verified in Fig. 4.1, because $L_B^1 \gg L_C^2$. This inevitably leads to e.g. an optimistically biased UL incoming CIR estimate as seen by [B]. Furthermore, since UEs typically use transmit power control, they will employ different power spectral densities, rendering the estimation even less accurate.

4.3 Performance of Fractional Power Control in Femtocells

The material in this section momentarily strays from ACCS in order to analyze the specific traits of FPC in the context of femtocells. Such digression is important because to the author's best knowledge there were no contributions in the literature prior to [102] taking into account the impact of FPC in local area deployments. The proper understanding of FPC in femtocell deployments allow us to decouple its effects from those of ACCS.

The performance figures were generated using the same LTE tool outlined in Section 2.4.1 whose comprehensive description is found in Appendix D. Two values for the deployment ratio parameter are considered, namely $\delta = 25\%$ and $\delta = 75\%$. In the absence of a FAP, a flat contains no active users. By default, a single floor is assumed; hence a scenario with up to 40 densely deployed femtocells is simulated. Both HeNBs and UEs are dropped uniformly at random positions. All users are located indoors assuming 1 UE per flat under Closed Subscriber Group (CSG) access mode. Co-channel interference from macro-cells is not considered in this study, or equivalently macro and femtocells operate in separate frequency bands. Lastly, proof-of-concept results consider 3 CCs, akin to the material in Section 3.6. Section 4.5.1 provides results for a 5-CC system. Table 4.1 summarizes the most important parameters.

In the following, UL performance results for the average user (cell due to single user assumption) and the 5% outage user throughput values are presented. All results are normalized with respect to the case where plain frequency reuse 1/1 is assumed (i.e. all cells use all 3 CCs), and no UL power control. The latter implies that UEs always transmit at their maximum power level (23 dBm).

However, before proceeding to the results per se, let us re-examine some of the key distinctions between macro and femtocells and how they affect the underlying assumptions behind FPC as mentioned in Section 4.2.1. Results shall be analyzed in the light of such differences:

Table 4.1: Assumptions for system-level simulations

System Model		
Spectrum allocation	3 CCs of 5 MHz each	
EVM	3%	
eNB parameters	Receiver noise figure	8 dB
	Antenna system	Omni (3dBi)
UE parameters	Max. TX power	23 dBm
	Min. TX power	−40 dBm
	Antenna system	Omni (0dBi)
Duplexing scheme	TDD	UL: 50%
Scenario Model [22]		
Home	Room size	10m x 10m
	Street width	10 m
	Internal walls	5 dB attenuation
	External walls	10 dB attenuation
	HeNB position	Uniform (Indoor)
Propagation Model [22]		
Minimum coupling loss	45 dB	
Shadowing std. deviation	Serving Cell	4 dB
	Other Cells	8 dB
Traffic Model		
User distribution	Uniform: 1 user/cell (Indoor)	
Data generation	Full buffer	

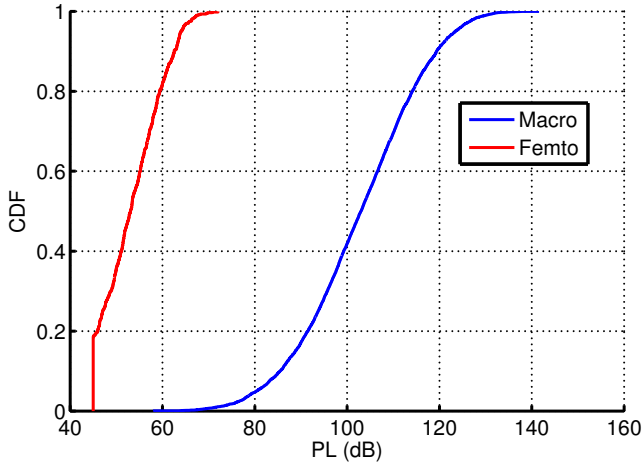

Fig. 4.2: Comparing the path loss distribution to the serving cell in Macro and Femto deployments. The macrocell case was generated assuming the 3GPP Macro-1 scenario corresponding to an inter-site distance of 500 m [63].

- In local deployments, so-called cell-edge users are **not** necessarily the main causers of UL interference[3].
- Interference coupling can be much more severe than in macro cells, sometimes "catastrophic".
- Path loss to serving cell distributions are much more compact than those found in macro cells as exemplified in Fig. 4.2.

It is worth stressing that such differences become even more pronounced in case of CSG deployments due to the fact that the cell selection procedure is not based on signal strength.

Figure 4.3 summarizes the relative performance results of FPC in local area deployments. The upper figures (Figs. 5.2a and 5.2b) refer to a very dense network, where HeNBs are present in $\delta = 75\%$ of the apartments. In the bottom (Figs. 4.3c and 4.3d), the deployment ratio, δ, equals 25%. Results for frequency reuse patterns 1/1 and 1/3 are shown on the left and right hand side figures, respectively. When reuse 1/3 is considered, each HeNB uses only one of the three CCs available. Curves are presented for different values of the FPC

[3]The work in [103] shows that the assumption that the users with lowest path gain generate most of the interference is not always true even for macrocells, especially in a three-sectorized cell layout with correlated shadow fading

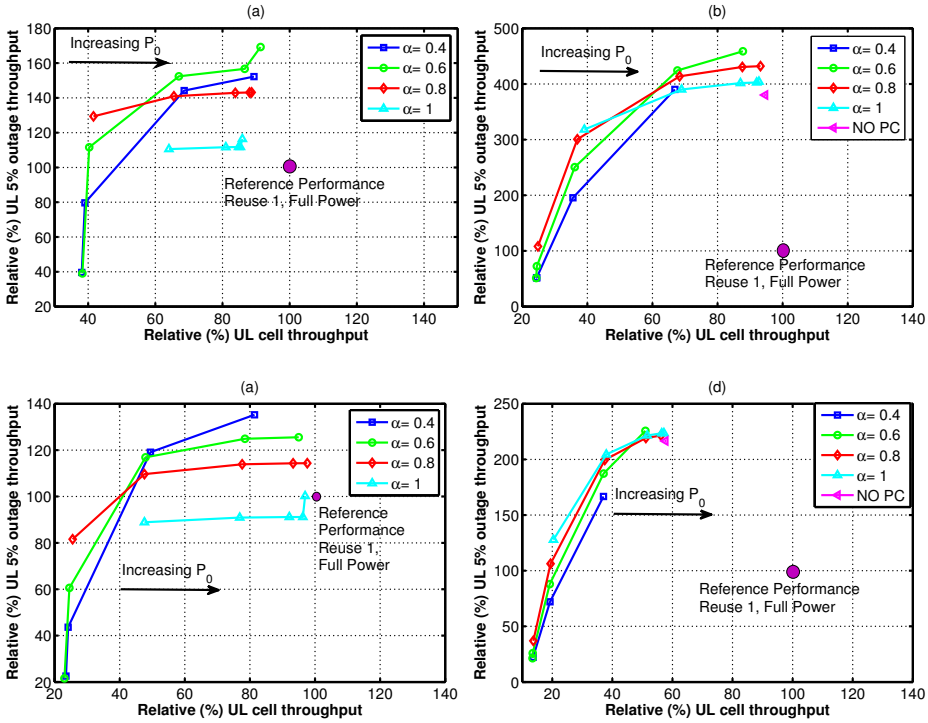

Fig. 4.3: Relative performance of FPC under different deployment conditions: (a) Reuse 1/1 and $\delta = 75\%$; (b) Reuse 1/3 and $\delta = 75\%$; (c) Reuse 1/1 and $\delta = 25\%$; (d) Reuse 1/3 and $\delta = 25\%$. Conclusion: FPC improves outage but always degrades average performance in femtocells.

parameter α, where each point of the curves corresponds to different values of P_0 in the range $[-100, -90, -80, -70, -60]$ dBm. All cells employed the same set of FPC parameters (P_0 and α), which together with the path loss between a UE and its serving cell, L_u^s, determine the transmitted PSD.

From these results it is observed that a proper FPC parametrization clearly results in better outage performance (as compared to no PC). Nonetheless there is a price to be paid as it *always* resulted in losses in terms of average cell throughput for the considered configurations. For example, losses in average throughput in the order of $(5 - 75)\%$ are seen in Figs. 5.2a and 5.2b. These results differ diametrically from those reported in [101] for macrocells, where FPC translated a small penalty in cell-edge throughput into a gain in average cell capacity. This behavior was not observed on any of the simulated configurations, even though a wide range of parameters was swept under several different frequency reuse

patterns and deployment ratios[4].

It is relevant to stress that in uncoordinated deployments, particularly in CSG residential scenarios, forcing UEs farther from their serving cell to power down more intensively is not always the most sensible strategy. A strong interfering UE might be close to its serving HeNB while generating strong UL interference to a neighbor just on the other side of the wall. Therefore one of the crucial assumptions behind FPC does not hold. This helps us grasp why it was not possible to observe a statistical improvement in overall performance.

Moreover, in the dense deployment, it can be seen that applying a simple 1/3 frequency reuse pattern with no power control delivered much better relative performance figures (380% vs 170%, respectively) for the same 5% average cell capacity loss when compared to the best FPC setting – $P_0 = -60$ and $\alpha = 0.6$ – under reuse 1/1. This effect is explained by the strong interference coupling, made even worse by CSG deployments, due to potential proximity of interfering devices, which cannot be entirely mitigated by means of power control. In sparser deployments, where only 25% of the FAPs were active, and interference is a bit less of a problem, results indicate that hard frequency reuse was less effective than FPC. The outage performance remained poorer (137% vs 217%), but average cell capacity was substantially less compromised due to the availability of the entire spectrum (57% vs 99%).

In general, one can conclude that despite the minor performance hits in terms of average throughput values, FPC can, when properly configured, deliver gains in terms of coverage and particularly power savings due to sensibly lower transmission power levels as observed in Fig. 4.4.

Finally, the previous results lead to the observation that a fully flexible and truly self-adjusting scheme is likely to require flexible adaptation capabilities in both power and frequency, in our case CC, domains. This idea is explored in Section 4.5 and more notably in Chapter 5 where this concept is applied in the DL to enrich the ACCS concept.

[4]Results shown in [101] and [104] do mention the possibility of optimizing the parameters to achieve improved cell-edge performance at the expense of average cell capacity similarly to the results presented here.

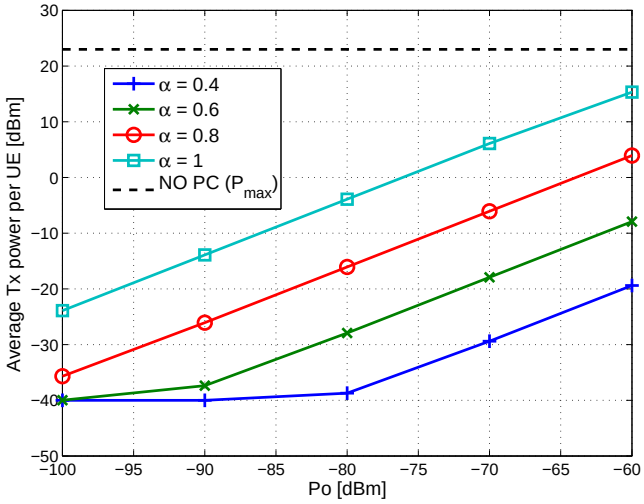

Fig. 4.4: Average total UE transmitted power for various FPC parametrization sets, assuming 1 UE per active cell and reuse 1/1. FPC leads to considerably lower transmit power levels.

4.3.1 Impact on the SINR Distribution

As explained in [101], as long as UEs do not become power limited, the experienced SINR per PRB, denoted γ, can be expressed in dB as:

$$\gamma = P_0 + (\alpha - 1) \cdot L \ - \text{IoT} - N \tag{4.4}$$

where N is the thermal noise power, and Interference over Thermal (IoT) is calculated as the ratio of interference plus thermal noise over thermal noise. For simplicity, if one assumes a constant level of interference and noise[5], the experienced SINR distribution is directly obtained as a scaled and shifted version of the path-loss distribution according to the FPC parameters. In this case, the expected value $E[.]$ and variance Var(.) of γ will be respectively given by:

$$E[\gamma] = (\alpha - 1) \cdot E[L] + P_0 - \text{IoT} - N \tag{4.5}$$

[5]In a real system, the IoT ratio is a function of P_0 and α as well. This dependency dampens the direct effect these parameters would have on the SINR distribution. For example, a global increase in P_0 boosts the received signal, but it also raises the total interference level.

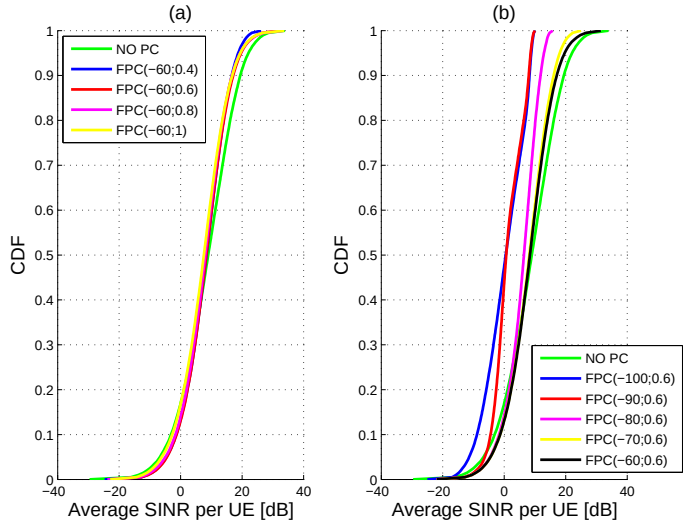

Fig. 4.5: CDFs of uplink SINR (a) for fixed $P_0 = -60$dBm and (b) for fixed $\alpha = 0.6$ compared to no power control under universal frequency reuse. One can observe that P_0 is the dominating factor affecting the average SINR.

$$\mathrm{Var}(\gamma) = (\alpha - 1)^2 \cdot \mathrm{Var}(L) \tag{4.6}$$

From (4.5) and considering that the path loss (L) distribution in femtocells is normally much more compact than those of macrocells as seen in Fig. 4.2, one can see that the value of P_0 is the dominating factor in terms of average SINR and consequently in terms of average cell performance. This can be inferred from Fig. 4.3 and becomes explicit in Fig. 4.5 through direct comparison of the left and right figures. The left figure depicts SINR distributions for a fixed $P_0 = -60$ dBm and variable α, while the figure on the right side shows curves for variable P_0 given a fixed $\alpha = 0.6$. In both cases, reuse 1/1 and $\delta = 75\%$ are assumed.

Notice that for high values of P_0 such as -60 dBm, the SINR distribution becomes nearly insensitive to the value of α. Nonetheless, lowering α spreads the distribution and allows for some improvements in the 5% percentile, which naturally leads to improved outage throughput as seen in Fig. 4.3. The dominance of P_0 becomes even more prominent at high α values since the variance of SINR is further decreased (4.6). In this case, the higher the value of P_0, the closer the performance becomes to that of the case without power control.

4.4 Uplink Performance of ACCS with Fractional Power Control

After considering the characteristics of FPC in the context of femtocells, the focus returns to ACCS and its performance associated with UL FPC. The associated questions are very simple: Can an unmodified (non-FPC aware) version of ACCS coexist in harmony with FPC? Are performance gains additive? Cutting to the chase, Fig. 4.6 undoubtedly answers the question and shows that ACCS concept works in the UL as well. And although the performance results shown in Fig. 4.6 assumed coupled decisions, i.e. symmetric UL/DL CC allocations, the same trends were observed when independent decisions were considered. The interested reader is refereed to Appendix B.3 and [105]. The main conclusion of the aforementioned paper is that even though DL-based C/I estimations are not perfectly accurate representatives of actual UL C/I values, potential performance discrepancies can be roughly compensated by properly setting the Base Component Carrier (BCC) and Supplementary Component Carrier (SCC) CIR thresholds, ξ_{BCC} and ξ_{SCC} respectively.

The numerical results were obtained as follows. In each snapshot, the deployed HeNBs were activated; one at a time in a random fashion, and a single BCC had to be selected without any UE-side information. The selection was based on the previous decisions made by other HeNBs as explained in Section 3.5.1. The subsequent phase of the simulation iterated over all active femtocells in a random order and an attempt to select SCCs is carried out. The estimated CIR thresholds were set at $\xi_{\mathrm{BCC}} = 15$ dB and $\xi_{\mathrm{SCC}} = 8$ dB.

Only full-buffer traffic is considered. Two deployment ratios have been simulated: $\delta = 25\%$ and $\delta = 75\%$, although results for the former are not depicted, because they led to the same conclusions. Results are presented for several different FPC parameterizations. In addition to the four curves (one for each α), Fig. 4.6a also includes three additional points: two corresponding to the performance of hard frequency reuse schemes with fine-tuned parameters from the previous section. These point are marked by a black cross and an orange star. The third point represents the UL performance of ACCS without FPC, marked by a magenta triangle. The performance benchmark is the same one used in Fig 4.3, namely universal frequency reuse without FPC.

It is observed that ACCS alone performs far better than the fine-tuned static reuse patterns, both in terms of both outage and average performance, boasting 316% and 26% relative performance gains respectively. In addition to that, when FPC is enabled, using a proper parametrization ($P_0 = -60$ dBm and $\alpha = 0.8$) the 5% outage performance of ACCS is boosted even further. Compare

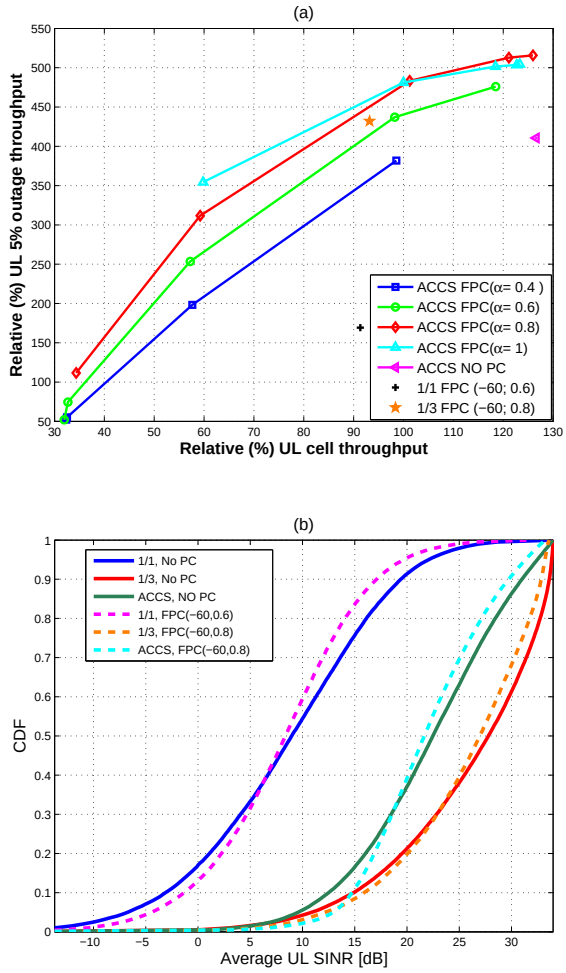

Fig. 4.6: Relative performance comparison with 75% of home eNBs active: (a) ACCS under FPC versus reuses 1/1 and 1/3 with fine-tuned FPC parameters and (b) Uplink SINR distributions with and without FPC. It can be stated that ACCS not only works in the UL, but it is also perfectly compatible with power control even without an explicit FPC awareness.

the magenta triangle with the uppermost red diamond. In fact, similarly to the results in Section 4.3, the combination of high P_0 and α values proved to be very attractive in all simulated cases, including those of sparser deployments ($\delta = 25\%$) not depicted here. Figure 4.6b complements the discussion by exhibiting the resulting SINR distributions for ACCS and hard reuse patterns 1/1 and 1/3. The solid curves depict the variants without FPC while the dashed show the corresponding performance with fine-tuned FPC parameters. The 5^{th} percentile gains are evident $(1-3)$ dB at the lower tail of the distributions.

Although the discussion in Section challenged the UL applicability of ACCS, the aforementioned results provide strong empirical evidence of its efficacy. Nonetheless, it is valid to try and evaluate what occurs if UL information is incorporated into the carrier selection procedure in order to exploit the inherent PSD variations. This is the subject of the next section, where a decentralized scheme yielding actual UL information is proposed. The proposed concept entails limited additional signaling requirements and in its most general formulation, the method facilitates UE-specific component carrier configurations in femtocells.

4.5 Enhanced Uplink Component Carrier Selection Scheme

UE-specific component carrier configuration, as explained in Section 3.4.3.1, is already possible in LTE-Advanced systems. As a matter of fact, the authors of [106] evaluate the performance gains that can be achieved by using Carrier Aggregation (CA) in the UL of LTE-Advanced systems by taking the effect of UE power limitations into consideration. Nonetheless, the evaluation therein is entirely based on macro-cells, where the limitation of UE transmission power might affect negatively the gains brought by multi-CC transmission. The distinction between power-limited and non-power-limited UEs and the subsequent CC and power allocations are based on the path loss to the serving cell. Notwithstanding, UEs, with all likelihood, will not become power-limited in a femtocell due to its small cell radius. Consequently, uplink CA decisions should be based on another metric in the case of femtocells, especially if inter-cell interference mitigation/coordination is taken into consideration.

The discussion in Section 4.3 made it clear that FPC is an integral part of LTE systems. Despite its ability to deliver gains in terms of outage performance, FPC alone may not suffice, and CC-based Inter-Cell Interference Coordination (ICIC) schemes, such as ACCS can boost the performance much further as shown in the previous section. However, ACCS did not fully explore the possibilities opened

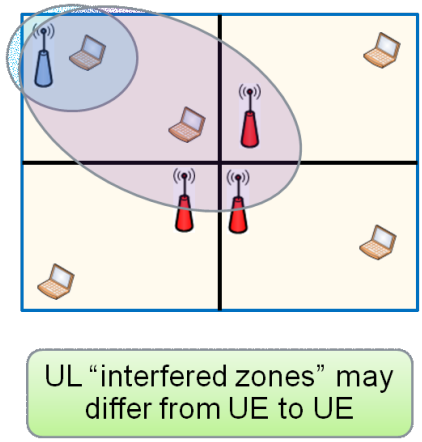

Fig. 4.7: A conceptual illustration of the different interference zones of different terminals. A FPC aware version of ACCS could explore the fact that some UEs can use certain CCs that other cannot.

by FPC, namely the differences in terms of transmit PSD. Firstly, the areas affected by UL interference generated by UEs will have a smaller radius than those created by non-power-controlled UEs. Secondly and more importantly, the “interference radius” will be UE, hence location dependent. The concept is illustrated in Fig. 4.7.

Yet, ACCS could simply not exploit this fact, since the information on the BIM assumes that both cells (serving and interferer) transmit with equal PSD. And to make matters worse, the DL-based information results in inaccuracies as described in Section 4.4. However, these inaccuracies can be fixed or at least toned down by realizing that DL interference coupling information can be adjusted according to differences in terms of transmit PSD and path loss differences of a small and upper bounded number of UEs to yield better approximations. This is accomplished by means of two equations described next:

$$\mathrm{UL}_{\{s\}\leftarrow\{n\}} \approx \mathrm{DL}_{\{s\}\rightarrow\{n\}} - \Delta(L_i, L_j) + \Delta(\mathrm{PSD}_i, \mathrm{PSD}_j) \tag{4.7}$$

$$\mathrm{UL}_{\{s\}\rightarrow\{n\}} \approx \mathrm{DL}_{\{s\}\leftarrow\{n\}} + \Delta(L_k, L_l) - \Delta(\mathrm{PSD}_k, \mathrm{PSD}_l) \tag{4.8}$$

The interpretation of (4.7) and (4.8) is made easier by exemplification. Resorting to Fig. 4.1 and assuming that HeNB $\{1\}$ is performing the evaluation; one would thus set $\{s = 1\}$ (serving) and $\{n = 2\}$ (neighbor) in the foregoing formulae, where $\Delta(x, y) \triangleq x - y$

The first $\Delta(.,.)$ terms in (4.7) and (4.8) account for the path loss difference between UEs (i, j) and UEs (k, l) towards their respective serving cells. If the transmit PSDs were identical for all UEs, these terms would suffice to provide correct UL information based on DL inputs. The PSD $\Delta(.,.)$ factors in (4.7) and (4.8) account for the transmit PSD differences between UEs (i, j) and UEs (k, l), respectively. If all UEs had equal path losses towards their serving cells, this factor would again suffice to correct possible imbalances in terms of transmit power per CC. In general, both corrections are needed and the UEs involved in the estimation are:

- UE (i) is the UE, among the ones served by HeNB $\{1\}$, with the largest path loss towards it, in this example UE [B]. This UE is potentially the worst victim of incoming UL interference.
- UE (j) is the UE responsible for cell's $\{1\}$ $\mathrm{DL}_{\{1\}\rightarrow\{2\}}$, i.e. cell's $\{2\}$ $\mathrm{DL}_{\{2\}\leftarrow\{1\}}$. This is the UE served by HeNB $\{2\}$ that is potentially the worst source of UL interference towards HeNB $\{1\}$ – in this example, it corresponds to UE [C].
- UE (k) in (4.8) is the one responsible for cell's $\{1\}$ $\mathrm{DL}_{\{1\}\leftarrow\{2\}}$, i.e. the worst source of outgoing uplink interference towards HeNB $\{2\}$. In this case, it is UE [B] as well $(k = i)$, but this is *not* necessarily always true. Either way, this has no impact in terms of signaling since UEs (i, k) are served by the same evaluating cell.
- Finally, UE (l) is analogous to UE (i), in that it is the UE with the largest path loss towards its serving cell $\{2\}$ and hence the worst potential victim of outgoing interference, in our example: UE [D].

The PSD and path loss pieces of information pertaining to UEs (j, l) must be signaled by cell $\{2\}$ as it cannot be known otherwise by cell $\{1\}$. However, as explained in Section 4.2.1, the PSD values can easily be calculated locally by cell $\{1\}$ if P_0 and α – which are normally the same for all cells and set a priori by the operator – are known. This limits the burden of additional inter-cell signaling to at most two path loss values irrespective of the number of UEs served by the femtocells. Once the UL interference coupling is estimated based on the proposed adjustments to the DL information, a more refined decision on whether to take a CC into use can be made.

A last, yet important remark, is that readers should notice that the two values given by (4.7) and (4.8) still characterize all UE and, as such, they provide cell-pair specific values, not UE specific estimations. In other words, when deciding ACCS uses the same UL information for all UEs within a cell. The distinction shall become clear in the upcoming section.

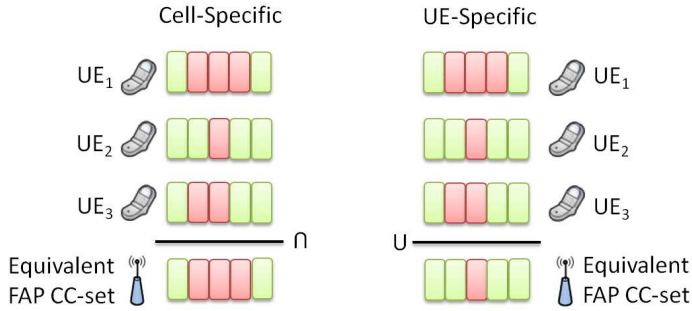

Fig. 4.8: Conceptual difference between cell- and UE-specific variants of ACCS. In the former (left), the resulting CC allocation is the set intersection of the permissable allocations of its served UEs, as opposed to the set union in the latter (right). Green blocks represent the allowed CCs.

4.5.1 User Specific Uplink Component Carrier Selection

It has just been stated that the decision to take a CC into use in a cell may be made on a UE basis given some DL BIM corrections. This can be done by extending the previous pair of equations to allow for UE-specific CC usage evaluations. The concept enables HeNBs to identify, for each of its served UEs, the set of CCs that can be used given the current CC allocation of neighboring cells. Subsequently, it would be up to the Packet Scheduler (PS) within the host HeNB to effectively distribute the radio resources of the permissable CCs according to any internal metric.

The merit of this approach is that from the perspective of the HeNB the resulting CC allocation becomes the set union of the allocations of its served UEs as opposed to the set intersection when (4.7) and (4.8) are utilized. Figure 4.8 illustrates the difference between these two approaches. Once again let us examine Fig. 4.1 to understand how this can be accomplished. Let us assume, due to the topology and the radio propagation conditions, that UEs [A] and [C] can potentially use the same UL CCs while UEs [B] and [D] cannot. ACCS would be able to tell UEs apart if equations (4.7) and (4.8) are extended as follows:

$$\mathrm{UL}_{u\leftarrow\{n\}} \approx \mathrm{DL}_{\{s\}\rightarrow\{n\}} - \Delta(L_u, L_j) + \Delta(\mathrm{PSD}_u, \mathrm{PSD}_j) \tag{4.9}$$

$$\mathrm{UL}_{u\rightarrow\{n\}} \approx \mathrm{DL}_{u\leftarrow\{n\}} + \Delta(L_u, L_l) - \Delta(\mathrm{PSD}_u, \mathrm{PSD}_l) \tag{4.10}$$

Similar to the reasoning presented previously, an interpretation of (4.9) – (4.10)

is given next. Using u as an index to distinguish individual UEs, then $\mathrm{UL}_{u\leftarrow\{n\}}$ and $\mathrm{UL}_{u\rightarrow\{n\}}$ represent the conditional UL incoming/outgoing CIRs for UE u if it reuses the same CC that is currently being used in neighboring cell $\{n\}$ (in this example, cell 2). One distinction between equations (4.9) – (4.10) and the previous pair of equations is the fact that u-th UE-specific PSD_u and path loss (towards the host cell),L_u, are considered in (4.9) and the use of $\mathrm{DL}_{u\leftarrow\{n\}}$ in (4.10). The latter is the ratio of path gains towards the serving and neighboring n cells as measured by UE u.

UEs (j, l) in (4.9) – (4.10) are the same ones used in (4.7) – (4.8) because there is no straightforward way for one cell (e.g. the host HeNB {1}) to know whether UE will be interfering with either UE [C] or [D] in the other cell, since that depends entirely on the packet scheduling carried out independently by HeNB {2}. All HeNB {1} knows – via the Component Carrier Radio Allocation Table (CCRAT) – is that a certain CC is currently in use in the UL in another cell. Therefore, in order to ensure that most detrimental reuse of resources does not take place, the most severe interferer/interfered UEs are still used in the estimations, namely UEs [C] and [D].

Finally, it is worth stressing that proposed idea differs from UL channel aware scheduling in that, when HeNB {1} schedules e.g. UE [B], it can take into account the interference this allocation generates towards existing allocations in HeNB {2}.

4.5.2 Performance Evaluation and Discussions

Finally, it is time to assess the performance of the proposed enhancements to compare them with the canonic ACCS. Moreover, in order to attain more general results, the basic simulation assumption described in Section 4.4 were extended to encompass multi-floor buildings. Now, each building consists of 3 floors, thus totaling 120 apartments. It is assumed that HeNBs are deployed in 75% of them. The number of available CCs has also been extended to 5.

Initially, a single UE/cell is considered, in which case equations (4.7) – (4.8) and (4.9) – (4.10) are fully equivalent. The cell-specific path loss compensation factor, α, was the same in all cells and varied from [0.2, 0.8] in steps of 0.2.

Figure 4.9 compares the average UL SINR achieved by the original ACCS scheme with that of the proposed method. The 0% to 10% outage region is highlighted for clarity. It can be seen that corrections are much more relevant for low α values where the imbalance between DL and UL estimations increases. The behavior can be understood if one realizes that, if P_0 is fixed and equal in all

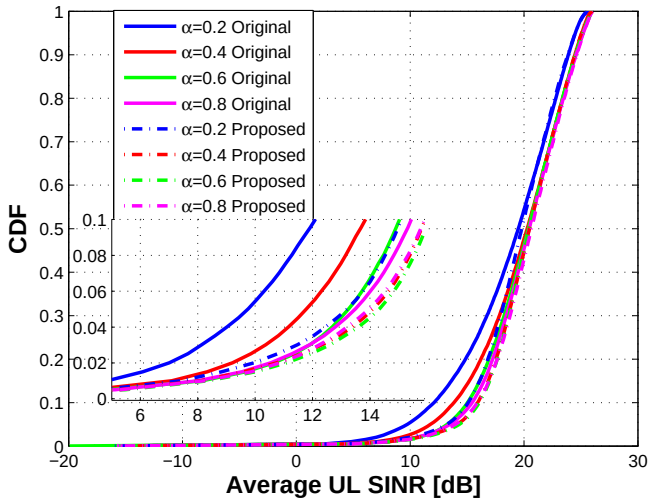

Fig. 4.9: UL SINR comparison between the original ACCS and the proposed UL FPC aware variant for various values of α.

cells, then (4.9) – similarly for (4.8) – reduces to:

$$\mathrm{UL}_{u\leftarrow\{n\}} \approx \mathrm{DL}_{\{S\}\rightarrow\{n\}} - \Delta(L_u, L_j)(1-\alpha) \tag{4.11}$$

Figure 4.10 complements the SINR information from Fig. 4.9. It can be seen that the share of UEs who have access to at least 2 CCs increases when compared to the original case. The increase in spectral availability combined with the SINR improvement has led to the relative gains in outage throughput seen in Fig. 4.11. The same figure also makes it evident that the biggest potential of the proposed scheme lies in the 5% outage throughput. Relative gains of up to 52% are seen with respect to the original ACCS concept. Recall that in the non-FPC-aware version, the UL CIR estimations are taken from (4.2) and (4.3).

Moreover, Fig. 4.12 compares the CC usage when cells serve multiple (3) UEs per cell. Since now the effective CC usage per cell is the set union of the CC usage of its served UEs, one can see that cells reuse CCs more aggressively when compared to UEs. The differences are expected to be even larger if the path loss distribution to the serving cell presents high variance. The analysis is purposefully limited to the CC distribution, because the actual user throughput figures are heavily dependent on the scheduling decisions, which are beyond the scope of this contribution. For example, the internal packet scheduler could

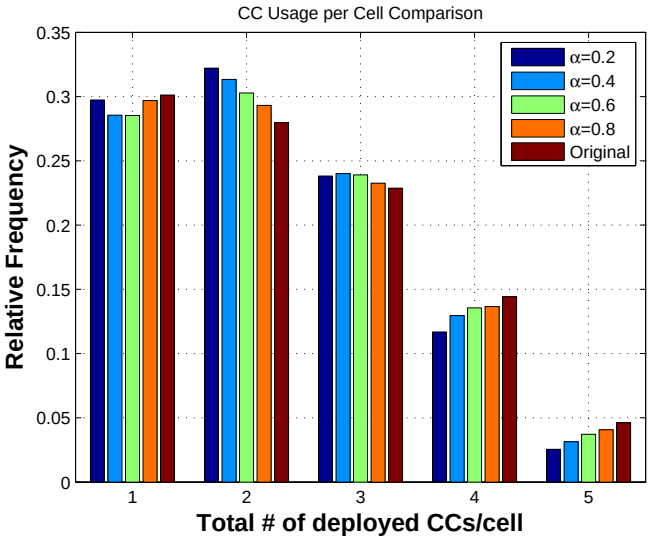

Fig. 4.10: Histogram of the component carrier usage per cell for various values of α as well as the original ACCS concept.

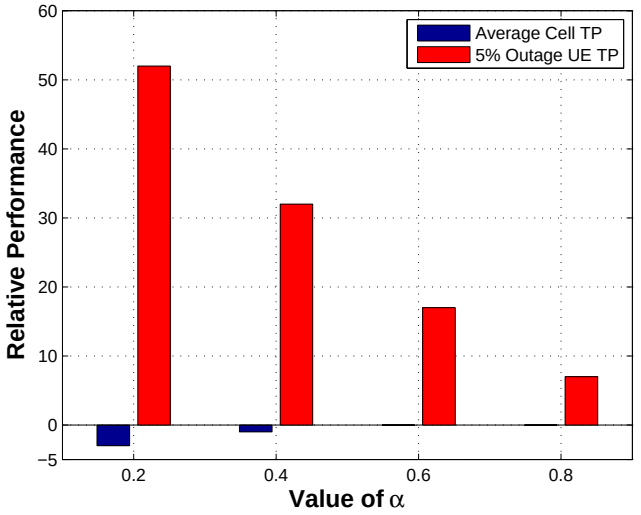

Fig. 4.11: Relative performance comparison between the original ACCS and the proposed UL FPC aware method for various values of α.

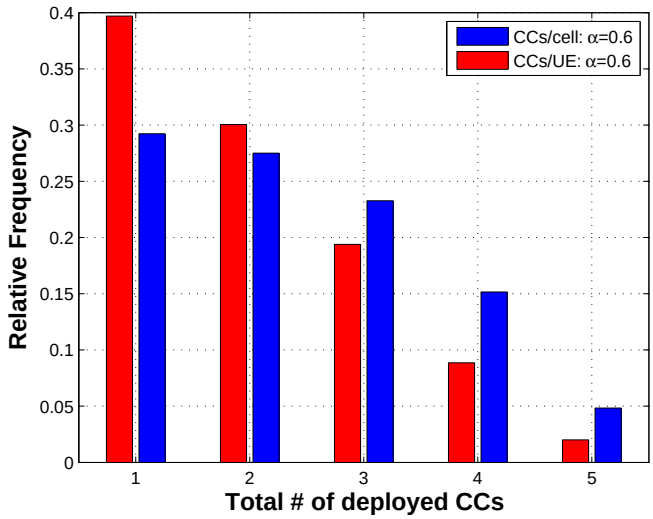

Fig. 4.12: FPC-aware ACCS: Histograms comparing the component carrier usage per cell and per UE for a fixed value of α in a deployment with multiple UEs per cell.

either try to increase fairness among its served UEs or boost the peak and average data rates.

Finally, it can be stated that the refinement of DL based information combined with the introduction of PC awareness improves the performance of the baseline ACCS concept, especially in terms of UL outage performance. One can thus conclude that the concept works at least in theory. Nonetheless, some self-criticism is never harmful. Most of the benefits were seen at very low α values. In fact, 0.2 is not even supported in 3GPP specifications. Complicating matters further is the observation that FPC leads to improved performance in local area deployments when α and P_0 are set at high values. The previous observations throw cold water on the proposed method by limiting its applicability.

In summary, in can be stated that the relative importance of corrections and consequently the utility of the method is high in the presence of significant PSD imbalances such as those due to radically different path loss distributions or different values of P_0. Nevertheless in very small cells, such as those assumed in the simulations, given the empirical evidence, and the recommended FPC settings, it is safe to claim that the unmodified version of ACCS is an excellent compromise.

4.6 Conclusions

The deployment of LTE-Advanced femtocells will pose new challenges in terms of interference management and efficient system operation. This uplink-centric chapter started off by investigating open-loop Fractional Power Control (FPC) in the context of dense-urban residential deployments, commonly referred to as femtocells, under closed subscriber group access mode and highlighted the differences with respect to macro cells.

It has been shown that any parametrization combining high values of P_0 and α ranging from 0.6 to 0.8 proved to be effective; leading to power savings, improved coverage and minor average throughput losses. Nonetheless, the same set of results led to the observation that a fully flexible and truly self-adjusting scheme is likely to require flexible adaptation capabilities in both power and frequency domains.

In view of this, additional results illustrating the applicability of the proposed ACCS concept in the UL have been presented. These have clearly shown that ACCS operates well in the presence of FPC, providing attractive UL gains, both in terms of 5% outage performance and average cell throughput. Notice, however, that UL performance improvements are achieved even though ACCS decisions are chiefly based on information collected from DL measurements. At least in principle, further improvements should arise from the inclusion of UL-specific knowledge in the decision process.

The last part of this chapter was devoted to such UL enhancements. A novel scheme was proposed and evaluated. It is shown that incorporating limited UL information to the baseline ACCS concept boosts the performance in terms of 5% outage throughput, especially in the presence of severe PSD imbalances. However, the results attained indicate that such imbalances tend to be rather modest in small cells, notably when the recommended FPC settings are employed. As a result, it can be concluded that the canonic ACCS, albeit chiefly based on DL measurements, is an extremely valid solution for the UL as well.

Investigations in scenarios with radically different path loss distributions among cells, such as those seen in heterogeneous networks are suggested for future studies. It is interesting to add that although the proposed scheme accounts for and capitalizes on inherent PSD differences stemming from FPC, it does so in a rather passive fashion. A more proactive approach would involve using the available information to set UE-specific parameters, such as P_0, in order to comply with the CIR targets imposed by ACCS, hence enabling CC allocations that would otherwise not be permitted. The next chapter entertains a similar idea, albeit in the DL.

Chapter 5

Variable Traffic and Generalized ACCS

5.1 Introduction

Chapter 3 described the framework proposed in this thesis facilitating dynamic spectrum assignment in uncoordinated femtocell deployments. Results therein have shown that the Background Interference Matrix (BIM) based Autonomous Component Carrier Selection (ACCS) method successfully captures and adapts to the spatial distribution of devices making up the "pseudo-random" network. In this respect, ACCS provides an automatic and fully distributed mechanism for dynamic frequency re-use on a Component Carrier (CC) resolution for Long Term Evolution (LTE)-Advanced.

Nonetheless, the original concept was designed with fully loaded networks in mind, which is clearly a worst-case scenario. Yet, the nearly unpredictable temporal traits of traffic – varying from light loads to near full-buffer – are elements that should not be overlooked when designing future-proof solutions for the next generation of femtocells. In this chapter, ACCS is extended (generalized) to adapt to traffic variations over time. The outcome, referred to as Generalized Autonomous Component Carrier Selection (G-ACCS) retains the virtues of the original method and, in many aspects, represents one step towards future cognitive networks. G-ACCS abandons the ordinary approach that would attempt

to track the bursty nature of packet-switched traffic, in favor of one where the power domain is opportunistically employed to overcome the potential restrictions imposed by CIR targets. As a matter of fact, the proposed idea does away with fixed thresholds yielding a truly autonomous technique. This is a consequence of relying on spectral efficiency estimation techniques instead of simple thresholds.

Although, the principles presented in this chapter are applicable in the Uplink (UL) as well, the work focuses on the Downlink (DL) due to the usual traffic asymmetry. Special attention is given to time-varying traffic, modeled by exponentially distributed arrivals of fixed size sessions. In what follows, Section 5.2 sets the scene with the assistance of a simple, yet insightful numerical example. Section 5.3 contains the main contribution of this chapter: G-ACCS is introduced alongside the pertinent nomenclature, the design principles and a detailed algorithm description. Sections 5.4 and 5.5 consist of an extensive comparative performance assessment. In the former, the simulation methodology is introduced; the latter presents the results and puts the findings into perspective. Finally, Section 5.6 concludes this chapter.

5.2 Variable Traffic and The Case for Cooperation

This section introduces a simple numerical analysis which will be used throughout this chapter to (i) provide intuitive explanations and (ii) to highlight the need for collaboration in local area deployments. The upshot is that selfish behavior by one cell can be utterly disruptive to neighboring cells depending on traffic and topology conditions.

The basic scenario is shown in Fig. 5.1. It consists of 2 Closed Subscriber Group (CSG) femtocells $\{A, B\}$, each cell serving a single User Equipment (UE), $\{\alpha, \beta\}$, respectively. For simplicity, let us assume that both cells share a single (spectral) resource – e.g. a component carrier – each with a (temporal) activity factor denoted by $0 < P_x \leq 1, x \in \{A, B\}$.

Although both cells have, at least in principle, equal rights to use the spectral resources, highly asymmetrical (unfair) situations may arise due to the uncoordinated nature of femtocell deployments. Let us begin by quantifying in (5.1)-(5.2) the value of selfishness relative to perfect cooperation (ideal interference

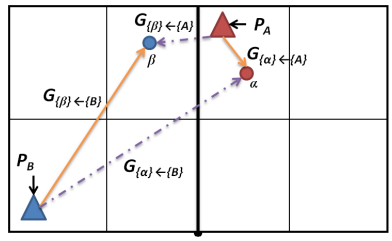

Fig. 5.1: An example of a highly asymmetrical deployment of two CSG femtocells. The solid and dashed lines represent signal and interference channel gains respectively. Circles represent UEs, while triangles represent the femtocells.

avoidance) as perceived by cells A and B, respectively.

$$\Xi_A \triangleq \frac{P_A P_B \, \varepsilon_A \, \mathrm{C_{MAX}} + P_A(1-P_B)\, \mathrm{C_{MAX}}}{\min\{P_A; \max[(1-P_B); 0.5]\}\, \mathrm{C_{MAX}}} \tag{5.1}$$

$$\Xi_B \triangleq \frac{P_B P_A \, \varepsilon_B \, \mathrm{C_{MAX}} + P_B(1-P_A)\, \mathrm{C_{MAX}}}{\min\{P_B; \max[(1-P_A); 0.5]\}\, \mathrm{C_{MAX}}} \tag{5.2}$$

The equations can be interpreted as follows: the numerators in (5.1)-(5.2) estimate the attained DL throughput in the absence of coordination. As such, P_A and P_B act as independent transmission probabilities. The resulting throughput of cell x is then given by a weighted sum. $\mathrm{C_{MAX}}$ – the highest achievable throughput due to Modulation and Coding Scheme (MCS) limitations – is achieved when there is no collision. Logically, in case of simultaneous transmissions, cell x attains only a topology dependent fraction, ε_x, of it.

On the other hand, the denominators quantify the achieved DL throughput when transmissions are always forced to be orthogonal. In this case, each cell cannot have an activity factor higher than 50% in general. The exception being the case where one cell's activity can be fully or at least partially accommodated due to modest resource needs of its neighboring cell, i.e. an ideal white-space filling strategy is assumed.

In summary, ratios higher than one imply that a cell benefits from no coordination whatsoever. Conversely, ratios smaller than one signify that the cell would favor a cooperative (orthogonal) approach even if that means capping its activity. Now, coming back to Fig. 5.1 and observing the existing asymmetry coupled with the CSG premise, the following is assumed: $\mathrm{DL}_{\{A\}\leftarrow\{B\}} =$

$G_{\{\alpha\}\leftarrow\{A\}}/G_{\{\alpha\}\leftarrow\{B\}} = 20\text{dB}$ and $\text{DL}_{\{B\}\leftarrow\{A\}} = G_{\{\beta\}\leftarrow\{B\}}/G_{\{\beta\}\leftarrow\{A\}} = -5\text{dB}$. Thus, numerically:

$$\varepsilon_A \triangleq C_{A|B}/\text{C}_{\text{MAX}} \approx 0.74 : C_{A|B} = \mathcal{S}\left(\text{DL}_{\{A\}\leftarrow\{B\}}\right)$$
$$\varepsilon_B \triangleq C_{B|A}/\text{C}_{\text{MAX}} \approx 0.06 : C_{B|A} = \mathcal{S}\left(\text{DL}_{\{B\}\leftarrow\{A\}}\right)$$

Here $\mathcal{S}(.)$ is a monotonically increasing function that maps C/I into spectral efficiency and $C_{X|Y}$ denotes the throughput achieved by cell X when cells X and Y have colliding transmissions. In our example, $\mathcal{S}(.)$ is an adjusted Shannon formula proposed in [64] for LTE. The curve fitting parameters were taken from tables 3 and 4 of the same paper. Nonetheless, the evaluation remains equally valid if the theoretical bounds for channel capacity [45] are used. The only three constraints are:

- Thermal noise is negligible and inter-cell interference is treated as noise by receivers.
- Below a minimal Signal to Interference plus Noise Ratio (SINR), the achieved throughput is zero because UEs are not even able to synchronize with their serving cells.
- Due to practical MCS limitations, the achievable throughput does not increase indefinitely with SINR.

The outcome is shown in Figs. 5.2a and 5.2b as a function of the activity factors P_A and P_B. The color indicates the value of $(\Xi_x - 1) \cdot 100$. The line segments in Figs. 5.2a and 5.2b demarcate the convex hull of the region where nodes have a strict preference for selfish behavior. Fig. 5.2a shows that cell A has a weak predisposition for cooperation when its activity is low. However, when P_A goes beyond 60%, the inclination towards selfishness is extremely strong. The achievable throughput due to selfish behavior is nearly twice as high as that attained by cooperating. Conversely Fig. 5.2b depicts that cell B strongly favors cooperation with the exception of a minuscule region where its activity ratio is nearly 100%, and cell A is rather inactive. Nonetheless, if cell A decides to seek its own benefit, cell B is virtually helpless and loses nearly all of its capacity as the numerator in (5.2) approaches zero in a very wide area of Fig. 5.2b. Briefly, Fig. 5.2 conveys two important messages:

- Selfish approaches might be optimal if sum-capacity is the metric of interest; notwithstanding, if fairness and outage-capacity are to be taken into account, cells – especially CSG ones – need to mind their surroundings.

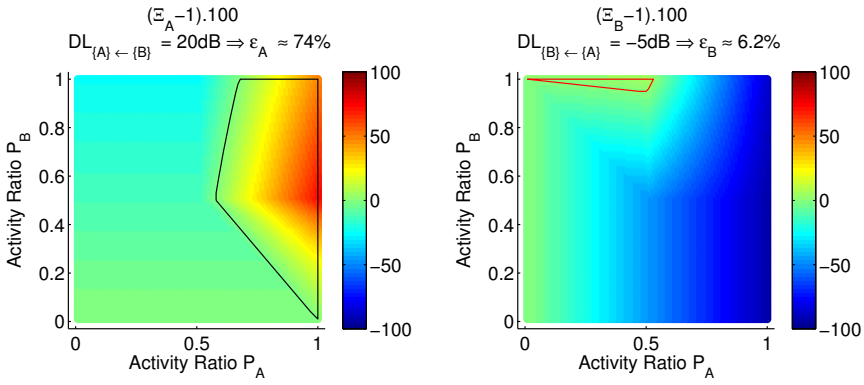

(a) (b)

Fig. 5.2: Relative value of selfishness with respect to perfect cooperation aiming at orthogonal transmissions: (a) $(\Xi_A - 1) \cdot 100$ and (b) $(\Xi_B - 1) \cdot 100$.

- Network topology essentially governs the interaction of cells, yet the activity patterns affect the perception cells have of their environment.

The first aspect is taken care of by BIMs, which render femtocells aware of the underlying network topology. Nonetheless, BIMs rely on expected rather than actual interference levels, i.e. interference coupling under full buffer. This means that the second aspect is not explicitly accounted for. Acknowledging that this approach can lead to overestimation of interference when the resources are not fully utilized, the material in the next section presents a solution that leverages the power domain to tone down the potential underuse of resources.

5.3 Generalized ACCS (G-ACCS)

In the basic ACCS concept introduced previously each CC is eligible for use in any cell provided that certain parameterized Carrier to Interference Ratio (CIR) requirements are satisfied. However, the CIR constraints cells are required to adhere to during Supplementary Component Carrier (SCC) selection may act as an overprotective limitation, especially when the rapid varying nature of packet switched is considered. Recap that BIMs reflect the interference coupling when $P_A = P_B = 100\%$ in the model discussed in Section 5.2. Consequently, the interference estimations will be off, unless the CC is fully utilized. As a result, resources that could otherwise be utilized are actually wasted.

Efficient utilization of CCs is relevant because in dense urban environments, the number of femtocells competing for additional resources may be much higher than the total number of CCs available, normally between 3 to 5. Consequently some cells might be unfavorably treated and become bandwidth limited due to potentially overprotective constraints if thresholds are set at high values. Conversely, if such thresholds are too permissive, the protection of unfavored UEs becomes less effective when the traffic intensity approaches that of full-buffer model. A straightforward approach is to track and respond to the actual SINR conditions yielding adaptive CIR targets. Unfortunately, adapting to temporal traffic variations compounds the inter-cell signaling and is quite challenging in a fully distributed framework due to inherent signaling delays. Therefore another smoother alternative was sought.

5.3.1 Outline of G-ACCS and Overall Targets

The original idea was extended to deal effectively with the time-domain related aspects of CC selection. In summary, the proactive usage of the information found in the BIMs to set the Power Spectral Density (PSD) of a desired CC autonomously is proposed. The goal is to provide a balance between the minimization of the outgoing interference and the usefulness of a given CC. Ultimately, the CC allocation rules are softened, the distribution of SCCs becomes less sensitive to the temporal evolution of the bandwidth acquisition/waiver process, outage performance is not sacrificed, and no additional parameters or inter-cell signaling are required. Furthermore, it should be appreciated that whilst the upcoming description is primarily concerned with the DL situation, the same principle can also be employed in the UL.

5.3.2 Conceptual Description

The proposed scheme retains the first-come first choice service policy of ACCS, but allows cells selecting their CCs later on to try and allocate new CCs provided that these cells reduce their PSD in order to minimize the outgoing interference towards the cell currently holding that CC. The cell which currently holds a particular CC is referred to as a *prior cell*. The cell which tries to deploy the same CC later on is denominated a *posterior cell*. In cognitive radio jargon [83], the prior femtocell acts as the primary device, while the posterior femtocell plays the role of a cognitive secondary radio.

In essence, G-ACCS embodies and extends the logical Table 5.1 to deal with combinations where setting the ideal PSD is non-obvious. The rationale is the

Table 5.1: The rationale behind G-ACCS

Loss (prior cell)	Yield (posterior cell)	Posterior cell action
Critical	Does not matter	Does not deploy CC
Moderate	High enough	Sets PSD properly and deploys CC
Negligible	Does not matter	Deploys CC

following. If the prior cell has very little or nothing to lose in terms of capacity, the posterior cells should allocate the CC even if the yield is low due to incoming interference. Conversely, if the prior cell is estimated to experience a critical capacity loss due to outgoing interference, the posterior cell shall refrain from allocating the CC irrespective of its potential capacity gain. The method then attempts to maximize the capacity of both posterior and prior cells under two restrictions[1]:

(a) Prior cells have higher priority and shall never incur capacity losses larger than the potential capacity gain attained by posterior cells.

(b) Posterior cells are the only cells performing power reductions. The PSD of prior cells remains unchanged and posterior cells utilize this assumption.

It is also very important to notice that such denominations are not absolute. After playing the role of a posterior cell when trying to deploy CC c, the same femtocell might be regarded as a prior by another cell attempting to allocate the same CC subsequently. The remainder of this section is devoted to an intuitive exposition of G-ACCS. Formal definitions and an algorithmic description are the subject of the next section.

Graphically, G-ACCS sets the PSD reduction such that the distance between the blue (yield) and red (loss) curves in Figs. 5.3-5.5 is maximized. The shape of the curves depends entirely on the interference coupling between cells. For example, Fig. 5.3 illustrates one scenario of weak outgoing interference coupling between the posterior and prior cells. Fig. 5.4 depicts a case where the posterior cell has a moderate outgoing interference coupling with the prior cell, hence a more aggressive PSD reduction is required. Additionally, the incoming interference coupling as perceived by the posterior cell is weak, and consequently PSD reductions have little impact on the blue curve. In Fig. 5.5 the allocation would

[1]Notice that the method is not a pure maximization of the sum capacity because the latter could imply a CC ownership exchange and/or power reductions from both cells.

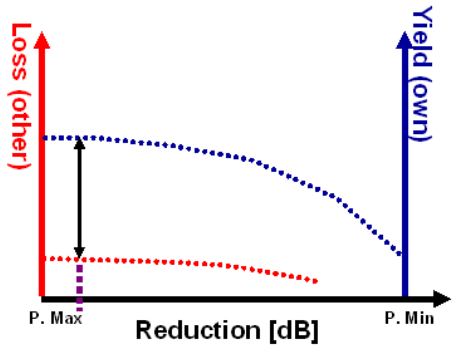

Fig. 5.3: In this case, only a soft reduction is required since the allocation of a CC by the posterior cell has little impact on the prior cell.

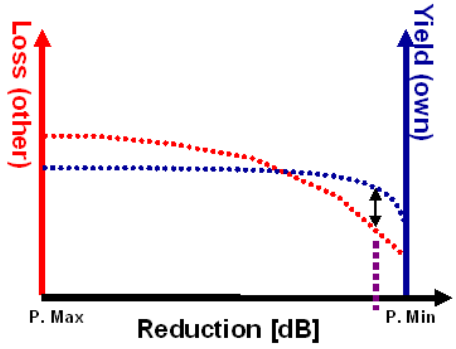

Fig. 5.4: Here the allocation is only allowed if an aggressive power reduction is applied to the desired CC, minimizing the loss incurred by the prior cell.

be denied as the loss is never smaller than the yield. This arises from strong outgoing interference coupling from the posterior towards the prior cell.

Finally, the careful reader can observe that, as far as G-ACCS is concerned, the only difference between a Base Component Carrier (BCC) and a Supplementary Component Carrier (SCC) is the fact that a cell is always the prior cell when it comes to its own BCC, since the latter is never relinquished. However, if additional protection/differentiation is strictly required one could introduce a maximum acceptable loss for BCC. This is illustrated in Fig.5.6. Yet, given the results presented in Section 5.5 the author posits that the additional complexity is not justified since considerable performance improvements in terms of outage performance remain visible even under dense and heavily loaded networks.

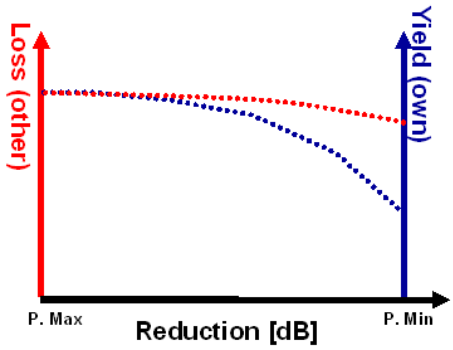

Fig. 5.5: This case illustrates an allocation that will not be performed, since the loss is never smaller than the gain. Reducing the transmission power lowers the loss marginally and decreases the yield significantly.

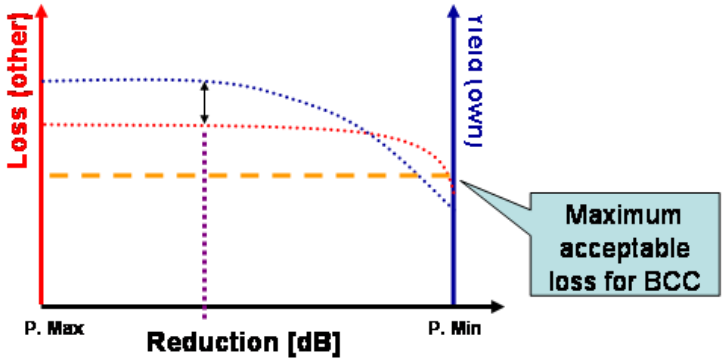

Fig. 5.6: The introduction of a maximum acceptable loss for BCC can offer additional protection for BCCs when other cells attempt to use the as SCCs. Here the posterior cell would not be able to deploy the CC due to the violation of this threshold.

5.3.3 Mathematical Formulation

The two aforementioned restrictions provide the mathematical framework under which the ideal PSD is calculated autonomously by posterior cells during the CC allocation attempt. Similarly to ACCS, Component Carrier Radio Allocation Tables (CCRATs) and BIMs are the two central pillars of G-ACCS. Both have been described in Sections 3.4.4 and 3.4.5 respectively.

Once cell k detects the need for additional CCs, it will use the information found in the BIM and the CCRAT to figure out whether or not the new allocation will jeopardize any existing allocation. Once again, recap that the BIM values are CIR estimates assuming equal Power Spectral Density (PSD) levels. Therefore, the PSD reductions of both the prior and posterior cell have to be taken into account on the C/I estimates. Additionally, the formulation described next does not necessitate an explicit distinction between BCCs and SCCs, hence only the PSD reduction information, i.e. the real part,$\Re(.)$, of z_n^c is required. For the sake of clarity, z_n^c will be used henceforth as the shorthand notation for $\Re(z_n^c)$.

G-ACCS exchanges the capacity yield of the posterior cell for the loss of the prior cell in order to make an allocation decision. The selected transmit power for each CC maximizes the difference of the yield and the loss, i.e., the net yield. The subsequent capacity estimations rely on the function $S(.)$ defined in Section 5.2.

The loss of the most critical prior cell, ω, is calculated as:

$$l(x) = S_{\text{free}} - \mathcal{S}\left(\text{DL}_{\{k\}\to\{\omega\}} - z_\omega^c + x\right) \tag{5.3}$$

where S_{free} represents the current capacity of the prior cell ω as discussed later in this section, x is the power reduction of the posterior cell and z_ω^c is the power reduction of the prior cell ω in dB[2]. The evaluation is done for each desired CC, c. Note that the argument of $S(.)$ in (5.3) is an effective outgoing BIM C/I as corrected by the PSD reductions. The most critical prior cell, ω, is determined for each CC as follows.

Denoting the set of neighboring prior femtocells currently using the candidate CC as $\boldsymbol{\psi}_{c\setminus\infty}$ ($\boldsymbol{\psi}_c$ excluding non-finite entries); then cell ω in (5.3) is such that:

$$\omega \triangleq n \mid \forall m \in \boldsymbol{\psi}_{c\setminus\infty} : \text{DL}_{\{k\}\to\{n\}} - z_n^c \leq \text{DL}_{\{k\}\to\{m\}} - z_m^c$$

i.e. it corresponds to the prior cell with the lowest effective – accounting for possible PSD reductions – outgoing BIM C/I entry amongst all those currently

[2]In (5.3)-(5.4) the arguments of $S(.)$ are assumed to have been converted to dB; hence the additions/subtractions.

using the desired CC as seen in the CCRAT table. In other words, the most affected prior cell in the case that the posterior cell uses the component carrier as well.

Similarly, the yield is defined in terms of the lowest effective – PSD reduction included – incoming BIM C/I:

$$y(x) = \mathcal{S}\left(\mathrm{DL}_{\{k\}\leftarrow\{\iota\}} + z_{\iota}^{c} - x\right) \tag{5.4}$$

where ι in (5.4) is defined to be the neighboring cell from $\boldsymbol{\psi}_{c\setminus\infty}$ responsible for the lowest effective incoming BIM C/I entry amongst all those currently using the desired CC as seen in the CCRAT table. It should be appreciated that such a cell is not necessarily the prior cell ω considered in (5.3) given a possible asymmetry of the interference coupling. Therefore:

$$\iota \triangleq n \mid \forall m \in \boldsymbol{\psi}_{c\setminus\infty} : \mathrm{DL}_{\{k\}\leftarrow\{n\}} + z_{n}^{c} \leq \mathrm{DL}_{\{k\}\leftarrow\{m\}} + z_{m}^{c}.$$

Finally, the net yield $n(x)$ is simply the difference between the yield $y(x)$ and the loss $l(x)$:

$$n(x) = y(x) - l(x) \tag{5.5}$$

G-ACCS searches for the power reduction x that maximizes the net yield. Naturally, if $\boldsymbol{\psi}_{c\setminus\infty} = \emptyset$ the CC can be taken without any further considerations. Otherwise, after analyzing $n(x)$ in (5.5); the CC will be deployed by the posterior cell if and only if:

$$\exists\, x \in [0 \quad \varrho] : n(x) \in \mathbb{R}^{+} \tag{5.6}$$

where ϱ denotes the maximum applicable PSD reduction, in which case, x is set at $\hat{x}$ given by:

$$\hat{x} = \underset{x\in[0\ \varrho]}{\arg\max}\ n(x) \tag{5.7}$$

The value of ϱ can either be parameterized or inferred from the BIM. Recall that G-ACCS assumes that the system is interference rather than noise limited. Therefore, care must be exercised in order to avoid extreme PSD reductions that would violate the previous assumption. As explained in Section 3.4.5, a cell's incoming BIM entry to itself, $\mathrm{DL}_{\{k\}\leftarrow\{k\}}$, expresses the Signal to Noise Ratio (SNR) experienced by the UE with the lowest channel gain. This information can be used to ensure that ϱ does not lead to very low SNR values at which point noise would dominate over interference, thus invalidating all calculations.

In a basic implementation the constant S_{free}, in (5.3), corresponds to the maximum spectral efficiency achievable by the system without any interference, i.e.

the bandwidth of the CC is absolutely free for that cell to use it with the highest MCS available. Optionally and more realistically, S_{free} could correspond to an estimation based on the average experienced SNR or even SINR at the prior cell just before the allocation attempt. Nevertheless these two alternatives entail additional signaling in order to inform the posterior cell about the conditions in the prior cell. Additionally, setting $S_{\text{free}} = \text{C}_{\text{MAX}}$ makes G-ACCS slightly more conservative – as it tends to overestimate the loss – which counterbalances its reuse-prone nature. For these reasons, the first and simpler approach is preferred.

Algorithm 1 summarizes the proposed method. G-ACCS resorts to iterative numerical optimization because the function $n(x)$ is not differentiable. This is not a limitation of the framework itself, but rather a consequence of $S(.)$ trying to mimic the behavior of a real system.

Algorithm 1 Calculate the PSD reduction $\hat{x}$

for each desired CC **do**
  Identify cell ω
  Identify cell ι
  if $\nexists$ cell ω **then**
    Allocate $\leftarrow$ **true** {CC is free.}
    $\hat{x} \leftarrow 0$
  else
    $\hat{x} \leftarrow \infty$, $x \leftarrow 0$, $N_{\max} \leftarrow 0$
    while $x \leq \varrho$ **do**
      Increase x
      Estimate $n(x)$
      if $N_{\max} < n(x)$ **then**
        $N_{\max} \leftarrow n(x)$
        $\hat{x} \leftarrow x$
      end if
    end while
    Allocate $\leftarrow N_{\max} \neq 0$
  end if
  return Allocate, $\hat{x}$
end for

5.4 Performance Evaluation

The current and the subsequent sections present a systematic evaluation of the effects of inter-cell interference on the overall performance of femtocells through detailed system level simulations. Recollecting the objectives of this thesis stated in Section 1.3 the complementary co-channel cross-tier interference is not treated here. Hence the analysis gravitates towards the inter-cell interference among femtocells operating in a dedicated band, i.e. macro cell and femtocell users are made orthogonal through bandwidth splitting. The analysis encompasses the effects of spatial density (network topology) and temporal sparseness (activity factor) on network performance. To the best of the author's knowledge, a comprehensive evaluation of these two aspects is not available in the context of interference coordination schemes for femtocells.

Recurring to the problem at hand and along the lines of the discussions in Sections 1.3 and 3.3, four Carrier Aggregation (CA) based solutions are evaluated. All investigated algorithms are essentially non-iterative and operate on time scales much longer than that of scheduling decisions. Moreover, all alternatives rely on a fully distributed architecture of autonomous decision makers to solve the interference management problem. The considered solutions are introduced in increasing order of complexity. The ultimate goal is to identify the trade-offs and assess how much complexity is effectively required to provide efficient interference coordination on a CC level in the context of LTE-Advanced femtocells. Henceforth, it is assumed that the system bandwidth consists of 5 CCs, the maximum supported by LTE-Advanced [107].

5.4.1 Component Carrier Selection Strategies

5.4.1.1 Universal Reuse

Although not strictly a CC selection strategy, there is no simpler approach than to grant all femtocells unrestricted access to all 5 CCs at all times without any power restrictions. Early work [88] based on LTE macro-cells indicate that among the static frequency schemes, plain reuse 1 performs best for wideband services. On the other hand, findings in [108] suggest that a properly chosen reuse factor leads to significant gains in 5%-outage user throughput in uncoordinated local area deployments. However, both studies assume full-buffer traffic. For this reason and also due to its inherent simplicity, universal reuse is included in the evaluation.

5.4.1.2 Network Listening Mode

A second possibility is to make use of the sensing capabilities of femtocells. Based on findings in [108] where a reuse factor of 1/2 showed promising results, a pragmatic approach is employed here. The 5 CCs are split into two semi-orthogonal subsets $\Lambda_1 = \{1, 2, 3\}$ and $\Lambda_2 = \{3, 4, 5\}$. During startup, each femtocell enters into a Network Listening Mode (NLM) [109] phase. Acting as a pseudo-UE, the femtocell scans the air interface searching for DL pilot signals from other femtocells in order to select the complementary subset to the one utilized by its "nearest" neighbor, i.e. the one with the smallest estimated path loss. The selected subset is not changed afterwards, at least not in a short time span, recognizing that the outcome cannot be expected to be the best possible.

5.4.1.3 Basic ACCS

The third strategy is the original ACCS introduced in Chapter 3 and originally presented in [96,110]. In this section, a slightly different variation is also considered. The latter shall be designated *Basic ACCS* in order to distinguish it from the *Original ACCS*. The two changes are: (i) usage of a separate and much lower C/I target, (0 dB), for the incoming interference estimation. (ii) Decoupled DL and UL decisions, whereas only the former is considered next.

The original ACCS concept treated incoming and outgoing estimations equally. By doing so, it failed to recognize that from a cell-centric perspective more bandwidth is never harmful as long as the expected incoming CIR is still above the lower bound imposed by MCS limitations. The outgoing evaluation remains exactly the same. Furthermore, decoupled decisions can better adapt to the potentially asymmetrical traffic requirements. Decoupling decisions have little impact on the DL, since ACCS is chiefly based on DL information. Additionally, the studies in [105] and especially those in Chapter 4 show that ACCS also works well with independent UL decisions.

5.4.1.4 G-ACCS

The fourth strategy is the novel G-ACCS solution that enables femtocells to jointly determine the subset of CCs and their corresponding transmission power levels, such that existing transmissions from neighboring cells are not disrupted.

Table 5.2: Link level parameters

MIMO Scheme	Diversity Order	Array gain (dB)	Spatial Streams	$BW_{eff} * \eta$	SNR_{eff}
2x2 CLM1	4	4.6dB	1	0.65	1.6
2x2 SM	1	-3dB	2	0.56	2

5.4.2 Simulation Assumptions

The performance figures were generated using the same quasi-dynamic LTE tool outlined in Section 2.4.1 whose comprehensive description is found in Appendix D. The simulation scenario is the one described in Section 1.4.3. A single femtocell and all its served user(s) are located inside the same apartment under CSG access mode. Their locations within each apartment are random and uniformly distributed. In the absence of a Femto Access Point (FAP), a flat contains no active users. Three floors are considered, thus totaling 120 apartments. Two values for the deployment ratio parameter are considered, the first one assumes a deployment ratio $\delta = 20\%$ while $\delta = 80\%$ in the second and even denser scenario.

Whereas the location of devices is static, Radio Resource Management (RRM) and the generation of traffic are dynamic processes. The simple finite-buffer traffic model is aligned with 3GPP recommendations [22] to facilitate independent validations. The model is based on sessions with fixed payloads. The interval $\mathcal{I}$ between the end of one session and the user's request for the next session obeys a negative exponential distribution, with an average length of $1/\lambda$, where λ is the rate parameter. For each scenario the arrival rate λ parameter took on the following values [0.1 0.2 1].

As in the preceding chapters, the packet scheduling algorithm is a simple equal resource sharing scheduler. The DL SINR is calculated per Physical Resource Block (PRB) for every simulation step. Error Vector Magnitude (EVM) modeling is included; therefore SINR is asymptotically limited. The achieved throughput is calculated using a modified Shannon fitting. In the simulations as well as in the numerical evaluations found in Section 5.2 the parameters from [64] are utilized. The following 2 modes are considered: single-stream (CLM1) and multi-stream (SM MIMO). The parameters taken from [64] are repeated in Table 5.2 for convenience.

Five CCs of 20 MHz are assumed. Although such a spectral availability seems optimistic for today's operators, it is not critical. In fact, all results are normal-

ized and therefore independent from the system bandwidth. The number of CCs available is a much more relevant aspect [110]. The total power is distributed evenly among CCs. The fixed payload size is $S = 62.5$ Mbytes[3] and the number of users per femtocell was set at $U = 1$.

Moreover, since ACCS and G-ACCS rely on information exchange among femtocells, a latency of 100 ms is included in order to account for signaling delays. Therefore, if two or more cells attempt to allocate SCCs within a time-window of 100 ms, the information will not be available in the CCRAT, and a "collision" may occur. Although there are practical ways of dealing with this problem, such solutions are beyond the scope of this work. Therefore, the results herein already include imperfections. Another design choice is that in G-ACCS multiple iterations are not allowed. For this reason $\hat{x}$ is calculated only once for the sake of (i) simplicity, (ii) stability, and (iii) minimal signaling requirements.

The numerical results were obtained as follows. In each snapshot, the deployed femtocells were activated; one at a time in a random sequence. When universal reuse is employed, all cells may use all 5 CCs, and there are no further considerations. In the NLM simulations, upon activation each femtocell selects one subset based on the preceding network state, and no further changes take place. In (G-)ACCS simulations a single BCC is selected as in Section 3.3 and is not changed afterwards. The process relies on previous decisions made by other femtocells and without any UE-side information. In the subsequent phase of (G-)ACCS simulations femtocells always attempt to select as many SCCs as possible whenever a download session starts, relinquishing them upon completion. This means that the underlying packet schedulers are inherently greedy, but do not occupy resources when there is no traffic at all. Yet, the BCC is always kept. There are no additional rules in order not to violate the scheduler independence principle. In all cases, the collection of results begins once all deployed femtocells have been switched on. Finally, the statistical reliability of the simulation is ensured by collecting the results of thousands of snapshots, each snapshot comprising 120s[4]. Table 5.3 provides an overview of the main simulation parameters.

[3]The artificial file size is due to the available bandwidth of 100 MHz. The goal is to exercise a wide range of workloads (from modest to near full-buffer traffic loads.) One could down-scale file sizes to the desired bandwidth.

[4]The simulation campaign was configured such that several UE locations ("drops") are simulated for any given layout, i.e the FAP positions. Several layouts were simulated as well.

Table 5.3: Assumptions for system-level simulations

System Model		
eNB parameters	Total TX power	20 dBm
	Tx Power/CC	$[0 \sim 13]$ dBm
	Antenna system	Omni (3dBi)
UE parameters	CA Capable	Yes
	Antenna system	Omni (0dBi)
Spectrum allocation	5 CCs of 20 MHz each	
C/I thresholds (ACCS)	BCC:15 dB	SCC: 8 dB
Information exchange latency	100 ms	
Total EVM	5%	
Propagation Model [22]		
Shadowing std. deviation	Serving Cell	4 dB
	Other Cells	8 dB
Minimum coupling loss	45 dB	
Deployment and Traffic Models [22]		
Deployment ratios	$\delta = 20\%$ and $\delta = 80\%$	
Inter-session intervals	$E[\mathcal{I}] = 1/\lambda = [10\ 5\ 1]$ s	
Payload Size	62.5 MBytes	

5.5 Simulation Results and Analysis

Results are analyzed using the three Key Performance Indicators (KPIs) introduced in Section 1.4.4. These are complemented by the average duty cycle, D, and the G-factor. Additionally, all throughput results presented next are normalized by the maximum throughput of the system. Hence, a normalized throughput of 100% implies a transmission over the whole bandwidth with the highest spectral efficiency allowed by MCS limitations. This emphasizes the relative trends rather than the absolute values. In summary, the five KPIs are:

- Average duty cycle (D): it is the fraction of time that the system has active transmissions. Calculated as the ratio of the average duration of

downloads $E[\tau]$ and the average total interval between sessions $E[\mathcal{I}+\tau]$.

- G-factor: defined as the ratio of the total wideband signal power and the interference plus noise power at the receiver (UE) side.
- Average HeNB throughput: the throughput averaged over all femtocells from all simulation snapshots. Recap that with a single served UE, the HeNB and user throughput values are the same (Measured during active periods).
- Peak user throughput: the achieved user throughput for the 95%-tile, i.e. the 5% best users achieve higher (if MCS allows) or at least equal throughput values.
- Outage user throughput: the achieved user throughput for the 5%-tile, the 5% worst users achieve equal or lower throughput values.

5.5.1 Topology, Traffic Variability and Network Performance

This section examines the statistical impact of the topology (density) and traffic variability on the overall network performance. The average duty cycle for all evaluated methods and both deployment ratios is plotted in Fig. 5.7a. It can be observed that the selected parameters cover a wide range of network loads, making the analysis rather comprehensive. The simpler NLM approach suffers from poor performance, especially at sparse deployments – solid magenta line – because it imposes a hard limit on the amount of allocated resources. Such limitation is only efficient when the duty cycle is very high. Although all methods achieve a similar average duty cycle, G-ACCS shows a consistently lower one in all scenarios considered. Two additional aspects can be observed in Fig. 5.7b which depicts the G-factor distributions for the simplest universal reuse strategy:

- Despite comparable average duty cycles (D=24% and D=19%) the share of users experiencing low G-factor, e.g. below 0 dB, jumps from 8% to nearly 20% in the denser deployment.
- When $\delta = 0.2$ even the highest loaded system at D=67% (uppermost red solid curve) presents higher G-factor values than the lowest loaded system for $\delta = 0.8$ at D=19% (lowermost dashed blue curve).

The last two findings fall in with the discussion in Section 5.2 and indicate that the density of the network plays indeed a more important role than the

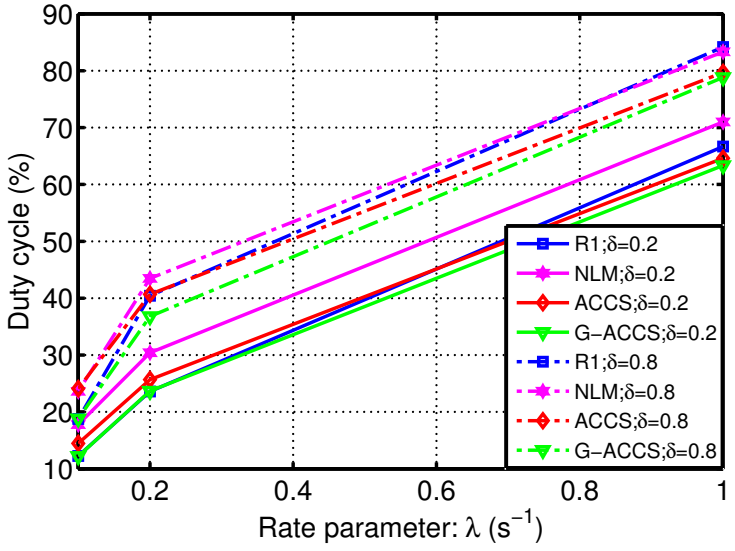

(a)

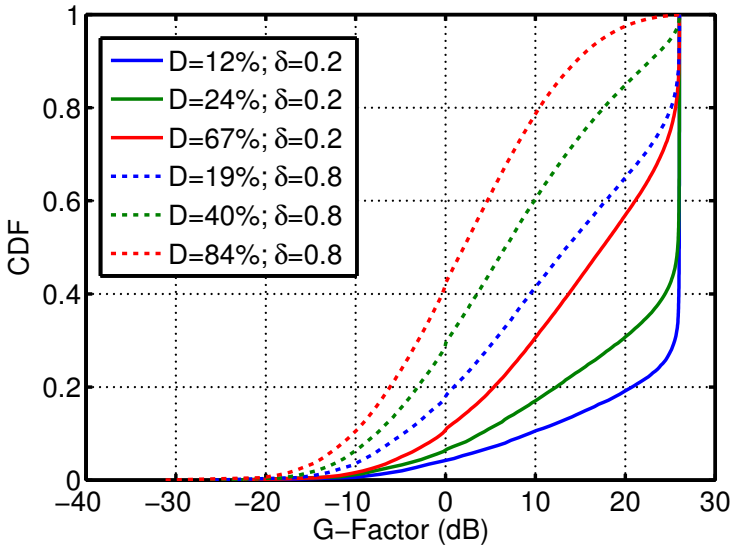

(b)

Fig. 5.7: (a) Average duty cycle comparison as a function of λ for all evaluated methods and deployment ratios. (b) Empirical G-factor distributions for variable deployment ratios and duty cycles assuming universal reuse.

traffic intensity in dictating the interaction of cells. Moreover, depending on the traffic intensity universal reuse might be an efficient solution in terms of average performance, but certainly not a fair one, especially in dense femtocell deployments. In fact, some users will simply starve due to extremely low G-factor conditions.

5.5.2 The Downside of Conditional C/I Ratios

The foregoing discussions in Section 3.3 highlighted the advantages of utilizing the expected interference coupling between cells rather than actual interference levels. The considerations in Sections 5.2 and 5.3 hinted at the potential pitfalls. Now let us examine the subject more carefully. Figs. 5.8a and 5.8b depict the empirical cumulative distribution functions of normalized DL cell throughput for $\langle \delta = 0.2, \lambda = 0.1 \rangle$ and $\langle \delta = 0.8, \lambda = 0.1 \rangle$, respectively. For the sake of completeness, performance results for the original ACCS scheme are presented as well.

Due to the light traffic load, the interference levels incurred are not necessarily detrimental, hence the superior performance of universal reuse. The overprotection effect of ACCS becomes evident. This arises because BIMs are oblivious to the actual activity ratio of both cells, i.e. all interference coupling estimations correspond to the upper-right corner of Figs. 5.2a and 5.2b.

Putting more emphasis on the outgoing BIM entries as suggested in Section 5.4.1.3, rather than treating incoming and outgoing entries equally, alleviates the problem. However, the effect is not significant, notably when $\delta = 0.8$. This occurs mainly because many CCs are anyway taken by neighbors as BCCs, which have much stricter C/I targets. Additionally, once a cell activates a low quality SCC, it might be preventing its usage by other cells where it could be utilized in a more spectrally efficient manner.

There are a few tactics to minimize this issue, but none really solves it without additional parametrization or trade-offs. For example, restricting the CCs selectable as BCCs to e.g. {1,2,3} will pack BCCs more tightly and therefore increase the probability of cells finding available SCCs. However, this will worsen BCC interference conditions. Alternatively, cells could adjust their respective C/I requirements according to the traffic load. Yet this implies extra signaling, and the dynamics of packet-switched traffic are not easily tracked, notably when signaling delays are involved.

G-ACCS greatly reduces the overprotection problem as shown in Fig. 5.8. In fact, its greatest merit is to achieve this goal without additional parameters and

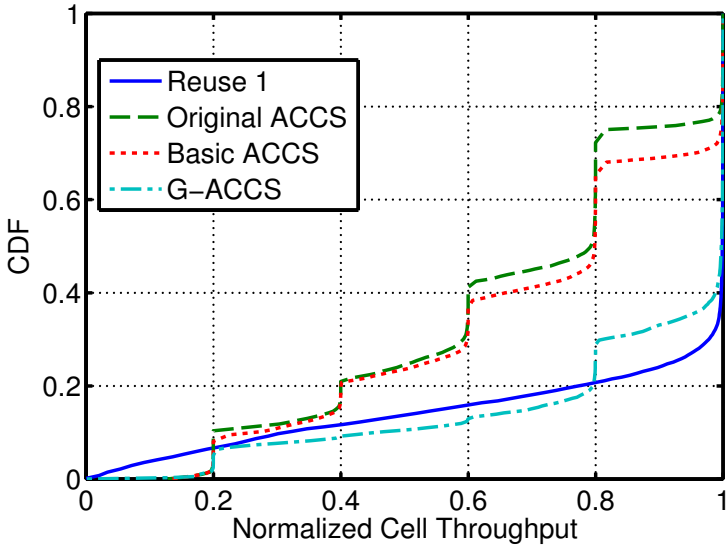

(a)

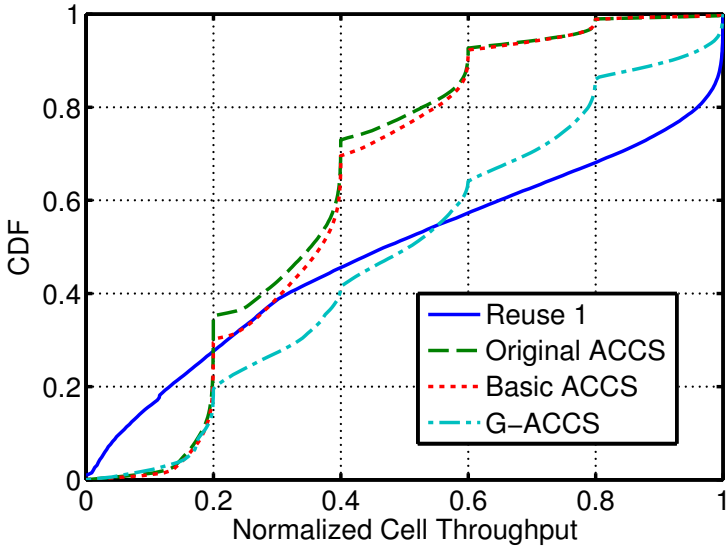

(b)

Fig. 5.8: Empirical cumulative distribution functions of normalized downlink cell throughput: (a) $\delta = 0.2$, $\lambda = 0.1$ and (b) $\delta = 0.8$, $\lambda = 0.1$. G-ACCS yields outage gains (lower tail) without sacrificing the performance along the rest of the distribution.

minimal sacrifice of fairness. It can be seen that the performance boost in the lower portion of the throughput distribution is maintained.

5.5.3 Analysis

This section condenses the results obtained and attempts to put them into perspective. But before moving on to the performance figures, the behavior of the four CC strategies considered in Section 5.4.1 is examined qualitatively in view of Fig. 5.2.

Universal reuse is a simple strategy whose overall performance strongly depends on favorable network topology and activity ratios. Therefore, cells with very high as well as cells with miserable throughput figures may be seen. As opposed to universal reuse, the NLM-based approach clearly leverages the network topology and can partially avoid interference. Once again looking at Fig. 5.2 and considering just one cell and its "nearest" neighbor, this solution can be understood as a hybrid one. Both cells attain orthogonal allocations for two CCs and share a third one where the outcome will again depend on the traffic intensity.

A parallel can also be drawn between ACCS and the discussion in Section 5.2. First, similarly to the NLM approach, ACCS gathers information related to the network topology. Notwithstanding, this information – the BIM – characterizes the receiving UE conditions and not those of the transmitting femtocell. Moreover, when it comes to allowing non-orthogonal transmissions, ACCS distinguishes between both cells. For example, if cell B in Fig. 5.1 is using a certain CC, and cell A decides to deploy it as well, the allocation will be denied in order to ensure minimal disturbance of ongoing transmissions. The opposite, however, would be allowed since cell B would not seriously harm UE α.

Finally, G-ACCS works similarly to ACCS, but with one key distinction. Since G-ACCS does not require hard decisions, it is capable of moving along the resource utilization plane. The rationale is a generalization of the temporal activity ratio concept to a resource utilization ratio. The previous argument is justified by the fact that transmit power is also a key resource in wireless networks.

Table 5.4 presents a summary of the performance of all considered component carrier selection strategies. The results are also plotted in Figs. 5.9a and 5.9b for $\delta = 0.2$ and $\delta = 0.8$, respectively. Each circle corresponds to a different λ, hence one session arriving on average every 10s, 5s and 1s after the end of the previous one. The points near the upper-right corner correspond to the lower lambda

Table 5.4: Summary of simulation results.

Deployment Ratio		$\delta = 0.2$			$\delta = 0.8$		
$E[\mathcal{I}]$	Scheme	Out	Avg	Peak	Out	Avg	Peak
$1/\lambda$=10s		14%	86%	100%	2.4%	51%	100%
$1/\lambda$= 5s	R1	9%	78%	100%	1.5%	35%	96%
$1/\lambda$= 1s		5%	60%	100%	0.9%	21%	64%
$1/\lambda$=10s		32%	55%	60%	4%	38%	60%
$1/\lambda$= 5s	NLM	31%	55%	60%	2.5%	30%	58%
$1/\lambda$= 1s		14%	49%	60%	1.7%	23%	50%
$1/\lambda$=10s		20%	71%	100%	16%	37%	74%
$1/\lambda$= 5s	ACCS	20%	69%	100%	14%	34%	69%
$1/\lambda$= 1s		19%	66%	100%	12%	30%	59%
$1/\lambda$=10s		20%	86%	100%	16%	52%	100%
$1/\lambda$= 5s	G-ACCS	19%	77%	100%	10%	41%	89%
$1/\lambda$= 1s		17%	70%	100%	6%	32%	72%

values. The x-axis is the average cell throughput, while the y-axis corresponds to the 5% outage user throughput. The diameter of the circles represents the peak user throughput with the actual values shown next to it for clarity. Finally, the dashed lines are polynomial trend lines.

Analyzing Fig. 5.9 it is natural to ask which strategy is the best. True to the engineering spirit, the answer is: it depends. Universal reuse is a competitive solution in terms of simplicity, peak date rates, and average cell throughput. Nevertheless, its outage performance, especially in denser deployments, is deplorable even at modest traffic loads. Therefore an operator opting for this strategy could face a throng of dissatisfied users. A situation that would be aggravated in case of heterogeneous co-channel deployments, since standardized schemes typically favor macro UEs at the expense of femto users [111].

One potential advantage of the NLM scheme is the absence of inter-cell signaling. Notwithstanding its decent outage performance, particularly in less dense deployments, the NLM strategy suffers a major degradation in terms of peak data rates and overall cell capacity. Moreover, NLM displayed very poor outage performance in denser deployments, barely outperforming universal reuse. The results are nowhere near those achieved by the genie-aided reuse 1/2 pattern of previous contributions [108]. One of the reasons is the random (spatial) order

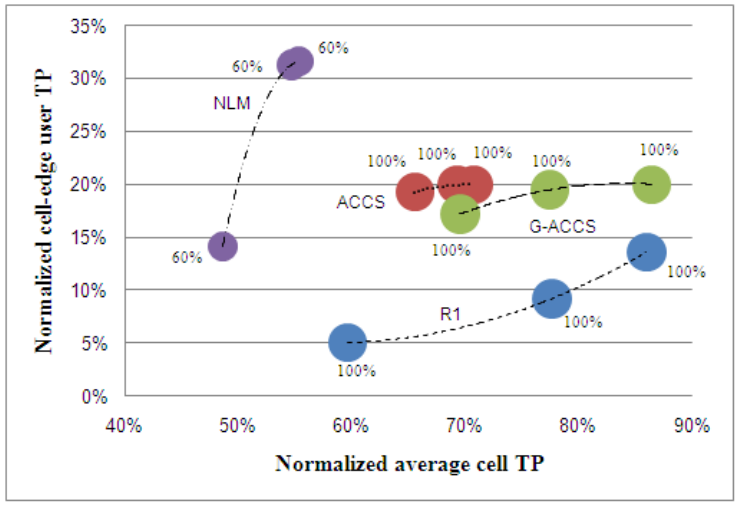

(a)

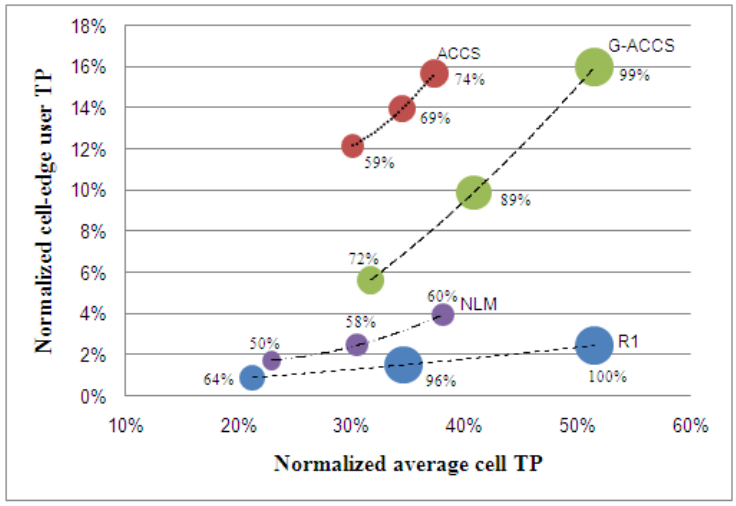

(b)

Fig. 5.9: Summary of attained performance for all considered component carrier selection strategies: (a) $\delta = 0.2$ and (b) $\delta = 0.8$. The bigger the "bubble" and the closer it is to the uppermost right corner the better. The numbers next to each bubble the percentage of the maximum throughput achieved by the best 5% users. The lines connecting the dots simply highlight the trends.

in which femtocells are switched on. Without reconfigurations, the achieved CC pattern is far from optimal due to deadlocks. The overall performance results from NLM would certainly vary if the cardinality and number of the subsets were chosen differently. Yet, that would not change the fact that the method relies on measurements performed at transmitter side rather than the receiver side. The "nearest" neighbor as seen by the femtocell is not necessarily the strongest DL interferer. Furthermore, NLM-like methods overlook one critical trait of the spectrum sharing problem, as the amount of CCs is fixed. Discovering not only which, but also how many CCs should be allocated at a given time is equally, if not more, important.

The basic ACCS offers considerable performance improvements compared to the two aforementioned simpler techniques. Additionally, with five CCs to choose from, ACCS was found to be quite insensitive to the order in which femtocells are switched on. Results from Section 3.6 and those reported in [96] indicate that the interference coupling expressed by BIMs successfully captures the spatial sparseness of the network. However, the same cannot be said about the temporal sparseness. The outcome is a visible degradation in the average cell throughput and a more subtle loss in peak performance when compared with universal reuse. The trade-off is not deterministic and can be controlled by adjusting the C/I targets employed. However, fine-tuning such targets is laborious, and the values tend to be case specific. In our studies we have used values optimized for full-buffer traffic, hence the excellent performance at high duty cycles and dense deployments.

G-ACCS is clearly the most well-rounded method. It retains the best aspects of ACCS and always outperforms universal reuse in terms of average cell-throughput, while attaining comparable peak data rates. An intuitive explanation comes from the model introduced in Section 5.2. Since G-ACCS does not require hard decisions, it is capable of moving along the resource utilization plane seeking the best compromise.

Moreover, because fairness is an important aspect when multiple autonomous agents share a limited set of resources; Jain's fairness index ($\mathcal{J}$) was employed to quantify it. Jain's index is a continuous and scale-independent metric. It can be understood as the square of the cosine of the angle between the data set x_i and the hypothetical equal allocation and is defined as [112]:

$$\mathcal{J}(x_1, x_2, \ldots, x_n) = \frac{(\sum_{i=1}^{n} x_i)^2}{n \cdot \sum_{i=1}^{n} x_i^2} \tag{5.8}$$

A value of $\mathcal{J} = 1$ implies that all femtocells in the network achieve the same

Table 5.5: Quantifying the joint performance in terms of efficiency and fairness.

Cases	δ	λ	R1	NLM	ACCS	G-ACCS
Joint Performance ($\mathcal{J}_{\text{scheme}} \times \mu^{\text{cell}}_{\text{scheme}}$)	0.2	0.1	0.788	0.529	0.635	0.794
		0.2	0.673	0.530	0.611	0.680
		1	0.456	0.448	0.575	0.597
	0.8	0.1	0.354	0.306	0.307	0.415
		0.2	0.206	0.224	0.274	0.304
		1	0.114	0.160	0.241	0.226

average DL throughput. Nonetheless, the fairness index per se says nothing about the absolute throughput attained by cells. It simply expresses the degree of equality. On the other hand, the average cell throughput (μ^{cell}) is a metric that masks inequality. Since there are two bounded metrics between 0 and 1, a natural development is to multiply both ($\mathcal{J}_{\text{scheme}} \times \mu^{\text{cell}}_{\text{scheme}}$) in order to quantify the joint performance in terms of efficiency and fairness[5]. Table 5.5 summarizes this product for the different CC selection strategies under different traffic loads and density of femtocells.

Readers can verify that G-ACCS is exceptionally well positioned when fairness and performance metrics are combined. ACCS does outperform G-ACCS in the densest and most heavily loaded scenario, but this is a consequence of (i) the fine-tuned parametrization employed in ACCS and (ii) the pessimistic signaling delay assumptions which penalize G-ACCS more severely than ACCS due to the more permissive nature of the former.

Finally, it can be stated that the results make it very evident that both the spatial distribution of devices and temporal traits of traffic (from light loads to near full-buffer) are elements that should not be overlooked when designing solutions for future femtocells. It is rather straightforward to protect the less-favored users; any sparse static reuse pattern will do it. However doing so without compromising average and peak user throughput values under a multitude of unpredictably varying conditions is rather tricky. Yet G-ACCS achieves this goal.

[5]Strictly speaking, the lower bound of $\mathcal{J}$ equals $1/n$, which tends to 0 as n tends to infinity.

5.6 Conclusions

The work in this chapter has further explored the possibilities offered by carrier aggregation in terms of interference management in the context of future LTE-Advanced femtocells. Both simple and more complex alternatives were considered. The ultimate goal was to assess how much complexity is required to provide efficient interference coordination on a component carrier level. The contribution is valuable as it provides guidelines for future deployments of femtocells. Moreover, a comprehensive characterization of the performance as a function of the network density and the traffic intensity was provided. While the majority of previous contributions in the literature focus on the full-buffer model; a finite-buffer traffic model has been considered here. The latter introduces rapid fluctuations of the interference levels, and therefore challenges the working assumptions of many techniques where the need for iterative reconfigurations is incautiously deemed a minor nuisance. The analysis of the simulation results shows that all considered component carrier selection strategies have their pros and cons. Nonetheless, the main contribution of this chapter, namely G-ACCS, retains the best elements of the other alternatives providing gains in terms of outage, average cell and peak throughput without any parametrization. Finally, the findings herein are also applicable to femtocells without CA support. For example, if femtocells are restrained to a single component carrier, a savvy (re-)selection of BCCs is desirable. The information from BIMs could be utilized to strike a balance between the minimization of the outgoing interference and the usefulness of the new BCC; thus minimizing the chances of propagating a wave of reselections arbitrarily far inside the local cluster of femtocells. Investigation of the aforementioned ideas, the extension to scenarios with picocells, as well as characterizing the impact of mobility on BIM in terms of inter-cell signaling are the subject of ongoing and future work.

Chapter 6

Conclusions and Future Work

This project undertook the challenge of designing practical and self-adjusting Component Carrier (CC) selection mechanisms to deal with interference in future LTE-Advanced femtocell deployments. In this brief final chapter, the main findings are summarized, distributed Inter-Cell Interference Coordination (ICIC) schemes are put into perspective, general recommendations are laid out, and, lastly, a few suggestions for further studies are provided.

6.1 Summary and Conclusions

Chapter 1 has set the scene and delimited the scope of this thesis. This work entertained the idea of exploiting the Carrier Aggregation (CA) framework introduced in LTE-Advanced as a natural enabler/enhancer of simple, yet effective frequency domain interference management schemes. The problem was then tackled in a systematic manner. The organization of the thesis tries to reflect this fact, in that, the necessary preconditions to accomplish the objectives of this project are built up chapter by chapter.

Chapter 2 has addressed the first two objectives of this project, namely (i) provide an understanding of the interference footprint of local area cellular deployments, and (ii) investigated the suitability of well-established contention

based solutions in the context of cellular systems. The latter could be perceived as a sanity check. After all, WiFi networks are virtually omnipresent nowadays. In short, two lessons have been learnt: Carrier Sense Multiple Access with Collision Avoidance (CSMA/CA) is in general not able to outperform scheduling strategies using a properly selected frequency reuse factor. CSMA/CA simply takes on too many responsibilities at the same time – duplexing, multiplexing and interference coordination – and is plagued by hidden nodes, exposed nodes and random collisions. All three factors contribute to suboptimal resource utilization. Lastly, as the wording – *properly selected* – implies, there is no static optimum frequency reuse pattern spanning all network topologies even when just full buffer traffic is considered.

Chapter 3 picked up where the previous chapter left off. Recap that in the cellular world, duplexing and user multiplexing are handled separately. Consequently, the work focused solely on developing a fully distributed and scalable solution to manage interference in uncoordinated networks. The outcome is the simple yet flexible and efficient Autonomous Component Carrier Selection (ACCS) framework. ACCS is based on sensing and lightweight information exchange and does not prevent femtocells from using the entire spectrum when this is a sensible choice. Endowing cells with the ability to "learn" what sensible means was the key aspect here. The proposed framework gives due focus to those users who suffer the most from inter-cell interference. Moreover, it does so without compromising average and peak user throughput values. Ultimately, this has been shown to render the system much less sensitive to the density of femtocells making up the uncoordinated network. The distinguishing element from prior work is the shift from a purely selfish and opportunist paradigm to a cooperative one. Cells need to heed their roles as sources of interference and not just mere victims. A notion that was subsequently followed by many other independent contributions in the literature in [91, 94, 95].

Chapter 4 is the uplink-centric counterpart of its predecessor. The work assessed the impact of Fractional Power Control (FPC) on femtocells, highlighting the main qualitative differences with respect to traditional macro-cells. The presence of FPC was also factored into the ACCS framework. Subsequently, two algorithmic formulations that incorporate Uplink (UL) power control information into the CC selection procedure were presented. Results demonstrated that it is indeed possible to capitalize on Power Spectral Density (PSD) variations brought about by FPC. This comes at the cost of, albeit little, signaling. The accompanying discussion also explained how the more elaborate formulation adds a twist to the originally cell-specific selection of CCs, leading to user-specific CC configurations in the uplink. Nonetheless, given the recommended FPC settings, the gains are small, and it is safe to conclude that the unmodified ACCS concept is an excellent compromise solution for the UL, despite being chiefly based on Downlink (DL) information.

The material in Chapter 5 introduced the Generalized Autonomous Component Carrier Selection (G-ACCS) algorithm, a parameterless capacity-based generalization of ACCS. Besides selecting carriers, G-ACCS is also capable of autonomously setting their transmit PSDs. This chapter has also exposed the pros and cons of a Background Interference Matrix (BIM)-based approach, that is to say, relying on expected rather than actual interference levels. Namely, this approach facilitates tremendously scheduler-independent decisions. On the other hand, this formulation can lead to overestimation of interference coupling when the resources are not fully utilized. Additionally, a comprehensive characterization of the performance as a function of the network density and the traffic intensity was provided as well. The encouraging results have shown that leveraging the power domain to circumvent the restrictive nature of expected interference coupling is a promising strategy. Ultimately, the take-home messages from the previous chapter, and perhaps from this entire thesis are:

- Selfish approaches might be optimal if sum-capacity is the metric of interest; notwithstanding, if fairness and outage-capacity are to be taken into account, cells – especially, but not limited to CSG ones – need to mind their surroundings.

- Both the spatial distribution of devices and temporal traits of traffic (from light loads to near full-buffer) are elements that should not be overlooked when designing future-proof solutions for femtocells.

- Realistic traffic introduces rapid fluctuations of the interference levels, and therefore challenges the working assumptions of many techniques where the need for iterative reconfigurations is incautiously deemed a minor nuisance.

It is safe to conclude that cooperative carrier-based ICIC is a viable alternative for future uncoordinated deployments of small LTE-Advanced cells. The results in this thesis provided strong evidence that even relatively simple approaches offer attractive performance benefits. Finally, it is noteworthy to stress that carrier-based ICIC schemes have the advantage of being fully compatible with legacy User Equipments (UEs) as well as offering protection to both data and control channels, even in the presence of closed, i.e. private cells. These properties have led 3GPP to initiate in March 2011 the "Carrier based HetNet ICIC for LTE" work item initially proposed by Nokia Siemens Networks. The description and objectives of the work item targeting Long Term Evolution (LTE)-Release 11 and beyond can be found at [51].

6.2 Recommendations and Guidelines

Before moving on to future endeavors, some recommendations pertaining to the applicability of ACCS in current networks are presented next. Clearly, the present reality is still far from the idealized "Femto Commons" 100 MHz spectrum scenario. Consequently, to be of any immediate practical value, the findings must be put into perspective.

In practice, if an operator spectrum is limited to e.g. 20 MHz, splitting the band into four 5 MHz or even two 10 MHz CCs will inflict a penalty in terms of peak throughput, if served UEs do not support CA (legacy devices). However, nothing prevents the framework from being extended to allow consistently "isolated" femtocells (as perceived through BIMs) to bind adjacent carriers, thereby judiciously undoing the spectral partition. Moreover, the tremendous gains perceived in outage performance speak in favor of ACCS even in the absence of CA-enabled UEs. Additionally, bandwidth splitting and ACCS automatically protect the control channels from disruptive interference. This trait is of critical importance, yet it seems to be quite often forgotten that improved data Signal to Interference plus Noise Ratio (SINR) is useless if UEs cannot decode control channels.

In summary, ACCS and bandwidth splitting into 3 or more CCs is recommended. For example, in a co-channel deployment, a 20 MHz band could be split into three 5 MHz CCs, where femtocells would operate. Macrocells would still operate on a single 20 MHz CC with the added benefit that 5 MHz would be free of femtocell interference. The recommendation for at least three CCs is based on the maximal clique (graph theory) analysis presented in Appendix A.2.

Finally, in order to come full circle, the design guidelines outlined in Chapter 1 are revisited and commented here based on insights acquired in the course of this project. The description below juxtaposes design principles and explanations on how the former have materialized in the proposed ACCS framework.

Keep it simple Hence the choice for a simple frequency domain concept. Frequency planning is a proven technique. ACCS capitalize on the carrier aggregation framework to provide self-adjusting frequency planning.

Look for a good design; it need not be perfect This principle goes hand in hand with the previous one. Ingenious people can always come up with some ultra-dense network topology that the algorithms cannot handle optimally. Rather than snarling the design up, pathological cases are brushed aside. However, this does not imply that those have been totally

ignored. The considered multi-floor dual-stripe scenario with full deployment is anyway incredibly dense and constitutes a special case per se.

Think about scalability If femtocells are deployed massively by end-users, no centralized databases of any kind are tolerable. Thus, the option for autonomous agents and pair-wise interference coupling characterizations.

Expect heterogeneity Femtocells are expected to be built by different vendors, with different types of hardware, scheduling strategies, etc. To handle them, the rules governing the network design must be simple, unambiguous, and flexible.

Exploit modularity This principle and the previous one are closely linked. Together, they vindicate the decision to keep things separate, ultimately leading to the scheduler independence principle.

Avoid static options and parameters If parameters are unavoidable try to keep their numbers at a reasonable level. This principle played a paramount role in the designs of ACCS and more prominently in that of G-ACCS.

6.3 Future Work

The purpose of this final section is to provide some food for thought, offering a brief, and by no means exhaustive, list of topics for posterior studies.

In this work, co-channel deployments have been deliberately neglected in favor of a "Femto Commons" vision. However, if that assumption is lifted, the inclusion of co-channel macro and pico cells into the ACCS picture becomes the obvious candidate for future studies.

As hinted at in Chapter 3, the same framework applied to the femto-femto scenario could be translated almost seamlessly to the pico-pico case. However, two aspects distinguish these deployments and they should not be overlooked. Firstly, picocells may serve a much larger number of users, hence a more elaborate data fusion procedure might be required to characterize the interference coupling between cells. One straightforward possibility is to employ a certain percentile rather than the lowest reported C/I value. Lastly, and probably more profoundly, picocells typically operate under Open Subscriber Group (OSG) as opposed to the Closed Subscriber Group (CSG) access mode of femtocells. As a result, load balancing becomes a possibility. This opens up new opportunities that should be investigated. For example, one cell could offload a neighboring cell in exchange for additional CCs.

Another logical next step is to factor in the presence of macro cells. CSG femtocells are typically, and rightfully so, portrayed as aggressors in co-channel deployments, due to their potential to turn the coverage area of a macrocell into a swiss cheese. Nevertheless, they are also victimized by macro and picocells due to the tremendous power imbalance. As a result, the framework could be slightly modified to introduce some form of "macro-awareness". Clearly, if the potential harm a femtocell may cause to its neighboring femtocells pales in comparison to the interference generated by the macro layer, it might as well allocate the extra CC without deeper considerations. Simply put, know your enemy.

A completely different line of extension of this work is the evaluation of the coexistence of ACCS and advanced short-term packet schedulers, such as those reported in [113]. In this thesis, the scope was limited to a basic channel blind scheduler. Qualitatively speaking, such opportunistic schedulers are expected to take away part of the gain offered by concepts akin to the one presented in this thesis. However, packet schedulers benefit data channels only, and can do very little or nothing for the control channels. A quantitative analysis of this interplay is therefore suggested for future studies. One possible conclusion is that a fixed and relatively low C/I target might suffice to preclude the most detrimental interference couplings. Moreover, the evaluation in scenarios displaying highly uneven traffic distributions, conforming to the Pareto Principle (the law of the vital few), as well as other traffic models is also strongly advocated.

A final remark concerns a key underlying assumption. Namely, most interference coordination research, including this work, is implicitly based on conservative transceiver designs. On the other hand, advanced transceivers with interference cancelation capabilities are mature and remain a very active research area. Ultimately, both research areas share a common goal – maximize spectral efficiency by means of interference avoidance/suppression, respectively. Unfortunately, work in both fronts has not exploited their intrinsic synergies so far and sometimes even moved in orthogonal directions: a typical design goal of ICIC schemes is the reduction of overall inter-cell interference levels. That approach clearly ignores the suppression capabilities of modern transceivers. In fact, it is potentially counterproductive, because such transceivers work better in the presence of strong dominant interferer(s).

Is this really the way forward? Future studies challenging the current working assumptions might be able to find the appropriate split of roles between the physical and medium access control layers; thus sensibly accommodating interesting new developments such as coordinated Multiple Input Multiple Output (MIMO) schemes.

Appendix A

Self-Organizing Coalitions for Conflict Evaluation and Resolution (SOCCER)

This appendix contains a reprint of the following two articles as well as an overview of the material contained therein, augmented by intuitive discussions. The upcoming discussion contextualizes the work by linking up both papers to the rest of this thesis.

1. Luis G. U. Garcia, Gustavo W. O. Costa, Andrea F. Cattoni, Klaus Pedersen and Preben Mogensen, "Self-Organizing Coalitions for Conflict Evaluation and Resolution in Femtocells," GLOBECOM 2010, 2010 IEEE Global Telecommunications Conference (Globecom 2010) ,Miami, Dec. 2010.

2. Gustavo W. O. Costa, Luis G. U. Garcia, Andrea F. Cattoni, Klaus Pedersen and Preben Mogensen, "Dynamic Spectrum Sharing in Femtocells: a Comparison of Selfish versus Altruistic Strategies," Vehicular Technology Conference Fall (VTC 2011-Fall), 2011 IEEE Vehicular Technology Conference, San Francisco, Sept. 2011.

A.1 SOCCER and this Thesis

Self-Organizing Coalitions for Conflict Evaluation and Resolution (SOCCER) was initially designed as an add-on to the original Autonomous Component Carrier Selection (ACCS) framework. The basic idea was to let the system operate in a simple "first-come, first-served" mode as long as the cell loads remained low to moderate. In this case, the basic Supplementary Component Carrier (SCC) selection rules and the inherently time- and spatially varying nature of traffic would help accommodating the demand for extra Component Carriers (CCs), preventing blind actions by greedy cells to wreak havoc on the network due to excessive interference levels.

However, in high load situations the situation could differ radically. The basic ACCS concept does not explicitly deal with traffic requirements and fairness rules governing neither the acquisition nor the release of SCCs. Such requests are up to lower Radio Resource Management (RRM) entities. ACCS simply grants or denies these requests for additional CCs. Ultimately, this could lead to the pre-emption of CCs as there are no guarantees that a cell would still be granted access to SCCs after its critical surrounding neighbors have made their choices. A femtocell could thus be forced to sacrifice itself continuously (starving resource wise) in favor of the greater good. Alternatively, the competition among neighboring cells could force them to "cheat", thereby engaging into mutually destructive behavior through greedy/blind competition for the same resource. SOCCER was then devised as a complementary means to solve such conflicts of interest, allowing cells to establish non-aggression pacts according to certain policies. Hence, leading to a cooperative competition setting, a.k.a. "coopetition". Figure A.1 depicts SOCCER acting as an add-on to ACCS.

Due to practical constraints and in order to come up with a proof of concept as quickly as possible, a decision to test SOCCER as a stand-alone method was made during the writing of the first paper. The promising results combined with the downright lack of time put off the implementation of SOCCER as an add-on, as initially conceived. This is the sole reason why this line of work is included here as an appendix rather than being part of the main body of the thesis. Nonetheless, SOCCER is one of the main contributions of this thesis due to its simplicity and efficacy.

In hindsight, it could be stated that SOCCER, when used as an add-on, is functionally related to Generalized Autonomous Component Carrier Selection (G-ACCS), albeit very different conceptually. Both methods attempt to overcome the restrictive nature of schemes relying on potential interference coupling by granting access to additional resources when the simpler threshold based approach would deny it.

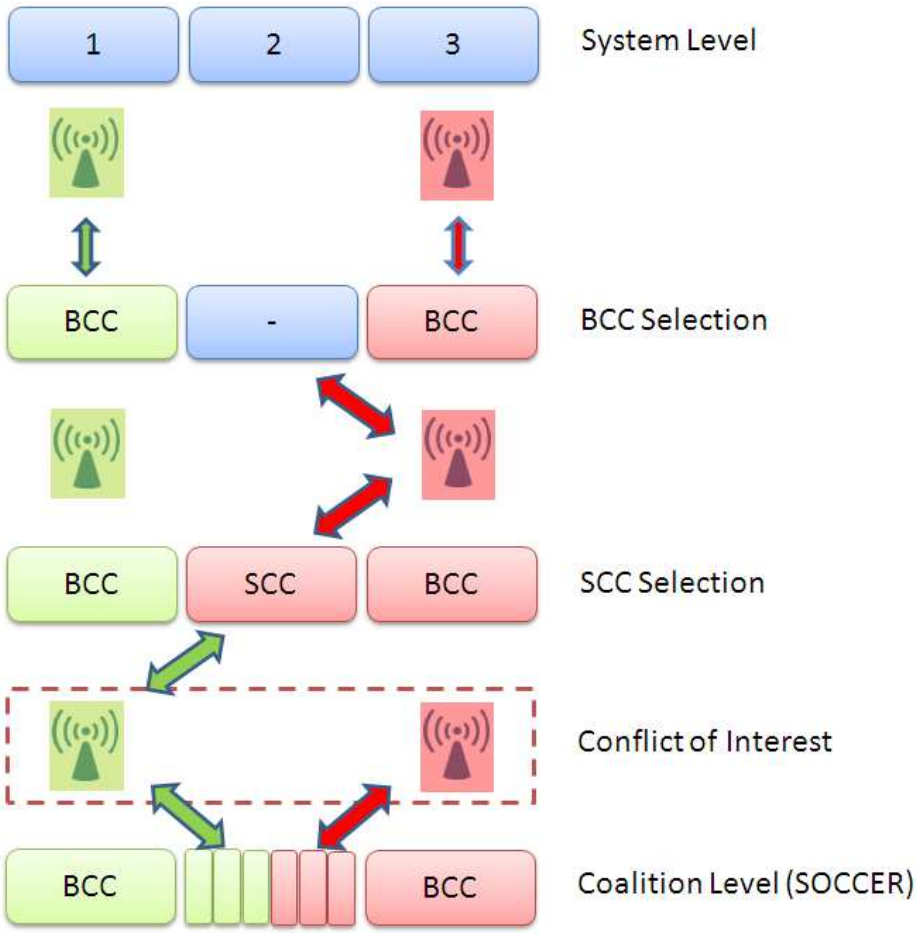

Fig. A.1: An illustration of SOCCER operating as an ACCS add-on. In this basic example, two femtocells form a coalition and share the second component carrier. Each femtocell is entitled to half of CC number 2. More details are given in the paper reprints.

A.2 SOCCER in a Nutshell

The SOCCER algorithm introduced in the first paper is a novel method inspired by graph and coalitional game theories. The proposed algorithm consists of a set of distributed and scalable rules for building coalitions; these rules essentially resolve the conflicts among avid femtocells competing for a limited amount of resources. SOCCER has been designed by targeting localized reconfigurations, thus avoiding reconfiguration storms in the network. Furthermore, the rules governing the resource redistribution ensure overall system performance improvements while maintaining a certain degree of fairness among the competing nodes.

The process consists of two stages: identifying the key contenders and subsequently dividing up the resources. The first phase is essentially driven by some policy, denoted identification of *strong bonding* in SOCCER terminology. The second phase embodies the truce attained via orthogonal resource allocations. The actual coordination of the resources takes place among Femto Access Points (FAPs); hence decisions are made on a cell level. Nonetheless, such decisions hinge on User-Equipment (UE) assistance.

From a graph-theory viewpoint, the policy is the rule defining the edges of the underlying graph representing the network, where each femtocell is a vertex. The reallocation algorithm is then analogous to a vertex coloring procedure. Notice that both elements are equally relevant. Defining a graph that incorporates traits that are pertinent to wireless networks is of paramount importance. That is the reason why the definition of strong bonding is irrevocably linked with channel capacity as defined by Shannon [45] and adjusted to fit the characteristics of the system in consideration [64]. Moreover, while several off-the-shelf graph coloring algorithms exist, in view of the discussions in Chapter 3, online, non-iterative (non-recoloring), localized methods were targeted here.

In our framework and by virtue of the proposed resource reallocation algorithm, femtocells may be part of zero, one or several coalitions at the same time. Furthermore, coalitions can be formed in different and independent ways on each resource unit, e.g. a component carrier or the entire band. The reallocation of resources, if deemed necessary according to the policy, is performed when a femtocell wishes to access resources already in use by other femtocell(s). This procedure can be executed e.g. at startup or delayed until traffic requirements lead to conflicts. In this view, the new entrant is the femtocell seeking access to the spectrum. In the first paper, the policy was defined such that a new entrant can proactively request coordination to at most two active players. The analysis in the first paper, based on elements from graph theory (size of maximal cliques), shows that coordinating with two other players is enough to

provide considerable gains, while avoiding unjustifiable spectrum fragmentation and reducing the need for signaling. Moreover, such simplification allowed the reallocation algorithm to be defined by six simple rules. Extensive simulation results proved the effectiveness of the proposed method.

A.3 SOCCER, Strategies and Game-Theory

As stated earlier, depending on the topology of the network, SOCCER allows femtocells to establish non-aggression pacts, the so-called coalitions, according to certain policies. The encouraging results in the first paper motivated further investigation of a particular aspect: what are the implications if cells are allowed to establish the agreements at their own discretion? Does one need to enforce certain policies or would the behavior of femtocells be "self-regulated"? These aspects were investigated in the second paper.

As opposed to the graph-theory view on SOCCER presented in the previous section, from a game-theoretic perspective, femtocells are greedy agents (players) and will act on a self-interested manner, striving to maximize their utilities. On the other hand, the definition of strong bonding used in the first paper is not truly selfish. Based on examples from society and nature, challenging the selfishness assumption was the main goal of the second article. In the end the two apparently conflicting views are reconciled by realizing that the payoff of each player (femtocell) is affected, not only by the way the channels are redistributed, but also by the very definition of the utility functions. These two elements define the spectrum allocation of each femtocell and the experienced SINR levels. Four alternative utility functions that incorporate altruistic elements were defined.

The analysis included cases where the cooperation level was kept to a strict minimum as well as cooperative cases towards a common goal. In particular, equal rights dynamic spectrum sharing among Closed Subscriber Group (CSG) cells was considered. Four different ways of selecting strategies were analyzed: (i) Selfish: All players select their strategies targeting the maximization of their own instantaneous throughput; (ii) Selfless new entrant: The new entrant intends to protect the existing players and it is completely altruistic. Other players still play selfishly; (iii) Max-min: a pair of players will choose to cooperate if this is of benefit to the player which is most sensitive to their mutual interference; 4) Max-sum: A pair of players will coordinate transmissions if this decision increases their sum capacity compared to uncoordinated transmissions.

The system level simulation results have shown that each femtocell should strive

for a balance between selfishness and altruism. It is possible to use this balance in favor of the overall network throughput or in favor of achieving a minimum performance for each cell. Another interesting observation was that a purely selfish approach (based on incoming only information) is significantly worse than a truly selfless (entirely based on outgoing information) strategy. In conclusion, theoretical assumptions should guide the design of practical solutions, but they should not be a limiting factor. In this case, it was possible to reconcile the policy with canonical assumptions, but this might not always be the case. The policies should be enforced at standardization or regulatory level, if one aims at pushing spectral efficiency to its limits.

A.4 Final Remarks

SOCCER as a stand-alone method is likely to become overprotective in the presence of bursty traffic, similarly to ACCS as discussed in Chapter 5. This occurs because SOCCER is also based on expected interference coupling, that is to say, it relies on the information found in the Background Interference Matrix (BIM). However, as an add-on managing inter-cell interference on a shared band, complementary to a pseudo-dedicated one embodied by Base Component Carrier (BCC), SOCCER is probably still very efficient even if the load conditions deviate from those of full-buffer traffic. Both scenarios have not been experimentally tested yet as are the obvious next subjects of investigation.

A.5 Paper Reprints

This full text paper was peer reviewed at the direction of IEEE Communications Society subject matter experts for publication in the IEEE Globecom 2010 proceedings.

Self-Organizing Coalitions for Conflict Evaluation and Resolution in Femtocells

Luis G. U. Garcia*, Gustavo W. O. Costa*, Andrea F. Cattoni*, Klaus I. Pedersen† and Preben E. Mogensen*†
*Aalborg University, Aalborg, Denmark
†Nokia Siemens Networks, Aalborg, Denmark

***Abstract*—The recent introduction of carrier aggregation in LTE-Advanced enables new possibilities in designing frequency domain interference reduction and management schemes. These methodologies are of extreme interest in the case of dense and uncoordinated deployments of femtocells. In such scenarios, dense deployment of cells coupled with the scarcity of frequency resources may lead to a potentially disruptive amount of interference, which severely affects the performance of the system. This contribution presents a novel method inspired by graph and coalitional game theories. The proposed algorithm consists of a set of distributed and scalable rules for building coalitions; these rules essentially resolve the conflicts among avid femtocells competing for a limited amount of resources. The proposed scheme has been designed by targeting localized reconfigurations, thus avoiding reconfiguration storms in the network. Furthermore, the rules governing the resource redistribution ensure overall system performance improvements while maintaining a certain degree of fairness among the competing nodes. Simulation results prove the effectiveness of the proposed method.**

***Index Terms*—Spectrum Sharing, Coalitions, Femtocells, LTE-Advanced, Self-organizing.**

I. Introduction

Carrier aggregation, i.e., simultaneous transmission over multiple component carriers, is emerging as a key feature of future wireless communication systems aiming at fulfilling the targets set by the International Telecommunication Union in [1]. It offers the possibility to increase physical layer data rates proportionally to the number of aggregated carriers and facilitates backward compatibility at the same time. Today, carrier aggregation is already present in the form of channel bonding (two adjacent carriers) in WiFi (IEEE 802.11n) and it is a central element of both LTE-Advanced and WiMAX (IEEE 802.16m), currently under standardization.

A side benefit of carrier aggregation is the potential to dynamically reconfigure the system bandwidth, which can be exploited in the form of simple yet effective frequency domain interference coordination schemes. This becomes especially attractive when one considers future deployments of femtocells. These are cost-effective, user-deployed, low-power base stations operating in licensed spectrum. The concept is extremely enticing due to the potential benefits that it offers to operators and end-users, e.g. improvement of indoor broadband wireless services and offload of the macro-cellular network [2], [3]. Nonetheless, unlike carefully planned macro cells, femtocell deployment will be uncoordinated and potentially chaotic. For that reason, femtocell deployment demands some form of interference management [4], [5].

In order to cope with the traffic demand, heavily loaded cells will need more component carriers than lightly loaded ones. Under low to moderate load conditions, a simple "first-in, first-served" mode of operation may be effective. In this case, the inherently time-varying nature of traffic in each cell will help accommodate the demand for extra component carriers. However, in high load situations the competition among neighboring cells can force them to engage into mutually destructive behavior through greedy/blind competition for the same resource. This can lead to severe inequities or result in an inefficient usage of the resources due to excessive interference levels, especially within dense local area network deployments.

In the following, we propose a practical and self-organizing method aiming at fair and efficient resource distribution whenever competition for the same resource arises among two or more cells. The main objective is to ensure access to additional resources in a rational and coordinated fashion. Our case study is based on LTE-Advanced, whose terminology is employed; nonetheless the proposed methodology is general and can be applied to other radio access technologies. The considered target deployment scenario is a dense-urban residential one, assuming a closed subscriber group access policy. We derive our results from a Monte Carlo performance evaluation according to the methodology defined in [6] by 3GPP.

The rest of this paper is organized as follows: Section II points to related research in the literature and introduces the proposed concepts in the detail. Section III states the simulation assumptions, while Section IV presents and discusses the obtained results. Finally, Section V concludes the paper and points out possibilities for future work.

II. System Model

In this section we introduce our framework and carefully describe the proposed method – Self-Organizing Coalitions for Conflict Evaluation and Resolution (SOCCER). Due to space limitations, a rigorous mathematical analysis is beyond the scope of this short contribution and it will be the subject of a future paper. We point interested readers to the pertinent literature on coalitional game theory [7] and we provide a quantitative proof of SOCCER effectiveness by means of numerical simulations.

978-1-4244-5638-3/10/$26.00 ©2010 IEEE

This full text paper was peer reviewed at the direction of IEEE Communications Society subject matter experts for publication in the IEEE Globecom 2010 proceedings.

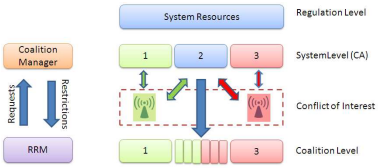

Fig. 1. Proposed framework.

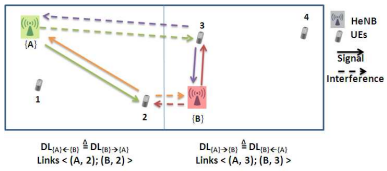

Fig. 2. Simplified scenario illustrating how the BIM is estimated. In the context of femtocells we take the lowest carrier-to-interference (C/I) ratio reported towards a given neighbor as representative of the interference coupling between a pair of cells.

A. The proposed framework

We define a network as a set of N femtocells, denoted by $\mathcal{N} = \{1, \ldots, N\}$ (home eNBs (HeNBs) in LTE-Advanced terminology), which operates in a licensed spectrum. The spectrum is divided into a set of Component Carriers (CC), $\mathcal{M} = \{1, \ldots, M\}$ of cardinality $|\mathcal{M}| = M$, each of bandwidth $BW_{m|m\in\mathcal{M}}$. CCs can be either contiguous or not. The framework is depicted in Fig. 1 along with a simplified representation of the system showing a coalition formed by two HeNBs. We discuss coalitions in detail in the next two sections. In the example, the total bandwidth is equally divided into 3 CCs and as soon as the requirements of each cell can no longer be met with a single CC, a conflict of interest arises. Under such circumstances, it is highly desirable to ensure that this resource is utilized in an efficient and fair manner. This task can be accomplished by forming coalitions.

We posit that coalition managers, local to each HeNB, keep coalition tables, one for each shared CC. This table stores the list of current coalitions and the corresponding allocation restrictions. We also suggest that Radio Resource Management (RRM) entities such as packet schedulers interact with coalition managers indicating the need for CCs subject to local traffic requirements. Additionally, coalition formation is binding, meaning that HeNBs must respect the agreement and packet schedulers shall abide to the imposed restrictions. Furthermore, it is relevant to stress: (i) coalition managers operate on a much longer time scale when compared to packet schedulers; (ii) the proposed multi-layered approach is not limiting; the coalition based concept can be employed both at intra- or inter-component carrier levels. Figure 1 depicts coalitions within (intra) CCs, however, if so desired, the entire system bandwidth can be seen as a single wideband resource to be shared via coalitions as seen in Section III.

In the following section we describe a set of distributed rules enabling the autonomous formation of coalitions among HeNBs, which can then be mapped into undirected graphs as explained in Section IV-B. The formation rules rely on simple capacity estimations based on prior system performance characterization and knowledge of mutual interference coupling between a pair of cells.

B. Strong bonding

The two central pillars of the proposed method are: determining the presence of *strong bonding* between pairs of HeNBs and the subsequent formation of coalitions following certain working principles. This section dissects strong bonding, while the coalitions are the subject of the next one. In simple terms, the presence of a strong bonding between two HeNBs implies that mutual cooperation by means of a coalition is beneficial. Conversely, in the absence of strong bonding, competition is fruitful and no restrictions are enforced.

Strong bonding is determined by a bidirectional relation between two HeNBs. This evaluation relies on so-called Background Interference Matrices (BIM) [4], which we postulate to be built by each HeNB based on standard downlink (DL) measurements, namely User Equipment (UE) Reference Signal Received Power (RSRP) [8]. Figure 2 illustrates the concept and depicts all involved links in the description that follows. Each UE measures the RSRP from both its serving cell and neighboring HeNBs, just as in handover measurements. The RSRP values are reported to its serving HeNB. In turn, the corresponding HeNB gathers this information and calculates differences of RSRP values (in dB). This calculation yields potential DL incoming C/I ratios in case the same CC is reused by the neighboring cell, as perceived by each of its served UEs. Clearly, there are many possible manners to utilize this knowledge, but in the context of femtocells we take the lowest C/I ratio reported towards a given neighbor as representative of the DL incoming interference coupling between the pair of cells, henceforth denoted by $DL_{\{.\}\leftarrow\{.\}}$.

Naturally, if the femtocell serves more than a single UE, the lowest C/I value for different neighbors can come from different UEs. In such a way, interference coupling among cells is quantified on a pair-wise basis, i.e. not considering the total effectively received interference power. In addition to incoming ratios, DL outgoing C/I ratios (calculated as incoming ratios by neighboring cells) are signaled back and represented here by $DL_{\{.\}\rightarrow\{.\}}$. The BIM information essentially "teaches" each cell about its mutual interference coupling with neighboring cells, which makes them capable of estimating the impact of any new allocation on surrounding cells, both as victims and sources of interference.

Now, let two neighbor HeNBs be denoted by A and B. Mathematically, a strong bonding occurs whenever (1) is satisfied,

$$v(G_{\{A,B\}}) > v(G_{\{A\}}) + v(G_{\{B\}}) \qquad (1)$$

978-1-4244-5638-3/10/$26.00 ©2010 IEEE

This full text paper was peer reviewed at the direction of IEEE Communications Society subject matter experts for publication in the IEEE Globecom 2010 proceedings.

where $v(G_{\{A\}})$, $v(G_{\{B\}})$ are the values of the single element coalitions, while $v(G_{\{A,B\}})$ is the value of a coalition formed by A and B in terms of Spectral Efficiency (SE in bits/s/Hz):

$$v(G_{\{A\}}) = \mathrm{SE}[(\mathrm{C/I})_{\mathrm{A|B}}] \quad (2)$$

$$v(G_{\{B\}}) = \mathrm{SE}[(\mathrm{C/I})_{\mathrm{B|A}}] \quad (3)$$

$$v(G_{\{A,B\}}) = \frac{1}{2} \cdot \{\mathrm{SE}[(\mathrm{C/I})_{\mathrm{A}}] + \mathrm{SE}[(\mathrm{C/I})_{\mathrm{B}}]\} \quad (4)$$

The function $v(.)$ is expressed by an adjusted Shannon capacity formula [9] based on *a priori characterization* of link level performance, where the bandwidth and the SNR efficiencies of the system are taken into account. It maps the potential C/I (taken from the BIM, such that $(C/I)_{A|B} = \min(DL_{\{A\}\leftarrow\{B\}}, DL_{\{A\}\rightarrow\{B\}})$) into spectral efficiency estimations. Moreover, while in (2) and (3) it is assumed that that both nodes decide to simply reuse the entire resource, in (4) each HeNB gets one orthogonal half of the resource, which takes a sensible and fair non-aggression pact as a model.

Note that the information both cells see is identical given the way the BIM is created. Obviously, this is a compromise in order to avoid additional signaling and any information mismatch. It implies that any externalities are *not* considered while determining strong bonding. This simplification entails that we assume $(\mathrm{C/I})_{\mathrm{B|A}} = (\mathrm{C/I})_{\mathrm{A|B}}$ instead of using $(\mathrm{C/I})_{\mathrm{A|}\mathcal{N}}$ and $(\mathrm{C/I})_{\mathrm{B|}\mathcal{N}}$ in (2) and (3). Additionally, if the other cell is not present (made orthogonal), the channel is estimated to be free such that $(\mathrm{C/I})_{\mathrm{A}} = (\mathrm{C/I})_{\mathrm{B}} = (\mathrm{C/I})_{\mathrm{free}}$ in (4). At the expense of additional signaling, the estimated C/I given the rest of the network ($(\mathrm{C/I})_{.|\mathcal{N}}$) that is currently using the same resource could be considered as well.

C. Formation rules

A coalition of otherwise interfering HeNBs is merely a *code of conduct*, which once established via bi- or multilateral agreements, dictates how its members shall share resources targeting resource orthogonalization. As such, a HeNB may be part of none, one or several coalitions at the same time. Furthermore, coalitions can be formed in different and independent ways on each CC. The cardinality of a coalition is the number of involved parts. We will use the notation n-coalition for a coalition of cardinality n.

Hereafter, a HeNB seeking for an additional CC is denominated a new entrant HeNB. The new entrant HeNB needs to determine which neighboring HeNBs should be considered as coalition candidates. Each candidate HeNB should fulfill two conditions: it is already using the desired CC and it has a strong interference bonding with the new entrant, as defined in (1). If there are no candidates, the solution is trivial: the new entrant HeNB can use the whole CC.

In order to reduce the complexity of the method, we consider here the case where the new entrant HeNB will send Coalition Formation Requests (CFR) for at most two coalition candidates. In Section IV-B we justify this choice, considering typical deployment scenarios. Then, the method can be implemented using six simple formation rules, depending on two aspects:

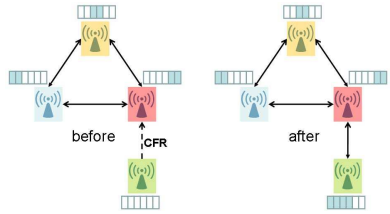

(a) "Free rider" scenario.

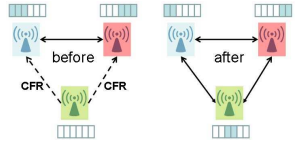

(b) Augmentation: from a 2-coalition to a 3-coalition.

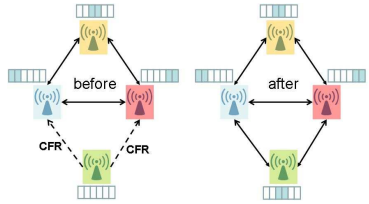

(c) "Follow suit" 3-coalition example.

Fig. 3. Before: the new entrant sends a CFR to one or more strongly bound interferers. After: the coalition is formed the resources are divided accordingly.

- Whether there is one or two coalition candidates.
- Whether the candidates are already involved or not in previously formed coalitions.

The formation rules can be summarized as follows:

1) Only one coalition candidate: There are two sub-cases:

- If the coalition candidate has full allocation of the CC, the resources shall be equally divided. Therefore, both the new entrant and the coalition candidate will have different halves of the CC, precisely as in Fig. 1.
- If the coalition candidate is already involved in other coalitions it will not have full allocation of the CC. In this case, the new entrant can use all the sub-resources which are not already allocated by the coalition candidate. Note that, in this case the new entrant may have even more than half of resources, characterizing a "free rider" situation, illustrated in Fig. 3a. If the coalition candidate has more than or exactly half the resources, then each of the parts shall allocate half of the resources.

2) Two coalition candidates: Here, there are four sub-cases:

- The coalition candidates are part of a 2-coalition. In this case, the resources shall be divided equally amongst the

978-1-4244-5638-3/10/$26.00 ©2010 IEEE

This full text paper was peer reviewed at the direction of IEEE Communications Society subject matter experts for publication in the IEEE Globecom 2010 proceedings.

three HeNBs, augmenting the 2-coalition to a 3-coalition as shown in Fig. 3b.

- The coalition candidates are part of one or more 3-coalitions with third party HeNBs. In this case, the new entrant has to allocate exactly the same resources as the third party, and no changes are made to the resource allocation of the candidates. A new 3-coalition is formed amongst the three involved parts, as exemplified in Fig. 3c.
- The coalition candidates are not part of the same coalition and their allocations can be made compatible with the new entrant allocating half of the resources. In this case, the new entrant will form 2-coalitions with both of them and will allocate half of the resources on the most efficient fashion. One example is illustrated in Fig. 4a.
- The coalition candidates are not part of the same coalition but their allocations can *not* be made compatible with the new entrant allocating half of the resources, due to restrictions imposed by other coalitions previously formed. In this case, the new entrant will form 2-coalitions with both of them, but the CC will be divided in the same way as if there was a 3-coalition, i.e., in three equal parts, as shown in Fig. 4b.

These rules have been designed considering resource fairness, efficiency and solving all conflicts locally, i.e., up to the first tier of neighbors. This choice was made to reduce the need for signaling and the complexity of the underlying inter-HeNB communication protocol, as well as avoiding reconfiguration storms. The main reason being that there is no straightforward way for a HeNB to know how far it is from the edge of the network. If further communication is considered, e.g. with the second tier of neighbors, refinements are possible at the cost of increased complexity, e.g. the left- and rightmost HeNBs in Fig. 4b could become free-riders.

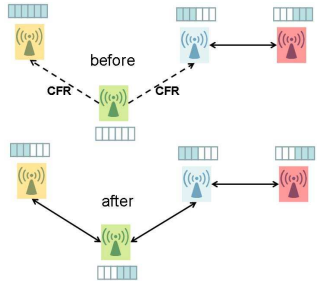

(a) Two new and compatible 2-coalitions.

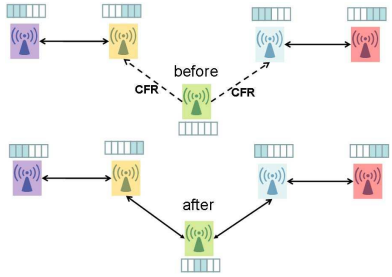

(b) Two new and incompatible 2-coalitions.

Fig. 4. Before: the new entrant sends a CFR to two strongly bound interferers. After: the coalition is formed the resources are divided accordingly.

III. Simulation Methodology

A. Simulation Tool

The performance was evaluated through semi-static system level simulations. The simulator is based on basic LTE specifications [10]. It relies on series of "snapshots". During each snapshot, path loss, shadowing and the location of devices remain constant. Fast fading is not explicitly simulated; therefore, results can be viewed as the performance averaged over a sufficiently long time period. Moreover thousands of snapshots are simulated to ensure statistical reliability.

We consider a full buffer traffic model and a 2x2 antenna configuration for all links allowing up to two code words. A simple equal resource sharing (round-robin) packet scheduling algorithm is assumed. Open-loop uplink Fractional Power Control (FPC) as standardized by 3GPP [11] for LTE is modeled as well.

For any given UE, the signal to interference and noise ratio (SINR) is calculated according to the UE's specific parameters (interfering cells, allocation of PRBs, etc.). Error vector magnitude (EVM) modeling is present in order to account for various imperfections in the implementation of Radio Frequency (RF) components and imposes an asymptotical limit to SINR values. Look-up tables map the SINR to corresponding throughput values according to a modified Shannon's formula from [9]. The raw spectrum efficiency is upper bounded to 10.04 bps/Hz due to modulation and coding scheme (MCS) limitations. The most important parameters are summarized in Table I.

B. Deployment Scenario

We consider a block consisting of two stripes of apartments, each stripe having 2 by 10 apartments per floor in a total of 6 floors, thus totalling 240 apartments. There is a 10m wide street between the two stripes of apartments. The area of the block is therefore 120m x 70m.

Partially owing to the full buffer assumption and in order to simulate an absolutely worst case scenario, the multi-layered resource allocation is not considered; therefore CCs are not further subdivided neither in time nor frequency. Instead, the entire bandwidth was divided into 6 equal CCs, thus permitting coalitions of cardinality up to 3, where HeNBs can be allocated 2,3,4 or 6 CCs according to the proposed rules.

It is assumed that with probabilities $P = 25\%$ (dense deployment) and $P = 75\%$ (denser deployment) there is one

978-1-4244-5638-3/10/$26.00 ©2010 IEEE

This full text paper was peer reviewed at the direction of IEEE Communications Society subject matter experts for publication in the IEEE Globecom 2010 proceedings.

TABLE I
ASSUMPTIONS FOR SYSTEM-LEVEL SIMULATIONS

System Model		
Spectrum allocation	6 CCs of 5 MHz each	
Duplexing scheme	TDD	UL: 50%
EVM	3%	
eNB parameters	TX power	23 dBm
	Antenna system	Omni (3dBi)
UE parameters	Max. TX power	23 dBm
	Min. TX power	−40 dBm
	Antenna system	Omni (0dBi)
Power control [11]	DL	NO PC
	UL	FPC (−60 dBm, 0.8)
Deployment Model [6]		
Dense Urban	Room size	10m x 10m
	Street width	10 m
	Internal walls	5 dB attenuation
	External walls	10 dB attenuation
Propagation Model [6]		
Minimum coupling loss	45 dB	
Shadowing std. deviation	Serving Cell	4 dB
	Other Cells	8 dB
Traffic Model		
User distribution	Uniform: 1 UE/cell (Indoor)	
Data generation	Full buffer	

low-power eNB in each flat. In the absence of a HeNB, we assume that there are no active users in the flat. Both HeNBs and UEs are dropped uniformly at random positions. All users are located indoors, assuming closed subscriber group access mode, i.e. UEs always connected to a HeNB in the same apartment. The indoor path loss modeling follows that defined in [6]. Macro-cells are not considered in this study.

IV. RESULTS AND DISCUSSIONS

A. Performance Analysis

All the throughput results were normalized by the maximum theoretical capacity of the system. Hence, a normalized throughput of 100% means transmission over the whole bandwidth at the maximum system spectral efficiency.

Figure 5 shows the empirical cumulative distribution function (CDF) of cell throughput, at 25% deployment ratio. Three cases are compared: universal reuse $(1/1)$, hard reuse $1/2$ and SOCCER. In a sparser deployment such as the one considered in Fig. 5, the reuse $1/2$ approach becomes clearly bandwidth limited for most of the cells. This can be concluded from the nearly vertical lines. Reuse $1/1$ provides a better average throughput than reuse $1/2$ since the band is doubled, but that inflicts a high penalty to those cells which have an unfavorable geometry due to the uncoordinated deployment. On the contrary, the proposed method can adaptively choose the spectrum allocation outperforming both reuse patterns in terms of average cell and 5% outage throughput. One can conclude that the proposed method is very efficient in attaining a minimal quality even for the cells which have a strong interference coupling.

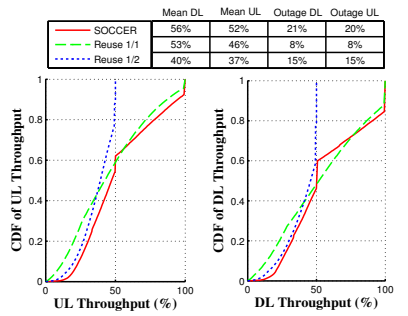

Fig. 5. Uplink and Downlink cumulative distribution functions of cell throughput, at 25% deployment ratio. Average and 5% Outage throughput results are highlighted.

Note, that in our method it is acceptable to have a small loss in one link direction for the common good. This can be seen from the small CDF range in Fig. 5 where reuse $1/1$ has better performance then the proposed method. We purposefully introduce symmetry, taking the lowest Incoming/Outgoing C/I value to represent the interference coupling between two cells. If there is a significant imbalance between outgoing and incoming C/I ratios, one cell loses a bit of capacity (e.g.in the DL) and the other one will gain. However, in the opposite direction (UL), the situation is reversed and in total, everybody benefits in one way or another. Therefore, the same cells which lose compared to universal reuse in one direction are the ones which gain the most in the opposite direction and, for that reason, the whole network can benefit from enhanced average capacity.

In Fig. 6 we consider a denser deployment, i.e. $P = 75\%$. On such a dense network most cells become interference limited instead of bandwidth limited. In a interference limited scenario, reuse two becomes a more interesting alternative to reuse one. In fact, in a dense deployment strong interference coupling appears more often and, hence, reuse one yields severely degraded outage performance. Our method adapts to this situation, providing similar results to reuse two in terms of 5% outage and average throughput. The peak capacity of SOCCER, at 95% of CDF, is 40% higher than reuse two in uplink and 28% in downlink.

B. Analysis of network graphs

In Section II-C, in order to limit the complexity, we suggested to limit the number of interferers to which each base station signals their intent to join coalitions. Now, we shall revisit this concept. Let us first model the network as an undirected graph, with a vertex for each HeNB and edges to represent *strong bonding*. Using graphs as a model, a maximal clique of size α represents a subset of α HeNBs such that every two HeNBs in the subset are connected by an edge and the

978-1-4244-5638-3/10/$26.00 ©2010 IEEE

This full text paper was peer reviewed at the direction of IEEE Communications Society subject matter experts for publication in the IEEE Globecom 2010 proceedings.

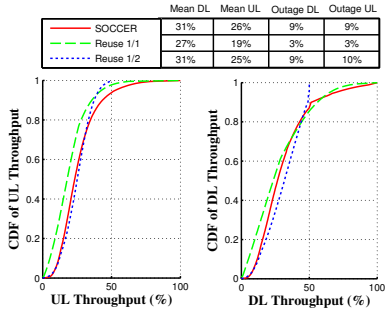

Fig. 6. Uplink and Downlink cumulative distribution functions of cell throughput, at 75% deployment ratio. Average and 5% Outage throughput results are highlighted.

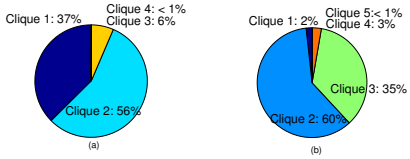

Fig. 7. Pie-charts of occurrences of maximal cliques in the interference graph. (a) Maximal clique occurrence for 25% and (b) 75% deployment ratios.

subset can not be extended to $\alpha + 1$ HeNBs.

The two pie charts in Fig. 7 show the relative occurrence of maximal cliques of various sizes in the interference graph of the simulated scenarios. Even in very dense scenarios, maximal cliques of cardinality larger than 3 are infrequent.

SOCCER forms coalitions that closely match the maximal clique sizes on the interference graph. This means that the simplified method will work very efficiently on most of the cases on the investigated scenario. Note also that the method is not necessarily inefficient if there are cliques larger than size 3. When a multi-layered resource allocation is considered as shown in Fig. 1, then the conflicts of cliques of size 4 or larger can be solved on the higher level. Considering the distributions of clique size in a typical deployment scenario (Figs. 7a and 7b), the traffic variability and the extensibility to multi-layered resource allocation we suggest to apply the simplifying assumption to practical cases.

C. Practical considerations

Potential applications beyond those described are numerous; the proposed resource sharing scheme can be adapted to other autonomic communication systems with relatively simple adjustments. The only requirements are the ability to flexibly (sub-)divide a resource and to be in possession of a representative characterization of the system performance in order to estimate the value of coalitions. For simplicity, we have demonstrated an LTE-Advanced system whose bandwidth was divided into 6 CCs to accommodate coalitions of up to three devices sharing the same resource. However, if 6 CCs are not readily available, the framework shown in Fig. 1 can be directly utilized, if 6 orthogonal resources are created via e.g. Time-Division Multiple Access (TDMA). In this case, TDMA could be employed in order not to sever an LTE-Advanced CC into smaller chunks. In these circumstances, cells would be entitled to one autonomously selected base/anchor carrier, which is "untouchable", i.e. it is always active, indivisible and may only be re-used by cells without *strong bonding*, while sharing supplementary or secondary CCs according to the formation rules.

V. Conclusion

This contribution introduced a new mechanism, which enables femtocells to self-adapt and autonomously share resources aiming at efficient network operation. The proposed method presents three highly desirable virtues; it is simple, practical and delivers very attractive performance results. Based on the evaluation of the mutual interference coupling between pairs of HeNBs, it leads to sensible cooperation via multilateral agreements following a simple set of rules, which by construction preclude disruptive reconfiguration avalanches. The algorithm has been extensively tested by means of computer simulations in dense urban deployment scenarios within an LTE-Advanced framework. The obtained results prove the proposed method is able to outperform traditional pre-planned frequency reuse patterns both in terms of average and 5% outage throughput per cell. Moreover, when modeling the network as a graph, results also demonstrated that maximal cliques larger than 3 are rather infrequent even in extremely dense networks operating at full load; this result illuminated an important aspect of the problem structure and justified the limit imposed by design on the maximal coalition size.

References

[1] ITU, "Guidelines for evaluation of radio interface technologies for IMT-Advanced," Tech. Rep., July 2008.
[2] V. Chandrasekhar, J. G. Andrews, and A. Gatherer, "Femtocell networks: A survey," *Communications Magazine, IEEE*, September 2008.
[3] H. Claussen, L. T. W. Ho, and L. Samuel, "Financial Analysis of a Pico-Cellular Home Network Deployment," in *IEEE ICC*, June 2007.
[4] L. G. U. Garcia, K. I. Pedersen, and P. E. Mogensen, "Autonomous Component Carrier Selection: Interference Management in Local Area Environments for LTE-Advanced," *Communications Magazine, IEEE*, September 2009.
[5] D. L. Pérez *et al.*, "OFDMA Femtocells: A Roadmap on Interference Avoidance," *Communications Magazine, IEEE*, September 2009.
[6] 3GPP RAN 4, "Simulation assumptions and parameters for FDD HeNB RF requirements," Tech. Rep. R4-092042, May 2009.
[7] W. Saad *et al.*, "Coalitional game theory for communication networks: A tutorial," *Signal Processing Magazine, IEEE*, September 2009.
[8] 3GPP, "TS 36.214, Physical layer Measurements," Tech. Rep., Feb 2008.
[9] P. E. Mogensen *et al.*, "LTE Capacity Compared to the Shannon Bound," in *VTC Spring*, April 2007.
[10] 3GPP, "TR 25.814, Physical layer aspects for evolved Universal Terrestrial Radio Access (UTRA), V 7.1.0," Tech. Rep., September 2006.
[11] ——, "TS 36.213, Evolved Universal Terrestrial Radio Access (E-UTRA); Physical layer procedures, V 9.0.1," Tech. Rep., December 2009.

978-1-4244-5638-3/10/$26.00 ©2010 IEEE

Dynamic Spectrum Sharing in Femtocells: a Comparison of Selfish versus Altruistic Strategies

Gustavo W. O. Costa*, Luis G. U. Garcia*, Andrea F. Cattoni*, Klaus I. Pedersen† and Preben E. Mogensen*†
*Aalborg University, Aalborg, Denmark
†Nokia Siemens Networks, Aalborg, Denmark

***Abstract*—Dynamic spectrum approaches are steadily gaining momentum, especially in the context of femtocells. Yet designing efficient, stable, fair and scalable distributed algorithms is no easy feat, specially if the cells in a wireless network tend to act selfish and independently. Game Theory is a powerful toolbox which models the interaction of autonomous agents. In this paper we present a game theoretic model for a dynamic spectrum sharing framework recently proposed for femtocells [1]. Our analysis includes cases where femtocells compete for spectrum as well as cooperative cases towards a common goal. The system level simulation results show that strict adherence to the game-theoretic selfish behavior performs poorly compared to the non-adherent rules which balance altruism and rational egoism. The main conclusion is that practical solutions should be guided but not limited by purely theoretical assumptions.**

***Index Terms*—Spectrum Sharing, Femtocells, Carrier Aggregation, Self-organizing.**

I. Introduction

The traffic growth in wireless networks is pushing the spectrum utilization toward dynamic spectrum allocation. The requirements for the design of practical dynamic spectrum sharing solutions are quite tight in terms of efficiency, stability, fairness and scalability. Furthermore, achieving these goals in a distributed fashion is complicated since wireless network can take independent decisions.

Game Theory (GT) deals with such autonomous decisions. Therefore, GT has been applied to dynamic spectrum sharing and cognitive radio in a number of recent proposals [2]–[4]. Nonetheless, canonical game-theoretic models assume a intrinsically selfish behavior. Consequently players will always attempt to maximize their own welfare disregarding those of other players.

Yet, this needs not to be the case for cognitive agents. Experimental settings of the ultimatum game [5] show that human subjects often behave in ways that completely erode the hypothesis that people only act in favor of their personal interest. Also, in nature, the concept of reciprocal altruism [6] introduced in the field of evolutionary biology shows that individuals can take actions that are detrimental to themselves at a particular moment in time. Yet, in the long run such behavior might be beneficial because there is a chance of being in a reverse situation and therefore be favored by other individuals.

In the field of wireless communications, the work in [7] has shown that a combination of egoistic and altruistic beamforming can play an important role in the optimization of the rates in a Multiple-Input-Multiple-Output interference channel (MIMO-IC) case. Coalition formation for spectrum sensing is investigated in altruistic and selfish settings in [4].

In this paper we investigate different degrees of altruism and selfishness in a dynamic spectrum sharing framework. The resource (spectrum) sharing problem is extremely pertinent in the context of femtocells due to the envisioned large scale uncoordinated deployment of these low-power base-stations [8]. Assuming a purely selfish behavior a femtocell only cooperates if that leads to an increase of its instantaneous throughput. The opposite occurs in a selfless approach: only the other cells matter. Cells cooperate without regarding any benefits and losses that such action may bring because they expect other cells to do exactly the same, as in reciprocal altruism. Finally, in balanced approaches each femtocell weighs the benefits and costs of cooperation when it determines its collaborative set of femtocells.

These different strategies are investigated under the framework we introduced in [1], namely Self-Organizing Coalitions for Conflict Evaluation and Resolution (SOCCER). In this contribution, we formalize this framework using a game theoretic model, which was not present in [1]. The game is analyzed using the basic game theoretic assumptions of selfishness. Furthermore, we analyze the overall performance of SOCCER under four different strategies for transmission coordination: (i) egoistic, (ii) selfless and (iii) a balanced approach aiming at the maximization of minimal throughput and (iv) a balanced approach aiming at maximal sum throughput. The analysis is corroborated by system-level simulations.

The rest of this paper is organized as follows: Section II describes our system model, whereas section III formalizes our spectrum sharing framework in light of Game Theory. Different strategies for the establishment of cooperative sets are introduced. Using game theoretic analysis in Section IV we discuss the strategies on a few example scenarios. In Section V, we present and discuss the system level simulation results obtained. Finally, Section VI recapitulates the main findings and concludes the paper.

II. System Model

We consider equal rights dynamic spectrum sharing among closed-subscriber group (CSG) femtocells. We investigate only the intra-tier interference avoidance [8] and the macrocells are assumed to operate in a separate band. Thus, macrocells are not explicitly modeled. The Femtocell Access Point (FAP)

978-1-4244-8325-9/11/$26.00 ©2011 IEEE

coordinates the spectrum allocation with the served User Equipments (UEs). Hence, the spectrum decisions are done on a cell basis. We assume that each femtocell can make autonomous decisions about spectrum allocations and, for this reason, the problem is modeled as a game in the next section. Hereafter, a CSG femtocell is also referred to as a player, following the GT nomenclature.

Furthermore, we assume that communication among femtocells is possible, at least, for neighbor femtocells. The particular communication requirements which enable this framework are:

- Exchange of measurements, which characterize the interference coupling between a pair of femtocells.
- Messages needed to establish coordinated transmissions. We assume the availability of a protocol to perform this task.

A simple way to characterize the interference coupling of a pair of cells is using Background Interference Matrices (BIMs). Essentially, a BIM entry is a measurement of signal-to-interference ratio (SIR) for a single interferer. For example, for a pair of cells, i and j, the incoming downlink BIM of i is denoted $\mathrm{DL}_{\{i\}\leftarrow\{j\}}$ and it is a representative value of the SIR experienced by UEs at femtocell i if the FAP at j is the only interferer. Conversely, the outgoing downlink BIM of i towards j is the SIR measured by UEs at femtocell j, when i is the only interferer. The outgoing BIM is denoted as $\mathrm{DL}_{\{i\}\rightarrow\{j\}}$. Naturally, for a pair of cells the incoming BIM of a cell is the outgoing BIM of the other, i.e., $\mathrm{DL}_{\{i\}\leftarrow\{j\}} \equiv \mathrm{DL}_{\{j\}\rightarrow\{i\}}$, by definition. Notice that players need to exchange the incoming BIM values, so that relevant interferers are also aware of their outgoing BIMs.

The system bandwidth is divided in orthogonal channels. We assume that there is a mechanism for the transmission over multiple channels. One example is carrier aggregation [9] which allows the femtocells to coordinate transmissions by selecting different sets of component carriers. Transmission coordination has a cost, which is the reduction of the total transmit bandwidth, but it also has an associated benefit, which is the increase in signal-to-interference-plus-noise-ratio (SINR). In general, even if SINR can be further increased, there is a limit on the maximum capacity gain because wireless systems have a limited number of modulation and coding schemes (MCSs). For this reason, a player needs to estimate capacity in order to evaluate whether or not to coordinate transmissions. Since all femtocells implement the same radio access technology, they can use pre-calculated SINR to throughput mapping tables to derive capacity estimations.

We are particularly interested in the performance during the most congested times, when several players are active such as illustrated in Fig. 1. Note that we do not specify a particular time scale for this model. The time granularity is ultimately restricted by the cell to cell and FAP to UE signaling capabilities. If the signaling can be done fast, then new spectrum decisions can be updated for every traffic session. More conservatively it could be done on FAP power on and updated from time to time.

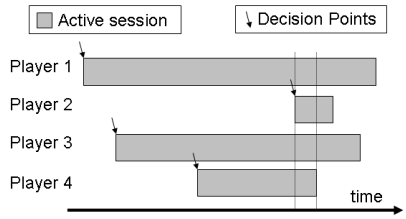

Fig. 1. Session activation is not controlled by the players. The most congested time is illustrated by the vertical bars.

III. Game Theoretic Modeling

A. Game Model

In Game Theory (GT), a game is a formal model of a particular problem and the players are the decision makers of a game. The players select their strategies among a strategy set in order to maximize an utility function, which models the players' preferences over a set of possible outcomes. In this paper, we assume that the utility of a femtocell is naturally given by its downlink throughput.

In our model, when a player becomes active, he has to decide on the spectrum allocation. Referring to Fig. 1, the activation of each player is naturally modeled as a dynamic game [10]. In dynamic games, there is a defined structure of decision points, named information sets. In an information set, a particular player is presented with a set of possible actions and it must make a decision based on the information he has at hand. When dynamic games have a regular structure which is repeated several times, such structure is called a game stage. The activation of a new player starts a new game stage in our model. Each game stage can be described as follows:

- A player is randomly selected for activation. Using GT nomenclature this is a move made by *Nature*, i.e., a random movement the players do not have control upon.
- The newly activated player can chose a subset of other players to request for coordinated (orthogonal) transmission. We name such a player a *new entrant*.
- The existing players may accept or decline the coordinated transmission request (CTR).

Basically, this stage game defines how the new entrant can establish mutual non-aggression agreements with other players. To the interested reader, this is a basic element of *Network Formation Games* [11]. A game stage is exemplified in Fig. 2, where player i is being activated and players j and k were already active. The information sets are represented by a circle marking the name of the player responsible for decision. In this example, the new entrant i has three possible actions: coordinate transmission with j, coordinate transmission with k or do not coordinate transmissions, i.e., reuse the spectral resources. Upon request, player j or player k can decide whether or not to accept to coordinate transmissions.

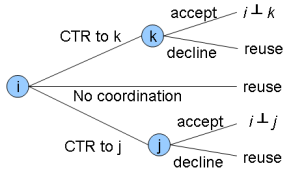

Fig. 2. Representation of a possible stage game. If two players agree to coordinate, then they will attain orthogonal spectrum allocation. Otherwise they reuse spectral resources.

B. Distributed Channel Allocation

The utility of the players is affected not only by the mutual agreements between pair of players, but also by the way the channels are re-distributed when new players join the game. Ultimately, these two elements will define the component carrier allocation of each femtocell and the actual SINR in each channel.

The reader interested in the details of the channel allocation algorithm may refer to [1]. Therein we consider a distributed channel allocation and re-allocation algorithm with the following characteristics:

- The allocation of resources respects the mutual agreements among players.
- All conflicts are solved locally, enforcing stability, i.e., only "neighbor" players can be affected by the activation of a new player.
- Any affected player will end-up with a subset of the channels from its previous allocation.
- The following invariant is kept: each player and his connections will reuse the whole spectrum.
- If possible, each directly connected player will receive the same share of component carriers.

In, [1] the spectrum allocation policy states that a new entrant can request coordination at most to two active players. The analysis in [1] shows that coordinating with two other players is enough to provide considerable gains, while avoiding spectrum fragmentation and reducing the need for signaling.

C. Strategies

In dynamic games, strategies are essentially a contingent plan of how to play the game on each possible information set [10]. Rational players are typically assumed to select their strategies on a purely selfish manner. Based on examples from society [5] and nature [6] we are interested in challenging the selfishness assumption and identify what are the desirable strategies for dynamic spectrum sharing in femtocells.

In this paper we consider four different ways of selecting strategies:

(i) *Selfish*: All players select their strategies according to the canonical GT assumptions, optimizing only their own instantaneous throughput.

(ii) *Selfless* new entrant: The new entrant intends to protect the existing players and it is completely *selfless*. Other players still play selfishly.

(iii) *Max-min*: a pair of players will choose to cooperate if this is of benefit of the player with lowest incoming BIM.

(iv) *Max-sum*: A pair of players will coordinate transmissions if this decision increases their sum capacity compared to uncoordinated transmissions.

Next, we turn to the analysis of these strategies.

IV. Analysis

First we discuss how selfish players would behave and later we discuss the alternative strategies. Henceforth, we assume that the players at a particular game stage only know about that stage. In other words, the players can not foresee if the game will have more stages or not. This seems to be a reasonable assumption since the players can not predict the arrival of new sessions in a non-causal way (see Fig. 1). Therefore, selfish players making decisions at stage t will attempt to maximize their utility at stage t, regardless of future unknown implications.

The analysis of dynamic games usually follows backward induction [10]. This essentially consists in predicting the behavior of the players in sub-branches of the game and then reducing the game. For example, in the game of Fig. 2, one can analyze the expected behavior of players j and k and later analyze the expected behavior from i.

So, the first question is how active players are expected to behave when they receive a CTR from a new entrant? "To coordinate or not to coordinate? That is the question". Any rational player would be willing to coordinate transmissions with a new entrant, as long as this does not imply further losses in spectrum allocation. After all, the less incoming interference the better. So any player satisfying this condition with coordinated transmissions will cooperate:

$$C_j(t) = C_j(t-1) \tag{1}$$

Where C_j is the downlink capacity of j (utility). Nevertheless, if a player had full spectrum allocation in stage $t-1$, then it will not be that easily willing to donate spectrum to the new entrant on stage t. After all, under a fair spectrum allocation rule, coordinating transmissions with the new entrant would imply losing half of the channels. Let j be the player deciding about the coordination request from i. If j has full spectrum allocation, then i may expect j to cooperate only if:

$$C(\mathrm{DL}_{\{i\}\to\{j\}}) \leq \frac{C(SNR_j)}{2} \tag{2}$$

where C represent the SINR to throughput mapping, and SNR_j is the signal-to-noise ratio (interference excluded) of player j. Essentially, equation (2) says that a selfish player will not be willing to coordinate transmission if the SINR gain does not outweigh the spectrum losses.

Then, we analyze what the expected behavior of the new entrant is. A rational new entrant will not send CTR to players

that will certainly decline it and he can determine that by backward induction. Furthermore, if the new entrant does not engage on coordination with any player, he will be able to reuse the whole spectrum. Therefore, a new entrant will only consider making bi-lateral agreements to players which satisfy:

$$C(\mathrm{DL}_{\{i\}\leftarrow\{j\}}) \leq \frac{C(SNR_i)}{2} \quad (3)$$

Recap that the policies may impose a maximum number of players to which the new entrant can send the CTR. Hence, the new entrant needs to prioritize the players according to his own interests, i.e., in terms of incoming BIM. In summary, the steps which the new entrant need to perform to maximize his stage utility are:

1) Create an ordered list of the existing players in terms of incoming BIM, $\mathrm{DL}_{\{i\}\leftarrow\{j\}}$.
2) Remove players which do not satisfy at least one of the two: (1) or (2).
3) Remove players which do not satisfy equation (3).
4) Send the CTR up to maximum number of players according to the policy.

This summarizes the expected strategy of a selfish new entrant.

In the second considered strategy the new entrant is selfless. Then, he has only to evaluate equation (2) to decide which players would benefit from coordination and order those players in terms of outgoing BIM. The existing players have no incentive to decline offers of coordination, since the new entrant selects them on their best interests.

A third possibility is to attempt to optimize the "welfare" by maximizing the minimum (*max-min*) throughput. This is the policy applied in [1]. The feasible set is formed by selecting players which will satisfy either (2) or (3) and sorting then accordingly. If all players behave according to max-min policy, then the relation is symmetric and the existing players will reach the same conclusions as the new entrant.

Finally, we consider players which try to maximize the sum throughput. In this case, the players will chose to coordinate transmissions if this move is expected to increase the sum throughput on a two by two basis:

$$\frac{C(SNR_i)+C(SNR_j)}{2} \geq C(\mathrm{DL}_{\{i\}\rightarrow\{j\}})+C(\mathrm{DL}_{\{i\}\leftarrow\{j\}}) \quad (4)$$

Fig. 3 shows some example interference scenarios and the expected outcome for different player strategies. Table I summarizes the considered strategies to a new entrant and formalizes them with an equivalent utility function. In Table I j is an already active player. k represents any player including i. C_k represents the capacity of player k, whereas N is the total number of players.

V. Results and Discussions

The performance was evaluated through semi-static system level simulations. We derive our results from a Monte Carlo performance evaluation and thousands of snapshots have been simulated to ensure statistical reliability. All four strategies, summarized in Table I, were compared.

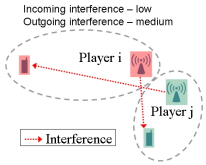

Strategy	Outcome
Selfish	Reuse
Selfless *i*	Orthogonal
Selfless *j*	Reuse
Max sum	Reuse
Max-min	Orthogonal

(a) Example Scenario 1 - Interference coupling is highly asymmetric. If the players reuse the resources, player j will be severally affected but the gains to player i may be considerable.

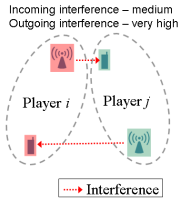

Strategy	Outcome
Selfish	Reuse
Selfless *i*	Orthogonal
Selfless *j*	Orthogonal
Max sum	Orthogonal
Max-min	Orthogonal

(b) Example Scenario 2 - Interference coupling partially asymmetric and generally strong.

Fig. 3. Example scenarios of the behavior of different strategies.

TABLE I
Summary of new entrant i behavior for different strategies.

Strategy	Prioritization to send CTR	Equivalent Utility
Selfish	$C(\mathrm{DL}_{\{i\}\leftarrow\{j\}})$	C_i
Selfless	$C(\mathrm{DL}_{\{i\}\rightarrow\{j\}})$	$min(C_j), j \neq i$
Max-min	$min\left\{\mathrm{DL}_{\{i\}\leftarrow\{j\}}, \mathrm{DL}_{\{i\}\rightarrow\{j\}}\right\}$	$min(C_k), \forall k$
Max Sum	$\frac{C(SNR_i)+C(SNR_j)}{C(\mathrm{DL}_{\{i\}\rightarrow\{j\}})+C(\mathrm{DL}_{\{i\}\leftarrow\{j\}})}$	$\frac{\sum_k C_k}{N}$

The scenario consists of a single 5x5 grid of houses assuming CSG femtocells. Each house contains 4 rooms where both FAPs and UEs are randomly located. Yet, there is at most one femtocell per house. The indoor propagation is modeled according to the WINNER A1 indoor home scenario [12]. Furthermore, if the UE and the FAP are located in the same room, we assume line-of-sight propagation and non-line-of-sight otherwise. The transmit power of femtocells was set to 24dBm. Look-up tables map the SINR to corresponding throughput values according to a modified Shannon's formula from [13]. The system bandwidth is divided into 6 Component Carriers of 15 MHz each.

All the throughput results were normalized by the maximum theoretical capacity of the system. Hence, a normalized throughput of 100% means transmission over the whole bandwidth at the maximum system spectral efficiency considering the MCS limitation. We study five different network densities: from sparsest to densest as the deployment ratio increases from $\delta = 20\%$ to $\delta = 100\%$ in steps of 20%.

Fig. 4 depicts the observed trends for the two performance indicators of interest, namely the 5% outage user-throughput and the average cell throughput. The performance of plain

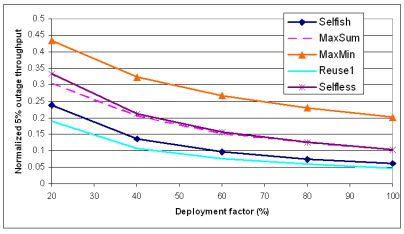

(a) Normalized downlink 5% outage cell throughput.

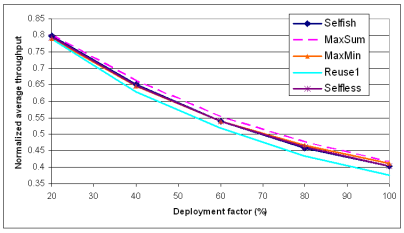

(b) Normalized downlink average cell throughput.

Fig. 4. System level simulation results.

reuse-1 is included in the figures as well as it provides an intuitive benchmark.

First and foremost it can be observed that the canonical GT selfish strategy provides only marginal benefits when compared to universal reuse, which entails no additional complexity. Referring to Fig 3, we can understand the behavior. Cooperation will only take place when the interference coupling is severe and "nearly-symmetrical". On the other side of the spectrum lies the max-min approach where the collaborative sets are formed much more frequently as cooperation will arise whenever the network topology renders one cell less fortunate.

The selfless and max-sum approaches lie in the in-between the other two in terms of outage performance. However the latter is a more natural strategy, especially if the model is extended to open subscriber groups (OSG). It is hard to conceive that nodes will act according to a truly selfless policy. Nonetheless, a parallel can be drawn between the selfless approach and the well-known prisoner's dilemma. If one node is willing to take the first step because it knows all other will act similarly (no cheaters), the achieved solution is better than the Nash equilibrium (selfish strategy).

Finally, all variants improve the average cell throughput, but the gain is rather modest. Even with $\delta = 100\%$ the gain ranges from 6% for the selfish strategy up to 11% for max-sum. The max-sum alternative always performs the best in terms of average throughput as it was designed to do so. It is also interesting to notice that the max-min approach does not sacrifice the average cell throughput in order to rectify the existing inequities.

VI. Concluding Remarks

Dynamic spectrum sharing is of increasing relevance due to the scarce availability of spectrum, and its importance is further increasing due to the massive growth of traffic demand. In particular, dense femtocell deployment is expected to take off during the next years in order to meet the demand. Distributed autonomous spectrum sharing approaches are preferred for the large scale deployment of femtocells. We investigated a practical solution, which consists in letting neighbor femtocells to establish mutual non-aggression agreements. Under some policies it is possible to devise efficient distributed channel allocation rules which smoothly reallocate the spectrum.

Using Game theory and, particularly, elements of Network Formation Games, we modeled the establishment of such agreements as a dynamic game. In addition to that, several strategies for this game were proposed ranging from purely egoistic to selfless. The system level simulation results show that each femtocell should strive for a balance between selfishness and altruism. It is possible to use this balance in favor of the overall network throughput or in favor of achieving a minimum performance for each cell. In conclusion, theoretical assumptions should guide the design of practical solutions, but they should not be a limiting factor.

References

[1] L. Garcia, G. Costa, A. Cattoni, K. Pedersen, and P. Mogensen, "Self-organizing coalitions for conflict evaluation and resolution in femtocells," in *GLOBECOM 2010, 2010 IEEE Global Telecommunications Conference*, 2010, pp. 1 –6.

[2] J. Ellenbeck, C. Hartmann, and L. Berlemann, "Decentralized inter-cell interference coordination by autonomous spectral reuse decisions," in *Wireless Conference, 2008. EW 2008. 14th European*, 2008, pp. 1–7.

[3] G. da Costa, A. Cattoni, I. Kovacs, and P. Mogensen, "A scalable spectrum-sharing mechanism for local area network deployment," *Vehicular Technology, IEEE Transactions on*, vol. 59, no. 4, pp. 1630–1645, May 2010.

[4] Z. Khan, J. Lehtomaki, M. Latva-aho, and L. DaSilva, "On selfish and altruistic coalition formation in cognitive radio networks," in *Cognitive Radio Oriented Wireless Networks Communications (CROWNCOM), 2010 Proceedings of the Fifth International Conference on*, 2010, pp. 1 –5.

[5] R. M. Nelissen, D. S. van Someren, and M. Zeelenberg, "Take it or leave it for something better? responses to fair offers in ultimatum bargaining," *Journal of Experimental Social Psychology*, vol. 45, no. 6, pp. 1227 – 1231, 2009.

[6] C. Stephens, "Modelling reciprocal altruism," *The British Journal for the Philosophy of Science*, vol. 47, no. 4, pp. 533–551, 1996.

[7] Z. Ho and D. Gesbert, "Balancing egoism and altruism on interference channel: The mimo case," in *Communications (ICC), 2010 IEEE International Conference on*, May 2010, pp. 1 –5.

[8] V. Chandrasekhar, J. Andrews, and A. Gatherer, "Femtocell networks: a survey," *Communications Magazine, IEEE*, vol. 46, no. 9, pp. 59–67, 2008.

[9] S. Parkvall, A. Furuskar, and E. Dahlman, "Evolution of lte toward imt-advanced," *Communications Magazine, IEEE*, vol. 49, no. 2, pp. 84–91, 2011.

[10] D. Fudenberg and J. Tirole, *Game Theory*. MIT Press, 1991.

[11] M. O. Jackson, "A survey of models of network formation: Stability and efficiency," EconWPA, Game Theory and Information 0303011, Mar. 2003.

[12] P. *et al.*. Kysti, "IST-WINNER D1.1.2 , "WINNER II Channel Models", ver 1.1," Winner II, Tech. Rep., 2007. [Online]. Available: https://www.ist-winner.org/WINNER2-Deliverables/D1.1.2v1.1.pdf

[13] P. E. Mogensen *et al.*, "LTE Capacity Compared to the Shannon Bound," in *VTC Spring*, April 2007.

Appendix B

Complementary Discussions

This appendix contains brief discussions on a series of topics that complement the framework introduced in Chapters 3 and 4. These subjects are examined separately, because some of them have not yet reached the same level of maturity as the other constituents of the Autonomous Component Carrier Selection (ACCS) framework, while others would simply disrupt the flow of the presentation. Nonetheless their relevance should not be dismissed.

B.1 Recovery Actions

As stated in Chapter 3, the Base Component Carrier (BCC) acts as an anchor and enjoys certain privileges. Whereas the main purpose of Supplementary Component Carriers (SCCs) is to provide additional cell capacity whenever possible; the BCC shall provide reliable full cell coverage as it is used by terminals to camp, to set up calls, etc. Consequently, the related ACCS scheme puts strong emphasis on assuring the quality of a BCC.

After the initial BCC selection, the Femto Access Point (FAP), also known as Home enhanced NodeB (HeNB), shall monitor the quality of its selected BCC to ensure desired quality and coverage levels. The quality can be measured in

terms of Reference Signal Received Power (RSRP) and Reference Signal Receive Quality (RSRQ) levels reported by User Equipments (UEs) to their serving HeNB [97]. If poor quality is detected, recovery actions will be triggered in an attempt to improve the situation. Such actions can be understood as additional defensive measures to safeguard against potentially erroneous SCC decisions made by neighboring FAPs.

Naturally some filtering might be required to tell apart quality problems that cannot be handled by recovery actions from those that can. For example, low RSRQ levels associated with very low RSRP fall into the first category. The reporting UE is likely to be out of coverage and it would not be sensible to trigger pointless actions that would simply disturb the rest of the network. Conversely poor RSRQ when RSRP levels are good is an indicator of strong co-channel interference that can be toned down by recovery actions. Two possible recovery actions are proposed and discussed next:

1. Interference Reduction Request (IRR)
2. Reselection of the BCC

B.1.1 Interference Reduction Requests

Interference Reduction Requests (IRRs) are the first and preferred option. Given the absolute priority of BCCs over SCCs, a FAP (victim) is entitled to send IRRs to all interfering FAPs (aggressors) that are currently using the victim's BCC as a SCC. It is posited that a FAP receiving an IRR shall react to that request within a relatively short time, e.g. 50 ms. The simplest reaction is to relinquish the Component Carrier (CC) altogether. Alternatively, the recipient could be forced to reduce its transmission power by a few dB. The IRR concept can also be used by new entrants (FAP being powered up) to dig a "spectrum hole" in case all CCs have been taken by a FAP that was previously isolated.

Naturally, sending IRRs to several neighbors does not favor the overall performance of the system. It is expected that a rather limited number of interferers will account for most of the total interference power. Identifying the main interferers and sending addressed requests (see Fig. B.1) possibly containing estimated required power reductions would prevent neighbors from unnecessarily muting some or all of their SCCs. The pair-wise interference characterizations contained in the Background Interference Matrix (BIM) could be used to establish the identity of the pertinent neighbors accounting for most of the interference. Future investigations are expected to shed light on the best IRR alternative.

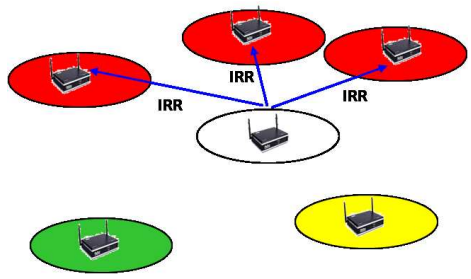

Fig. B.1: A HeNB experiencing poor BCC quality can send IRRs to the neighboring cells. HeNBs receiving an IRR shall relinquish the CC, unless the specified carrier it utilized as a BCC.

B.1.2 BCC Reselection

Simply put, a BCC reselection means that a FAP will switch to another CC because the current one is experiencing severe quality problems. Ideally, BCC reselections should be as infrequent as possible because this process is equivalent to resetting a cell. Therefore a HeNB should only change its BCC if: (i) significant performance gains from doing that are foreseen; (ii) IRR have failed to improve the experienced conditions; (iii) the reselection will most likely not lead to a reconfiguration storm propagating arbitrarily deep into the network.

Clearly, the most straightforward reselection strategy is to revaluate the algorithm used for the initial BCC selection. However, this naive solution has a few drawbacks. Firstly, it cannot accurately quantify the potential performance gains. Recap that the bootstrap procedure simply tries to ensure that BCC are reused as sparsely as possible given only the HeNB-to-HeNB path loss measurements.

Secondly, if IRRs have failed (or have not been sent out at all), it means that the interference is coming from nearby cell(s) reusing the CC as a BCC too. This could occur if the number of CCs to choose from is low, the network is very dense, and the activation order of FAP has led to a deadlock. Therefore, there is a good chance that the same CC is selected again, which will not improve the state of affairs, or worse, that a reselection will trigger an infinite domino effect.

This problem can be understood as follows: If the cellular network is mapped into an interference graph $G = (V, E)$ where the node set V denotes FAPs and the edge set E represents the possibility of disruptive co-channel interference. It is well known that in the presence of e.g. an odd-cycle[1], three frequencies (colors)

[1]The odd numbered of vertices are connected in a closed chain forming a polygon, such as

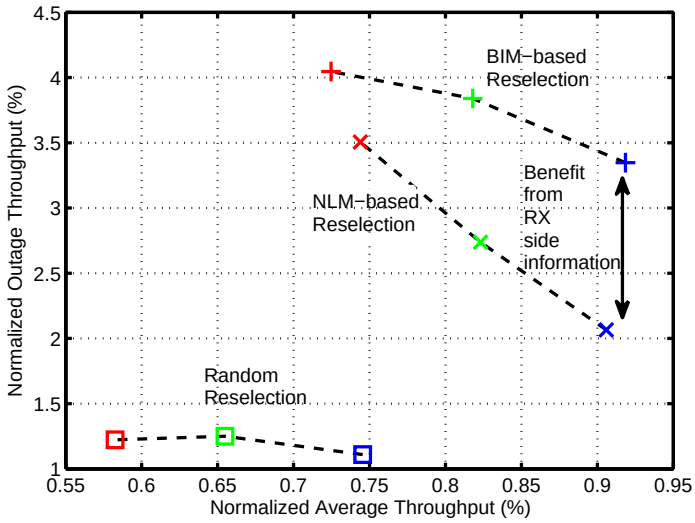

Fig. B.2: A preliminary comparison of three alternative reselection alternatives. Blue, green and red markers indicate, 3, 4 and 5 CCs to choose from respectively. All results are normalized with respect to the corresponding performance of universal reuse. The value of receiver side information becomes evident.

are needed to obtain a conflict-free coloring, i.e. no two adjacent vertices use the same frequency. Now if one assumes a network with just two CCs (colors) to choose from, one dissatisfied FAP could jump to the other CC available. If this FAP is indeed part of an odd-cycle, then it and its neighboring FAPs would reselect CCs ad infinitum. Furthermore, many other graph-theoretic aspects beyond the scope of this discussion can dictate a higher number of colors. However, without a central entity, no single FAP has global knowledge of the underlying graph. Consequently, there is no simple way of knowing how many colors are required and how far-reaching the impact of a unilateral reselection is. This poses a serious challenge. Given that the number of carriers (colors) is always limited, and bandwidth splitting takes its toll on capacity, it might be preferable to trade-off optimality for stability. This is the strategy employed for example by the scheme introduced in Appendix A, which could be understood as an imperfect graph coloring algorithm.

Finally, the original selection could not rely on receiver-side information. It seems reasonable to use the richer information contained in the BIM to guide the reselection decisions. In possession of outgoing interference coupling knowledge, a FAP can infer whether or not its actions will have significant impact on the

a triangle or a pentagon.

neighbors, ultimately leading to them reselecting the BCC.

Figure B.2 presents a preliminary comparison of three BCC reselection strategies. The results were generated using the same Long Term Evolution (LTE) tool and deployment scenario (3 floors) described used throughout this thesis. Full-buffer traffic and deployment ratio, $\delta = 1$, were assumed. In all cases, FAPs were restricted to a single CC. The first one is similar to the initial selection algorithm, that is, it is based on HeNB-to-HeNB path loss measurements and each FAP tries to select a CC differing from those selected by the $C - 1$ worst-interferers as seen by the FAP, where C is the number of CCs to choose from. The second alternative is a totally random reselection. Finally, the BIM-based approach defines the edges of the graph using the *strong-bonding* definition introduced by the Self-Organizing Coalitions for Conflict Evaluation and Resolution (SOCCER) algorithm presented in Appendix A. It then avoids the $C - 1$ worst-interferers as seen by receivers. In Fig B.2, all results are normalized by the performance of universal reuse. The fixed system bandwidth was split into three four and five CCs, represented by the blue, green and red markers respectively. The value of receiver side information becomes evident. Moreover, when a single CC restriction is imposed, 3 CCs to choose from is arguably the best choice for the Network Listening Mode (NLM)- and BIM-based methods. Finally, looking at the performance from the random strategy it can be stated, as radical as it may sound, that it might be better, and certainly safer, to preclude event/condition-driven BCC reselections completely if the information available is very limited.

B.2 Timing Aspects

While BCC reselections are suggested to occur over hours or even days in order to promote stability, SCCs can, at least in principle, be reselected on a much faster basis

Clearly the optimal reselection and hence signaling rate is a compromise between performance and control plane overhead. On one hand, Internet traffic is highly bursty (temporally sparse) and because the ACCS framework relies on the cooperative exchange of relatively small control plane messages between FAPs, attempts to track variations on a packet-basis could easily exhaust the inter-cell signaling capacity and might even be proven futile due to inherent signaling delays. Ultimately, the latency of the interface among cells dictates how fast ACCS can operate.

On the other hand, cells should not delay the activation for too long, otherwise

they could risk doing so after the session that triggered the evaluation in the first place is over. Neither should cells hold on to CCs much longer than strictly required because they might unnecessarily be preventing other cells from using the same CCs.

In sum, the selection of SCCs is suggested to occur over a time span of hundreds of milliseconds up to seconds, hence being fairly slow when compared to packet scheduling (1 millisecond in LTE). As result, ACCS shall take care of large scale load variations, so-called elephant flows [114], while opportunistic and independent schedulers would deal with instantaneous traffic variations, the mice flows.

B.2.1 Distinguishing Elephants from Mice

A simple idea proposed here is to resort to a cross-layered [115] approach. Akin to Medium Access Control (MAC) layer buffer status reports, the application layer could inform ACCS (or an equivalent entity) about the size and possibly other Quality of Service (QoS) requirements of the file to be downloaded/uploaded. This would allow Radio Resource Management (RRM) entities and eventually ACCS itself to distinguish very clearly short-lived traffic spikes from actual elephant flows [114], extremely large (in bytes) continuous flows. Naturally, much work is required to turn this idea into a real concept.

B.2.2 Dealing with Signaling Delays

Theoretical research typically assumes that the coordination and sharing of information is instantaneous. However, if the information exchange takes place over a backhaul with non-negligible latency, decisions will be based on stale and potentially incorrect information. In Chapter 3, signaling was assumed ideal, whereas simulations in Chapter 5 included the effect of coordination delays.

When a signaling delay of τ seconds is considered, then if any neighboring femtocell needs to make a decision during the time $[-\tau, \tau]$, this decision will be based on imperfect information. In other words, the Component Carrier Radio Allocation Table (CCRAT) will be outdated. This may or may not be a serious issue depending on the interference coupling among the cells making their decisions. In order to tackle this problem a simple practical solution is proposed. The description assumes a reliable exchange of decision information.

Whenever a cell decides to acquire more CCs, it shall *announce* its decision

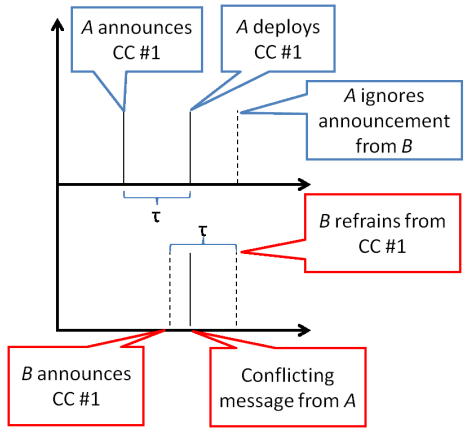

Fig. B.3: A simple contention mechanism based on announcements to ensure decisions are not based on stale information caused by information exchange delays.

and *wait* for a period of τ seconds. If no conflicting coordination messages arrive within this period, the cell can finally activate the CC. Any messages arriving after τ seconds are ignored because they are based on later decisions and the neighboring cell(s) originating the message(s) will have received the first announcement within their contention period and shall refrain from effecting their announced decision. The process is illustrated in Fig. B.3.

B.3 Decoupling Downlink (DL) and Uplink (UL) Decisions

In the original formulation introduced in [96], ACCS only considered coupled CC allocations. Therefore the set and the number of CCs used by a given cell in the UL would always equal that employed in DL[2]. Referring to Chapter 3, this restriction entails that both equations, (3.7) and (3.8), must be satisfied in order to activate a CC.

The obvious downside of a coupled approach is that such assumption precludes asymmetric allocations. Additionally, coupled decisions might hinder the activation of extra CCs, for example in the UL, where CIR conditions might be favorable, due to unfavorable conditions in the DL. On the other hand, since

[2]The set of CCs is strictly the same in a Time Division Duplexing (TDD) system. If Frequency Division Duplexing (FDD) is used, this equivalence implies paired set of CCs.

BIMs are based on DL measurements, the the more reliable DL estimations could still prevent erroneous and potentially harmful UL decisions. In fact, when it comes to duplexing, ACCS comes in three different flavors.

1. Coupled and dependent decisions as originally presented. A single CCRAT and a single BIM per cell. Both directions share the same view on interference coupling and CC usage.
2. Two independent ACCS processes per cell relying on the same interference coupling information, but with two CCRATs, one for each link. The CC usage would then differ due to the traffic asymmetry.
3. Two independent ACCS processes and UL decisions rely on BIMs adjusted to match the conditions seen in the reverse link, akin to the material in Section 4.5. In this case, cells have different views for each link, due to independent interference coupling and CC usage information.

The work reported in [105,116,117] investigated the three variants and concluded that having two independent ACCS processes relying on the same DL-based BIM is a good compromise solution. The addition of UL information, which is difficult to estimate in the real world, does not provide substantial performance improvements. That is the reason why simulations in Chapters 3 to 5 always assume independent decisions for each link, unless explicitly stated otherwise.

For the interested reader, the aforementioned contributions have also shown that – if actual UL information is available and the same Carrier to Interference Ratio (CIR) thresholds are considered – the UL is more restrictive than the DL direction. The resulting distribution describing the number of CCs employed in the UL has a lower mean value than that of the DL. As a final remark, when compared to the third variant, the first and second versions of the ACCS mechanism suffer a notorious degradation in terms of UL outage user throughput if very permissive (low) thresholds are used, whereas the UL average user throughput is not correspondingly improved. This is a consequence of wrong decisions based on inaccurate estimates. This is aligned with the findings from Chapter 4 that concluded that most of the benefits stemming from actual UL information come in terms of outage rather than average performance. Therefore, the usage of very aggressive CIR thresholds in the absence of accurate UL information is not recommended if the UL outage user throughput is a relevant Key Performance Indicator (KPI).

Appendix C

On Open versus Closed LTE-Advanced Femtocells

This appendix contains a reprint of the conference paper below. The paper complements the discussion presented in Chapter 2.

- Luis G. U. Garcia, Klaus Pedersen and Preben Mogensen,"" On Open versus Closed LTE-Advanced Femtocells and Dynamic Interference Coordination," Wireless Communications and Networking Conference (WCNC), 2010 IEEE , vol., no., pp.1-6, 18-21 April 2010.

C.1 Paper Reprint

This full text paper was peer reviewed at the direction of IEEE Communications Society subject matter experts for publication in the WCNC 2010 proceedings.

On Open versus Closed LTE-Advanced Femtocells and Dynamic Interference Coordination

Luis G. U. Garcia
Aalborg University, Denmark
Email: lug@es.aau.dk

Klaus I. Pedersen
Nokia Siemens Networks, Aalborg
Email: klaus.pedersen@nsn.com

Preben E. Mogensen
Aalborg University, Denmark
Nokia Siemens Networks, Aalborg

***Abstract*—Low-power home base stations, also known as femtocells, are one of the strong candidates for high data rate provisioning in indoor environments. Unfortunately, the benefits are not without new challenges in terms of interference management and efficient system operation. In this paper we take a closer look at several aspects associated with the deployment of LTE-Advanced home eNBs under two different access policies: closed subscriber group (CSG) and open subscriber group (OSG). Our results are derived from extensive downlink system level simulations. We limit our scope to dense-urban deployment of femtocells assuming dedicated carriers, i.e. no interference to/from the macro layer. Particularities of each access mode are discussed under different hard frequency re-use configurations. Our results indicate that an OSG deployment is indeed able to cut short the lower end of the SINR distribution when universal frequency re-use is employed. However, when other re-use configurations are considered, OSG no longer guarantees improved SINR conditions. In addition, we present additional results for the autonomous component carrier selection (ACCS) concept introduced in earlier contributions, providing strong suggestions that the scheme yields attractive performance benefits independently of the access policy selected by the operator. Finally, we point out that uplink results including realistic power control settings need to be considered before definitive conclusions can be safely drawn.**

***Index Terms*—Femtocells, LTE-Advanced, Spectrum-sharing, Autonomous Component Carrier Selection.**

I. Introduction

LTE-Advanced, an evolved version of LTE, with bandwidths up to 100 MHz is currently under study to fulfill the targets defined in [1] and [2]. Here the 100 MHz system bandwidth is achieved via aggregation of individual component carriers (CCs) following the Rel'8 numerology. Now, in addition to traditional macro and micro cell deployment scenarios, local area deployments have become relevant as well due to the expected large scale deployment of cost-effective low-power base stations.

Low-power base stations will appear as normal eNBs for the user equipment (UE) and are commonly referred to as "femtocells" or home eNBs, in LTE-Advanced terminology. Throughout this paper, we use these terms interchangeably. Femtocells are low-cost user-deployed cellular base stations that operate in licensed spectrum using an IP based wired backhaul such as cable or DSL designed to provide service in local environments similarly to WiFi access points.

Dense deployment of low-power base stations offers significantly higher capacity per area as compared to macro cells, arising from using smaller cell sizes and more efficient spatial re-use. Additionally, femtocells can be used to provide deep in-building broadband wireless services while offering savings associated with offloading traffic onto the femtocell, in particular for heavy data users. Therefore, home eNBs have recently reemerged as a promising technology component and many believe it will definitely be one of the next steps in the evolutionary path of cellular wireless systems [3], [4].

However, as attractive as femtocells may seem, the benefits are not without new challenges in terms of interference management and efficient system operation. The roll-out of femtocells is intrinsically uncoordinated and potentially chaotic, as the average end user will normally install home base stations without carefully considering where other people in the immediate surroundings have installed other home base stations. Additionally, the required proximity to an internet connection will often dictate the placement of the home eNB. As a consequence, assuming universal frequency re-use heavy inter-cell interference may arise, leading to poor system performance, especially for cell-edge users [5].

In this paper we concentrate on the differences between two foreseen access modes [1] and how they impact the deployment of femtocells. We focus on dense-urban residential deployments and derive our results from a Monte Carlo performance evaluation according to the evaluation methodology defined in [6] by 3GPP. Our results assume a 2x2 MIMO configuration and include error vector magnitude (EVM) modeling to account for various imperfections, such as IQ imbalance, in the implementation of Radio Frequency (RF) components as detailed subsequently.

We consider free-for-all, i.e. open subscriber group (OSG) and closed subscriber group (CSG) access policies. The former is desirable from a spectrum efficiency point of view, as it allows all UEs of an operator to share the resources of the femtocell, thereby curbing interference levels. The limiting factors here are the capacity of the home eNB and the capacity of the backhaul connection. Closed access might be preferred from a security, privacy and fair resource distribution of the wired (x-DSL/cable) internet connection. This mode entails that only a relatively low number of "known" UEs belonging to friends and family members can be served by the home

[1] A third hybrid mode, which combines the first two, is expected as well but is outside the scope of this contribution.

978-1-4244-6398-5/10/$26.00 ©2010 IEEE

This full text paper was peer reviewed at the direction of IEEE Communications Society subject matter experts for publication in the WCNC 2010 proceedings.

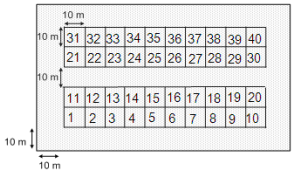

Fig. 1. Dense urban building layout with two apartment buildings, each having 20 flats with own low-power eNB.

eNB. In other words, the cell and consequently the end-user's internet connection is blocked to neighbors and passersby. A related study addressing the co-existence of 3G macro and femto base stations on the same frequency carrier under both CSG and OSG modes is found in [7]. Nonetheless, while the authors of that contribution focus on macro-femto interactions, here, we only deal with femto-femto interactions, as co-channel deployments are not considered.

Additionally, previous work found in [8] also highlighted the need for for new self-adjusting interference management techniques. In this light we present a new set of downlink results which tries to answer the question whether or not the previously proposed dynamic interference coordination scheme for LTE-Advanced known as Autonomous Component Carrier Selection (ACCS) [9], [10] is equally valid for both access policies.

The rest of this paper is organized as follows: Section II introduces our system model and simulation assumptions. In Section III we discuss the CSG x OSG results assuming well known hard frequency re-use patterns. Section IV deals with the downlink performance evaluation of autonomous component carrier selection under both access modes. Finally, we conclude the paper in Section V.

II. Simulation Assumptions

A. Deployment Model

We consider a block consisting of two stripes of apartments, each stripe having 2 by 10 apartments. Apartments dimensions are 10m x 10m and there is a 10m wide street between the two stripes of apartments. Each block is therefore of size 120m x 70m. The scenario is illustrated in Figure 1. Cells are numbered to facilitate the analysis in Section III.

It is assumed that with a probability P there is one low-power eNB in each flat. In the absence of an eNB, we assume that there are no active users in the flat. Moreover, we assume a single floor only; hence a scenario with up to 40 eNBs is simulated if $P = 1$. Both eNBs and UEs are dropped uniformly at random positions. All users are located indoors (no outdoor users) and we evaluated cases with 1 and 4 users per flat.

B. Propagation Model

Path loss and log-normal shadowing are considered, but fast fading is not explicitly simulated. Therefore, the results can be viewed as the performance averaged over a sufficiently long time period. The indoor path loss modeling follows those found in [6]. For convenience, the UE to home eNB path loss models for the cases where the UE and eNB are in the same or in different apartment stripes are given here by (1)-(2), respectively:

$$PL(\text{dB}) = 38.46 + 20\log R + 0.7 d_{\text{2D indoor}} + q * L_{\text{iw}} \quad (1)$$

$$PL(\text{dB}) = \max(15.3 + 37.6\log R, 38.46 + 20\log R) + \\ + 0.7 d_{\text{2D indoor}} + q * L_{\text{iw}} + L_{\text{ow}} + L_{\text{ow}} \quad (2)$$

In the equations, R is the total distance between transmitter and receiver. An additional log-linear loss is added (0.7 dB/m), which is calculated on the basis of the indoor part of the separation distance ($d_{\text{2D indoor}}$). This additional loss is used to simulate indoor elements such as furniture, doors, and walls not modeled individually. For the modeled buildings two types of walls are considered: external walls with 10 dB penetration loss (L_{ow}) and internal walls with a 5 dB penetration loss (L_{iw}). Wall penetration loss is applied on each internal wall (q) crossing the direct signal path. Wall attenuation variations are not taken into account. Doors and windows, typical in e.g. office or apartment type spaces, could lead to significant power leakage, and thus the cell isolation simulated may be optimistic compared to actual deployments. Finally, the component dependent on the number of traversed floors is not included as it was not considered.

C. Simulation Methodology

The performance was evaluated through semi-static system level simulations. The simulator is based on basic LTE specifications [11], but with bandwidth extensions up to 100 MHz. It relies on series of "snapshots". During each snapshot, path loss, shadowing and the location of devices remain constant. A few thousands of snapshots are simulated to get the averaged performance.

We consider a full buffer traffic model and a 2x2 antenna configuration for all links allowing up to two code words. A simple equal resource sharing packet scheduling algorithm is assumed, therefore for cells with N UEs, each UE is granted $1/N$ of the total bandwidth allocated to the cell. Additionally, there is no downlink power control.

For any given UE, the signal to interference and noise ratio (SINR) is calculated in accordance to the UE's specific parameters (position, height, serving and interfering low power eNBs, etc.). The SINR maps were generated by calculating the ratio between the received signal power from the serving cell and those coming from all interfering cells plus noise at the grid points within the considered area.

In order to account for various imperfections in the implementation of RF components and to avoid unrealistically high SINR values, an error vector magnitude (EVM) model was introduced, therefore imposing a soft SINR limit. EVM

This full text paper was peer reviewed at the direction of IEEE Communications Society subject matter experts for publication in the WCNC 2010 proceedings.

TABLE I
ASSUMPTIONS FOR SYSTEM-LEVEL SIMULATIONS

System Model		
Spectrum allocation	100 MHz at 3.4 GHz	
EVM	3%	
eNB parameters	Max. TX power	23 dBm
	Antenna system	Omni (3dBi)
UE parameters	Receiver noise figure	9 dB
	Antenna system	Omni (0dBi)
Radio Standard	LTE-Advanced	DL: OFDMA UL: SC-FDMA
Duplexing scheme	TDD	DL: 50% UL: 50%
Scenario Model [6]		
Home	Room size	10m x 10m
	Street width	10 m
	Internal walls	5 dB attenuation
	External walls	10 dB attenuation
	eNB position	Randomized
Propagation Model [6]		
Minimum coupling loss	45 dB	
Shadowing std. deviation	Serving Cell	4 dB
	Other Cells	8 dB
Traffic Model		
User distribution	Uniform: 4 users/cell	
Data generation	Full buffer	

is one of the widely accepted figure of merits used to evaluate the quality of communication systems. In simple terms, it quantifies how far the actual received constellation symbols are from their ideal locations had they been sent by an ideal transmitter. With the EVM defined as a percentage, the maximum achievable SINR is calculated as by: $\gamma_{\max} = -20.\log_{10}(\mathrm{EVM}/100)$. As a result the EVM-limited effective SINR γ_{evm} is given by

$$\frac{1}{\gamma_{\mathrm{evm}}} = \frac{1}{\gamma_{\max}} + \frac{1}{\gamma_{\mathrm{ideal}}} \tag{3}$$

The important aspect to notice here, is that due to inherent RF impairments, potential SINR improvements might not be fully realized, which limits even further the effectiveness of looser re-use schemes. Look-up tables map the SINR to corresponding throughput values according to a modified Shannon's formula from [12]. Implicitly this entails ideal link as well as single-/multi-stream adaptation along with hybrid automatic repeat-request (HARQ). The raw spectrum efficiency is limited to 10.8 bps/Hz. Furthermore, for each frequency re-use factor other than universal re-use, an in-advance simple frequency plan is assumed so that inter-cell interference is minimized, i.e. two adjacent apartments never employ the same part of the spectrum. We summarize the most important parameters in Table I.

III. CSG VERSUS OSG RESULTS

In this section, we consider both closed and open femtocells and analyze the results from a interference and average cell throughput perspective. Additionally, we consider the effects that two different frequency re-use schemes have on CSG and OSG deployments.

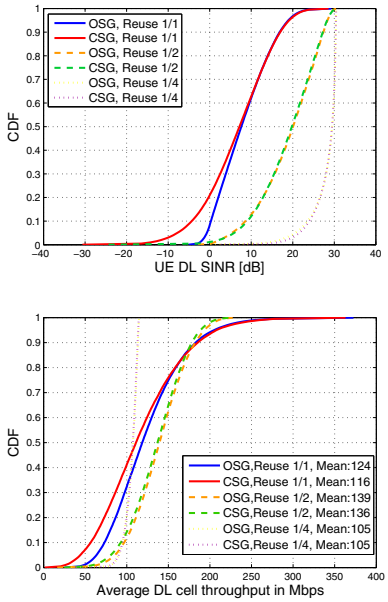

Fig. 2. CSG x OSG: CDFs of downlink UE SINR, average downlink cell throughput under different frequency re-use configurations.

As stated in Section I, in private or closed mode, apart from the macro-cells which are not considered here, UEs can only connect to the home eNB in the same residence. While a public or open mode allows for UEs to be served by the low power eNB providing the strongest signal, even if that eNB is inside another flat. In this case, the serving cell is selected based on the smallest total path loss (including the deterministic total path loss and shadow fading).

Besides, universal plain frequency re-use 1/1 which establishes the baseline performance, hard frequency re-use 1/2 and 1/4 configurations are analyzed.

Figure. 2 depicts SINR and average downlink cell throughput empirical cumulative distribution functions (CDF). These results assume up to 4 UEs per flat and the densest network topology ($P = 1$), which is clearly the most challenging in terms of inter-cell interference. From the curves in Fig. 2a it is evident that benefits in terms of SINR from introducing open access are much more significant when universal frequency re-use is used. In all other configurations, OSG does not provide a clear advantage over CSG. However, the possibility to be

This full text paper was peer reviewed at the direction of IEEE Communications Society subject matter experts for publication in the WCNC 2010 proceedings.

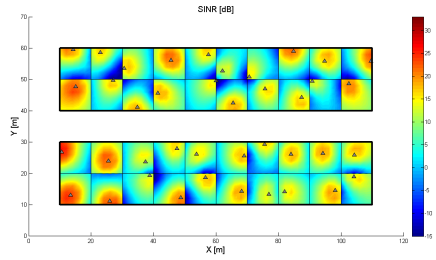

(a) Closed subscriber group.

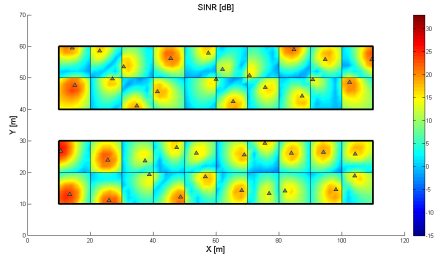

(b) Open subscriber group.

Fig. 3. Available downlink SINR with frequency re-use $1/1$.

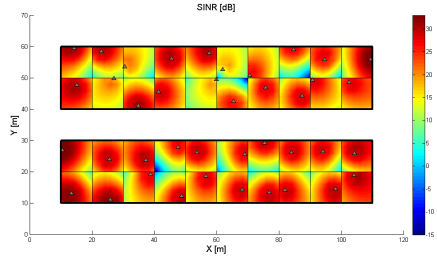

(a) Closed subscriber group

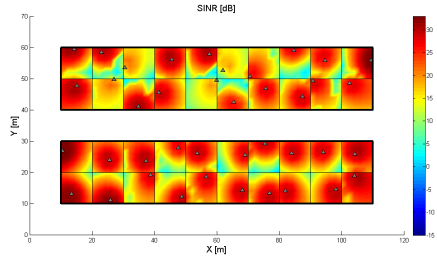

(b) Open subscriber group

Fig. 4. Available downlink SINR with frequency re-use $1/2$.

served by the home eNB with the strongest signal makes the occurrence of extremely low SINR values much less frequent, i.e. it shortens the left tail of the distribution in all cases.

Figure 2b reflects the improvements in terms of average cell throughput. As expected, sparser re-use factors will not always boost the average system performance due to the reduced transmission bandwidth. This can be easily understood in view of Shannon's capacity theorem [13] and limited SINR range. Re-use $1/4$ becomes clearly bandwidth limited. The access mode does not alter the situation dramatically, except once again for re-use $1/1$. In this case, at the 10% percentile of the CDF, the average cell throughput improves roughly 30%.

In order to get further visual insight, Fig. 3 and Fig. 4 show SINR availability maps for two hard frequency re-use configurations and both access modes. The small gray triangles represent the random location of the home eNB inside each apartment. Shadow fading is not simulated here for clarity, thus each cell becomes a contiguous area, instead of consisting of multiple "islands".

Besides the obvious removal of all "deep blue" (very low SINR) regions when OSG is introduced, perhaps the most interesting aspect is the fact that while all equivalent areas in Fig. 3b always have better or equal SINR than those in Fig. 3a; however this is not true for Figures 4b and 4a, see cells 32 and 35 for example. In the first case, the otherwise worst interfering cell becomes the serving cell. However due to the in-advance frequency plan it is very likely that the strongest source of interference already employs a different frequency. Therefore the strongest signal is not necessarily the least interfered one. To illustrate the situation, adjacent cells such as 1, 2 and 11 will always use different halves of the spectrum (assuming re-use $1/2$), however diagonally adjacent cells such as 1 and 12 will share the same half.

Figure. 5, presenting UE throughput empirical CDFs, highlights yet another important aspect of OSG versus CSG deployments: A fully open access deployment calls for some form of admission control. Additionally, load balancing schemes might also be required if one intends to ensure fair distribution of data rates among different cells. In a fully open access, if cell selection is entirely performed based on signal strength, certain cells will offload some traffic to neighboring ones which will become more severely loaded. This means that the spectrum available must be shared by a higher number of UEs. When one looks at the results down to UE throughput level, it becomes clear that gains in terms of SINR arising from open access are not fully translated into improved user experience. This renders the 5% outage throughput values to be higher in CSG cases than those in OSG ones, when sparser hard frequency re-uses are considered. On the other hand, also due to traffic offloading, peak UE rates can also be increased in some cells, this is evidenced by the upper parts of the orange

This full text paper was peer reviewed at the direction of IEEE Communications Society subject matter experts for publication in the WCNC 2010 proceedings.

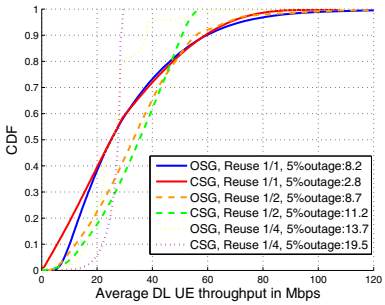

Fig. 5. CSG x OSG: CDFs of downlink UE throughput under different frequency re-use configurations.

and yellow curves when compared to the green and purple curves respectively.

Finally, when Fig. 2b and Fig. 5 are considered jointly, we can infer that open access is not necessarily the best way to improve either average cell throughput or 5% outage throughput values. Hard re-use $1/2$ under CSG provided roughly 10% higher average cell capacity than universal re-use under OSG. This can be easily explained by the fact that OSG mainly favors cell edge UEs in terms of SINR, but does very little for other UEs. With regard to outage throughput, re-use $1/2$ led to 36% higher performance. This is due to the aforementioned traffic offloading permitted by open access.

IV. ACCS Results

The results in the previous section and earlier contributions [5] indicate that dynamic interference coordination is needed for cases with dense deployment of lower power eNBs, such as pico or femtocells. One proposed solution, known as Autonomous Component Carrier Selection (ACCS) is described in [9], [10]. In this section we shortly summarize the basic idea of ACCS for LTE-Advanced,point readers to pertinent references and provide extensive simulation results in order to assess the suitability of ACCS when both access modes are considered.

The total system bandwidth is divided into M frequency chunks or component carriers. It is then proposed that each cell automatically selects one of the component carriers as its primary carrier (also sometimes called the base carrier) when the home eNB is powered on. As the offered traffic increases, the home eNB may start to take additional component carriers into use. These are called secondary component carriers. Nonetheless, a cell is only allowed to take more secondary component carriers into use provided that this is possible without causing excessive interference to the surrounding cells. For that evaluation, each home eNB collects so-called background interference matrices (BIM) based on UE measurements. Based on this information, each cell essentially "learns" about the local environment, thus making it capable of estimating the impact on the surrounding cells from taking more carriers into use. For more information on the BIM, and rules for selecting more secondary component carriers, we refer to [9], [10].

Here we present normalized performance results for average throughput per cell, as well as the 95% coverage per user throughput. For simplicity the transmit power per component carrier is assumed fixed and given by $P_{cc} = P_{\max}/M_{cc}$, where $M_{cc} = 4$ is the number of components into which the system bandwidth is divided. Hence home eNBs will only transmit at full power if they employ all component carriers. Note that the complexity and behavior of ACCS is only dependent on the number of component carriers and not on the system bandwidth itself, therefore the trends and results shown next remain perfectly valid for other system bandwidths provided that the number of component carriers remains the same. The interested reader can refer to [10] for a brief discussion about the sensitivity of ACCS to the number of component carriers. The primary and secondary component carriers target SINR values [9] were set to 10 dB and 8 dB respectively. Additionally, it is worth stressing that due to the full load assumption, a cell will always allocate as many additional carriers as possible given the existing allocation of its neighbors and interference coupling.

Results are normalized with respect to the performance of full frequency re-use and CSG, i.e. for the case where all eNBs use the entire frequency band. In addition to showing the performance results for ACCS, we also show results for fixed frequency re-use configurations of $1/2$ and $1/4$. For each of these three configurations, we present results for P (probability of eNB being active) equal to $[0.25, 0.50, 0.75, 1.00]$. Hence, for the performance results in Fig. 6, each of the four points on the curves corresponds to different values of P. The points on the curve with highest 5% outage UE throughput gains corresponds to $P = 1$ (i.e. the densest home eNB deployment, and therefore with the highest profit from inter-cell interference coordination). From the results in Fig. 6a we observe that ACCS performs consistently better than the fixed frequency re-use schemes. The ACCS scheme automatically adapts to the environment and therefore capitalizes on favorable interference conditions due to switched-off eNBs. Compared to plain frequency re-use one, we observe that ACCS provides a consistent improvement of 18% (factor 1.18) higher cell throughput and 140%-330% higher coverage (factor 2.4-4.3).

Figure 6b contains results for OSG, but note that the performance is still normalized with respect to the baseline performance of plain frequency re-use one and CSG. Looking at the orange curve for OSG and plain frequency re-use one (1/1) results in Fig. 6b, we can see that OSG delivers increasing performance benefits performance in terms of average cell performance and cell-edge performance. Also for this case the ACCS appears to have a very attractive performance when compared to the fixed frequency re-use configurations over all different home eNB deployment densities as it offers

This full text paper was peer reviewed at the direction of IEEE Communications Society subject matter experts for publication in the WCNC 2010 proceedings.

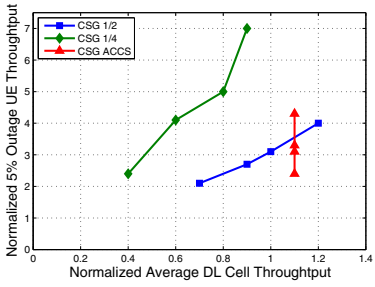

(a) CSG deployment.

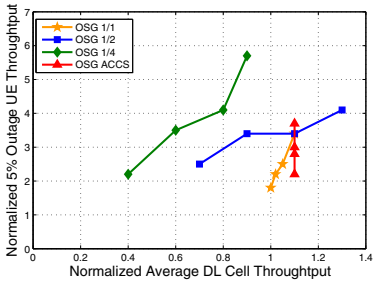

(b) OSG deployment.

Fig. 6. Downlink performance comparison.

uncompromising average cell performance while retaining most of the coverage benefits from sparser re-uses. Thus, this leads to the conclusion that the ACCS scheme works equally independent on whether we have OSG or CSG cases.

V. Conclusion

The deployment of LTE-Advanced femtocells will pose new challenges in terms of interference management and efficient system operation. In this paper we present downlink simulation results for a dual stripe apartment block in a dense-urban deployment of LTE-Advanced home eNBs following current models from 3GPP. We compared the interference footprint of closed subscriber group (CSG) and open subscriber group (OSG) deployments under different hard frequency re-use configurations. It was shown that in case of multiple CSG home eNBs, regions with extremely low SINR values occur.

Naturally, the assessment of deployment aspects depend heavily on assumed traffic and user distributions. Our downlink results assuming full buffer traffic model demonstrate that benefits in terms of SINR from introducing open access are much more significant when universal frequency re-use is considered. In all other configurations, OSG does not provide a clear advantage over CSG. However, it should be emphasized that the latter observation is solely based on downlink investigations, hence uplink performance also needs to be considered before drawing definitive conclusions on OSG vs CSG.

Interestingly, when frequency re-use and OSG are considered, connecting to the cell providing the strongest signal is not always the most sensible choice, as the strongest signal is not necessarily the least interfered one. Notwithstanding, the possibility to be served by the home eNB with the strongest signal ensures that the occurrence of extremely low SINR values is much less frequent.

Finally, our simulation results indicated that the proposed dynamic interference coordination scheme for LTE-Advanced known as Autonomous Component Carrier Selection (ACCS) performs consistently better than the fixed frequency re-use schemes over a wide range of network deployment densities due to its self-adjusting capability. Compared to plain frequency re-use one, we observe that ACCS provides a consistent improvement of 18% (factor 1.18) higher cell throughput and 140%-330% higher coverage under closed access. When open access is considered, ACCS appears to have a very attractive performance as well, leading to the conclusion that the ACCS scheme works equally well independently of access mode of operation of femtocells.

References

[1] 3GPP, "TR 36.913, Requirements for further advancements for E-UTRA (LTE-Advanced)," Tech. Rep., June.

[2] ITU, "Guidelines for evaluation of radio interface technologies for IMT-Advanced," Tech. Rep., July 2008.

[3] V. Chandrasekhar, J. G. Andrews, and A. Gatherer, "Femtocell networks: A survey," *Communications Magazine, IEEE*, September 2008.

[4] H. Claussen, L. T. W. Ho, and L. Samuel, "Financial analysis of a pico-cellular home network deployment," in *IEEE ICC*, June 2007, pp. 5604–5609.

[5] Y. Wang, S. Kumar, L. G. U. Garcia, K. I. Pedersen, I. Z. Kovacs, S. Frattasi, N. Marchetti, and P. E. Mogensen, "Fixed Frequency Reuse for LTE-Advanced Systems in Local Area Scenarios," in *VTC Spring*. Barcelona, Spain: IEEE, April 2009.

[6] 3GPP RAN 4, "Simulation assumptions and parameters for FDD HeNB RF requirements," Tech. Rep. R4-092042, May 2009.

[7] J. Gora and T. E. Kolding, "Deployment Aspects of 3G Femtocells," in *IEEE PIMRC*, Tokyo, Japan, September 2009.

[8] H. Claussen, "Distributed algorithms for robust self-deployment and self-configuration in autonomous wireless access networks," in *IEEE ICC*, vol. 4, Istanbul, Turkey, June 2006, pp. 1927–1932.

[9] L. G. U. Garcia, K. I. Pedersen, and P. E. Mogensen, "Autonomous component carrier selection: Interference management in local area environments for lte-advanced," *Communications Magazine, IEEE*, September 2009.

[10] ——, "Autonomous Component Carrier Selection for Local Area Uncoordinated Deployment of LTE-Advanced," in *VTC Fall*. Anchorage, Alaska: IEEE, 2009.

[11] 3GPP, "TR 25.814, Physical layer aspects for evolved Universal Terrestrial Radio Access (UTRA), V 7.1.0," Tech. Rep., September.

[12] P. Mogensen, W. Na, I. Kovacs, F. Frederiksen, A. Pokhariyal, K. Pedersen, T. Kolding, K. Hugl, and M. Kuusela, "LTE Capacity Compared to the Shannon Bound," in *Vehicular Technology Conference*, April 2007, pp. 1234–1238.

[13] C. Shannon, "A Mathematical Theory of Communication," *the Bell System Technical Journal*, 1948.

Appendix D

Detailed Simulation Assumptions

This appendix describes in detail the underlying simulations assumptions and both simulators developed during this thesis. The system parameters are taken from the Long Term Evolution (LTE) system, which are likely to be used for LTE-Advanced as well.

D.1 The Simulation Tools

Both simulators have been coded in Matlab. This section is dedicated to the commonalities, which were purposefully maximized in order to obtain a meaningful comparison of inter-cell interference management techniques. The differences are treated in upcoming sections. The code is highly modular and each individual module was meticulously tested during the development phase. The code also contains basic error treatment and several runtime sanity checks to ensure that the integrated system would remain logically consistent.

The high level flowchart of both simulation tools is shown in Fig D.1. Note that the simulation methodology is based on a "snap-shot" based approach, including simulation of a number of time-steps for each snap-shot. For each snapshot, a

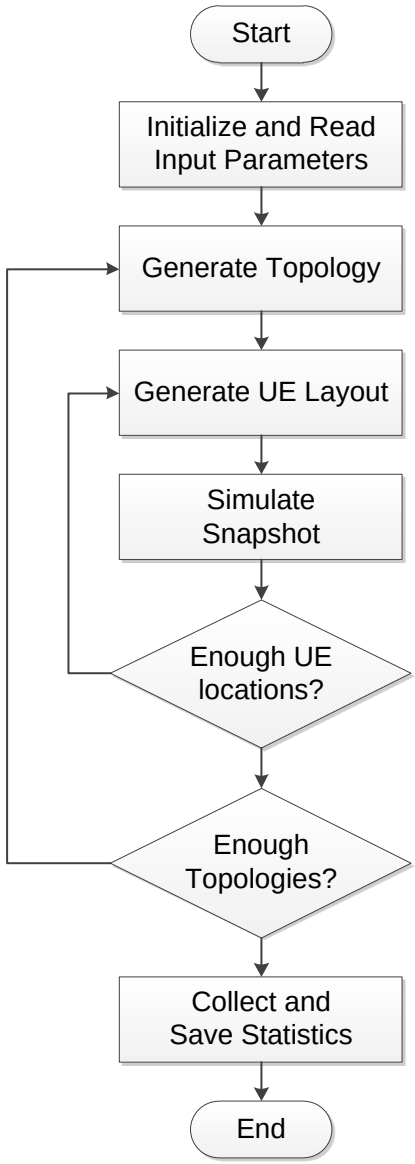

Fig. D.1: High level flowchart of both simulators. The distinctions are concentrated in the "snapshot" module.

new set of active Femto Access Points (FAPs) and users is generated. In order to get the statistically averaged performance, a few thousands of snapshots are simulated and the throughput is collected from all these snapshots. During each time-trace, the location of User Equipments (UEs), FAP as well as the radio channel conditions remain constant. However, Physical Resource Block (PRB) allocation and therefore interference levels can vary dynamically due to finite buffer traffic models and/or the contention mechanism.

D.1.1 Deployment Scenario

All results included in this thesis assume the simulation scenario and indoor path loss modeling defined by Third Generation Partnership Project (3GPP) in [22] for the evaluation of femtocells. The so-called dense-urban dual-stripe scenario consists of two buildings, each with two stripes of apartments, each stripe having 10 apartments per floor. Apartments dimensions are 10m x 10m. There is a 10m wide street between the two buildings. The scenario is illustrated in Fig. D.2.

Both FAPs and UEs are dropped uniformly at indoor random positions. A FAP is a low transmit power base station also known as Home enhanced NodeB (HeNB) in LTE parlance. The random location of FAPs within each apartment mimics the end-user placement of these devices. Note that there is at most one FAP per apartment, whereas the number of UEs can be larger. Throughout this project the number of users typically ranged from 1-4.

Depending on the access mode, Closed Subscriber Group (CSG) or Open Subscriber Group (OSG), UEs are either served by the FAP in the same apartment (CSG) or the femtocell providing the strongest received signal (OSG). CSG implies that, apart from the macro-cells which are not considered here, UEs can only connect to the HeNB in the same residence even if the signal strength from a neighboring FAP is higher. In OSG, the serving cell is selected based on the smallest total path loss (including the deterministic total path loss and shadow fading).

To emulate the realistic case that an apartment may or may not have a femtocell, the "*deployment ratio*", δ, parameter was utilized. The deployment ratio controls the density of the network and varies from 0 to 1.0. Objectively, δ represents the probability of a femtocell being present in each apartment. In the absence of a FAP, no UEs are generated in the apartment. During the simulations, the presence of a FAP is the outcome of a Bernoulli trial (an independent yes/no experiment). Hence, the actual number of deployed HeNBs, H, follows the binomial distribution with parameters $n = 40.F$ and $p = \delta$, where F is

the number of floors simulated. Buildings were simulated with 1 up to 6 floors in this project. Mathematically, the average number of deployed femtocells is $\mathrm{E}[H] = np$ while the probability of having exactly h HeNBs in n apartments is given by the probability mass function:

$$f(H; n, p) = \Pr(H = h) = \binom{n}{h} p^h (1-p)^{n-h} \tag{D.1}$$

D.1.2 Propagation Model

Path loss and log-normal shadowing are considered, but fast fading is not explicitly simulated because the channel varies slowly in indoor system. The indoor wall-counting path loss model is taken from [22, 118]. Two cases have been implemented: the UE and HeNB are either in the same or they are in different apartment stripes. These scenarios are modeled according to (D.2) and (D.3), respectively:

$$\begin{aligned} PL(\mathrm{dB}) = {} & 38.46 + 20 \log R + 0.7 d_{\mathrm{2D\,indoor}} + q * L_{\mathrm{iw}} + \\ & + 18.3 n^{((n+2)/(n+1)-0.46)} \end{aligned} \tag{D.2}$$

$$\begin{aligned} PL(\mathrm{dB}) = {} & \max(15.3 + 37.6 \log R, 38.46 + 20 \log R) + q * L_{\mathrm{iw}} + \\ & + L_{\mathrm{ow}} + L_{\mathrm{ow}} + 0.7 d_{\mathrm{2D\,indoor}} + 18.3 n^{((n+2)/(n+1)-0.46)} \end{aligned} \tag{D.3}$$

In the equations, R is the total distance between transmitter and receiver. An additional log-linear loss is added (0.7 dB/m), which is calculated on the basis of the indoor part of the separation distance ($d_{\mathrm{2D\,indoor}}$). This additional loss is used to simulate indoor elements such as furniture, doors, and walls not modeled individually. For the modeled buildings two types of walls are considered: external walls with 10 dB penetration loss (L_{ow}) and internal walls with a 5 dB penetration loss (L_{iw}). Wall penetration loss is applied on each internal wall (q) crossing the direct signal path. Wall attenuation variations are not taken into account. Doors and windows, typical in e.g. office or apartment type spaces, could lead to significant power leakage, and thus the cell isolation simulated may be optimistic compared to actual deployments. Finally, n denotes the number of traversed floors in multi-floor deployments.

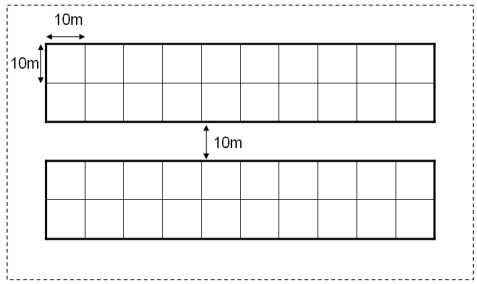

Fig. D.2: Top view of the deployment scenario. Multiple floors are considered.

Log-normal shadowing applies to all links. For links between a HeNB and a UE served by it, the standard deviation is assumed to be 4 dB. Otherwise for all other links (including interference links) the standard deviation is 8dB.

D.1.3 Traffic Models

Both full buffer and finite buffer traffic models are considered in the simulations, according to the guidelines in [22]. The full buffer, also known as the backlogged, traffic model leads to continuous traffic and non-varying interference in LTE simulations. In the Carrier Sense Multiple Access with Collision Avoidance (CSMA/CA) based simulation tool, traffic is not continuously transmitted due to the contention mechanism. Nonetheless, when full-buffer is assumed, user buffers never become empty and sessions last for as long as the simulation runs irrespective of the simulation tool. Although not very realistic in many cases, the full buffer traffic is extensively used due to its simplicity.

Finite buffer traffic models allow evaluations with time-varying interference to be carried out. This traffic model is characterized by the fact that the users have a finite amount of data to transmit or receive. In this study, the models was based on sessions with fixed payloads . The interval $\mathcal{I}$ between the end of one session and the user's request for the next session obeys a negative exponential distribution according to (D.4), with an average length of $1/\lambda$, where λ is the rate parameter.

$$f(\mathcal{I};\lambda) = \begin{cases} \lambda e^{-\lambda \mathcal{I}}, & \mathcal{I} \geq 0, \\ 0, & \mathcal{I} < 0. \end{cases} \tag{D.4}$$

The expected value of $\mathcal{I}$ thus equals $\mathrm{E}[\mathcal{I}] = 1/\lambda$. The total offered traffic per

cell, L, is given by

$$L = \lambda' SU, \tag{D.5}$$

and it depends then on the number of users in each cell, U, the file size, S, and the expected inter-session arrival rate λ'. The latter depends on the session duration, T_s, and the interval between the end of one session and the beginning of the next one, such that:

$$\lambda' = \frac{1}{T_s + E[\mathcal{I}]} \tag{D.6}$$

Although the average user data rate R is not known a priori because it depends on the interference conditions and received signal levels, the session duration can be approximated by the ratio between the file size S and the average data rate R (assumed equal for all users), therefore:

$$T_s = \frac{S}{R} \tag{D.7}$$

Combining (D.6) and (D.7) with (D.5) leads to the total offered load, expressed as:

$$L = \lambda' SU = \frac{1}{S/R + 1/\lambda} SU \tag{D.8}$$

In this work, the number of users and the file sizes were fixed, different loads were obtained by changing the rate parameter λ. The model is illustrated in Fig D.3. Finite buffer model simulations are typically much longer than full-buffer ones (with duration of hundreds of seconds). In order to have representative interference variation, numerous sessions must start and finish. Lastly, finite-buffer is not present in the CSMA/CA based simulator and was therefore not evaluated.

D.1.4 The Physical Layer Modeling

For any given transmission, the receiver side Signal to Interference plus Noise Ratio (SINR) is calculated in accordance to the received signal, interference

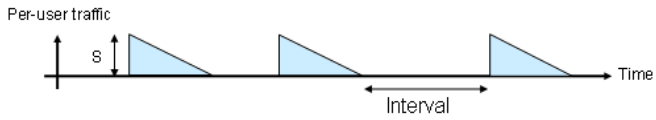

Fig. D.3: Finite-buffer traffic model used in this thesis.

power and the noise power levels. Moreover, in order to account for various imperfections in the implementation of Radio Frequency (RF) components and to avoid unrealistically high SINR values, an Error Vector Magnitude (EVM) model was introduced. EVM is one of the widely accepted figure of merits used to evaluate the quality of communication systems. In simple terms, it quantifies how far the actual received constellation symbols are from their ideal locations had they been sent by an ideal transmitter. With the EVM defined as a percentage, the maximum achievable SINR is calculated as by:

$$\gamma_{\text{max}} = -20 \log_{10}(\text{EVM}/100) \tag{D.9}$$

As a result the EVM-limited effective SINR γ_{evm} is given by (D.10), where γ_{ideal} represents the calculated SINR before imperfections are taken into account.

$$\frac{1}{\gamma_{\text{evm}}} = \frac{1}{\gamma_{\text{max}}} + \frac{1}{\gamma_{\text{ideal}}} \tag{D.10}$$

The important aspect to notice here, is that due to inherent RF impairments, potential improvements might not be fully realized, which limits even further the effectiveness of looser re-use schemes. Figure D.4 illustrates the asymptotical SINR limitation and the corresponding gap between ideal and the effective SINR values for an EVM value of 3%, or equivalently $\gamma_{max} = 30.5$ dB.

The LTE link-level capacity curve is used to map the effective SINR to spectral efficiency and finally to throughput values. The mapping is independently done per Component Carrier (CC). The methodology proposed in [64] is a modification of Shannon's famous capacity bound and was utilized here because it facilitates the benchmarking. The capacity can be estimated using the adjusted Shannon formula:

$$S = BW_{eff} log_2(1 + SINR/SINR_{eff}), \tag{D.11}$$

where S is the estimated spectral efficiency in $bit/s/Hz$. The adjustment terms

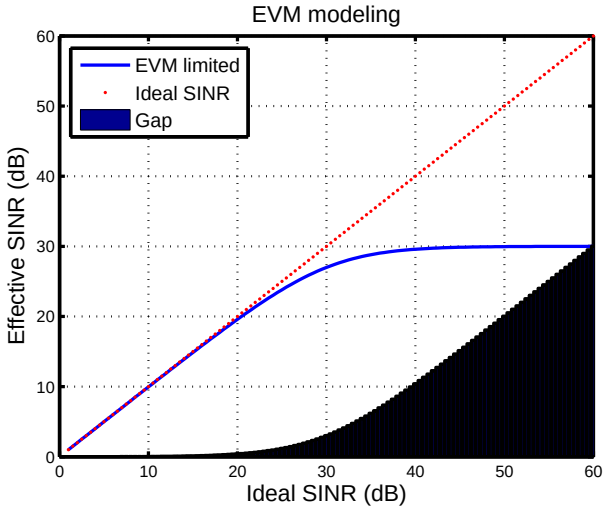

Fig. D.4: An illustration of the asymptotical behavior induced by EVM modeling. Above, $\gamma_{\max} \approx 30.5$ dB.

account for various practical aspects that limit the achievable throughput, such as the effects of achievable bandwidth efficiency, control channel overhead, Modulation and Coding Scheme (MCS) limitations, etc. BW_{eff} adjusts for the system bandwidth efficiency and $SINR_{eff}$ adjusts for the SINR implementation efficiency. A 2x2 MIMO configuration is considered throughout this thesis, therefore allowing up to two code words. Lastly, although (D.11) regards interference as Gaussian noise, it has been shown in [64] to provide an accurate throughput estimation in a multi-cell system with non-Gaussian interference.

D.2 LTE-Advanced Simulator

The simulator is based on basic LTE [3] specifications, whose time domain structure is depicted in D.6, but with bandwidth extensions up to 100 MHz via Carrier Aggregation (CA) of 5 20 MHz CCs. The differences between both simulators materialize in the behavior during the "snapshot" module, which is outlined in Fig. D.5 and examined next.

As discussed in Chapter 2, duplexing is an important element of cellular networks. The tool assumes synchronized Time Division Duplexing (TDD) with a fixed yet configurable 50-50 capacity split between Downlink (DL) and Uplink

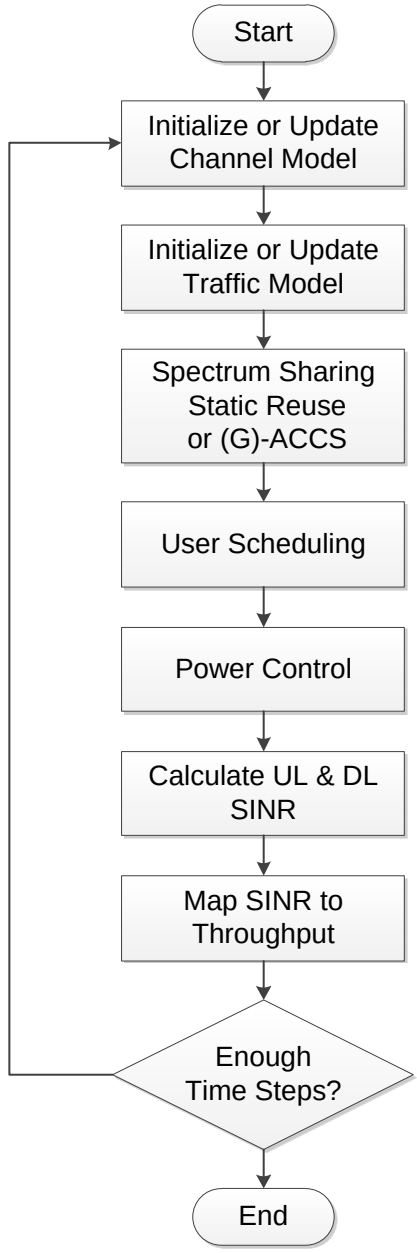

Fig. D.5: High level flowchart of the snapshot module in the LTE tool.

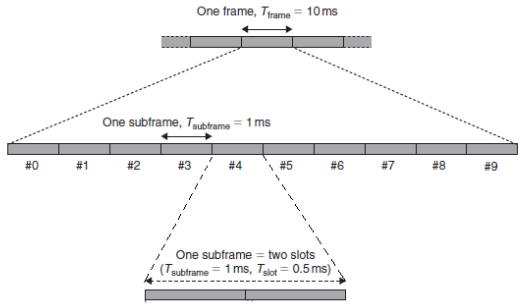

Fig. D.6: A high level description of LTE time domain structure [4].

(UL). In other words, UL (reverse link) and DL (forward link) transmissions do not interfere with each other.

Another distinction regards the SINR calculation. In the LTE tool, the SINR is calculated independently per PRB, whereas the CSMA/CA based version estimates it over the entire band. Finally, static frequency planning with hard frequency reuse patterns is implemented. Different frequency reuse factors are supported.

Both ACCS and G-ACCS algorithms (See Chapters 3 and 5) are implemented in this simulator as well. When these algorithms are considered, the deployed HeNBs are activated one at a time in a random fashion and a single base component carrier Base Component Carrier (BCC) is selected without any UE-side information. The subsequent phase of the simulation iterates over all active HeNB in a random order and a single attempt to select Supplementary Component Carriers (SCCs) is carried out in full-buffer cases. When finite-buffer traffic models are considered, thousands of frames are simulates and SCC selection takes place whenever a new session arrives. The next sections detail the remaining differences.

D.2.1 Power Control

According to the 3GPP standard [119], home base stations may transmit with a maximum power of 20 dBm in the DL. In all simulations with the exception of G-ACCS ones, there is no DL power control. Additionally, the total transmission power is evenly divided among the CCs into which the system bandwidth is divided; hence, HeNBs only transmit at full power if they employ all CCs.

In the UL transmission, unless stated otherwise, Fractional Power Control (FPC) is applied to minimize the interference as well as to prolong the user battery life. The uplink power control mechanism contains both open-loop and closed-loop operations. The latter is not considered in this work because fast-fading was not explicitly modeled. Consequently, adaptation to the short-term channel quality variations become irrelevant. The transmit power for a user is [100]:

$$P_{TX} = max\left\{P_{min}, \min\{P_{max}, P_0 + 10\log_{10} M + \alpha L_u^s\}\right\}, \tag{D.12}$$

where $P_{min} = -30$ dBm, $P_{\max}$ is the maximum UE transmit power – typically 23 dBm – , P_0 is a UE-specific parameter, M is the number of PRBs assigned to a certain user, α is the cell-specific path loss compensation factor and L_u^s is the DL path loss value in decibels measured by UE u towards its serving cell.

D.2.2 User Scheduling

To simplify the problem and focus mainly on cell level spectrum sharing, a frequency domain channel blind fair-resource scheduler is used in each cell. Therefore, each user gets an equal share of the available resources of its own cell. It is also assumed that all possible PRBs are used by the active user(s). Furthermore, only LTE-Advanced users are considered, which can access the whole spectrum through CA.

D.3 CSMA/CA Based Simulator

The key distinction between this tool and the one presented in the previous section pertains to the manner stations access the medium. This difference implies a new snapshot implementation whose flowchart is depicted in Fig. D.7. Power control and scheduling are not present and the pivotal CSMA/CA module is detailed next.

The sensing part detects whether or not the channel is busy. Whenever the channel is perceived idle by a station with data waiting to be transmitted – sensed power below -76 dBm – the station's back-off timer is decremented. When the countdown ends, the station seizes the entire spectrum for some period, denoted here as the *holding time*. The back-off timer mechanism works as described in Chapter 2 and the 0.5 ms LTE radio slot (half of a Transmission Time Interval (TTI) [3]) is employed as the time quantum during the countdown.

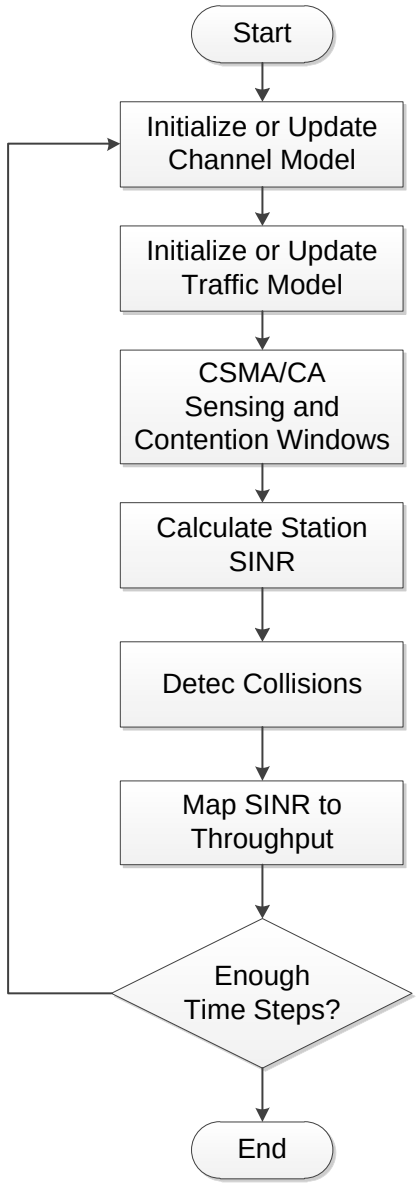

Fig. D.7: High level flowchart of the snapshot module in the CSMA/CA tool.

The holding time value was set by design at 10 ms. This mode of operation admittedly diverges from that of true WiFi networks, where time scales are much shorter (μs), and holding times vary as those depend on both the MAC Service Data Unit (MSDU) size and the physical layer throughput. Nevertheless this choice serves multiple purposes. First, it matches the LTE frame structure as depicted in Fig. D.6. Besides, since latency is not being investigated the absolute time scale has little impact on the overall performance.

Second, and more importantly, 10 ms comprise 20 radio slots (countdown units). This 20/1 ratio matters in this context because the Medium Access Control (MAC) layer efficiency in WiFi systems increases with growing MSDU sizes – the time spent transmitting becomes larger relative to the waiting/sensing period. The selected ratio is roughly equivalent to the 23.5/1 ratio between the time needed to transmit the largest IEEE 802.11n MSDU of 7935 bytes at 300 Mbps and the WiFi countdown unit ($9\mu s$). This combination led to a good match between LTE time structure (frames and slots) and reasonable WiFi parameters. Furthermore, all throughput results are measured at the MAC rather than the Physical Layer (PHY) layer [49]. Due to the contention mechanism, transmissions are typically interference free and will attain high instantaneous throughput. Nonetheless, due to the discontinuous transmissions induced by the very same mechanism, user perceived throughput, is much lower. The temporal structure employed in the CSMA/CA-based simulator is shown in Fig.D.8.

Finally, the collision detection module interacts indirectly with the CSMA/CA module. Whenever a collision takes place, this information is used to increment the contention windows in the subsequent step. The implementation however does not rely on explicit acknowledgements. Rather, collisions are detected based on:

Low SINR When the SINR value averaged over 10 ms on the receiver side is below -10 dB, the throughput is zero and the transmission fails[1].

Simultaneous transmissions It can occur that a client station and its access point decide to transmit to each other at the same time. In this case both transmissions are lost.

Hidden nodes Two or more nodes, which cannot sense each other, transmit to the same serving access point. The access point cannot decode two transmissions. The first transmission is assumed to capture the channel and, if

[1]The SINR threshold was set to 20 dB in order to emulate imperfect link adaptation. However, due to the small apartment dimensions, and the single client station per access point, hidden nodes were hardly an issue and co-channel interference did not seem to increase the collision rates substantially. Devices were able to sustain very high PHY layer data rates when active.

its SINR is above -10 dB, it survives. Otherwise the first transmission is lost just like the other transmissions.

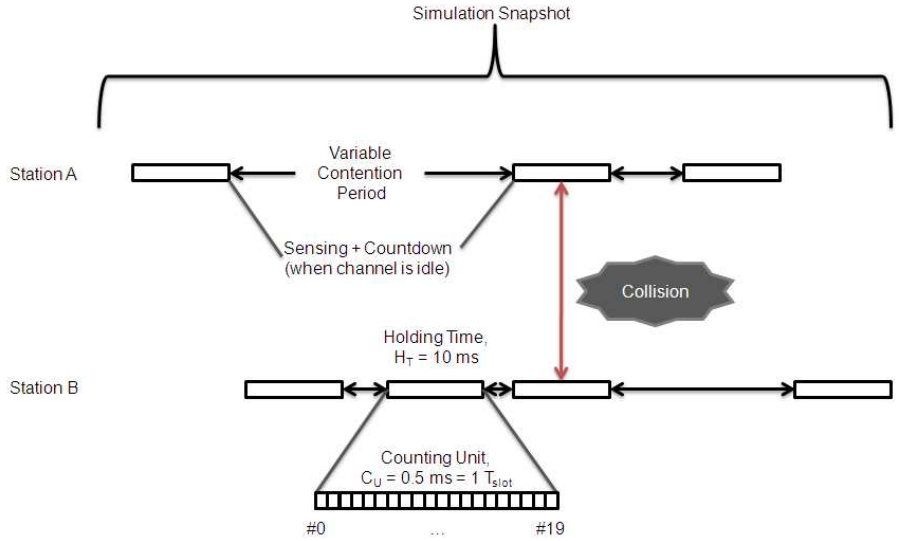

Fig. D.8: A high level description of the timing employed in the CSMA/CA tool.

Appendix E

Signum, Heaviside step and Q-functions

E.1 The Signum Function

The signum, also known as the sign, function $f : \mathbb{R} \to \{-1, 0, 1\}$ extracts the sign of a real number (x) and is defined such that:

$$\operatorname{sgn}(x) = \begin{cases} -1 & \text{if } x < 0, \\ 0 & \text{if } x = 0, \\ 1 & \text{if } x > 0. \end{cases} \tag{E.1}$$

E.2 The Heaviside Step Function

The discrete Heaviside step function, also known as the unit step function, is frequently denoted by $H[n]$ or $u[n]$ It is a discontinuous piecewise constant function whose value is zero for non-positive values of the integer argument n

and one otherwise. The unit step function is formally defined as:

$$H[n] = \begin{cases} 0 & n < 0, \\ 1 & n \geq 0. \end{cases} \tag{E.2}$$

E.3 The Q-Function

The Q-function often arises when one needs to compute probabilities that involve Gaussian distributions. For any Gaussian random variable x with mean m and standard deviation σ, the probability that x exceeds x_0, that is $Pr(x > x_0)$, is quantified as:

$$Pr(x > x_0) = \frac{1}{\sigma\sqrt{2\pi}} \int_{x_0}^{\infty} \exp\left(-\frac{(x-m)^2}{2\sigma^2}\right) dx \tag{E.3}$$

The integral in (E.3) corresponds to the area underneath the tail of the Gaussian probability density function (pdf). Defining a new variable y and using the substitution

$$y = \frac{x-m}{\sigma}, \tag{E.4}$$

(E.3) can be recast as

$$Pr\left(y > \frac{x_0 - m}{\sigma}\right) = \frac{1}{\sigma\sqrt{2\pi}} \int_{\left(\frac{x_0-m}{\sigma}\right)}^{\infty} \exp\left(-\frac{y^2}{2}\right) dy \tag{E.5}$$

The evaluation of the integral in (E.5) is denoted the Q-function. Thus $Q\left(\frac{x_0-m}{\sigma}\right) = Q(z)$ such that:

$$Q(z) = \frac{1}{\sqrt{2\pi}} \int_{z}^{\infty} \exp\left(-\frac{y^2}{2}\right) dy \tag{E.6}$$

There is no closed form for the expression above. However the kernel of the integral is the pdf of the standard normal distribution $\mathcal{N}$ $(m = 0, \sigma^2 = 1)$ and it

either tabulated or calculated using numerical methods. An important property of the Q-function is that:

$$Q(-z) = 1 - Q(z) \tag{E.7}$$

Finally, Table contains the values of the Q-function for various values of z.

Table E.1: Tabulation of the Q-function.

z	Q(z)	z	Q(z)
0.0	0.500000000	2.0	0.022750132
0.1	0.460172163	2.1	0.017864421
0.2	0.420740291	2.2	0.013903448
0.3	0.382088578	2.3	0.010724110
0.4	0.344578258	2.4	0.008197536
0.5	0.308537539	2.5	0.006209665
0.6	0.274253118	2.6	0.004661188
0.7	0.241963652	2.7	0.003466974
0.8	0.211855399	2.8	0.002555130
0.9	0.184060125	2.9	0.001865813
1.0	0.158655254	3.0	0.001349898
1.1	0.135666061	3.1	0.000967603
1.2	0.115069670	3.2	0.000687138
1.3	0.096800485	3.3	0.000483424
1.4	0.080756659	3.4	0.000336929
1.5	0.066807201	3.5	0.000232629
1.6	0.054799292	3.6	0.000159109
1.7	0.044565463	3.7	0.000107800
1.8	0.035930319	3.8	0.000072348
1.9	0.028716560	3.9	0.000048096

List of Acronyms

3GPP Third Generation Partnership Project

ACCS Autonomous Component Carrier Selection

AP Access Point

BCC Base Component Carrier

BIM Background Interference Matrix

CA Carrier Aggregation

CC Component Carrier

CCRAT Component Carrier Radio Allocation Table

CDF Cumulative Distribution Function

CIR Carrier to Interference Ratio

CR Cognitive Radio

CRN Cognitive Radio Networks

CSG Closed Subscriber Group

CSMA/CA Carrier Sense Multiple Access with Collision Avoidance

DCF Distributed Coordination Function

DL Downlink

DL RS TX Downlink Reference Signal Transmit

ECDF Empirical Cumulative Distribution Function

eICIC Enhanced Inter-Cell Interference Coordination

eNB enhanced NodeB

EPC Evolved Packet Core

EVM Error Vector Magnitude

FAP Femto Access Point

FDD Frequency Division Duplexing

FPC Fractional Power Control

G-ACCS Generalized Autonomous Component Carrier Selection

GT Game Theory

HetNet Heterogeneous Network

HII High Interference Indicator

HeNB Home enhanced NodeB

HeNB-GW Home eNB Gateway

HSPA High Speed Packet Access

ICIC Inter-Cell Interference Coordination

IMT-A International Mobile Telecommunications-Advanced

IoT Interference over Thermal

IPR Intellectual Property Rights

IRR Interference Reduction Request

ITU-R International Telecommunications Union - Radio Communication Sector

JSAC IEEE Journal on Selected Areas in Communications

KPI Key Performance Indicator

LAN Local Area Network

LA Link Adaptation

LTE Long Term Evolution

MAC Medium Access Control

MSDU MAC Service Data Unit

MCS Modulation and Coding Scheme

MIMO Multiple Input Multiple Output

NLM Network Listening Mode

OFDM Orthogonal Frequency Division Multiplexing

OFDMA Orthogonal Frequency Division Multiple Access

OI Overload Indicator

OSG Open Subscriber Group

PC Power Control

pdf probability density function

PHY Physical Layer

PPP Poissson Point Process

PRB Physical Resource Block

PS Packet Scheduler

PSD Power Spectral Density

QoS Quality of Service

RF Radio Frequency

RIP Received Interference Power

RNTP Relative Narrowband Transmit Power

RRM Radio Resource Management

RSRP Reference Signal Received Power

RSRQ Reference Signal Receive Quality

SCC Supplementary Component Carrier

SC-FDMA Single-carrier Frequency Division Multiple Access

SIR Signal to Interference Ratio

SINR Signal to Interference plus Noise Ratio

SISO Single Input Single Output

SNR Signal to Noise Ratio

SOCCER Self-Organizing Coalitions for Conflict Evaluation and Resolution

TCP Transmission Control Protocol

TDD Time Division Duplexing

TTI Transmission Time Interval

UE User Equipment

UL Uplink

WCDMA Wideband Code Division Multiple Access

WLAN Wireless Local Area Network

Bibliography

[1] Ovum, "Global mobile market outlook: 2009-14," Premium Report, February 2010.

[2] Cisco, "Cisco Visual Networking Index: Global Mobile Data Traffic Forecast Update,2010-2015," White Paper, February 2011.

[3] H. Holma and A. Toskala, *LTE for UMTS Evolution to LTE-Advanced*. John Wiley & Sons, 2 ed., 2011.

[4] E. Dahlman, S. Parkvall, J. Sköld, and P. Beming, *3G evolution: HSPA and LTE for mobile broadband*. Elsevier, 2007.

[5] S. Sesia, B. Matthew, and T. Issam, *LTE, the UMTS long term evolution: from theory to practice*. John Wiley & Sons, Feb 2009.

[6] D. Astély, E. Dahlman, A. Furuskar, Y. Jading, M. Lindstrom, and S. Parkvall, "LTE: the evolution of mobile broadband," *Communications Magazine, IEEE*, vol. 47, pp. 44–51, Apr 2009.

[7] Y. Zheng, "How to operate– boosting WiMAX indoor coverage," *Huawei Communicate*, pp. 31–32, Apr 2009.

[8] "IEEE Standard for Information Technology-Telecommunications and Information Exchange Between Systems-Local and Metropolitan Area Networks-Specific Requirements - Part 11: Wireless LAN Medium Access Control (MAC) and Physical Layer (PHY) Specifications," *IEEE Std 802.11-2007 (Revision of IEEE Std 802.11-1999)*, pp. C1–1184, 12 2007.

[9] V. Chandrasekhar, J. Andrews, and A. Gatherer, "Femtocell networks: a survey," *Communications Magazine, IEEE*, vol. 46, no. 9, pp. 59–67, 2008.

[10] ETSI MCC, "Report of 3GPP TSG RAN IMT-Advanced Workshop," tech. rep., April 2008.

[11] S. Parkvall, A. Furuskar, and E. Dahlman, "Evolution of lte toward imt-advanced," *Communications Magazine, IEEE*, vol. 49, no. 2, pp. 84–91, 2011.

[12] M. Iwamura, K. Etemad, M.-H. Fong, R. Nory, and R. Love, "Carrier aggregation framework in 3GPP LTE-Advanced [WiMAX/LTE Update]," *Communications Magazine, IEEE*, vol. 48, no. 8, pp. 60–67, 2010.

[13] ITU-R, "Framework and overall objectives of the future development of IMT-2000 and systems beyond IMT-2000," *Recommendation M. 1645*, Jun 2003.

[14] A. Hashimoto, H. Yoshino, and H. Atarashi, "Roadmap of IMT-advanced development," *Microwave Magazine, IEEE*, vol. 9, pp. 80–88, Aug 2008.

[15] D. Lopez-Perez, A. Valcarce, G. de la Roche, and J. Zhang, "Ofdma femtocells: A roadmap on interference avoidance," *Communications Magazine, IEEE*, vol. 47, no. 9, pp. 41–48, 2009.

[16] D. Lopez-Perez, A. Valcarce, G. De La Roche, E. Liu, and J. Zhang, "Access methods to wimax femtocells: A downlink system-level case study," in *Communication Systems, 2008. ICCS 2008. 11th IEEE Singapore International Conference on*, pp. 1657–1662, 2008.

[17] H. Claussen, "Performance of macro- and co-channel femtocells in a hierarchical cell structure," in *Personal, Indoor and Mobile Radio Communications, 2007. PIMRC 2007. IEEE 18th International Symposium on*, pp. 1–5, 2007.

[18] M. A. Ergin, K. Ramachandran, and M. Gruteser, "An experimental study of inter-cell interference effects on system performance in unplanned wireless lan deployments," *Computer Networks*, vol. 52, pp. 2728–2744, October 2008.

[19] G. J. Foschini, "Layered space-time architecture for wireless communication in a fading environment when using multi-element antennas," *Bell Labs Technical Journal*, vol. 1, no. 2, pp. 41–59, 1996.

[20] D. Gesbert, M. Shafi, D. shan Shiu, P. J. Smith, and A. Naguib, "From Theory to Practice: An Overview of MIMO Space-Time Coded Wireless Systems," *IEEE Journal on Selected Areas in Communications*, 2003.

[21] 3GPP, "Technical Specification Group Radio Access Network; Requirements for Further Advancements for E-UTRA (LTE-Advanced) (Release 8)," Tech. Rep. 36.913 V8.0.0, Jun 2008.

[22] 3GPP , "Evolved Universal Terrestrial Radio Access (E-UTRA); Further advancements for E-UTRA physical layer aspects," Tech. Rep. 36.814 v9.0.0, March 2010.

[23] P. Mogensen, T. Koivisto, K. Pedersen, I. Kovacs, B. Raaf, K. Pajukoski, and M. Rinne, "Lte-advanced: The path towards gigabit/s in wireless mobile communications," in *Wireless Communication, Vehicular Technology, Information Theory and Aerospace Electronic Systems Technology, 2009. Wireless VITAE 2009. 1st International Conference on*, pp. 147–151, May 2009.

[24] A. Ghosh, R. Ratasuk, B. Mondal, N. Mangalvedhe, and T. Thomas, "Lte-advanced: next-generation wireless broadband technology [invited paper]," *Wireless Communications, IEEE*, vol. 17, no. 3, pp. 10–22, 2010.

[25] A. Khandekar, N. Bhushan, J. Tingfang, and V. Vanghi, "Lte-advanced: Heterogeneous networks," in *Wireless Conference (EW), 2010 European*, pp. 978–982, 2010.

[26] 3GPP , "Evolved Universal Terrestrial Radio Access (E-UTRA) and Evolved Universal Terrestrial Radio Access Network (E-UTRAN); Overall description; Stage 2," Tech. Spec. 36.300 v10.3.0, April 2011.

[27] 3GPP , "Evolved Universal Terrestrial Radio Access (E-UTRA); FDD Home eNode B (HeNB) Radio Frequency (RF) requirements analysis," Tech. Spec. 36.921 v10.0.0, April 2011.

[28] 3GPP , "Architecture aspects of Home Node B (HNB) / Home enhanced Node B (HeNB)," Tech. Rep. 23.830 v9.0.0, October 2009.

[29] H. Holma and A. Toskala, *WCDMA for UMTS - HSPA evolution and LTE, fifth edition.* John Wiley & Sons, 2010.

[30] H. Claussen, L. Ho, and L. Samuel, "Financial Analysis of a Pico-Cellular Home Network Deployment," in *Communications, 2007. ICC '07. IEEE International Conference on*, pp. 5604–5609, june 2007.

[31] N. Shetty, S. Parekh, and J. Walrand, "Economics of Femtocells," in *Global Telecommunications Conference, 2009. GLOBECOM 2009. IEEE*, pp. 1–6, 30 2009-dec. 4 2009.

[32] J. Gora and T. Kolding, "Deployment aspects of 3G femtocells," in *Personal, Indoor and Mobile Radio Communications, 2009 IEEE 20th International Symposium on*, pp. 1507–1511, sept. 2009.

[33] P. Xia, V. Chandrasekhar, and J. Andrews, "Open vs. Closed Access Femtocells in the Uplink," *Wireless Communications, IEEE Transactions on*, vol. 9, pp. 3798–3809, december 2010.

[34] A. J. David Ló´pez-Pérez, Ákos Ladányi and J. Zhang, "OFDMA Femtocells: Intracell Handover for Interference and Handover Mitigation in Two-Tier Networks," in *Wireless Communications and Networking Conference (WCNC), 2010 IEEE*, pp. 1–6, april 2010.

[35] Nokia Siemens Networks, "Macro+HeNB performance with escape carrier," 3GPP Standard Contribution (R1-101453), Feb 2010.

[36] 3GPP, "Evolved Universal Terrestrial Radio Access (E-UTRA); FDD Home eNode B (HeNB) Radio Frequency (RF) requirements analysis," tech. rep., April.

[37] "IEEE Standard for Information technology–Telecommunications and information exchange between systems–Local and metropolitan area networks–Specific requirements Part 11: Wireless LAN Medium Access Control (MAC) and Physical Layer (PHY) Specifications Amendment 5: Enhancements for Higher Throughput," *IEEE Std 802.11n-2009 (Amendment to IEEE Std 802.11-2007 as amended by IEEE Std 802.11k-2008, IEEE Std 802.11r-2008, IEEE Std 802.11y-2008, and IEEE Std 802.11w-2009)*, pp. c1–502, 29 2009.

[38] J. Peha, "Sharing Spectrum Through Spectrum Policy Reform and Cognitive Radio," *Proceedings of the IEEE*, vol. 97, pp. 708–719, april 2009.

[39] P. Anker, "Cognitive Radio, the Market and the Regulator," in *New Frontiers in Dynamic Spectrum, 2010 IEEE Symposium on*, pp. 1–6, april 2010.

[40] Michael Garey and David S. Johnson, *Computers and Intractability: A Guide to the Theory of NP-Completeness*. W. H. Freeman, 1979.

[41] G. Boudreau, J. Panicker, N. Guo, R. Chang, N. Wang, and S. Vrzic, "Interference coordination and cancellation for 4g networks," *Communications Magazine, IEEE*, vol. 47, no. 4, pp. 74–81, 2009.

[42] F. Mullany, L. Ho, L. Samuel, and H. Claussen, "Self-deployment, Self-configuration:Critical Future Paradigms for Wireless Access Networks," in *Autonomic Communication* (M. Smirnov, ed.), vol. 3457 of *Lecture Notes in Computer Science*, pp. 234–238, Springer Berlin / Heidelberg, 2005.

[43] H. Claussen, "Distributed Algorithms for Robust Self-deployment and Load Balancing in Autonomous Wireless Access Networks," in *Communications, 2006. ICC '06. IEEE International Conference on*, vol. 4, pp. 1927–1932, june 2006.

[44] Brian E. Carpenter (ed.), "Architectural Principles of the Internet," *Internet RFC 1958*, June 1996.

[45] C. Shannon, "A Mathematical Theory of Communication," *the Bell System Technical Journal*, 1948.

[46] J. Andrews, S. Shakkottai, R. Heath, N. Jindal, M. Haenggi, R. Berry, D. Guo, M. Neely, S. Weber, S. Jafar, and A. Yener, "Rethinking information theory for mobile ad hoc networks," *Communications Magazine, IEEE*, vol. 46, pp. 94 –101, december 2008.

[47] M. Haenggi, J. Andrews, F. Baccelli, O. Dousse, and M. Franceschetti, "Stochastic geometry and random graphs for the analysis and design of wireless networks," *Selected Areas in Communications, IEEE Journal on*, vol. 27, no. 7, pp. 1029–1046, 2009.

[48] J. Andrews, R. Ganti, M. Haenggi, N. Jindal, and S. Weber, "A primer on spatial modeling and analysis in wireless networks," *Communications Magazine, IEEE*, vol. 48, pp. 156 –163, november 2010.

[49] Andrew S. Tanenbaum, *Computer Networks, Fourth Edition*. Prentice Hall PTR, 2002.

[50] WINNER II, D1.1.2, "WINNER II Channel Models part I- Channel Models," tech. rep., September 2007.

[51] Nokia Siemens Networks, "Carrier based HetNet ICIC for LTE," 3GPP Standard Contribution (RP-110437), March 2011.

[52] T. S. Rappaport, *Wireless communications principles and practice, second edition*. Prentice Hall, 2001.

[53] Gábor Fodor and Chrysostomos Koutsimanis and András Rácz and Norbert Reider and Arne Simonsson and Walter Müller, "Intercell Interference Coordination in OFDMA Networks and in the 3GPP Long Term Evolution System," *Journal of Communications*, vol. 4, no. 7, 2009.

[54] A. Akella, G. Judd, S. Seshan, and P. Steenkiste, "Self-management in chaotic wireless deployments," in *Proceedings of the 11th annual international conference on Mobile computing and networking*, MobiCom '05, (New York, NY, USA), pp. 185–199, ACM, 2005.

[55] G. Bianchi, "Performance analysis of the IEEE 802.11 distributed coordination function," *Selected Areas in Communications, IEEE Journal on*, vol. 18, pp. 535 –547, mar 2000.

[56] Jan Erik Håkegård, "Multi-Cell WLAN Coverage and Capacity," *Telektronikk*, 2006.

[57] J. Zhu, B. Metzler, X. Guo, and Y. Liu, "Adaptive CSMA for Scalable Network Capacity in High-Density WLAN: A Hardware Prototyping Approach," in *INFOCOM 2006. 25th IEEE International Conference on Computer Communications. Proceedings*, pp. 1–10, april 2006.

[58] I. Tinnirello, G. Bianchi, and Y. Xiao, "Refinements on IEEE 802.11 Distributed Coordination Function Modeling Approaches," *Vehicular Technology, IEEE Transactions on*, vol. 59, pp. 1055–1067, march 2010.

[59] A. Pokhariyal, T. Kolding, and P. Mogensen, "Performance of Downlink Frequency Domain Packet Scheduling for the UTRAN Long Term Evolution," in *Personal, Indoor and Mobile Radio Communications, 2006 IEEE 17th International Symposium on*, pp. 1–5, Sep 2006.

[60] J. G. Proakis, "Capacity of multiple access methods," in *Digital Communications*, McGraw-Hill Science/Engineering/Math, Aug 2000.

[61] A. Goldsmith, *Wireless Communications*, ch. 14, pp. 464–466. Cambridge, 2005.

[62] R. Miles, "On the homogeneous planar poisson point process," *Mathematical Biosciences*, vol. 6, pp. 85–127, 1970.

[63] 3GPP, "Physical layer aspects for evolved Universal Terrestrial Radio Access (UTRA)," Tech. Rep. 25.814 v7.1.0, September 2006.

[64] P. Mogensen, W. Na, I. Kovacs, F. Frederiksen, A. Pokhariyal, K. Pedersen, T. Kolding, K. Hugl, and M. Kuusela, "LTE Capacity Compared to the Shannon Bound," in *Vehicular Technology Conference*, pp. 1234–1238, April 2007.

[65] I. Mitola, J. and J. Maguire, G.Q., "Cognitive radio: making software radios more personal," *Personal Communications, IEEE*, vol. 6, pp. 13–18, Aug. 1999.

[66] Jeffrey G. Andrews and Wan Choi and Robert W. Heath Jr, "Overcoming Interference in Spatial Multiplexing MIMO Cellular Networks," *Wireless Communications Magazine, IEEE* , December 2007.

[67] I. Katzela and M. Naghshineh, "Channel assignment schemes for cellular mobile telecommunication systems: A comprehensive survey," *Communications Surveys Tutorials, IEEE*, vol. 3, no. 2, pp. 10–31, 2000.

[68] M.-L. Cheng and J.-I. Chuang, "Performance evaluation of distributed measurement-based dynamic channel assignment in local wireless communications," *Selected Areas in Communications, IEEE Journal on*, vol. 14, pp. 698–710, May 1996.

[69] M. Serizawa and D. Goodman, "Instability and deadlock of distributed dynamic channel allocation," in *Vehicular Technology Conference, 1993 IEEE 43rd*, pp. 528–531, May 1993.

[70] L. Narayanan, *Channel Assignment and Graph Multicoloring*, pp. 71–94. John Wiley & Sons, Inc., 2002.

[71] M. C. Necker, "Scheduling Constraints and Interference Graph Properties for Graph-based Interference Coordination in Cellular OFDMA Networks," *Mob. Netw. Appl.*, vol. 14, pp. 539–550, August 2009.

[72] Furqan Ahmed and Olav Tirkkonen and Matti Peltomäki and Juha-Matti Koljonen and Chia-Hao Yu and Mikko Alava, "Distributed Graph Coloring for Self-Organization in LTE Networks," *Journal of Electrical and Computer Engineering*, vol. 2010, August 2010.

[73] M. Huson and A. Sen, "Broadcast scheduling algorithms for radio networks," in *Military Communications Conference, 1995. MILCOM '95, Conference Record, IEEE*, vol. 2, pp. 647–651 vol.2, Nov. 1995.

[74] A. Mishra, S. Banerjee, and W. Arbaugh, "Weighted coloring based channel assignment for wlans," *SIGMOBILE Mob. Comput. Commun. Rev.*, vol. 9, pp. 19–31, July 2005.

[75] D. Leith and P. Clifford, "A Self-Managed Distributed Channel Selection Algorithm for WLANs," in *Modeling and Optimization in Mobile, Ad Hoc and Wireless Networks, 2006 4th International Symposium on*, pp. 1–9, 2006.

[76] A. MacKenzie and S. Wicker, "Game theory and the design of self-configuring, adaptive wireless networks," *Communications Magazine, IEEE*, vol. 39, pp. 126–131, Nov. 2001.

[77] J. Ellenbeck, C. Hartmann, and L. Berlemann, "Decentralized inter-cell interference coordination by autonomous spectral reuse decisions," in *Wireless Conference, 2008. EW 2008. 14th European*, pp. 1–7, 2008.

[78] G. da Costa, A. Cattoni, I. Kovacs, and P. Mogensen, "A scalable spectrum-sharing mechanism for local area network deployment," *Vehicular Technology, IEEE Transactions on*, vol. 59, pp. 1630–1645, May 2010.

[79] Junhong Nie and Haykin, S., "A Q-learning-based dynamic channel assignment technique for mobile communication systems," *Vehicular Technology, IEEE Transactions on*, vol. 48, pp. 1676–1687, sep 1999.

[80] C.J.C.H. Watkins, *Learning from Delayed Rewards*. PhD thesis, Cambridge University, 1989.

[81] M. Bennis and D. Niyato, "A Q-learning based approach to interference avoidance in self-organized femtocell networks," in *GLOBECOM Workshops (GC Wkshps), 2010 IEEE*, pp. 706–710, Dec. 2010.

[82] A. Galindo-Serrano, L. Giupponi, and M. Dohler, "Cognition and docition in ofdma-based femtocell networks," in *GLOBECOM 2010, 2010 IEEE Global Telecommunications Conference*, pp. 1–6, dec. 2010.

[83] N. Devroye, M. Vu, and V. Tarokh, "Cognitive radio networks," *Signal Processing Magazine, IEEE*, vol. 25, no. 6, pp. 12–23, 2008.

[84] I. Akyildiz, W.-Y. Lee, M. Vuran, and S. Mohanty, "A survey on spectrum management in cognitive radio networks," *Communications Magazine, IEEE*, vol. 46, no. 4, pp. 40–48, 2008.

[85] J. Xiang, Y. Zhang, T. Skeie, and L. Xie, "Downlink spectrum sharing for cognitive radio femtocell networks," *Systems Journal, IEEE*, vol. 4, no. 4, pp. 524–534, 2010.

[86] D. Gesbert, S. G. Kiani, A. Gjendemsjø, and G. E. Øien, "Adaptation, Coordination, and Distributed Resource Allocation in Interference-Limited Wireless Networks," *Proceedings of the IEEE*, 2007.

[87] N. Himayat, S. Talwar, A. Rao, and R. Soni, "Interference management for 4G cellular standards [WIMAX/LTE UPDATE]," *Communications Magazine, IEEE*, vol. 48, pp. 86–92, august 2010.

[88] A. Simonsson, "Frequency Reuse and Intercell Interference Co-Ordination In E-UTRA," in *Vehicular Technology Conference, 2007. VTC2007-Spring. IEEE 65th*, pp. 3091–3095, 2007.

[89] G. Li and H. Liu, "Downlink Radio Resource Allocation for Multi-Cell OFDMA System," *Wireless Communications, IEEE Transactions on*, vol. 5, pp. 3451–3459, december 2006.

[90] N. Jindal, J. Andrews, and S. Weber, "Bandwidth partitioning in decentralized wireless networks," *Wireless Communications, IEEE Transactions on*, vol. 7, pp. 5408–5419, december 2008.

[91] L. Zhang, L. Yang, and T. Yang, "Cognitive interference management for lte-a femtocells with distributed carrier selection," in *Vehicular Technology Conference Fall (VTC 2010-Fall), 2010 IEEE 72nd*, pp. 1–5, 2010.

[92] R. Madan, J. Borran, A. Sampath, N. Bhushan, A. Khandekar, and T. Ji, "Cell Association and Interference Coordination in Heterogeneous LTE-A Cellular Networks," *Selected Areas in Communications, IEEE Journal on*, vol. 28, pp. 1479–1489, december 2010.

[93] R. Madan, A. Sampath, N. Bhushan, A. Khandekar, J. Borran, and T. Ji, "Impact of Coordination Delay on Distributed Scheduling in LTE-A Femtocell Networks," in *GLOBECOM 2010, 2010 IEEE Global Telecommunications Conference*, pp. 1–5, dec. 2010.

[94] K. Zheng, F. Hu, L. Lei, and W. Wang, "Interference coordination between femtocells in LTE-advanced networks with carrier aggregation," in *Communications and Networking in China (CHINACOM), 2010 5th International ICST Conference on*, pp. 1–5, aug. 2010.

[95] A. Prasad, K. Doppler, M. Moisio, K. Valkealahti, and O. Tirkkonen, "Distributed Capacity Based Channel Allocation for Dense Local Area Deployments," in *Vehicular Technology Conference Fall (VTC 2011-Fall), 2011 IEEE 74th*, pp. 1–5, 2011.

[96] L. Garcia, K. Pedersen, and P. Mogensen, "Autonomous component carrier selection: interference management in local area environments for lte-advanced," *Communications Magazine, IEEE*, vol. 47, no. 9, pp. 110–116, 2009.

[97] 3GPP, "Evolved Universal Terrestrial Radio Access (E-UTRA); Physical layer; Measurements," Tech. Spec. 36.214 V10.1.0, March 2011.

[98] L. Garcia, G. Costa, A. Cattoni, K. Pedersen, and P. Mogensen, "Self-Organizing Coalitions for Conflict Evaluation and Resolution in Femtocells," in *GLOBECOM 2010, 2010 IEEE Global Telecommunications Conference*, pp. 1–6, dec. 2010.

[99] S. Kumar, *Techniques for Efficient Spectrum Usage for Next Generation Mobile Communication Networks. An LTE and LTE-A Case Study.* Institut for Elektroniske Systemer, Aalborg Universitet, 2009.

[100] 3GPP, "Evolved Universal Terrestrial Radio Access (E-UTRA); Physical layer procedures," Tech. Spec. 36.213 V9.1.0, March 2009.

[101] C. Castellanos, D. Villa, C. Rosa, K. Pedersen, F. Calabrese, P.-H. Michaelsen, and J. Michel, "Performance of uplink fractional power control in utran lte," in *Vehicular Technology Conference, 2008. VTC Spring 2008. IEEE*, pp. 2517 –2521, may 2008.

[102] L. Garcia, K. Pedersen, and P. Mogensen, "Uplink Performance of Dynamic Interference Coordination under Fractional Power Control for LTE-Advanced Femtocells," in *Vehicular Technology Conference Fall (VTC 2010-Fall), 2010 IEEE 72nd*, pp. 1–5, sept. 2010.

[103] M. Boussif, N. Quintero, F. Calabrese, C. Rosa, and J. Wigard, "Interference Based Power Control Performance in LTE Uplink," in *Wireless*

Communication Systems. 2008. ISWCS '08. IEEE International Symposium on, pp. 698 –702, oct. 2008.

[104] A. Simonsson and A. Furuskar, "Uplink Power Control in LTE - Overview and Performance, Subtitle: Principles and Benefits of Utilizing rather than Compensating for SINR Variations.," in *VTC Fall*, IEEE, 2008.

[105] F. Sanchez-Moya, J. Villalba-Espinosa, L. G. U. Garcia, K. I. Pedersen, and P. E. Mogensen, "On the Impact of Explicit Uplink Information on Autonomous Component Carrier Selection for LTE-A Femtocells," in *Vehicular Technology Conference Spring (VTC 2011-Spring), 2011 IEEE 73rd*, pp. 1–5, may 2011.

[106] H. Wang, C. Rosa, and K. Pedersen, "Performance of Uplink Carrier Aggregation in LTE-Advanced Systems," in *Vehicular Technology Conference Fall (VTC 2010-Fall), 2010 IEEE 72nd*, pp. 1–5, sept. 2010.

[107] K. Pedersen, F. Frederiksen, C. Rosa, H. Nguyen, L. Garcia, and Y. Wang, "Carrier aggregation for lte-advanced: functionality and performance aspects," *Communications Magazine, IEEE*, vol. 49, pp. 89 –95, june 2011.

[108] Y. Wang, S. Kumar, L. Garcia, K. Pedersen, I. Kovacs, S. Frattasi, N. Marchetti, and P. Mogensen, "Fixed frequency reuse for lte-advanced systems in local area scenarios," in *Vehicular Technology Conference, 2009. VTC Spring 2009. IEEE 69th*, pp. 1–5, 2009.

[109] J. Zhang and G. de la Roche, *Femtocells: Technologies and Deployment*, ch. 8.5, pp. 234–235. John Wiley and Sons, 2010.

[110] L. Garcia, K. Pedersen, and P. Mogensen, "Autonomous component carrier selection for local area uncoordinated deployment of lte-advanced," in *Vehicular Technology Conference Fall (VTC 2009-Fall), 2009 IEEE 70th*, pp. 1–5, 2009.

[111] D. Lopez-Perez, I. Guvenc, G. de la Roche, M. Kountouris, T. Quek, and J. Zhang, "Enhanced intercell interference coordination challenges in heterogeneous networks," *Wireless Communications, IEEE*, vol. 18, pp. 22–30, june 2011.

[112] J.-Y. Le Boudec, *Performance Evaluation of Computer and Communication Systems*. EPFL Press, Lausanne, Switzerland, 2010.

[113] G. Monghal, *Downlink Radio Resource Management for QoS Provisioning in OFDMA Systems*. PhD thesis, 2009.

[114] L. Guo and I. Matta, "The war between mice and elephants," in *Network Protocols, 2001. Ninth International Conference on*, pp. 180–188, nov. 2001.

[115] V. Srivastava and M. Motani, "Cross-layer design: a survey and the road ahead," *Communications Magazine, IEEE*, vol. 43, pp. 112–119, dec. 2005.

[116] Juan Villalba Espinosa and Fernando Sánchez Moya, "Statistical Characterization and Uplink Improvements in Autonomous Carrier Selection for Femtocells," Master's thesis, Aalborg University.

[117] L. G. U. Garcia, F. Sanchez-Moya, J. Villalba-Espinosa, K. I. Pedersen, and P. E. Mogensen, "Enhanced Uplink Carrier Aggregation for LTE-Advanced Femtocells," in *Vehicular Technology Conference Spring (VTC 2011-Fall), 2011 IEEE 74th*, pp. 1–5, sept. 2011.

[118] 3GPP RAN 4, "Simulation assumptions and parameters for FDD HeNB RF requirements," Tech. Rep. R4-092042, May 2009.

[119] 3GPP, "Evolved Universal Terrestrial Radio Access (E-UTRA); Base Station (BS) radio transmission and reception (Release 9)," Tech. Spec. 36.104 v9.4.0, June 2010.